DEVELOPMENT OF THERMOSENSITIVE GEL OF DOXYCYCLINE HYCLATE CONTAINING ZINC OXIDE

By

Jongjan Mahadlek

A Thesis Submitted in Partial Fulfillment of the Requirements for the Degree

MASTER OF PHARMACY

Program of Pharmaceutical Technology

Graduate School

SILPAKORN UNIVERSITY

2008

DEVELOPMENT OF THERMOSENSITIVE GEL OF DOXYCYCLINE HYCLATE CONTAINING ZINC OXIDE

By

Jongjan Mahadlek

A Thesis Submitted in Partial Fulfillment of the Requirements for the Degree

MASTER OF PHARMACY

Program of Pharmaceutical Technology

Graduate School

SILPAKORN UNIVERSITY

2008

การพัฒนาเจลชนิดไวต่อการเปลี่ยนแปลงอุณหภูมิของด็อกซีไซคลินไฮเคลต ที่ประกอบด้วยซิงค์ออกไซด์

โดย
นางสาวจงจันท์ มหาดเล็ก

วิทยานิพนธ์นี้เป็นส่วนหนึ่งของการศึกษาตามหลักสูตรปริญญาเภสัชศาสตรมหาบัณฑิต
สาขาวิชาเทคโนโลยีเภสัชกรรม
บัณฑิตวิทยาลัย มหาวิทยาลัยศิลปากร
ปีการศึกษา 2551

The Graduate School, Silpakorn University has approved and accredited the Thesis title of " Development of Thermosensitive Gel of Doxycycline Hyclate Containing Zinc Oxide " submitted by Miss Jongjan Mahadlek as a partial fulfillment of the requirements for the degree of Master of Pharmacy in Pharmaceutical Technology

…….....

(Associate Professor Sirichai Chinatangkul, Ph.D.)

Dean of Graduate School

...../...../.....

The Thesis Advisor

Associate Professor Thawatchai Phaechamud, Ph.D.

Assistant Professor Juree Charoenteeraboon, Ph.D.

The Thesis Examination Committee

..... Chairman

(Parichat Chomto, Ph.D.)

...../...../.....

..... Member

(Associate Professor Pienkit Dangprasirt, Ph.D.)

...../...../.....

..... Member

(Associate Professor Somlak Kongmuang, Ph.D.)

...../...../.....

..... Member

(Associate Professor Thawatchai Phaechamud, Ph.D.)

...../...../.....

..... Member

(Assistant Professor Juree Charoenteeraboon, Ph.D.)

...../...../.....

50353202 : MAJOR : PHARMACEUTICAL TECHNOLOGY
KEY WORDS : THERMOSENSITIVE GEL/ LUTROL® F127/DOXYCYCLINE HYCLATE/ ZINC OXIDE
JONGJAN MAHADLEK : DEVELOPMENT OF THERMOSENSITIVE GEL OF DOXYCYCLINE HYCLATE CONTAINING ZINC OXIDE. THESIS ADVISORS : ASSOC. PROF. THAWATCHAI PHAECHAMUD, Ph.D., AND ASST. PROF. JUREE CHAROENTEERABOON, Ph.D. 177 pp.

This study investigated the development of thermosensitive gel of doxycycline hyclate containing zinc oxide. The characterization for chemical properties of typical and nano zinc oxide were investigated using FTIR, DSC and SEM. The effect of types and amounts of zinc oxide on antimicrobial activity were evaluated. The effects of zinc oxide, *N*-methyl-2-pyrrolidone and doxycycline hyclate on the gel properties including gelation-gel melting temperature, rheology, syringeability, antimicrobial activity and the drug release were investigted. From SEM, the size of powder zinc oxide was smaller than that of micronized zinc oxide and zinc oxide BP, whereas the shape of tetrapod I and II were four needle like arms with pyramidal tips with various paticle sizes. The antibaterial activity depended on the size of zinc oxide. The increased amounts of NMP and zinc oxide decreased gelation temperature of the Lutrol® F127system. Whereas, the increased amount of doxycyline hyclate increased gelation temperature of the Lutrol® F127 system. The syringeability of samples showed to ease of administration into periodontal pockets. The syringeability of the doxycycline hyclate-Lutrol® F127 system were increased as the amount of zinc oxide was increased, however the syringeability of them were decreased as the temperature was decreased. Incorporation of zinc oxide into the Lutrol® F127 systems prolonged the drug release in phosphate buffer pH 7.2. Therefore, this development provided a potential gel system to delivery the drug into the periodontal pockets for the periodontitis therapy.

Program of Pharmaceutical Technology Graduate School, Silpakorn University Academic Year 2008
Student's signature .....
Thesis Advisors' signature 1. ..... 2. .....

50353202 : สาขาวิชาเทคโนโลยีเภสัชกรรม
คำสำคัญ : เจลชนิดไวต่อการเปลี่ยนแปลงอุณหภูมิ/ลูทรอล® เอฟ127/ด็อกซีไซคลินไฮเคลต/ซิงค์ออกไซด์

จงจันท์ มหาดเล็ก : การพัฒนาเจลชนิดไวต่อการเปลี่ยนแปลงอุณหภูมิของด็อกซีไซคลินไฮเคลตที่ประกอบด้วยซิงค์ออกไซด์. อาจารย์ที่ปรึกษาวิทยานิพนธ์ : ภก.รศ.ดร.ธวัชชัย แพชมัด และ ภญ.ผศ.ดร.จุรีย์ เจริญธีรบูรณ์. 177 หน้า.

การศึกษานี้เป็นการพัฒนาเจลชนิดไวต่อการเปลี่ยนแปลงอุณหภูมิของด็อกซีไซคลินไฮเคลตที่ประกอบด้วยซิงค์ออกไซด์ ศึกษาลักษณะทางเคมีของซิงค์ออกไซด์ธรรมดาและนาโนซิงค์ออกไซด์โดยใช้เครื่องโฟรเรียทรานสฟอร์ม อินฟราเรด สเปคโตรสโคปี เครื่องดิฟเฟอร์เรนเชียล สแกนนิ่ง แคลอริเมทริ และกล้องจุทรรศน์อิเลคตรอน และศึกษาผลของปริมาณ ซิงค์ออกไซด์ชนิดต่าง ๆ ต่อฤทธิ์ยับยั้งเชื้อจุลชีพ ศึกษาผลของซิงค์ออกไซด์ เอ็นเมทิลสองไพโรลิโดนและยาด็อกซีไซคลินไฮเคลตต่อคุณสมบัติต่าง ๆ ของเจลลูทรอล® เอฟ127 ได้แก่ อุณหภูมิที่ทำให้เกิดเจลและอุณหภูมิที่เจลหลอมเหลว รูปแบบการไหล ความสามารถในการฉีด ฤทธิ์ยับยั้งเชื้อจุลชีพ รวมทั้งศึกษาการปลดปล่อยยา พบว่าขนาดของซิงค์ออกไซด์พาวเดอร์มีขนาดเล็กกว่าไมโครไนซ์ ซิงค์ออกไซด์และซิงค์ออกไซด์บีพี ขณะที่เททราพอดซิงค์ออกไซด์ I และ II มีรูปร่างเป็นแขนสี่ด้านคล้ายพีระมิด และมีขนาดแตกต่างกันฤทธิ์ยับยั้งเชื้อแบคทีเรียของซิงค์ออกไซด์ขึ้นอยู่กับขนาดสาร ปริมาณของเอ็นเมทิลสองไพโรลิโดนและซิงค์ออกไซด์ที่เพิ่มขึ้น ทำให้อุณหภูมิที่ทำให้เกิดเจลของระบบลูทรอล® เอฟ127 ลดลง ขณะที่ปริมาณของยาด็อกซีไซคลินไฮเคลตที่เพิ่มขึ้น ทำให้อุณหภูมิที่ทำให้เกิดเจลของระบบลูทรอล เอฟ127 เพิ่มขึ้น ค่าไซริงจีอะบิลิตี้แสดงถึงความสามารถในการนำส่งยาเข้าสู่ร่องลึกปริทันต์ ค่าไซริงจีอะบิลิตี้ของระบบด็อกซีไซคลินไฮเคลต-ลูทรอลเพิ่มขึ้นตามปริมาณของซิงค์ออกไซด์ แต่จะลดลงตามอุณหภูมิที่ลดลง การเติมซิงค์ออกไซด์ในระบบลูทรอล® เอฟ127 ทำให้การปลดปล่อยยายาวนานขึ้น ดังนั้นการพัฒนาดังกล่าวทำให้ได้ระบบเจลที่มีศักยภาพในการนำส่งยาเข้าสู่ร่องลึกปริทันต์สำหรับรักษาโรคปริทันต์อักเสบ

ภาควิชาเทคโนโลยีเภสัชกรรม บัณฑิตวิทยาลัย มหาวิทยาลัยศิลปากร ปีการศึกษา 2551
ลายมือชื่อนักศึกษา.....
ลายมือชื่ออาจารย์ที่ปรึกษาวิทยานิพนธ์ 1. ..... 2. .....

ACKNOWLEDGEMENTS

This thesis was successfully achieved through the cooperation of many individuals. First of all, I would like to express my appreciation to my advisor, Assoc. Prof. Dr. Thawatchai Phaechamud for his encouragement, patience, valuable comments and support given throughout my time in graduate school.

I also would like to thank my co-advisor, Asst. Prof. Dr. Juree Charoenteeraboon for her meaningful consultancy, helpful comments and suggestion. An appreciation in extended to Dr. Parichat Chomto, Assoc. Prof. Dr. Somlak Kongmuang and Assoc. Prof. Dr. Pienkit Dangprasirt for the creative guidance and encouragement.

To all my teachers, all my friends, follow graduates students and the staff in Faculty of Pharmacy, Silpakorn University, I would like to thank them for their support, assistance and friendship.

Finally, I would like to express my deep gratitude and appreciation to my parents and my sister for their attention and loving support.

CONTENTS

LIST OF TABLES

Tables Page

LIST OF FIGURES

Figures Page

Figures Page

Figures Page

Figures Page

Figures Page

CHAPTER I

INTRODUCTION

Periodontitis is an inflammation of periodontium that support the teeth in the mouth such as gums, periodontal ligaments, alveolar bone and dental cementum. This disease caused by bacterial infection of a periodontal pocket arising from the accumulation of subgingival plaque and inflammatory response, which can result in tooth loss (Schwach *et al.*, 2000; Kelly *et al.*, 2004). The aim of periodontitis therapy is to remove the bacterial deposits from the tooth surface. Hence, therapeutic approaches involving the use of antimicrobial agents for the treatment of periodontitis have been developed. Systemic and local administration of antibiotics also aid in pocket elimination with nonsurgical periodontal therapy. However, to obtain an effective concentration of the antimicrobial drug in the periodontal pocket after systemic administration, repeated intakes over a prolonged period of time are required. Moreover, this application induces some side effects like hypersensitivity, gastrointestinal intolerance and development of bacterial resistance. Therefore, a more satisfactory approach to administer antimicrobial drugs directly into the pocket involves the use of a controlled release device. Local drug delivery limits the drug to its target site, with little or no systemic uptake, so a much smaller dose is required for effective therapy and harmful side effects can be reduced or eliminated.

Various intra-pocket drug delivery systems have been proposed, including fibers, strips, films, injectable gels and microparticles (Jain *et al*., 2008). Injectable systems are particularly attractive for the delivery of drugs into the periodontal pocket. This application can be easily and rapidly carried out, without pain, by using a syringe. Many polymer-based intra-pocket devices containing drugs for this treatment had been studies as tetracycline loaded into poloxamer and monoglycerides (Esposito *et* al., 1997). Tetracycline-loaded bioadhesive semisolid, polymeric system based upon hydroxyethylcellulose and polyvinylpyrrolidone (Jones *et al*., 1996) and metronidazole-loaded systems based upon Carbopol 974P, hydroxyethylcellulose and polycarbophil (Jones *et al*., 1997). Tetracycline base loaded into the microtubular excipient halloysite and coated with chitosan to further retard the drug release

(Kelly *et al*., 2004). Tetracycline-serratiopeptidase containing pluronic gel were designed (Maheshwari *et al*., 2006). Doxycycline hydrochloride and/or secnidazole loaded into biodegradable polymers, poly (lactide) and poly (lactide-co-glycolide) has been reported (Gad *et al*., 2008).

Doxycycline, a semi-synthetic derivative of oxytetracycline is a broad-spectrum antimicrobial agent used as doxycycline hyclate that againsts many bacterial species including enterococci, *Streptococcus pyogenes*, *Staphylococcus aureus* and various anaerobes. This drug is used for periodontal therapy because of interfere with bacterial protein synthesis and inhibition of tissue collagenase activity. The Atrigel® is injectable biodegradable delivery system containing 10% doxycycline hyclate. This system is based on poly(DL-lactide) dissolved in a biocompatible solvent *N*-methyl-2-pyrrolidone (NMP) (Schwach *et al*., 2000).

N-methyl-2-pyrrolidone (NMP) is chemical compound with 5-membered lactam structure. It was a clear to slightly yellow liquid miscible with water and solvents as ethyl acetate, chloroform, benzene and lower alcohols or ketones. It was thermally stable (boiling point 202°C) and cought be used in formulations that require heat sterilization. These properties of NMP can be used as an attractive solubilizer in the pharmaceutical field (Sanghvi *et al*., 2008). NMP increased the skin permeation of estradiol (Koizumi *et al*., 2004). In the preliminary study, this solvent could change the sol-gel transition temperature of the Lutrol® F127 gels. Thus, the NMP was used as cosolvent in the injectable gel systems based on Lutrol® F127 in this study.

Lutrol® F127 (Poloxamer 407) is synthetic polymer consisting hydrophilic poly(oxy ethylene) and hydrophobic poly(oxy propylene) blocks arranged in a triblock structure. It has a molecular weight about 12,600. It is soluble in water, ethanol and isopropanol. Lutrol® F127 aqueous solutions show thermosensitive properties, which are of the utmosts interest in optimizing drug formulation. It is in general liquid at low temperature but change to gel at a given higher temperature (Dumortier *et al*., 2006). Lutrol® F127 aided as the solubilizing agent for poorly water-soluble molecules, indometacin (Dimitrova *et al*., 2000) or insulin (Barichello *et al*., 1999).

Zinc oxide (ZnO) is a chemical compound. It has been used for various applications. ZnO is of interest for a variety of applications in the pharmaceutical, cosmetics and other industries. It is used as the basis for the production of a number of dental cements; mixed with

clove oil or eugenol. It is used as temporary dental filling (Cassanho *et al*., 2005). It is the interested material because of its antimicrobial activity (Sawai, 2003; Sawai *et al*., 1998). Nano ZnO was ZnO with nano size and wildly studies nanomaterial in a variety of nanodevices such as in sensors, transducecers, solar cells and biomedical science (Wang 2004). Nowadays, nano ZnOs were synthesized by various techniques. Nano ZnO is made with the nano engineering process which shrinks the materials to nano scales that changes its physical, chemical and biological properties to develop the superior material. There are many types of nano ZnO such as nanorods, nanowires, nanocombs naobelts and tetrapods (Gui *et al*., 2006; Leung *et al*., 2004; Lim *et al*., 2006).

The aim of this study was to develop the thermosensitive gels of doxycycline hyclate containing zinc oxide. The Lutrol® F127 gels were prepared by cold method. Doxycycline hyclate, zinc oxide and NMP were added in the systems to investigate their the effect on properties of gels such as physicochemical property, pH, gelation and gel melting temperature, rheology, viscosity and antimicrobial activity against standard microbes, *Staphylococcus aureus*, *Escherichia coli* and *Candida albicans*. Effects of type and amount of zinc oxide on antimicrobial activity were investigated. Effects of doxycycline hyclate, zinc oxide and NMP on the gel physical properties and antimicrobial activities were evaluated. *In vitro* doxycycline hyclate release behavior of the systems were investigated.

The objectives of this study were :

1. To investigate the physicochemical properties of typical and nano zinc oxide and the effects of type and amount of them on the antimicrobial activity.
2. To investigate the preparation and characterization of Lutrol® F127 gel prepared by cold method.
3. To investigate the effects of *N*-Methyl-2-Pyrrolidone, zinc oxide and doxycycline hyclate in the system of gels on the physical properties and the antimicrobial activity of Lutrol® F127.
4. To develop the doxycycline hyclate thermosensitive gel containing zinc oxide and *N*-Methyl-2-Pyrrolidone

CHAPTER II

REVIEW OF LITERATURE

1. Periodontal disease

Periodontal diseases are group of conditions, including gingivitis and periodontitis, which affect the supporting structures of the teeth such as gums, periodontal ligaments, alveolar bone and dental cementum (Listgarten *et* al., 1987; Vyas *et al*., 2005). It is a localised inflammatory response caused by bacterial infection of a periodontal pocket associated with subgingival plaque (Haffajee *et* al., 1986). Although the bacteria are the primary cause, the expression of microbial pathogenic factors alone may not be sufficient to cause periodontitis but they initiate damage directly or indirectly by triggering host-mediated responses that lead to self-injury (Vyas *et al*., 2005). In the early phase of the disease, the gingiva inflamed and extended to deeper tissues in periodontitis, leading to gingival swelling, bleeding and bad breath. In the late phase of the disease, the supporting collagen of the periodontium was degenerated, alveolar bone began to resorb and the gingival epithelium along the tooth surface migrated to 'periodontal pocket' (Haffajee *et* al., 1986; Iqbal *et al*., 2008).

The periodontal pocket provides an ideal environment for the growth and proliferation of microorganisms as primarily gram negative bacteria and further, facultative anaerobic species. Prominent amongst these are *Bacteroides* spp.: *B. intermedius* and *B. gingivalis*; fusiform organisms: *Actinobacillus actinomycetemcomitans*, *Wolinella recta* and *Eikenella* spp.; and various bacilli and cocci; spirochetes; amoebas and trichomonads (Haffajee *et* al., 1986). However, the periodontal pocket remains to harbour the bacteria associated with the disease, a potentiate for a further destructive phase exists which the teeth may be lost. The pathogenesis of periodontal diseases is shown in Figure 1 (Jain *et al*., 2008).

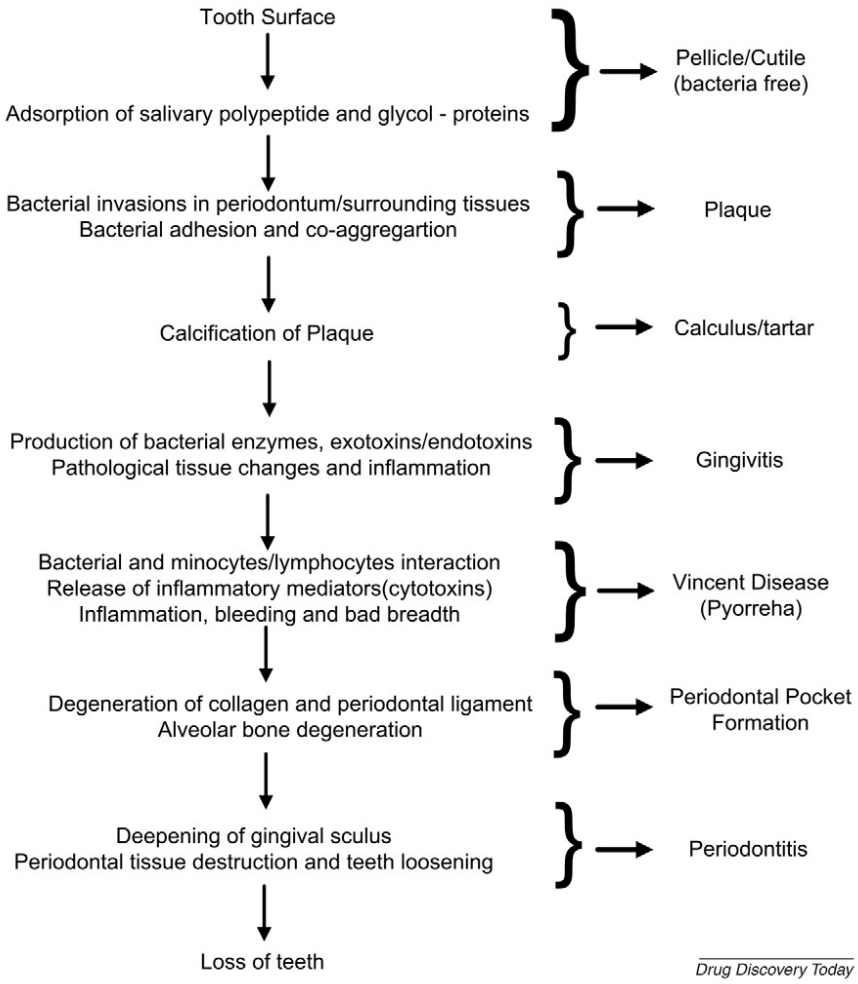

Figure 1 Flow chart representing pathogenesis of periodontal diseases (Jain *et al*., 2008)

The stages of periodontitis involved in the transition from healthy gingivae to the pathological periodontitis were represented as following and shown in Fig 2 (Iqbal *et al*., 2008).

Stage 1: healthy gum tissue (gingiva)

Stage 2: plaque formation due to bacterial invasion

Stage 3: bacterial toxins irritate gums and trigger host-mediated responses that lead to gingivitis

Stage 4: destruction of gingiva and bone that support the tooth leading to periodontitis

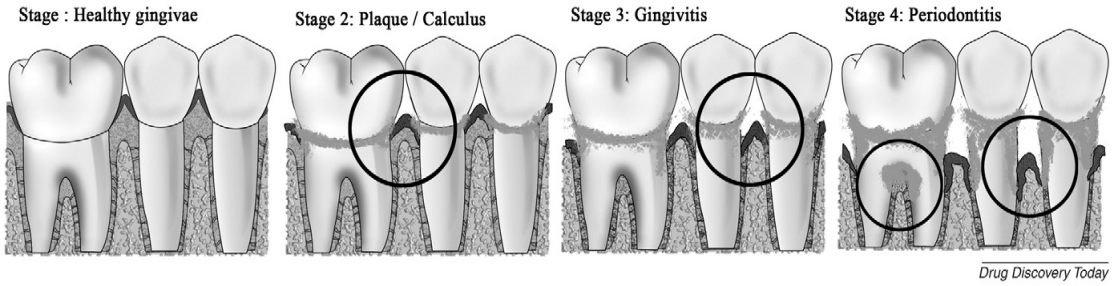

Figure 2 Diagrammatic representation of the pathological periodontitis changes (Iqbal *et al*., 2008)

Most treatments are based on strategies that shift the microflora within the periodontal pocket to that observed around healthy teeth and gingiva, and a widely used procedure consists of mechanically removing plaque and calculus, followed by systemic or local treatment with antimicrobial agents. However, multiple systemic doses of antibiotics have shown several drawbacks including: inadequate antibiotic concentration at the site of the periodontal pocket (Pitcher *et al.,* 1980); a rapid decline of the plasma antibiotic concentration to subtherapeutic levels (Gates *et al*., 1994); development of microbial resistance (Bollen *et al.,* 1996); and high peak-plasma antibiotic concentrations, which may be associated with side effects (Slots and Rams 1990). These obvious disadvantages have evoked an interest in the development of local drug delivery systems for the treatment of periodontal diseases.

Intra-pocket drug delivery systems are highly desirable due to the potentially lower incidence of undesirable side effects, improved efficacy and enhanced patient compliance. The attractiveness of treating periodontal diseases by the intra-pocket drug delivery systems is based on the prospects of maintaining effective high levels of drug in the gingival crevicular fluid (GCF) for a prolonged period of time to produce the desirable clinical benefits.

To date, a great number of local drug delivering devices have been proposed, including fibers, strips, films, gels, microparticles, and are listed in Table 1. Intra-pocket delivery devices in the periodontal pocket had various types such as fibres (Goodson *et al*., 1979; Tonetti *et al*., 1990), strips (Addy *et al*., 1984; Higashi *et al*., 1990; Maze *et al*., 1995; Paolantonio *et al*., 2008), films (Golomb *et al*., 1984; Ahuja *et al*., 2006) and injectable gels (Bruschi *et al*., 2007;Polson *et al*., 1997; Noyan *et al*., 1997). The various drugs were used for periodontal

therapy such as chlorhexidine, tetracycline, doxycycline, minocycline and metronidazole (Table 1).

Table 1 Summary of some investigated intra-pocket delivery systems (Jain *et al*., 2008).

Summary of some investigated intra-pocket delivery systems		
System	**Polymer matrix**	**Drug Incorporated**
Fibers	Cellulose acetate	Tetracycline HCl
		Chlorhexidine
	Ethylene vinyl acetate	Tetracycline HCl
	Poly(ε-caprolactone) (PCL)	Tetracycline HCl
Strip	Polyethylmetha acrylate (acrylic)	Tetracycline HCl
		Metronidazole
	Hydroxypropyl cellulose	Chlorhexidine, tetracycline
		Doxycycline
	Hydroxypropyl cellulose + methacrylic acid	Ofloxacin
	Polyhydroxybutyric acid	Tetracycline HCl
	Polylactide-co-glycolic acid (PLGA)	Tetracycline HCl
		Chlorhexidine
	Ethyl cellulose	Chlorhexidine
Films	Ethyl cellulose	Metronidazole
		Tetracycline HCl
		Minocycline
	Cross-linked atelocollagen	Tetracycline
	Gelatin (Byco® protein)	Chlorhexidine diacetate
	Cross-linked gelatin + glycerine	Chlorhexidine digluconate
	Chitosan	Taurine
	Chitosan + PLGA	Iproflavone
	Chitosan + PCL	Metronidazole
	Polyvinyl alcohol + carboxymethyl chitosan	Ornidazole
	PLGA	Tetracycline
		Amoxycillin + metronidazole
	Poly(*ortho* ester)	Metronidazole
	Eudragit L® and Eudragit S®	Clindamycin
	PCL	Minocycline
Gels	Chitosan	Metronidazole
	Hydroxyethyl cellulose + polyvinylpyrrolidone	Tetracycline
	Hydroxyethyl cellulose + polycarbophil	Metronidazole
	Poloxamer 407 + Carbopol 934P	Propolis
	Poly(DL-lactide) + *N*-methyl 2-pyrrolidone	Saguinarium
		Doxycycline hyclate
	Glycerol monooleate + sesame oil	Metronidazole
	PLGA	Tetracycline
Microparticles	Pluronic F 127	Tetracycline
	PLGA	Tetracycline
		Histatin peptides
	PLGA + PCL	Doxycycline
Nanoparticles	2-Hydroxyethyl methacrylate + polyethylene glycol dimethacrylate	–
	PLGA	*Harungana madagascariensis* leaf extract
	Chitosan	Antisense oligonucleotide
	Cellulose acetate phthalate	Triclosan
	PLGA	Triclosan
Vesicular system	Phosphatidylinositol	Triclosan
	Immunoliposomes	Anti-oralis
Other system	Poly(ethylene-co-vinyl acetate)	Acyclovir
		Chlorhexidine

Injectable systems are particularly attractive for the delivery of antibiotic agents into the periodontal pocket. The application can be easily and rapidly carried out, without pain, by

using a syringe. Thus, the cost of the therapy is considerably reduced compared to devices that need time to be placed and secured. Moreover, an injectable delivery system should be able to fill the pocket and generate the drug to reduce the pathogen. Sauvetre *et al*. (1993) suggested a mucoadhesive gel formulation based on 4% carbopol® containing 1% clindamycin hydrochloride was evaluated *in vivo* on microbial flora of periodontal pockets deeper than 5 mm that it could reduce the microbial content in the periodontal pockets. A gel formulation based on 2.5% hydroxypropylmethylcellulose containing 0.125% histatin was studied *in vivo* in beagle dogs and demonstrated significantly lower plaque index scores (Paquette *et al*., 1997). Kelly *et al*. (2004) developed the tetracycline formulations based on 20% poloxamer 407 containing 0.5% PEG 2000 and 1% octyl cyanoacrylate, and found that it deliver easily the drug to pockets. Maheshwari *et al*. (2006) developed the tetracycline-serratiopeptidase containing periodontal gel formulation. Viscosity and bioadhesivity increased with an increase in the concentration of Aerosil®. Release of tetracycline was sustained as the concentration of Aerosil® increased.

2. Doxycycline hyclate

Doxycycline hyclate is a broad-spectrum antibiotic synthetically derived from oxytetracycline. It is a yellow crystalline powder soluble, which solubles in water and slightly soluble in alcohol. The synonyms of doxycycline hyclate is doxycycline hydrochloride. Structure of doxycycline hyclate is shown in Figure 3.

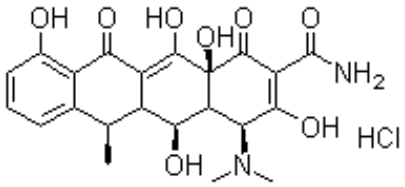

Figure 3 Chemical structure of doxycycline hyclate ($C_{22}H_{24}N_2O_8$, HCl).

Doxycycline is more active than tetracycline against many bacterial species including *Streptococcus pyrogene*, enterococci, *Nocardia* spp., *Staphylococcus aureus* and various anaerobes (Martindale 2005). It exhibits greater oral absorption. It had more prolonged the half-life, and enhanced lipid solubility, which is important for antibacterial action (Seymour

and Heasman 1995). Doxycycline hyclate is introduced for controlling the baterial in periodontal pockets of periodontitis. It has an extra anti-inflammatory effect by inhibiting the proinflammatory cytokines, IL-1 and TNF-alpha (Alexander and Damoulis, 1994; Reynolds and Meikle, 1997). It is bacteriostatic antibiotics which interfere with bacterial protein synthesis and also inhibit tissue collagenase activity (Yu *et al*., 1993; Seymour *et al*., 1995). It had a broad spectrum of activity inhibiting both gram negative and gram positive microorganisms, including the beta-lactamase producing strains which occurred in deep periodontal pockets. Doxycycline therapy at sub-antimicrobial dose had been shown to reduce periodontal disease activity by reducing matrix metalloproteinases (MMPs) and pro-inflammatory cytokines (Choi *et al*., 2004; Gapski *et al*., 2004).

The doxycycline hyclate preparation was used for treatment of periodontitis such as poly (lactide-co-glycolide)(PLGA) containing doxycycline hydrochloride were used to formulate the *in situ* implants (Gad *et* al., 2008). Doxycycline hyclate loaded microspheres composed of SynBiosys™ could be obtained with injectable systems (Gillissen., 2009). The Atrigel® is injectable biodegradable delivery system containing 10% doxycycline hyclate. This system is based on poly (DL-lactide) dissolved in a biocompatible solvent *N*-methyl-2-pyrrolidone (NMP) (Schwach *et al*., 2000).

3. Zinc oxide

Zinc oxide (ZnO) is chemical compound with molecular weight of 81.41. It is nearly insoluble in water and alcohol but soluble in acids and alkalis (Codex 12th edition 1994). It is odorless powder. It occurs as white hexagonal crystals or a white powder commonly known as zinc white. It remains white when exposed to hydrogen sulfide or ultraviolet light. Crystalline ZnO exhibits the piezoelectric effect and is thermochromic (it will change colour from white to yellow when heated, and back again when cooled down). ZnO decomposes into zinc vapor and oxygen at around 1975 °C

ZnO has been used for various applications because of its superior properties. ZnO is of interest for a variety of applications in the pharmaceutical industry, cosmetics and the other industry (the microelectronics industry including sensors, photocatalysis, solar cells, transparent electrodes, electroluminescent devices, and laser diodes). Gas sensing properties of sensors using

ZnO ceramics, thin films and nanostructures have been widely investigated (Choopun *et al*., 2007). ZnO is mainly used in zinc soap and ointment. ZnO is mildly astringent and used topically as a soothing and protective application in eczema, slight excoriations, wound and hemorrhoids. ZnO exhibited antibacterial activity (Sawai, 2003) and antifungal activity (Cassanho *et al*., 2005). Topical ZnO is an efficacious, painless and safe therapeutic option for wart treatment (Khattar *et al*., 2007).

At the nanoscale, ZnO formed in many different shapes as nanorods, nanohelixes, nanobows, nanowires, nanocombs, nanosheets, nanobelts and more exotic branched structures such as tetrapods and multipods (Figure 4). The dimensions of which are often closely related to specific properties. ZnO nanostructures may be grown using templates, physical vapour deposition, electrodeposition, thermal evaporation or hydro-thermal and solvo-thermal methods (Barnard *et al*., 2006). ZnO is an extremely widely studied nanomaterial, in part due to many properties promising new applications in a variety of nanodevices such as in optoelectronics, sensors, transducers and biomedical science (Wang 2004).

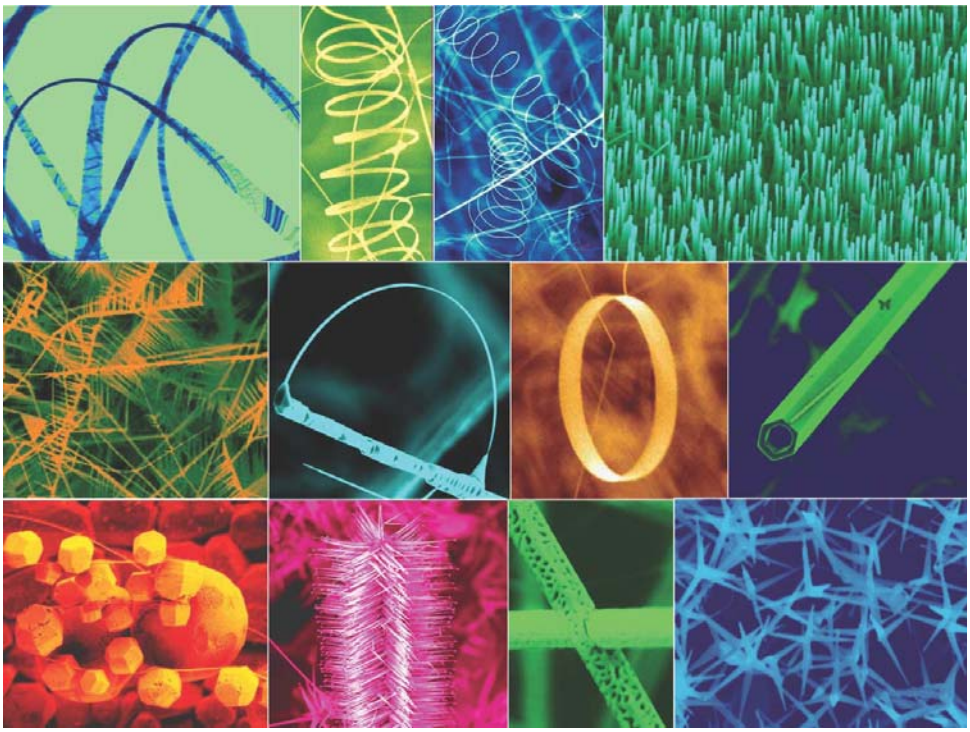

Figure 4 A collection of nanostructures of ZnO synthesized under controlled conditions by thermal evaporation of solid powders (Wang, 2004).

The antimicrobial activities of zinc oxide

Many reports showed the antimicrobial activity of zinc oxide. ZnO had bactericidal action against *S. aureus* and *P. aeruginosa* (Coleman *et al*., 2009). Sawai *et al*. (1996) found that MgO, CaO and ZnO powders had antibacterial activities against some bacteria strains, *S. aureus* and *E. coli*. Many factors related to the antibacterial activities such as the concentrations of the metal oxides particles, the particle size of the metal oxide powder and the specific surface area of the powder (Yamamoto *et al*., 1998). The mechanisms of the antibacterial activity of ZnO particles are not well understood. Sawai *et al*. (1996) proposed that the generation of hydrogen peroxide might be a main factor of the antibacterial activity. While Stoimenov *et al*. (2002) indicated that the binding of the particles on the bacteria surface due to the electrostatic forces could be the mechanism of action. Yamamoto *et al*. (1998) reported that the antibacterial activity depended on the surface area and concentration, while the crystalline structure and particle shape have little effect. The antibacterial activity is better, when the concentration is the higher and the surface area is the larger (Yamamoto *et al*., 1998). Tam *et al.* (2008) investigated antibacterial activity of ZnO nanorods prepared by a hydrothermal method against a gram-negative bacterium *Escherichia coli* and a gram-positive bacterium *Bacillus atrophaeus*.

4. *N*-Methyl-2-Pyrrolidone

N-Methyl-2-pyrrolidone (NMP) is the lactam of 4-methylaminobutyric acid and a very weak base. NMP is a colourless, high-boiling, mobile, characteristic odour, low viscosity and low toxicity. The chemical structure of NMP is shown in Figure 5.

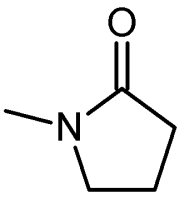

Figure 5 Chemical structure of *N*-Methyl-2-Pyrrolidone (NMP), C_5H_9NO

NMP is a chemically stable and powerful polar solvent. It is a water-miscible organic solvent. NMP is widely used in the petrochemical industry, and in the manufacturing of various compounds, including pigments, cosmetics, insecticides, herbicides, and fungicides. NMP increasingly is used as a substitute for chlorinated hydrocarbons. NMP is known as a good solvent for sparingly soluble drugs in water. The solubility parameter of NMP is similar to those of ethanol and dimethyl sulfoxide (DMSO) (Hanzen and Just, 2001). It has been reported that skin irritation is low for pyrrolidone derivatives (Sasaki *et al*., 1990). NMP is a strongly polar liquid and has the potential for use in solvent extraction process for separating polar substances from non-polar substances (Kumari *et al*., 2009). NMP increased transdermal absorption of some drugs such as phenolsulfonphthalein, ibuprofen and flurbiprofen (Akhter *et al*., 1985; Sasaki *et al*., 1988) and also estradiol (Koizumi *et al*., 2004). Kranz and Bodmeier (2008) reported the systems comprising PLA or PLGA dissolving in NMP. Atrigel®, the commercial injectable system based on poly(DL-lactide) dissolved in a biocompatible solvent N-methyl-2-pyrrolidone (NMP), was used for the periodontal therapy (Polson *et al*., 1997).

5. Lutrol® F127

Lutrol® F127 (Pluronic F127 or Poloxamer 407) consists of ethylene oxide (EO) and propylene oxide (PO) blocks arranged in a triblock structure PEO_x-PPO_y-PEO_x. The chemical formula is shown in Figure 6. It has a molecular weight of about 12,600. In general, poloxamers are composed of white, waxy, free-flowing granules that are practically odorless and tasteless. It is a nonionic surfactant and nontoxic and exhibit reversible thermal characteristics. Poloxamer 407 was used for many preparations (e.g., IV, inhalation, oral solution, suspension, ophthalmic, topical formulations). Sterilisation by autoclaving (120°C, 15 min, 1 bar) appears compatible and does not significantly alter viscosity characteristics of Poloxamer 407 solution, which is interesting to prepare sterile formulations (i.e., ophthalmic or injectable) (Veyries *et al*., 1999; Dimitrova *et al*., 2000).

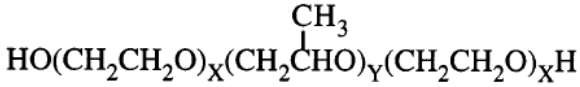

Figure 6 Chemical structure of poly(ethylene oxide-co-propylene oxide-co-polyethylene oxide) (PEO_x-PPO_y-PEO_x) (Lutrol® F127); x = 101 and y = 56

Poloxamers, like other surfactants when dispersed in the liquid, at low concentrations, exist individually as monomolecular micelles. This leads to decrease in the surface tension as well as surface free energy. But as the concentration of the pluronic® in the system increases, this results in the formation of multimolecular aggregates (Guzman *et al*., 1994). Polypropylene oxide (PPO) forms central hydrophobic core wherein methyl groups interact via Vanderwaals forces with substance undergoing solubilization. However, water solubility is believed to be due to the polyethylene oxide (PEO) block by hydrogen bonding interactions of ether oxygen with water molecules. Due to these interactions, pluronic are readily soluble in polar solvent and non-polar organic solvents and established themselves in formulation of dosage forms. Micellar behavior of different block copolymers is found to be dependent upon solvent composition and temperature (Rassing and Atwood 1983; Wanka *et al*., 1990). Micelle structure consists of hydrophobic PPO block lying in the micelle core and the PEO block in the corona (Alxandridis *et al.,* 1994; Jorgenson *et al.,* 1997).

It was reported by many workers that the various salts and additives added, surfactants, polymers, cosolvents have marked effect on micellization, clouding, solubilization behavior of pluronic solutions (Table 2). The addition of sodium chloride lowered the CMC bevause it developed the hydrophobicity in PPO moiety and hydrophilicity of PEO moiety was reduced (Desai *et al*., 2001). On the other hand, addition of urea increased the CMC since it increased solubility of semipolar PPO as well as PEO moiety. While the addition of sodium dodecyl sulphate caused the formation of polymer–sodium dodecyl sulphate complex or mixed micelle indicating polyelectrolyte nature (Desai *et al*., 2001). Pandit *et al*. (2000) studied the effect of NaCl, Na_2SO_4, Na_3PO_4, and NaSCN on pluronic® F-127 solutions. The structure making salts lowered the critical micellar temperature significantly, following Hofmeister series as Na_3PO_4 > Na_2SO_4 > NaCl. Whereas, NaSCN, which is water structure breaker, increased critical

micellar temperature. Ivanova *et al*. (2001) examined ternary isothermal (25°C) systems of pluronic® F127 in presence of various cosolvents such as water and polar water immiscible solvents like glycerol, propylene glycol or ethanol, a partially water immiscible solvent like glycerol triacetate and in presence of surfactants like sodium dodecyl sulphate and cetyl trimethyl ammonium bromide using Small Angle X-ray Scattering (SAXS). The effects that the different cosolvents or surfactants exhibit on the poloxamer phase behavior are interpreted in terms of the preference of the cosolvent/surfactant molecules to locate in different domains of the PEO–PPO–PEO block copolymer self-assembly. Organic solvents, depending on their relative polarities, locate preferably in the PEO-rich or the PPO-rich domains of the microstructure. Some solvents (e.g. ethanol and glycerol triacetate) may show amphiphilic behavior and act as cosurfactants by preferably locating at the interface between the PEO-rich and the PPO-rich domains.

The phase behavior of this polymer depends upon relative volumes of polar PEO rich domains and of relatively nonpolar PPO rich domains. If water is the solvent used in making the solutions, it swells PEO blocks and causes formation of structures of higher curvature. As concentration of water increases, the hexagonal structure reverts to micellar cubic structure and melts to form micellar water-rich solution. Polar water-miscible solvents maintain microstructure to high solvent/water ratios. Large varieties of lyotropic liquid crystalline structures are observed in partially water miscible solvents. These solvents show fewer types of structures in contrast to non-polar solvents (Ivanova *et al*., 2001).

Table 2 Influence of drugs or various agents on the transition temperature of poloxamer formulation (Dumortier *et al*., 2006)

Drug or Agent	Influence on the Transition Temperature (Method Used) ±Influence on Gel Strength and Mucoadhesive Force
Benzalkonium chloride	Transition temperature ↓ (glass tube)
Cysteine	Transition temperature ↓ (magnetic bar method) Gel of strength ↑
Carbopol	Transition temperature ↓ (magnetic bar method) Gel strength and mucoadhesive force ↑
Delta 5-aminolevulinic acid	Transition temperature ↑ (glass tube)
Diclofenac	Transition temperature ↑ (magnetic bar method) Gel strength and the bioadhesive force ↓
Ethanol	Transition temperature ↑ (magnetic bar method) Gel strength and the bioadhesive force ↓
Hydrochloric acid	Transition temperature ↑ (magnetic bar method) Gel strength and the bioadhesive force ↓
Hydroxypropylcellulose	No significant modification of the Transition temperature (magnetic bar method) and gel strength
Lidocaine	No significant modification (rheological method)
Morphine	No significant modification (rheological method)
Poloxamer 188	Transition temperature ↑ (magnetic bar method)
PEG 15000	Transition temperature ↑ (glass tube)
Polycarbophil	Transition temperature ↓ (magnetic bar method) Gel strength and mucoadhesive force ↑
Polyvinylpyrrolidone	No significant modification of the Transition temperature (magnetic bar method) and gel strength
Propylene glycol	Transition temperature ↑ (magnetic bar method) Gel strength and the bioadhesive force ↓
Short-chain fatty acid	Transition temperature ↓ (rheological method)
Sodium alginate	Transition temperature ↓ (magnetic bar method) Gel strength and mucoadhesive force ↑
Sodium chloride	Transition temperature ↓ (magnetic bar method) Gel strength and mucoadhesive force ↑
Sodium dihydrogen phosphate	Transition temperature ↓ (magnetic bar method) Gel strength and mucoadhesive force ↑
Sodium monohydrogen phosphate	Decrease of the Transition temperature ↓ (magnetic bar method) Gel strength and mucoadhesive force ↑
Vitamin B12	Transition temperature ↓ (glass tube)

Thermosensitive behavior of poloxamers

The phenomenon of thermogelling is perfectly reversible and is characterised by a sol-gel transition temperature (Tsol-gel). Below this temperature, the sample remains fluid though above the solution becomes semi-solid. The thermogelation results from interactions between different segments of the copolymer (Dumortier *et al*., 1991). As temperature increases, Poloxamer 407 copolymer molecules aggregate into micelles. This micellization is due to the dehydration of hydrophobic PO blocks, which represents the very first step in the gelling process (Fig. 7). These micelles are spherical with a dehydrated polyPO core with an outer shell of hydrated swollen PEO chains (Juhasz *et al*., 1989). This micellization was followed by gelation

for sufficiently concentrated samples. This gelation was attributed to the ordered packing of micelles. The different structures that can be observed with Poloxamer 407 in water or in mixed solvents were mainly elucidated by small angle X-ray scattering (SAXS) (Liu and Chu 2000). According to Liu and Chu (Liu and Chu 2000), a face centred cubic structure is obtained for Poloxamer 407 concentrations in water ranging between 20 and 40%. At higher concentrations (50%), a body centred cubic packing of micelles is observed. These micellar cubic structures and possible micellar entanglements produce high viscosity, partial rigidity and slow dissolution of the gels. Such properties facilitate the incorporation of both hydrophilic and hydrophobic drugs.

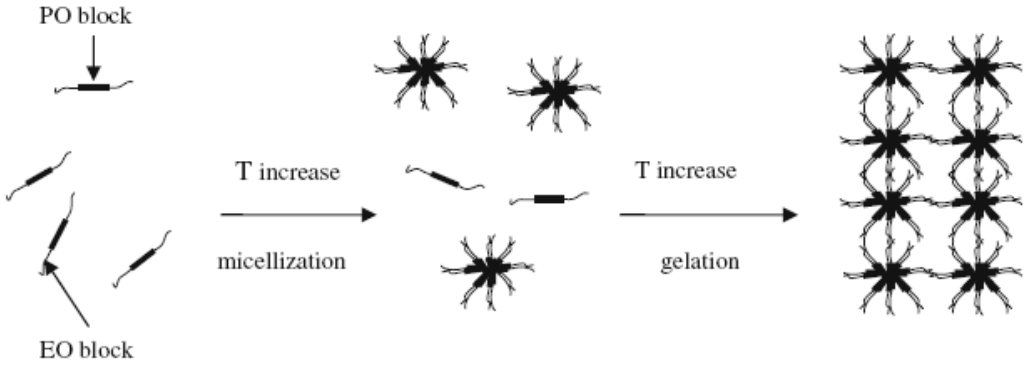

Figure 7 Schematic representation of the association mechanism of Poloxamer 407 in water (Dumortier *et al*., 2006).

The poloxamer copolymers exist in solution as unimers but self-assemble into micelles (Huang *et al*., 2002). At concentrations above the critical micelle concentration (CMC), the copolymer self-aggregates forming micelles of various aspects (Pandit *et al*., 2000). The hydrophobic PO core can incorporate water insoluble molecules and then protects fragile agents from exterior compnents (Attwood *et al*., 1985; Bohorquez *et al*., 1999; McDonald *et al*., 1974).

Properties of poloxamers

Poloxamer 407 facilitated the solubilisation of poorly water-soluble molecules like indomethacin (Dimitrova *et al*., 2000) or insulin (Barichello *et al*., 1999). Solubility of piroxicam in water was increased by 11-fold by adding 22.5% w/w Poloxamer 407 (Shin *et al*., 1997).

Poloxamer 407 promoted the stabilisation of included drugs in particular proteins such as urease and interleukin-2 (Wang and Johnston 1993), insulin (Morishita *et al.,* 2001), alpha chymotrysin and lactate dehydrogenase (Stratton *et al*., 1997) and peptides such as deslorelin and gonadotrophin-releasing hormone (GnRH) (Wenzel *et al*., 2002). Poloxamer 407 has also been used with W/O/W multiple emulsion to promote the stability of the preparation (Olivieri *et al*., 2003).

Gel strength increased with temperature and Poloxamer 407 concentration. This property might be altered in the presence of drugs or additives. Diclofenac, ethanol and propylene glycol weaken Poloxamer 407 gel, whereas sodium chloride, sodium monohydrogen phosphate and glycerine did the opposite (Choi *et al*., 1999; Yong *et al*., 2001). Bioadhesive force generally increased with gel strength and its value was modified by the same parameters (i.e., temperature and Poloxamer 407 concentration). The solvents or ionic agents might alter the adhesion characteristics of poloxamer formulations as it has been previously noted. NaCl has been included in some Poloxamer 407 gels to prolong the residence-time in the site of administration (Choi *et al*., 1999).

Rheological studies

Owing to the thermosensitive property of the poloxamer solutions, different studies focused on the effect of additives on the rheological behavior of these gels. Rheological behaviour represented a key-part in the formulation of poloxamer 407 preparations and had to be fully studied. Some studies determined the temperature range and consequently detects, with great sensitivity, interactions between additives and poloxamer 407 (Miller and Drabik 1984). Most of the authors determined either rheograms (i.e., shear stress versus shear rate or flow curve studies) or oscillatory studies. Rheograms were used for the applications in the development and the control phases whereas oscillatory tests gave more information on the structure and the behaviour of poloxamer 407 in the research studies.

1. Flow curves studies (shear stress versus shear rate)

The rheological behaviour was either Newtonian or non-Newtonian depending on the temperature. Below Tsol-gel, Poloxamer 407 solutions exhibit a Newtonian behaviour. Viscosity slightly increased with temperature. Above Tsol-gel, the rheological type becomes non-Newtonian and was characterised by a significant measured yield value (Charrueau *et al*. 2001;

Chang *et al*. 2002; Shawesh *et al*., 2002). Tsol-gel has been determined as the inflection point on the curve of the apparent viscosity as a function of the temperature (Charrueau *et al*. 2001). Moreover, the flow type of the Lutrol® F127 gels can be characterized using the following exponential formula (Martin 1993):

$$F^N = \eta G$$

$$\text{Log } G = N \text{ Log } F - \text{Log } \eta$$

Where F is shear stress, G is shear rate, N is an exponential constant, and η is a viscosity coefficient, respectively.

2. Oscillatory studies (strain and frequency sweep)

The two types of oscillatory measurements were studies. An oscillatory strain sweep was applied in which the dynamic moduli were recorded at a constant frequency. Strain sweep was used to determine the visco-elastic properties, which responded to the characteristic of materials. A second dynamic measurement (frequency sweep) was performed in which strain amplitude was kept constant and the frequency was varied. The structure of system could be kept intact during the measurement by choosing the amplitude of strain within the linear viscoelastic region (Maheshwari *et al*., 2006). In generally, the material could respond to the deformation on applied stress through 2 mechanisms such as elastic modulus (G'), which provides information about the elastic properties of the material, and viscous modulus (G"), which provides information about the viscosity of the material (Marriott 1988).

6. The release pattern of the prepared systems

The pattern of delivery achieved by a sustained release system can vary over a wide range but release profiles can be mainly categorized into three type:

1. Zero-order release model
2. Square-root-time release model
3. First order release model

6.1 Zero-order release model

An ideal controlled release device is one which can delivery the drug at constant rate until the device is exhausted of active agent. Mathematically, the release rate from this device is given as:

$$\frac{dM_t}{dt} = k \quad [1]$$

Where k is a constant, t is a time and M_t is the mass of active agent released. This model of release is called zero-order release model.

6.2 Square-root-time release model (Higuchi's model)

The second common release model is frequency referred to as square-root-of-time or $t^{1/2}$ release, providing compound release that is linear with the reciprocal of the square root of time. The release rate is then given as:

$$\frac{dM_t}{dt} = \frac{k}{\sqrt{t}} \quad [2]$$

In contrast to first-order release, the release rate here remained finite as the device approached exhaustion.

The release model of this type can be described by Higuchi's equation (Higuchi, 1963)

$$Q = [D\varepsilon/\tau (2A - \varepsilon C_s) C_s t]^{1/2} \quad [3]$$

Where Q is weight in grams of drug release per unit surface area, D is diffusion coefficient of drug in the release medium, ε is porosity of the matrix, τ is tortuosity of system, C_s is solubility of drug in the release medium and A is concentration of drug in the system, expressed as g/mL.

The assumptions made deriving equation are as follows:

1. A pseudo-steady state is maintained during release
2. A>>>Cs, i.e. excess solute is present
3. The system is in perfectly sink condition in which Cs is approximately to zero at all time
4. Drug particles are much smaller than those in the system
5. The diffusion coefficient remains constant
6. No interaction between the drug and the system occurs

In general Higuchi's equation is usually desired and used as:

$$Q = k_h t^{1/2} \quad [4]$$

Where k_h = higuchi's constant

Therefore the plot of amount of drug released from system versus square root of time should be increased linearity if drug release from the system is diffusion controlled. Although the above equation is based on release from a single face, it may use to describe diffusion-controlled release from all surface system.

In order to further verify that the release follows Higuchi's model, Higuchi's equation is converted into logarithmic from as:

$$\log Q = \log k_h + ½ \log t \quad [5]$$

The plot of log Q versus log t must not only yield a straight line, but must have a slope of 0.5.

6.3 First-order release model

The first-order release model is the third common type of the release model. The release rate in this case is proportional to the mass of active agent contained within the device. The rate is then given as:

$$\frac{dM_t}{dt} = k(M_0 - M_t) \quad [6]$$

Where M_0 is the mass of agent on the device at t=0. On rearrangement, this given

$$\frac{dM_t}{dt} = kM_0 \exp^{-kt} \quad [7]$$

In first-order model, therefore, the rate declines exponentially with time, approaching a release rate of zero as the device approaches exhaustion.

On the assumption that the exposed surface area of system decreases exponential of time, Wagner (1969) suggested that drug release from most controlled-release matrices could be described by apparent first order kinetics, thus:

$$A^t = A_0 e^{-k_1 t} \quad [8]$$

Where k_1 is first order release constant, A_0 is initial amount of drug and A_t is amount of drug remaining in the matrix at time t

Simplifying and taking the logarithm of equation 8 yields

$$\log A^t = \log A_0 - \frac{k_1 t}{2.303} \quad [9]$$

First order model can be predicted by plotting the logarithm of the percentage of drug remaining against time. If the drug release pattern follows first order model, linear relationship is obtained. Since both the square root of time release and first-order release plots are linear, as indicated by correlation coefficient, it is necessary to distinguish between to the models. The treatment has been based upon using the differential forms of the first order and square root of time equations (Schwartz *et al*., 1968)

For Higuchi's model, the rate will be inversely proportional to the total amount of drug release in accordance with equation (Higuchi, 1963 and Sa *et al*., 1990).

$$\frac{dQ}{dt} = \frac{k_h^2 S^2}{2Q'} \quad [10]$$

Where $Q' = Q*S$ (S is the surface area of matrix). The rate predicted by first-order model was given by:

$$\frac{dQ}{dt} = kA_0 - kQ \qquad [11]$$

Where $A = A_0 - Q'$. This indicated rate will be proportional to Q'. The rates of release are determined by measuring the slope at different points on the percentage of drug release versus times curves.

The plots of rates of release versus $1/Q'$ are linear, indicating that the release is fitted with Higuchi model. If the plots of rates of release versus Q' are linear, indicating that first order model is operative.

The release model for each classes of device is illustrated in Figure 8 (Baker, 1987). The release models of zero-order, square-root time and first-order are depicted, respectively (equation 1, 2 and 6).

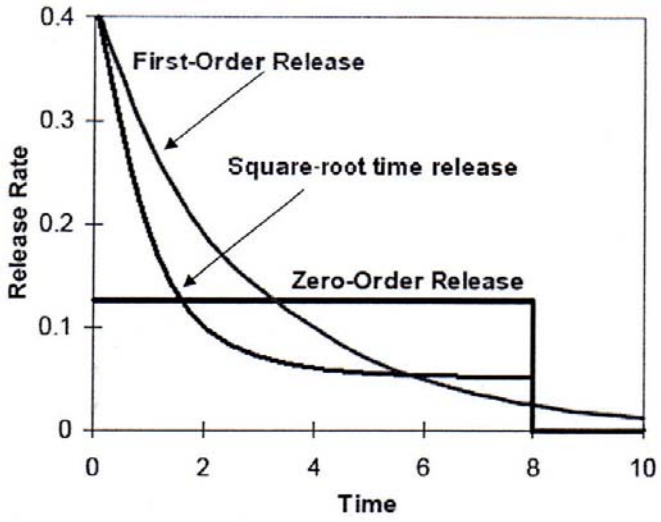

Figure 8 Zero-order, first-order and square-root time release patterns from devices containing the same initial active agent content (Baker *et al*., 1987).

7. Release mechanism of controlled release system

In order to analyze the mechanism of the drug from the systems, the dissolution data may be analyzed using the semiempirical equation of Peppas (1985) given below.

$$\frac{M_t}{M_\alpha} = kt^n \quad [12]$$

Where $\frac{M_t}{M_\alpha}$ = the fractional of release of drug up to time t

t = the release time

k = a constant incorporating structure and geometric characteristics of the controlled release device

n = the release exponent, indicative of the mechanism of drug release

Clearly, at desirable mechanism for many applications that which leads to be equals 1, this characterizes zero-order release behavior. Table 3 summarizes the general dependence of n on the diffusional mechanism (Peppas, 1985).

Table 3 Interpretation of diffusional release mechanism from drug release data from thin polymer film (Peppas, 1985).

Release exponent (n)	Drug transport mechanism	Rate as a function
0.5	Fickian diffusion	$t^{1/2}$
0.5<n<1.0	Anomalous (non-Fickian) Transport	t^{n-1}
1.0	Case-II transport	Zero-order (time-independent)
n>1.0	Super case-II transport	t^{n-1}

The empirical equation 12 could be modified for application to non planar geometric. The relationship between the diffusional exponent n and corresponding release mechanism is clearly depend on the geometry employed as shown in Table 3, 4 and 5 (Rigger and Peppas, 1987).

In non-swellable systems, the values of n are 0.45 and 1.0 for Fickian and case-II transport, respectively. Case-II transport is a special case readily identified and characterized by the constant velocity of the moving solvent front and the resulting linear weight gain with time. However, its characteristics are not as well understood, nor are they as fundamental in origin as those of Fickian diffusion. When the value of is $0.45 < n < 1.0$, the release was said to be non-Fickian (Rigger and Peppas, 1987). A value of n=1, however, mean that the drug release is independent of time, regardless of the geometry. Thus, zero-order release can exist for any geometry.

Table 4 Diffusional exponent and mechanisms of diffusional release from various non-swellable controlled release systems (Ritger and Peppas, 1987).

Release exponent			Drug release mechanism
Thin film	Cylindrical sample	Spherical sample	
0.5	0.45	0.43	Fickian diffusion
0.5<n<1.0	0.45<n<1.0	0.43<n<1.0	Anomalous (non-Fickian) transport
1.0	1.0	1.0	Zero-order (time-independent)

In swellable controlled release systems, case-II (Fickian diffusion) and case-II solute release behavior are unique in that each can be described in terms of a single parameter. Case-I transport described by diffusion coefficient, while case-II transport described by a characteristic constant. Non-Fickian behavior, by comparison, requires two or more parameters to describe the coupling of diffusion and relaxation phenomena.

In swellable matrices, when the system does not swell more than 25% of its original volume, the values of n are 0.45 and 0.89 for Fickian and case-II transport, respectively. When the value of n is > 0.45 and < 0.89, the release was said to be non-Fickian (Rittger and peppas, 1987). When the value of n was greater than that of the case-II transport, the release is said to be super case-II transport. Table 9 summarizes the range of values of diffusional exponent, n, and the released transport mechanism for each a geometry (Rittger and Peppas, 1987). A value of n =1, mean that the drug release can exist for any geometry; only slabs do this release coincide with case-II transport.

Table 5 Diffusional exponent and mechanisms of drug from various swellable controlled release systems (Ritger and Peppas, 1987).

.

Diffusion exponent, n			Drug release mechanism
Thin film	Cylindrical sample	Spherical sample	
0.5	0.45	0.43	Fickian diffusion
0.5<n<1.0	0.45<n<0.89	0.43<n<0.89	Anomalous (non-Fickian) transport
1.0	0.89	0.89	Zero-order (time-independent)

8. MicroMath® Scientist™ for Windows™

It is specifically designed to fit model equations to experimental data. Other programs focus on technical graphics, symbolic manipulation, matrix operations or worksheets for engineering calculations. Scientist™ incorporates all these elements, but its primary function is fitting equations to experimental data. Scientist™ can fit almost any mathematical model from the simplest linear functions to complex systems of differential equations, non-linear algebraic equations or models expressed as Laplace transforms. The Scientist Chemical Kinetic Library is a set of chemical kinetics models that can be used to simulate or analyze experimental data. The Chemical Kinetic Library includes models for zero, first and second order irreversible reactions,

first order reversible reactions, and parallel first order irreversible reactions with up to three products.

Least square fitting the experimental dissolution data (cumulative drug release > 10% and up to 80%) to the mathematical equations (power law, first order, Higuchi's and zero order) was carried out using a nonlinear computer programme, Scientist for Windows, version 2.1 (MicroMath Scientific Sofware, Salt Lake City, UT, USA). The coefficient of determination (r^2) was used to indicate the degree of curve fitting. Goodness-of-fit was also evaluated using the Model Selection Criterion (msc) (MicroMath Scientist Handbook, 1995), given below.

$$msc = \ln\left\{\frac{\sum_{i=1}^{n} w_i (Y_{obs_i} - \overline{Y}_{obs})^2}{\sum_{i=1}^{n} w_i (Y_{obs_i} - Y_{cal_i})^2}\right\} - \frac{2p}{n} \qquad [13]$$

When Y_{obsi} and Y_{cali} are observed and calculated values of the i-th point, respectively, and w_i is weight that applies to the i-th point, n is number of points and p is number of parameters.

9. X-ray Diffraction Principle

Recall electrons orbiting an nucleus are tightly bound. When source electrons strike these outer shell/orbital electrons, the electrons get bounced out of position (or the electrons undergo an energy transition) (Fig 9). This event is immediately followed by another electron dropping back toward the nucleus. The loss in energy appears as an emitted photon with a characteristic frequency. The energy difference between electron levels are quantum and the energy released will depend upon the number of protons and neutrons in the nucleus and the shell from which the electron was displaced.

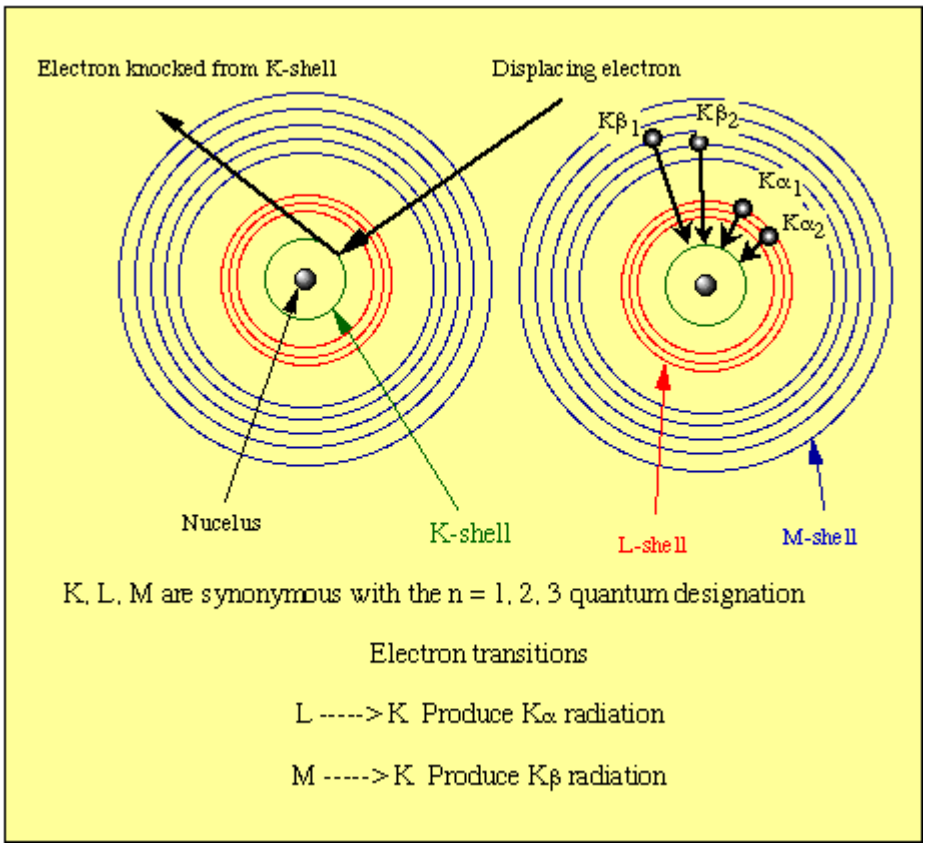

Figure 9 X-ray diffraction principle (Available from http://www.gly.uga.edu/schroeder/geol6550/CM03

CHAPTER III

METHOD OF STUDY

1. Materials

Di-sodium hydrogen orthophosphate (lot no. 405300, Ajax Finechem, Australia)

Doxycycline hyclate (Batch No. 20071121, Huashu pharmaceutical corporation., Shijiazhuang, China)

Hydrophilic colloidal silicondioxide; Aerosil® 200 (batch No.1305053, Wacker-Chemie GmBH, Germany)

Hydrophobic colloidal silicondioxide; Aerosil® R972 (batch No.1274041, Wacker-Chemie GmBH, Germany)

N-methyl-2-pyrrolidone (lot no. A0251390, Fluka, New Jersey, USA)

Potassium dihydrogen orthophosphate (lot no. E23W60, Ajax Finechem, Australia)

Sabouraud Dextrose Agar (SDA) (lot no. 7312647, Difco™ , USA)

Sabouraud Dextrose Broth (SDB) (lot no. 6345690, Difco™ , USA)

Sodium hydroxide (lot no. AF 310204, Ajax Finechem, Australia)

Tryptic Soy Agar (TSA) (lot no. 7341698, Difco™ , USA)

Tryptic Soy Broth (TSB) (lot no. 8091999, Difco™ , USA)

Zinc oxide BP (lot no. 000150, Vidhyasom, Thailand)

Zinc oxide micronized (Numchiang, Bangkok, Thailand)

Zinc oxide powder (Sigma-Aldrich Inc., Germany)

Zinc oxide tetrapod I and II (produced by Dr. Supab Choopun, Department of Physic, Faculty of Science, Chiangmai Univerity, Thailand)

Dialysis tube (Spectra / Por® membrane MWCO: 6,000 - 8,000, lot no. 32644, Spectrum Laboratories, Inc., CAL, USA)

2. Equipments

Analytical balance (Sartorius model BP2100S and Sartorius model CP224S, Germany)

Brookfield viscometer DV-III ULTRA (Brookfield Engineering Laboratories.Inc., USA)

Differential scanning calorimetry (Pyris Sapphrie DSC, Standard 115V, Perkin Elmer instruments, Japan)

Fourier transform infrared spectroscopy (Nicolet 4700, Becthai, USA)

Freeze dryer (Triad™ Labconco, Missouri, USA)

Particle size distribution analyzer (Partica LA-950, HORIBA, Japan)

pH meter (Professional Meter PP-15 Sartorius, Goettingen, Germany)

Scanning electron microscope (Maxim 200 Camscan, Cambridge, England)

Shaking incubator Model SI4 (Shel Lab, Cornelius, USA)

Texture analyzer (Charpa Techcenter, Godalming, Stable micro Systems Ltd., UK)

UV-vis spectrophotometer (Perkin-Elmer, Germany)

Water bath (Julabo, Japan)

3. Methods

3.1 Characterization of various zinc oxide

3.1.1 Differential scanning calorimetry (DSC)

DSC thermograms of all materials (ZnO BP, micronized ZnO, powder ZnO, tetrapod I and II ZnO) were recorded on a differential scanning calorimeter. The temperature axis and cell constant of DSC cell were calibrated with Indium. A heating rate of 10 ºC/min was employed over a temperature range of 25-300ºC with nitrogen purging (30 ml/min). The sample, approximately 5 mg, was weighed into aluminum pan and analyzed in a sealed aluminum pan. An empty aluminum pan was used as the reference.

3.1.2 Fourier transform infrared spectroscopy (FT-IR)

FT-IR spectra of all materials (ZnO BP, micronized ZnO, powder ZnO, tetrapod I and II ZnO) were recorded by the FT-IR spectrophotometer using the KBr pellet method in the region of 4000-400 cm^{-1}.

3.1.3 Scanning electron microscopy-energy dispersive X-ray spectrometer (SEM-EDS)

Surface morphology and element analyses of all materials (ZnO BP, micronized ZnO, powder ZnO, tetrapod I and II ZnO, Aerosil® 200 and R972) were analyzed using SEM-EDS. The samples were sputter coated with gold before examination.

3.1.4 Particle size distribution

The particle size of various zinc oxides and colloidal silicon dioxides were measured using a laser light scattering instrument with the widest measurement range (0.01-3000 μm). The distilled water was used as dispersing medium whereas absolute ethanol was used as a dispersing medium for micronized ZnO and Aerosil® R972 since micronized ZnO and Aerosil® R972 could not be wetted with water. Mean diameters of samples were determined (n=3).

3.2 Preparation of Lutrol® F127 gel

Twenty percent w/w Lutrol® F127 aqueous solutions were prepared by the cold method (Schmolka 1972). Lutrol® F127 was slowly added to cold water (4°C). Each dispersion left in a refrigerator for 24 hrs at 4°C then a clear solution was formed. To manipulate the various formulation properties, *N*-methyl-2-pyrrolidone, zinc oxide, doxycycline hyclate were added into the gel.

3.2.1 Effect of *N*-methyl-2-pyrrolidone

20%w/w Lutrol® F127 gels containing various amount of *N*-methyl-2-pyrrolidone were prepared. The different amount of *N*-methyl-2-pyrrolidone such as 10, 20, 30, 40, 50, 60 and 80%w/w were added as cosolvent to investigate the effect of them on the physicochemical properties and antimicrobial activity of gel. The formula (F1-F8) containing different amount of *N*-methyl-2-pyrrolidone are shown in Table 6.

Table 6 Composition formula of Lutrol® F127 gels containing different amount of *N*-methyl-2-pyrrolidone

Formula	Lutrol® F127 (%w/w)	*N*-methyl-2-pyrrolidone (%w/w)
F1	20	0
F2	20	10
F3	20	20
F4	20	30
F5	20	40
F6	20	50
F7	20	60
F8	20	80

3.2.2 Effect of zinc oxide

The effect of amount of zinc oxide on the physicochemical properties and antimicrobial activity of gel was investigated. Gels containing 20%w/w Lutrol® F127, with and without *N*-methyl-2-pyrrolidone (20%w/w) and various amount of zinc oxide BP such as 0.5, 1, 1.5, 2, 5 and 10%w/w were prepared and evaluated. The formula (F9-F20) containing zinc oxide are shown in Table 7.

Table 7 Composition formula of Lutrol® F127 gels containing different zinc oxide with and without *N*-methyl-2-pyrrolidone

Formula	Lutrol® F127 (%w/w)	Zinc Oxide (%w/w)	*N*-methyl-2-pyrrolidone (%w/w)
F9	20	0.5	-
F10	20	1	-
F11	20	1.5	-
F12	20	2	-
F13	20	5	-
F14	20	10	-
F15	20	0.5	20
F16	20	1	20
F17	20	1.5	20
F18	20	2	20
F19	20	5	20
F20	20	10	20

3.2.3 Effect of doxycycline hyclate

The effect of amount of doxycycline hyclate on the physicochemical properties and antimicrobial activity of gel was investigated. Gels containing 20%w/w Lutrol® F127, with and without *N*-methyl-2-pyrrolidone (20%w/w) and different amount of doxycycline hyclate were prepared. The different amounts of doxycycline hyclate were 2.5, 5, 7.5 and 10%w/w. The formula (F21-F28) containing doxycycline hyclate are shown in Table 8.

Table 8 Composition formula of Lutrol® F127 gels containing different doxycycline hyclate with and without *N*-methyl-2-pyrrolidone

Formula	Lutrol® F127 (%w/w)	Doxycycline hyclate (%w/w)	*N*-methyl-2-pyrrolidone (%w/w)
F21	20	2.5	-
F22	20	5.0	-
F23	20	7.5	-
F24	20	10.0	-
F25	20	2.5	20
F26	20	5.0	20
F27	20	7.5	20
F28	20	10.0	20

3.2.4 Effect of doxycycline hyclate and zinc oxide

The effect of amounts of all zinc oxide on the physicochemical properties and antimicrobial activity of doxycycline hyclate gel were investigated. Gels containing Lutrol® F127 (20%w/w), doxycycline hyclate (5%w/w), with or without *N*-methyl-2-pyrrolidone (20%w/w) and different amount of zinc oxide BP were prepared. The formula (F29-F40) containing doxycycline hyclate and different amount of zinc oxide are shown in Table 9.

Table 9 Composition formula of doxycycline hyclate gels containing different amounts of zinc oxide with and without *N*-methyl-2-pyrrolidone

Formula	Lutrol® F127 (%w/w)	Doxycycline hyclate (%w/w)	Zinc Oxide (%w/w)	*N*-methyl-2-pyrrolidone (%w/w)
F29	20	5	0.5	-
F30	20	5	1.0	-
F31	20	5	1.5	-
F32	20	5	2.0	-
F33	20	5	5.0	-
F34	20	5	10.0	-
F35	20	5	0.5	20
F36	20	5	1.0	20
F37	20	5	1.5	20
F38	20	5	2.0	20
F39	20	5	5.0	20
F40	20	5	10.0	20

3.3 Evaluation of gel properties

3.3.1 Study of the physical properties

The appearance of formulations were observed by visual observation. The observed appearance of the prepared systems were tested as color, homogeneity, phase of systems. The pH of formulations (after 1:100 (w/v) dilution with distilled water) was measured using a pH meter. All measurements were performed in triplicate for each sample (n=3).

3.3.2 Gelation and gel melting temperature

Typically, the determination of the boundary between the sol and gel phases depends on the selected experimental method. In this study a simple test-tube inverting method as described by Miller and Donovan (1982) and Jeong *et al*. (1999) was employed to roughly determine the phase boundary. Gelation and gel melting temperatures were assessed using a modification of the Miller and Donavan technique (Miller *et al.,* 1982). A 5-mL aliquot of gel was transferred to test tubes (internal diameter about 1.8 cm) and immersed in a thermostat water bath at 4°C, and sealed with aluminum foil. The temperature was increased with the increments of 1°C and left to equilibrate for 1 minute at each new setting. The samples were then examined for gelation, which was said to have occurred when the meniscus would no longer move upon tilting through 90°. The gel melting temperature, the temperature at which a gel started flowing upon tilting through 90°, was recorded.

3.3.3 Gel property using differential scanning calorimetry (DSC)

Typically, when the gelation is induced by temperature, the endothermic peak during heating obtained from differential scanning calorimetry (DSC) determined the transition temperature as well as the enthalpy of gelation (Wanka *et al*., 1990). The DSC thermograms of prepared systems were obtained using DSC technique. Samples approximately 5.0 mg were weighted into non-hermetically sealed aluminium pans aluminium pans. The heating range was -10-65°C using nitrogen as purge gas (20 mL/min).

3.3.4 Rheological behavior studies

The rheological behaviors of the Lutrol® F127 gels were investigated by studying their shear stress as functions of shear rate in a Brookfield DV-III Ultra programmable rheometer. To test the effect of temperature, the measurements were conducted at three different temperatures, namely 4°C, 27°C and 37°C.

3.3.5 Antimicrobial studies

Antimicrobial activity of the samples were tested using the contact direction method and the agar diffusion method. The standard microbes were used in this study were *Staphylococcus aureus* (ATCC 6538P)*, Escherichia coli* (ATCC 10536) and *Candida albicans* (ATCC 17110). The culture media for antibacterial and antifungal assay were Tryptic soy agar (TSA) and Sabouraud dextrose agar (SDA), respectively. The numbers of the microbes with and without the presence of different ZnO were investigated to estimate the antibacterial activities of the ZnO. For the antibacterial tests, different amounts of the ZnO were added to 10 mL medium to get different concentrations in range of 5-200 mg/10mL. The number of the bacteria was estimated by the direct plate counting method. Microbes with an approximate concentration of 10^4 colony forming units per milliliter (CFU/ml) was inoculated in a 10 ml broth medium as a blank control and in a solution mixture containing broth medium and different amounts of ZnO. The cultures were grown at 37°C under an agitation condition (200 rpm) for 4 h. After dilution, 100 μL of the proper dilution was transferred directly onto the agar plate. The solution was then spread over the surface of the agar. Three agar plates were used for each dilution. After incubating at 37°C for 24 h, the plates having an ideal number of colonies between 30 and 300 were counted. By knowing how much the sample was diluted prior to being plated, along with the amount of the dilution used in plating, the concentration of the viable cells per milliliter in the original sample was calculated. To be comparable, the inhibition ratio of the bacteria was evaluated by the following equation (Wang *et al*., 2006):

$$\text{Percent inhibition (\%)} = [(A - B) / A] \times 100\ \%$$

where A is the number of bacterial colonies from the untreated bacteria suspension (without ZnO) and B is the number of bacterial colonies from the bacteria culture treated by ZnO. The same antibacterial tests were done on all types of ZnO.

Antimicrobial activities of prepared gels were determined using agar-cup diffusion method. The actively growing broth culture of microbes were prepared, the turbidity was adjusted to be contain approximately 10^8 cells/mL. Then, the swab spreaded onto the agar plate in three directions to ensure complete the plate area and the spread culture were to dry. The sterilized cylinder cups were placed carefully on the surface of the swabbed agar. The prepared gels were filled into the cylinder cup and incubated at 37°C for 24 h. The antimicrobial activities

were measured as the diameter (cm) of clear zone of growth inhibition. The tests were carried in triplicate and the mean inhibition zone ± S.D. were calculated.

3.3.6 *In vitro* release studies

The release studies were performed using the dialysis method. One gram of gel was placed in a dialysis tube (MW cutoff, 6000 - 8000). The dialysis tube was then placed in a glass bottle containing 100 mL of phosphate buffer pH 7.2, maintained at 37°C, and stirred at 100 rpm. Samples (10 mL) were collected periodically and replaced with fresh dissolution medium. The concentration of doxycycline hyclate was determined spectrophotometrically at 349 nm. All of the experiments were triplicately done, and the mean cumulative drug release ± S.D. were calculated.

Calibration curve of doxycycline hyclate in phosphate buffer pH 7.2

Doxycycline hyclate of 7.5 mg was accurately weighed, dissolved in 25 mL distilled water and adjusted the volume to 50 mL with distilled water. This solution was used as a standard stock solution. The 0.833, 1.667, 2.5, 3.333, 4.167 and 5.833 mL stock solution was pipetted and adjusted with phosphate buffer pH 7.2 to volume in 25 mL volumetric flask to make approximately 0.005 - 0.035 mg/mL of doxycycline hyclate. The relationship between concentration and absorbance was determined using UV-vis spectrophotometer at 349 nm. The calibration curve of doxycycline hyclate in phosphate buffer pH 7.2 was exhibited in appendix (Fig. 61).

3.3.7 Determination of surface morphology of gels

Samples were prepared and then they were freeze dried using the freeze dryer for 48 hours until the samples were dried to avoid the collapse of porous structures. Samples were fixed on the adhesive tape and the fine gold sputtering was applied onto the samples. The surface and cross-sectional morphology of the dried samples were determined using scanning electron microscope (SEM). Micrographs were taken with a scanning electron microscope at an accelerating voltage of 15 kV.

Another test, the samples were determined after the release studies under conditions identical to those described above in 3.3.6 after 216 hours. Then they were prepared as the above methods for analysis of their surface morphology. The morphology of samples were observed as the porosity of structures, surface structure and drug crystalline.

3.3.8 Texture analysis

Recently, a dynamic mechanical analysis was used to determine the sol-gel transition in a more reproducible manner (Jeong *et al*., 2002). An abrupt change in the storage modulus or viscosity reflects the sol-gel transition. Textural analysis of the gel systems was performed using a TA.XT2i texture analyzer equipped with a 5 kg load cell and Texture Expert software. The samples of 150 mL were prepared for this test. The sol-gel transition temperature of Lutrol® F127 gels containing various ingredients were determined from oscillating measurements at 1 Hz and heated in a temperature controllable water bath from 4°C to 45°C at heating rate 1°C/min. The sol-gel transition temperature was calculated by 'time cure test' obtained by plotting the elasticity modulus (G') as function of temperature. The gelling temperature was defined as the point where the elasticity modulus (G') was half way between G' for the solution and G' for the gel as mentioned by Edsman *et al*. (1998).

3.3.9 Syringeability

Syringeability of various gel systems was examined to determine the effect of both temperature and the addition of excipients on the force required to expel the prepared product. The ease with which gel systems containing samples could be expressed after filling into syringes and through their fitted needles, was measured using a texture analyzer in compression mode. A filled 1 ml syringe was held in place with a clamp and the upper probe of the texture analyzer moved downwards until it came in contact with the syringe barrel base. A constant force of 0.1 N was applied to the base and the distance required to expel the contents for a barrel length of 20 mm was measured. All of the experiments were triplicately done (n=3) at temperatures of 4°C and 20°C. Force displacement profiles were performed, which the force at distance of 10 mm were selected for analysis. These forces (N) indicated syringeability of the samples that showed to ease of administration.

3.3.10 Data evaluation

To investigate the mechanism of drug release, the cumulative percentage of drug release profiles were fitted with different mathematical release equations. Least square fitting the experimental dissolution data (cumulative drug release > 10% and up to 80%) to the mathematical equations (power law, zero order, first order and Higuchi's) was carried out using a nonlinear computer programme, Scientist for Windows, version 2.1 (MicroMath Scientific

Software, Salt Lake City, UT, USA). The coefficient of determination (r^2) was used to indicate the degree of curve fitting. Goodness-of-fit was also evaluated using the Model Selection Criterion (msc) (MicroMath Scientist Handbook, 1995), given below. Model files used in this study are shown in Table 10.

$$msc = \ln\left\{\frac{\sum_{i=1}^{n} w_i (Y_{obs_i} - \overline{Y}_{obs})^2}{\sum_{i=1}^{n} w_i (Y_{obs_i} - Y_{cal_i})^2}\right\} - \frac{2p}{n} \qquad [14]$$

When Y_{obsi} and Y_{cali} are observed and calculated values of the *i-th* point, respectively, and w_i is weight that applies to the *i-th* point, n is number of points and *p* is number of parameters.

Table 10 Model files used with Scientist™

// MicroMath Scientist Model File: Power law IndVars: T DepVars: F Params: K,Tl, N F=K*((T-Tl)^N ***
// MicroMath Scientist Model File: Higuchi's model IndVars: T DepVars: F Params: K,Tl, F=K*((T-Tl)^(1/2)) ***
// MicroMath Scientist Model File: First order IndVars: T DepVars: F Params: K,Tl, F=1-EXP(-K*(T-Tl)) ***
// MicroMath Scientist Model File: Zero order IndVars: T DepVars: F Params: K,Tl, F=K*(T-Tl) ***

CHAPTER IV

RESULTS AND DISCUSSIONS

1. Physicochemical properties of typical and nano zinc oxide

1.1 Differential scanning calorimetry (DSC) thermograms and IR spectra

DSC is the thermal analysis which accurately measures the heat absorption or release of samples as a function of temperature. ZnO BP and ZnO in form of micronized, powder, tetrapod I and tetrapod II were analyzed with DSC. DSC thermograms of various zinc oxide are shown in Figure 10. The quantity of energy that was absorbed or released from samples was not found in DSC thermograms. Increased amount of ZnO from 3.3 mg to 8.0 mg was also tested but there was no any peak in thermogram as shown in Figure 11. FT-IR spectra of all samples did not exhibit any peak (Figure 12). The appeared peak at 2,500 – 2,300 cm^{-1} was the peak of C=O of carbon dioxide from air. These results thus indicated that nano ZnOs were not chemically different from typical ZnO (ZnO BP).

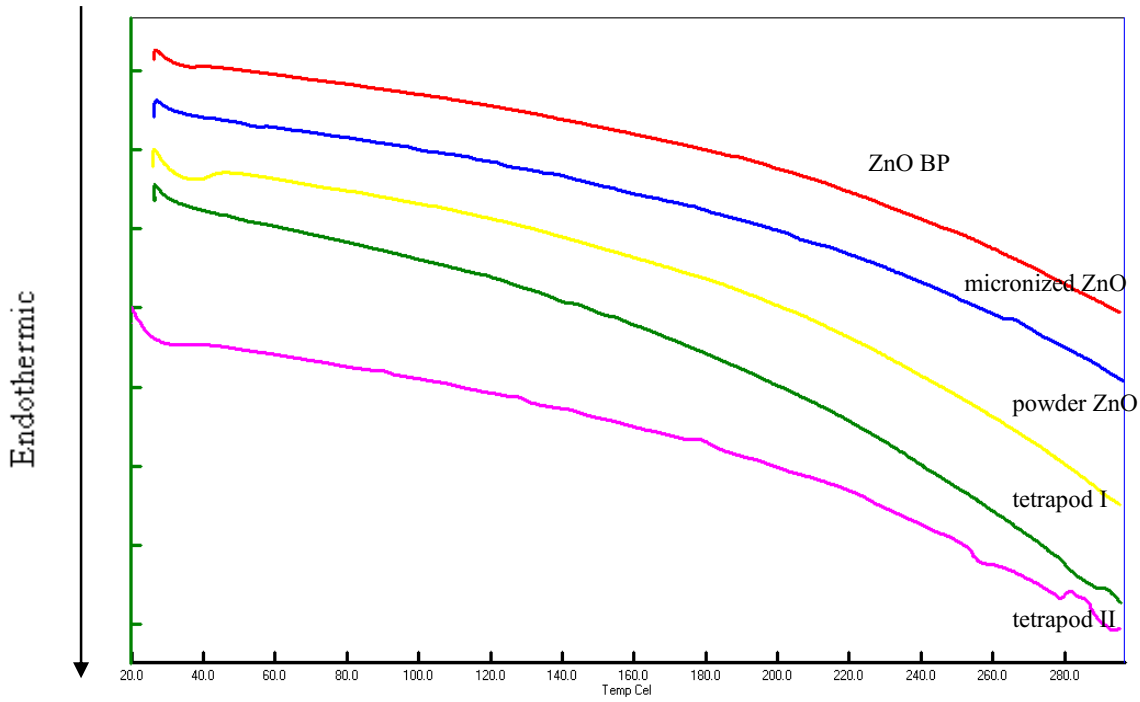

Figure 10 DSC thermograms of various zinc oxide: BP, micronized, powder, tetrapod I and tetrapod II zinc oxide (arranged from top to bottom).

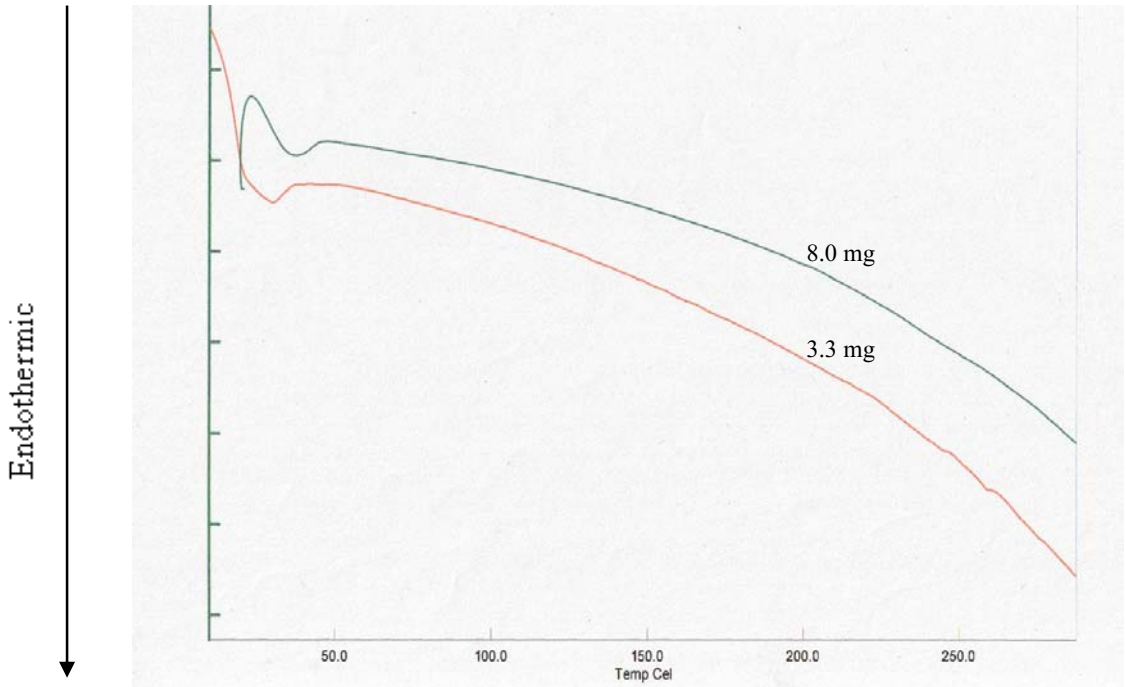

Figure 11 DSC thermograms of zinc oxide BP at various amounts: zinc oxide BP 8.0 and 3.3 mg (arranged from top to bottom).

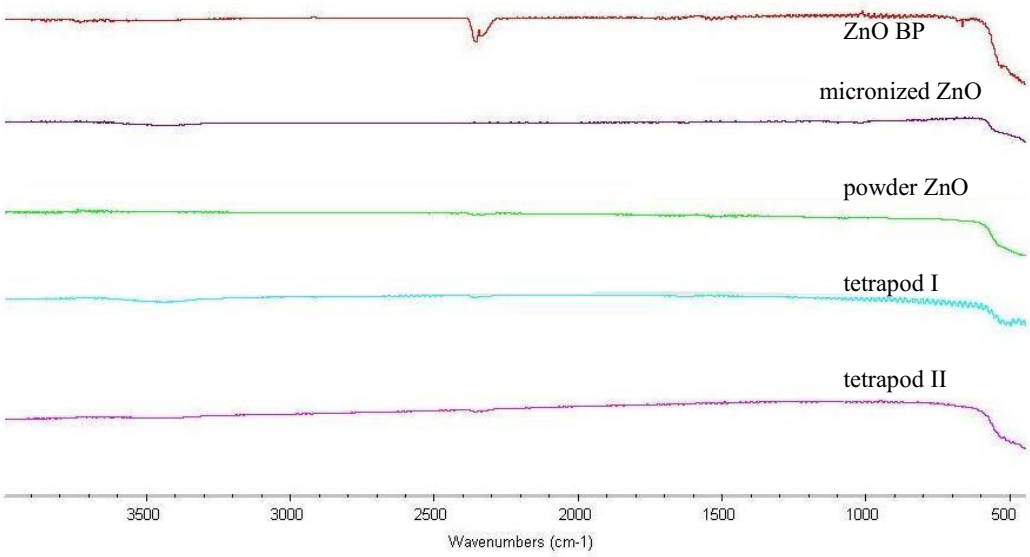

Figure 12 FT-IR spectra of various zinc oxides: BP, micronized, powder, tetrapod I and tetrapod II zinc oxide

1.2 Shape and surface morphology of various zinc oxide

Shape, surface morphology and element analyses of all materials were characterized using SEM-EDS. SEM images of various ZnOs are shown in Figures 13. ZnO BP exhibited as a group of hexagonal crystals with diameter in the range of 0.20-0.70 μm, and length in the range of 0.30-1.20 μm. The spherical ZnO agglomerated with a variety of size (0.10-2.60 μm) of micronized ZnO is shown in Figure 13. The shape of powder and micronized ZnO were spherical but the size of powder (< 0.20 μm) were smaller than that of micronized forms (0.05-0.70 μm). ZnO tetrapods comprised the four needle-like arms with pyramidal tips with various particle sizes. Colloidal silicon dioxides, Aerosil® 200 and Aerosil® R972, were agglomerative nanosphere (Figure 14).

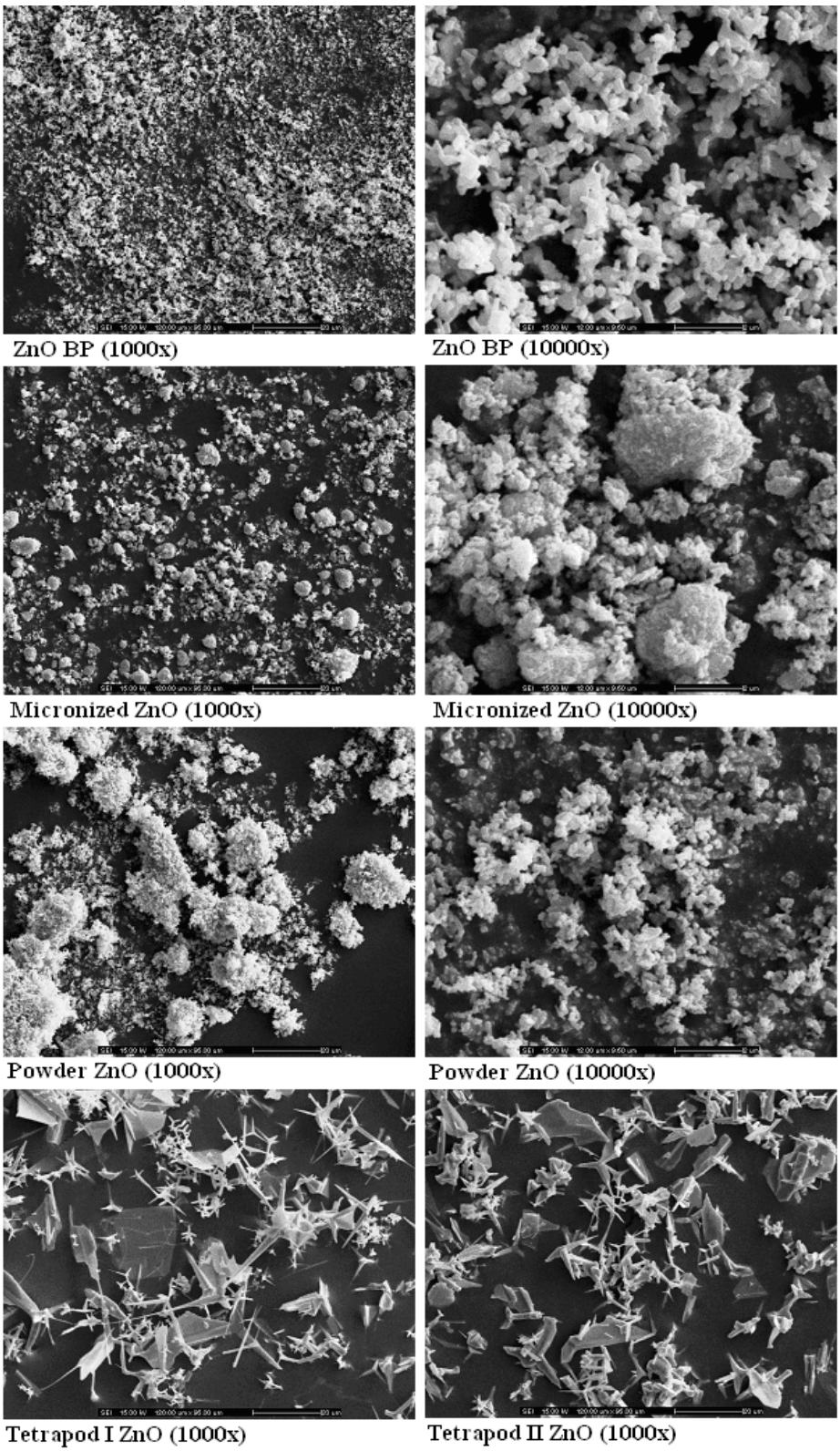

Figure 13 SEM micrographs of different forms zinc oxide: ZnO BP, Micronized ZnO, Powder ZnO, Tetrapod I ZnO and Tetrapod II ZnO

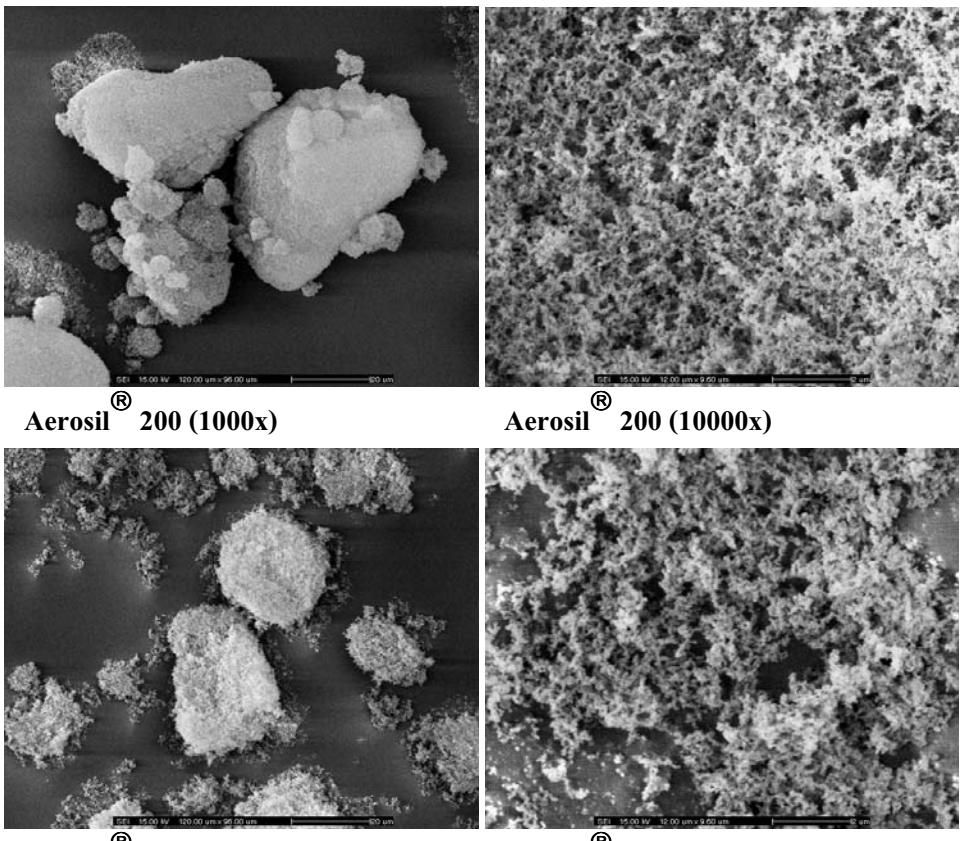

Aerosil® 200 (1000x) **Aerosil® 200 (10000x)**

Aerosil® R972 (1000x) **Aerosil® R972 (10000x)**

Figure 14 SEM micrographs of colloidal silicon dioxide: Aerosil® 200; 1000X, 10000X, and Aerosil® R972; 1000X, 10000X

Energy Dispersive Spectrometer (EDS) analysis is performed by measuring the energy and intensity distribution of X-ray signals generated by a focused electron beam on the specimen. With the attachment of the energy dispersive spectrometer, the elemental composition data of materials can be obtained. EDS pattern of various ZnOs: ZnO BP, micronized and powder ZnO are shown in Figure 15. There were four peaks (ZnL_{α_1}, ZnL_{β_1}, ZnK_{α}, and ZnK_{β_1}) with peak intensity of ZnL_{α} higher than that of ZnK_{α} and that of ZnL_{β} higher than ZnK_{β}. Thus, the energy released from L shell was higher than that from K shell. ZnO powder showed the peak of SiK_{α_1} since its surface was coated with silicone. In contrary, the ZnK_{α} peak intensity of tetrapod I and II ZnOs were higher than that of ZnL_{α} and the ZnL_{β} peak intensity were higher than that of ZnK_{β}. The SiK_{α_1} peak was found in EDS pattern of Aerosil® 200 and Aerosil® R972 (Fig. 16). It was obvious that ZnO with different shapes could release the different energy after activation

due to the arrangement of molecules were distincted formed. Kumar *et al*. (2008) observed that the intensity of the peak enhanced with the increase in the number of deposition cycle in the growth condition.

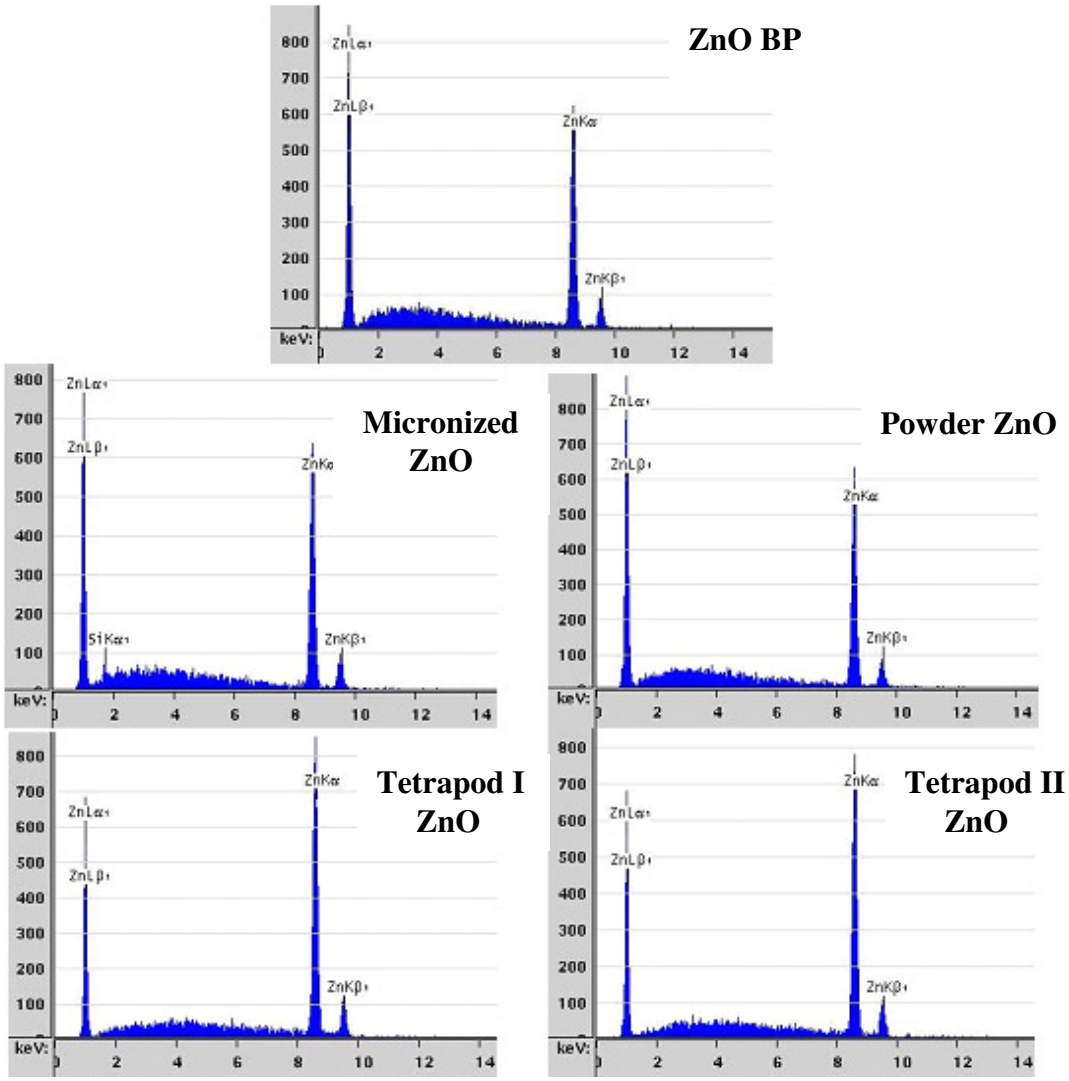

Figure 15 EDS patterns of various ZnOs; ZnO BP, Micronized ZnO, Powder ZnO, Tetrapod I and Tetrapod II ZnO

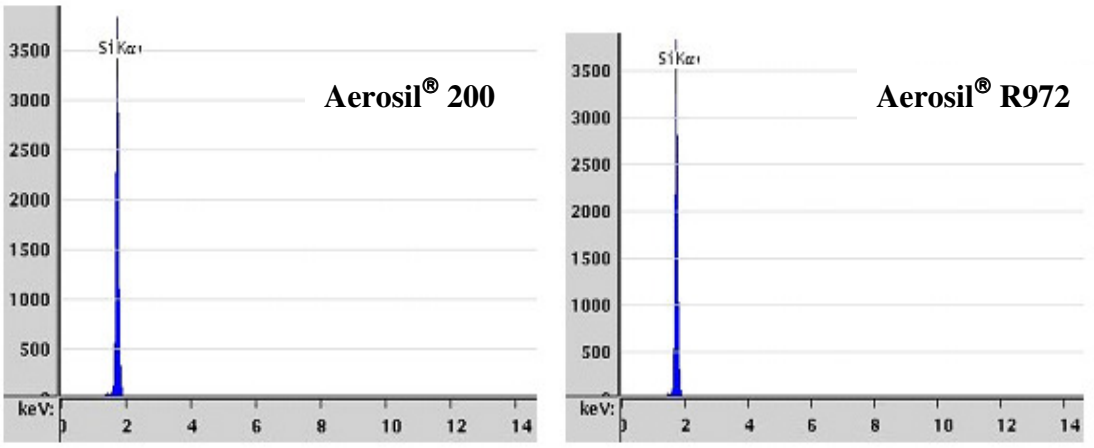

Figure 16 EDS patterns of various colloidal silicon dioxide; Aerosil® 200 and Aerosil® R972

1.3 Particle size of various zinc oxides

All samples were analyzed for their particle size using laser light diffraction spectroscopy. The distilled water was employed as a dispersing medium whereas absolute ethanol was used as a dispersing medium for micronized ZnO and Aerosil® R972 since micronized ZnO and Aerosil® R972 could not be wetted with water. This determination for each sample was repeated to three time. Mean of diameter were presented in Table 11. Micronized ZnO exhibited the smallest particle size (4.436 $\pm$ 2.891 µm). The particle size of powder ZnO (13.585 $\pm$ 6.715 µm) was smaller than that of ZnO BP (18.427 $\pm$ 7.493 µm), tetrapod I ZnO (33.072 $\pm$ 21.138 µm), tetrapod II ZnO (37.411 $\pm$ 30.874 µm), Aerosil® 200 (52.748 $\pm$ 31.276 µm) and Aerosil® R972 (89.634 $\pm$ 64.358 µm), respectively. Due to their structural arm form characteristic of tetrapods, ZnO tetrapod I and II were larger than ZnO BP, micronized and powder ZnO. According to the study of morphology from the SEM supported that the structures of both tetrapod ZnO were four needle-like arms with pyramidal tips and various particles sizes. Owing to the agglomeration of Aerosil® R972, the analyzed particle size of this material was larger than that of the others. Typically, Aerosil® 200 was hydrophilic fumed silica, whereas Aerosil® R972 was hydrophobic fumed silica (Takeuchi *et al*., 2004). However, these results were different from previous report that the particle size of Aerosil® 200 and Aerosil® R972 were 12 and 16 nm, respectively (Degussa 2009). However, our studies found the large particles were aggregated

from the fine particles as shown in SEM. Zhang *et al*. (2008) investigated the ZnO nanoparticles that the ZnO particles were not uniform, there were still some large particles, which might be the aggregates of the nanoparticles. The particle size measured by the Malvern Nano-Sizer which is the hydrodynamic diameter was expected to be larger than the actual size. Thus, the average particle sizes of all samples were measured by this method was bigger than the one found in the SEM image (Fig. 13), which might be the aggregates of the particles.

Table 11 Particle size of various samples (n=3)

	particle size (μm)	
	Mean	S.D.
ZnO BP	18.427	7.493
micronized ZnO*	4.436	2.891
powder ZnO	13.585	6.715
tetrapod I	33.072	21.138
tetrapod II	37.411	30.874
Aerosil® 200	52.748	31.276
Aerosil® R972*	89.634	64.358

* dispersed in absolute ethanol

2. Effect of *N*-methyl-2-pyrrolidone (NMP) on gel properties

2.1 The appearance of gel containing NMP

The gel base was transparent liquid at 4°C whereas the transparent semisolid gel was formed at 27°C and 37°C. The 20%w/w Lutrol® F127 gels containing various amounts of NMP were prepared. The prepared gels containing ≤ 30%w/w NMP were transparent liquid at 4°C. The 40%w/w NMP gel had a lot of bubble gas and the gel preparations containing ≥ 50% NMP exhibited as the cloudy gel. On the other hand, at 27°C and 37°C, the prepared gel containing ≤ 30%w/w NMP exhibited as the transparent gel whereas the 40%w/w NMP gel exhibited as a bubble gel and the gel preparations containing NMP more than 50%w/w exhibited as the yellowish transparent solution. These results indicated that the appearance of Lutrol® F127

systems were affected by the amount of NMP. Ivanova *et al.* (2001) reported that the phase behavior and microstructure of poloxamer block copolymers was also affected by various organic solvents as glycerol, propylene glycol and ethanol. To rationalize the preference of the various polar water-miscible solvents to locate in different domains of the self-assembled structure, we have proposed correlations on the solvent effects on the Poloxamer phase behavior on the basis of the solvent relative polarity. The polar solvents were further classified as PEO-resembling and PPO-resembling. It was shown that although polar and completely miscible with water, the PEO-resembling and the PPO-resembling solvents could affect the curvature of the self-assembled structure in opposite directions. The PEO-resembling solvents (glycerol) are located in the polar PEO-rich domains far from the interface and increase the curvature. The PPO-resembling solvents (propylene glycol and ethanol) are preferably located in the relatively apolar PPO rich domains and at the interface, and keep the curvature constant.

2.2 The pH of gels containing NMP

The pH values of the 20%w/w Lutrol® F127 gel containing 10-80% w/w NMP were presented in Table 12. The pH of 20% Lutrol® F127 gel without NMP was 5.20 ± 0.01. The pH values of gel preparations comprising NMP were in the range of 5.00 ± 0.03 to 5.27 ± 0.02. The pH of 1%w/v NMP was 5.64 ± 0.04. These results indicated that the amount NMP slightly changed pH value of gel preparations due to the pH value of NMP was near to that of the gel base.

Table 12 pH values of Lutrol gels comprising different *N*-methyl-2-pyrrolidone concentrations

Concentration of NMP (%w/w)	pH ± S.D. (n=3)
0	5.20 ± 0.01
10	5.16 ± 0.03
20	5.22 ± 0.02
30	5.26 ± 0.04
40	5.17 ± 0.02
50	5.17 ± 0.01
60	5.19 ± 0.07
80	5.27 ± 0.02

2.3 The gelation and gel melting temperature of 20%w/w Lutrol® F127 system containing NMP

The effect of *N*-methyl-2-pyrrolidone concentration on sol-gel and gel-sol transition is shown in Figure 17. Gelation temperature is temperature that system was changed from sol to gel state, whereas gel melting temperature is temperature that system was changed to sol state. Sol-gel transition temperature of Lutrol® F127 gel (20%w/w) without NMP was 23.7 ± 0.6°C. The addition of NMP influenced on the sol-gel and gel-sol transition of gels. Lutrol® F127 system with lower NMP (≤ 30%w/w) could shift the sol-gel transition to a lower temperature but the gel-sol transition was shifted to a higher temperature. Lutrol® F127 system with higher NMP (≥ 40%w/w) could shift both sol-gel and gel-sol transition to a lower temperature. Thus, the gelation range of systems containing ≤ 30%w/w NMP was broader than that of the systems containing ≥ 50%w/w NMP. The sol-gel transition temperature of gel comprising 40%w/w NMP was not found because this system formed gel at even low temperature. These results suggested that the added NMP decreased the gelation temperature of a Lutrol® F127. The prior studies reported that the gelation of thermosensitive gel was affected by various factors, such as

temperature, polymer concentration, concentration of active ingredients/excipients and electrolytes (Pandit *et al.,* 2000; Rhee *et al*., 2006; Maheshwari *et al*., 2006). The gel formation was related to micellar packing and volume fraction. The type of structures obtained in the presence of selective solvent appearred to be a function of the volume fraction of the polar/apolar component (Ivanova *et al.,* 2002) and the effects could be viewed in terms of a reduction in the water activity leading to an increase in the active concentration of polymer in the system. The decreased gelation temperature was owing to the interaction between the hydrophobic portion of the polymer molecules, which could disrupt the micellar structure and increase the entanglement of micelles (Meheshwari *et al.*, 2006). Most of flavors increased the viscosity of the poloxamer aqueous solution and decreased the gelling point of poloxamer 407 aqueous solution in proportion to amount added. The flavors might bind to the hydrophilic end chains of poloxamer, promoting dehydration and causing gelation of polymer solution at lower temperature (Rhee *et al.,* 2006).

Practically, the structure of NMP contained both lipophilic and hydrophilic portions. The dominant hydrophobic portion of NMP caused the decrement of gelation temperature. This is in agreement with previous findings on the effects of hydrophobic compounds on the gel formation of PEO-PPO-PEO block copolymer systems. For example, Malmsten and Lindman (1992) investigated the gelation of Lutrol® F127 and found that t-butylbenzene lowers the gelation temperature for this polymer. Gilbert *et al*. (1987) found that benzoic acid and *p*-hydroxybenzoate esters caused a decrease in the gelation temperature of the block copolymer and that the more hydrophobic the solute the greater the decrease in gelation temperature. Scherlund *et al*. (2000) found that the gelation point decreased with increasing amount of lidocaine and prilocaine. The origin of this effect was the presence of a hydrophobic component inducing micellization and resulting thereafter a micellar growth.

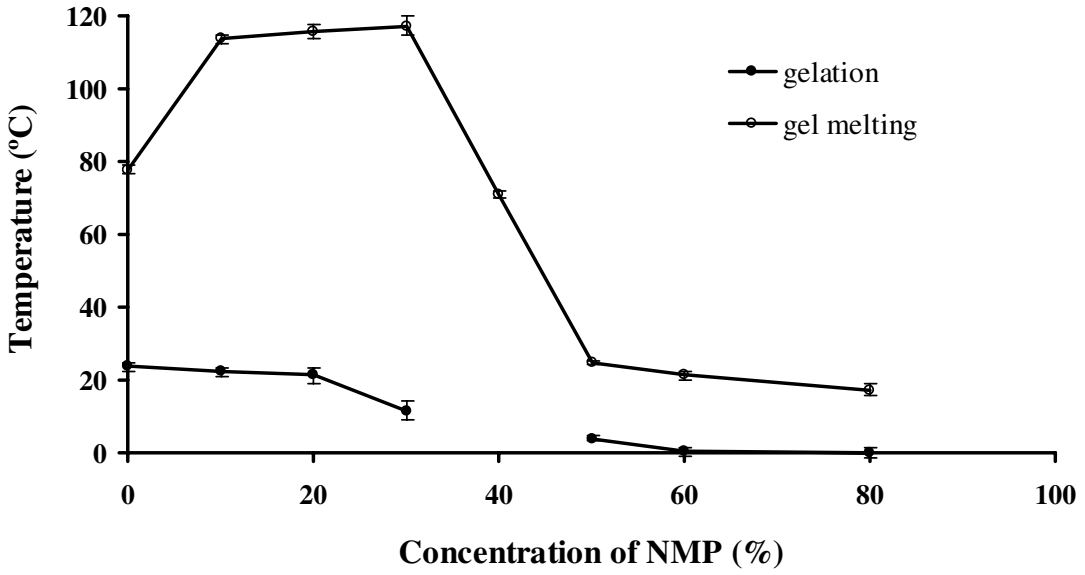

Figure 17 Effect of *N*-methyl-2-pyrrolidone on gelation temperature and gel melting temperature of 20% Lutrol® F127 gel (n=3)

2.4 The rheology of gels containing NMP

The flow curves of the Lutrol® F127 gels comprising different concentrations of *N*-methyl-2-pyrrolidone at different temperatures, 4°C, 27°C and 37°C, are shown in Figs 18, 19 and 20, respectively. The incorporation of NMP caused an apparent change in the flow curve of the Lutrol® F127 system. In the case of the concentration of NMP was less than 20%, the flow curve shifted from low shear stress to higher shear stress along the temperature increased. As the concentration of NMP was higher than 50%, the flow curve shifted from high shear stress to lower shear stress when the temperature was increased. The temperature change slightly affected the flow of systems containing 30 - 40%w/w NMP. The flow curve of system demonstrated as the non-Newtonian behavior that the up curve did not coincide with the down curve indicating the presence of thixotropy, with a hysteresis loop. But the area of the hysteresis loop of the all prepared systems did not increase as an increase of NMP concentration. This suggested that NMP could not enhance the thixotropic properties of the gel. However, the flow curve moved to a higher shear stress value, indicating the higher compactness for structure of the gels (Masheshwari *et al.,* 2006).

The flow parameters of Lutrol® F127 gels containing different concentrations of NMP at 4°C, 27°C and 37°C are listed in Table 13. The N values of the Lutrol® F127 gel containing 0 - 20% NMP increased as the temperature was enhanced. The N values of 0 - 20% NMP gels at 4°C were near to 1 indicating a Newtonian flow characteristic, while the non-Newtonian flow characteristic with the N values > 1 was obtained with an increase in the temperature. The N values of the prepared gels containing 30 - 40% NMP were > 1, which they were not affected by increasing of temperature. The increased NMP concentration from 50 to 80%w/w decreased the N values when the temperature increased. The N values of the prepared gels containing 50 - 80% NMP at 4°C were more than one indicating the non-Newtonian flow. Moreover, the N values with near to 1 of 50 - 80% NMP gels at 37°C indicated the Newtonian flow characteristic. The viscosity coefficient (η) of systems containing 0 - 20% NMP was increased but that of systems containing 30 - 40% NMP was slight increased during temperature increasing. On the other hand, the viscosity coefficient of systems containing 50 - 80%w/w NMP was decreased when the temperature was increased. These results were corresponding to the obtained flow curve.

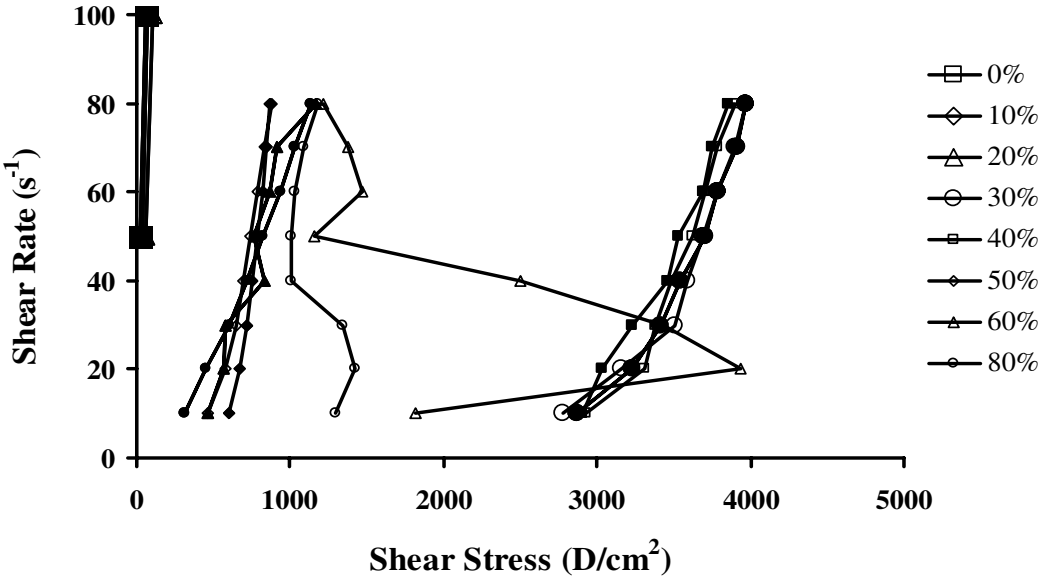

Figure 18 Flow curve of Lutrol® F 127 gel containing different concentrations of *N*-methyl-2-pyrrolidone at 4°C. Open symbols represent the up-curve, and closed symbols represent the down-curve.

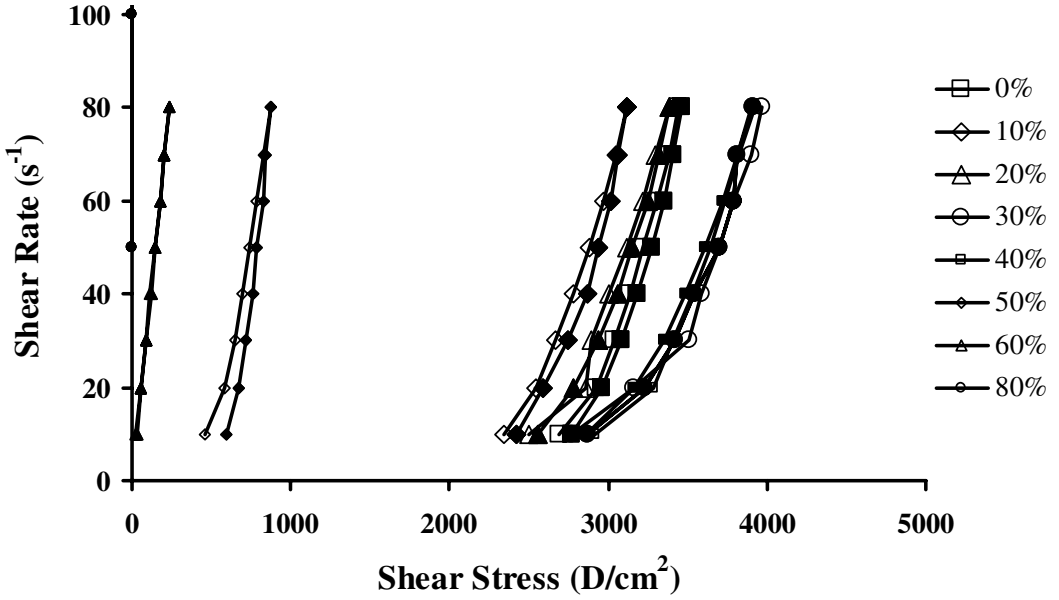

Figure 19 Flow curve of Lutrol® F 127 gel containing different concentrations of *N*-methyl-2-pyrrolidone at 27°C. Open symbols represent the up-curve, and closed symbols represent the down-curve.

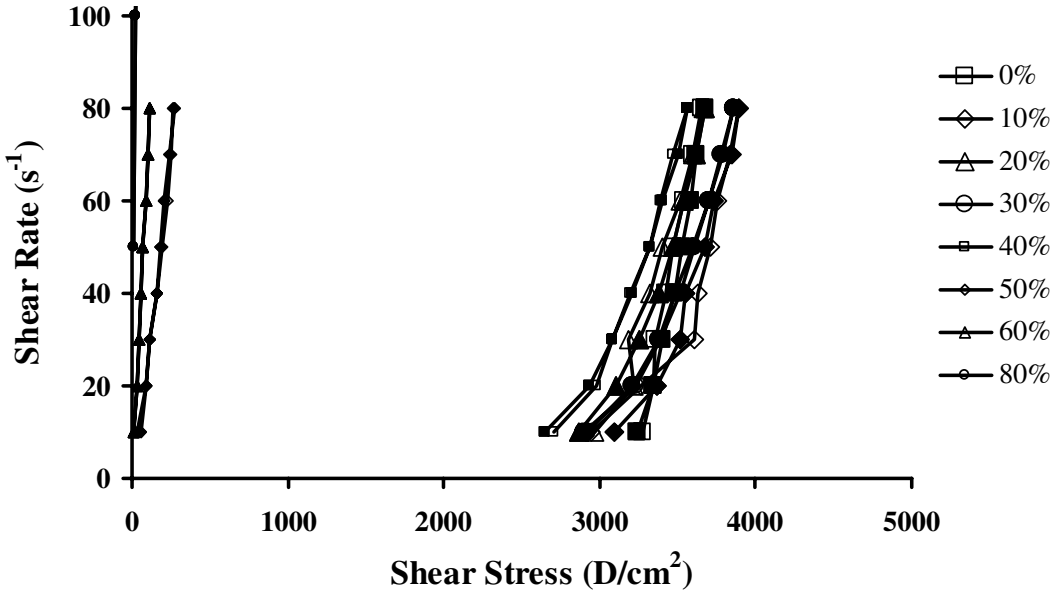

Figure 20 Flow curve of Lutrol® F 127 gel containing different concentrations of *N*-methyl-2-pyrrolidone at 37°C. Open symbols represent the up-curve, and closed symbols represent the down-curve.

Table 13 Flow parameters of Lutrol® F127 gel containing different concentrations of *N*-methyl-2-pyrrolidone at 4°C 27°C and 37°C (n=3)

Lutrol® F127 systems						
Concentration of NMP (% w/w)	4°C		27°C		37°C	
	N (mean±S.D.)	Viscosity Coefficient (mean±S.D., $[D/cm^2]^N$ s)	N (mean±S.D.)	Viscosity Coefficient (mean±S.D., $[D/cm^2]^N$ s)	N (mean±S.D.)	Viscosity Coefficient (mean±S.D., $[D/cm^2]^N$ s)
0	1.01 ± 0.02	-0.29 ± 0.04	6.95 ± 1.43	22.89 ± 4.84	10.50 ± 2.24	35.77 ± 8.05
10	0.99 ± 0.01	-0.20 ± 0.01	7.00 ± 0.45	22.71 ± 1.48	8.67 ± 1.32	29.18 ± 4.69
20	1.02 ± 0.01	0.05 ± 0.02	6.89 ± 0.73	22.67 ± 2.63	8.25 ± 1.30	27.59 ± 4.49
30	6.09 ± 0.35	20.04 ± 1.17	6.66 ± 0.97	22.00 ± 3.33	7.42 ± 1.14	24.61 ± 3.88
40	6.67 ± 0.84	22.14 ± 2.90	7.25 ± 0.37	24.12 ± 1.35	7.45 ± 0.56	24.60 ± 1.93
50	6.74 ± 1.27	22.33 ± 4.63	2.92 ± 0.46	6.47 ± 1.51	1.08 ± 0.05	0.70 ± 0.13
60	1.84 ± 0.39	4.44 ± 1.26	1.01 ± 0.03	0.49 ± 0.08	1.01 ± 0.03	0.21 ± 0.06
80	3.16 ± 1.05	7.57 ± 3.66	1.05 ± 0.17	-0.58 ± 0.26	1.04 ± 0.05	-0.59 ± 0.12

2.5 The thermal property of gel containing NMP investigated using differential scanning calorimetry (DSC)

The micelle transition of the formulation was investigated using differential scanning calorimetry (DSC). The critical micellization temperature (cmt) was taken as the onset of the endothermic peak. This peak has previously been attributed to a hydrophobic entropy gain on micellization (Alexandridis *et al.,* 1994; Wanka *et al*., 1994; Scherlund *et al.,* 2000). DSC investigations of Lutrol® F127 gel containing different NMP concentrations are shown in Figures 21 and 22. The critical micellization temperature (cmt) did not correlate with the added amount of NMP. The decrease of heating rate to 5°C/min was also conducted (Fig. 22). There was endothermic peaks appeared for the systems containing 60 and 80%w/w NMP. Scherlund *et al.* (2000) reported that the critical micellization temperature and gelation temperature of Lutrol® F68 and Lutrol® F127 were found to interconnect and influence by cosolutes, such as electrolyted and hydrophobic substances. Both cmt and gelation temperature increased upon diluting the system with water, and decreased with an increasing pH of the system due to the solubility reduction of the active ingredients. The ratio between the two block copolymers presented in the system had an impact on both cmt and the gelation temperature, resulting in a

decrease of onset temperature of both processes with an increase in Lutrol® F127. However, that mentioned characteristics did not obtain from this study.

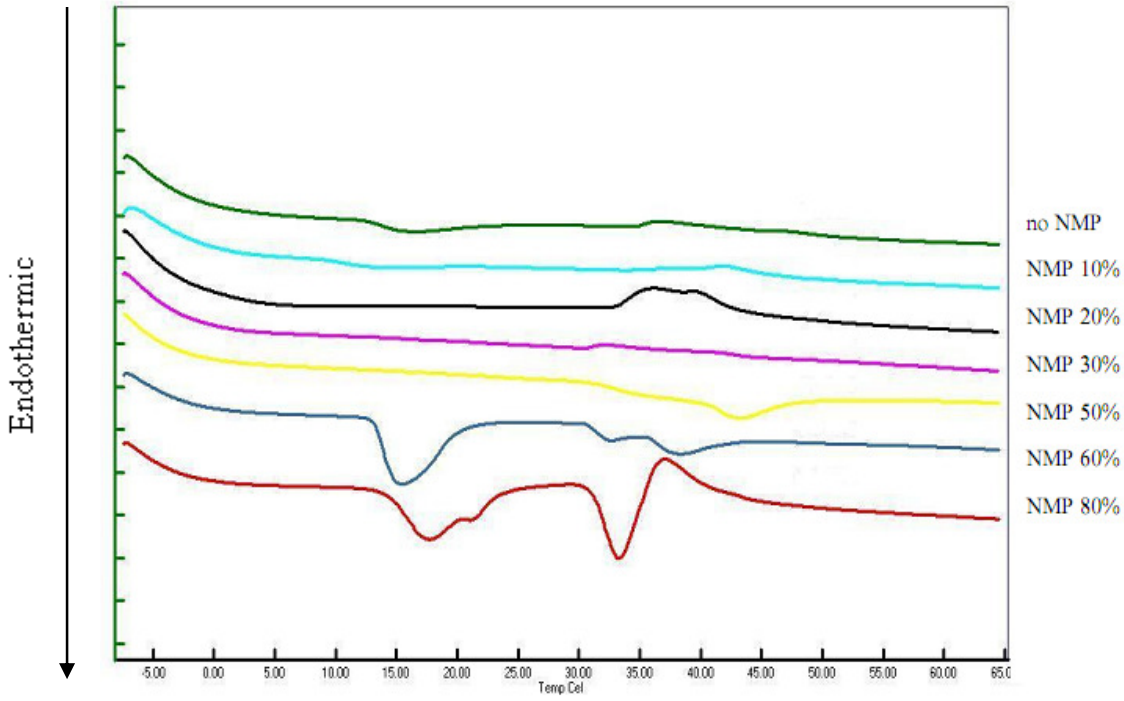

Figure 21 DSC thermograms of sytems contains 20%w/w Lutrol® F 127 gel and different concentrations of *N*-methyl-2-pyrrolidone with heat rate of 10°C/min

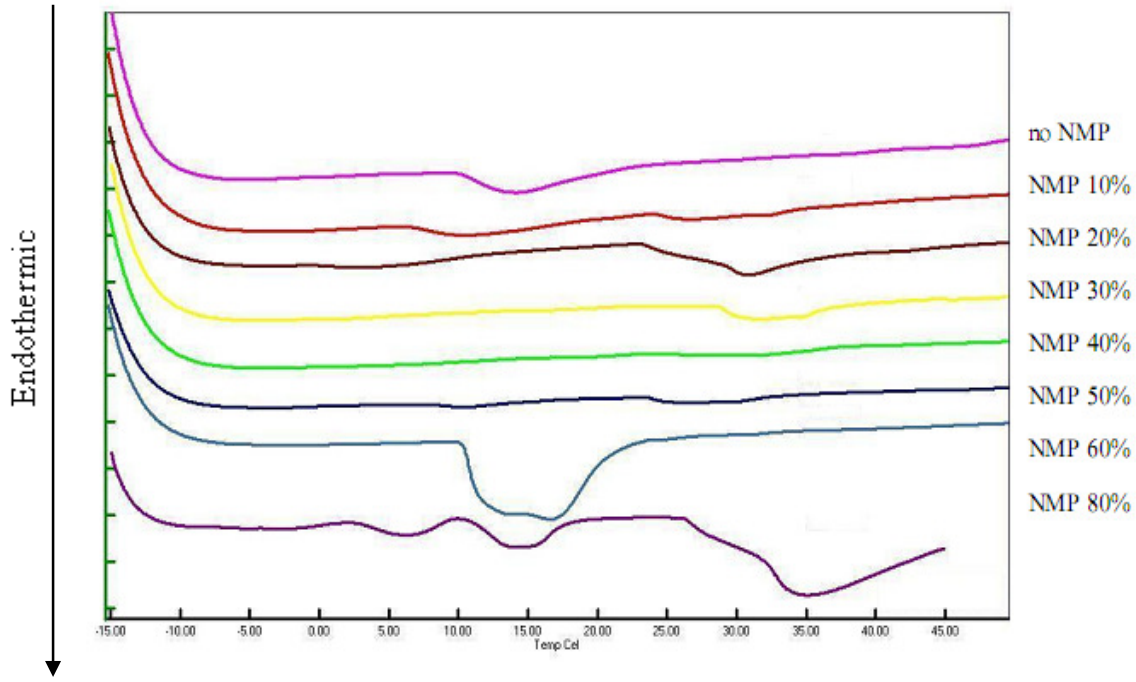

Figure 22 DSC thermograms of sytems contains 20%w/w Lutrol® F 127 gel and different concentrations of *N*-methyl-2-pyrrolidone with heat rate of 5°C/min

3. Effect of zinc oxide and doxycycline hyclate on gel properties

3.1 The influence of amount of zinc oxide on gel properties

3.1.1 The appearance of gels containing ZnO

ZnO BP (0, 1, 5 and 10%w/w) was incorporated into the 20%w/w Lutrol® F127 system. The appearance of the 20%w/w Lutrol® F127 gels was clear. The systems containing ZnO were cloud white gels. The homogeneous of systems were increased with the increased amount of ZnO**.**

3.1.2 The pH of gels containing ZnO

The pH values of gels containing different amount of ZnO BP with or without NMP are shown in Table 14. The pH of the gel bases with or without 20% NMP were 6.59 $\pm$ 0.02 and 6.54 $\pm$ 0.01, respectively. The pH values of all gels with ZnO were in the range of 7.43 - 7.70 which were higher than that of the gel bases (6.54 - 6.59). The pH of the prepared gel containing 20%w/w NMP were slightly lower than that of system without NMP. Therefore the pH value of gels was influenced with an addition of ZnO. Physically, the pH of ZnO was practically neutral (Remington 2000, pp. 1207).

Table 14 pH of Lutrol® F127 gel containing different amount of zinc oxide BP with or without *N*-methyl-2-pyrrolidone (n=3)

	pH									
Amount of	without NMP					20% NMP				
ZnO BP (%w/w)	1	2	3	Mean	S.D.	1	2	3	Mean	S.D.
0	6.57	6.61	6.58	6.59	0.02	6.54	6.53	6.55	6.54	0.01
1	7.61	7.74	7.75	7.70	0.08	7.43	7.44	7.46	7.44	0.02
5	7.48	7.53	7.55	7.52	0.04	7.48	7.40	7.42	7.43	0.04
10	7.46	7.54	7.50	7.50	0.04	7.44	7.46	7.50	7.47	0.03

3.1.3 The gelation and gel melting temperature of gels containing various amount of ZnO

The effect of amount of zinc oxide on the gelation and the gel melting temperature are shown in Figure 23 and Table 15. Incorporation of ZnO shifted the sol-gel transition to a lower temperature but the gel-sol transition was shifted to a higher temperature. Gelation point gradually decreased with increasing amount of ZnO. Block copolymer pluronic® F127 gel was mentioned to be formed by H-bonding in the aqueous system, caused by the attraction of the pluronic ether oxygen atom to a proton of water (Maheshwari *et al*., 2006). If the hydrogen bonding was supplemented by adding compounds with a hydroxyl group, the gelation point decreased (Malmsten *et al.,* 1992). Maheshwari *et al*. (2006) found that Aerosil® caused a significant increase in viscosity and a decrease gelation temperature of the 20%w/w Pluronic® F127, whereas the higher amount of the Aerosil® increased the gel structure since it became more closely packed, with the arrangement in a lattice pattern. On the other hand, the disruption of lattice melting of the gel occurred at higher temperature. Pandit *et al*. (2000) reported the effect of salts on Pluronic® F127 solutions. NaCl, Na_2SO_4 and Na_3PO_4 decreased the cmc and cmt of that system, which could be related to the enhanced dehydration of PPO block. The solubility of PPO in water decreased as structure making-salts were added. This decrease in solubility of the PPO block of F127 in water would favor micellization and reduce the cmt.

Therefore, our study that ZnO lowered the gelation temperature of Lutrol® F127 could be suggested to the enhanced dehydration of the PPO block resulting in the micelle formation and micelle entanglement.

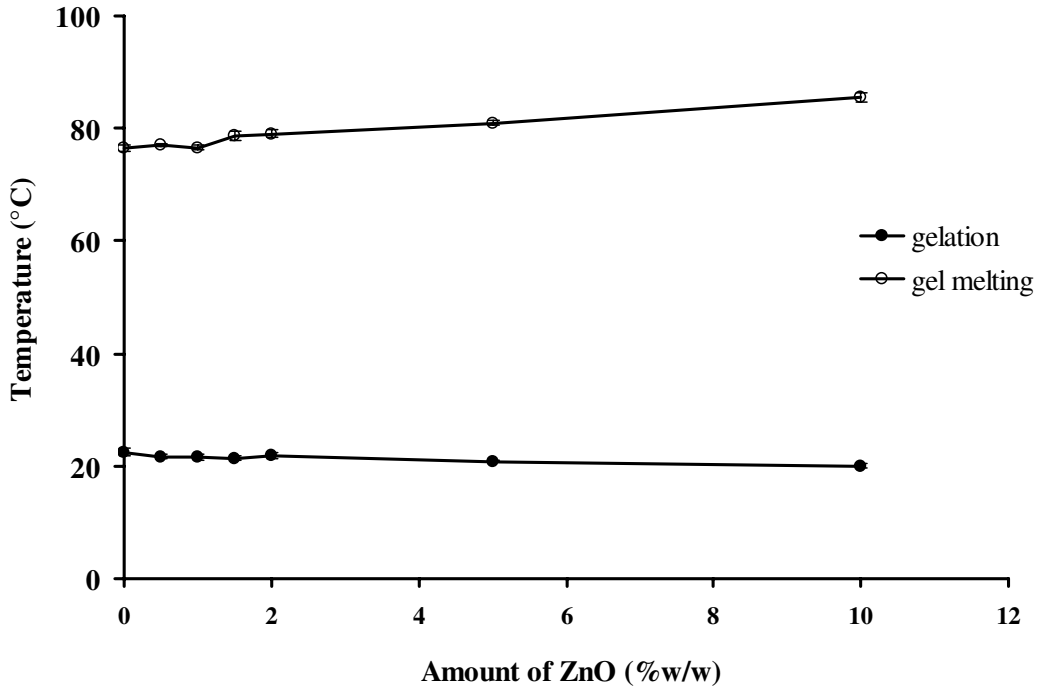

Figure 23 Effect of amount of zinc oxide on gelation and gel melting temperature.

Table 15 Gelation and gel melting temperature of Lutrol® F127 gel containing different amount of zinc oxide (n=3)

Amount of	Gelation temperature (°C)					Gel melting temperature (°C)				
ZnO (%w/w)	1	2	3	Mean	S.D.	1	2	3	Mean	S.D.
0.0	22.0	22.2	23.2	22.5	0.6	76.1	76.5	77.2	76.6	0.6
0.5	21.4	21.6	22.1	21.7	0.4	77.2	77.4	76.8	77.1	0.3
1.0	21.3	21.2	22.1	21.5	0.5	77.0	76.5	76.2	76.6	0.4
1.5	21.2	21.1	22.0	21.4	0.5	77.8	79.1	79.3	78.7	0.8
2.0	21.2	22.2	22.1	21.8	0.6	78.4	79.2	79.6	79.1	0.6
5.0	20.6	21.1	21.0	20.9	0.3	81.5	80.8	80.6	81.0	0.5
10.0	20.3	19.5	20.1	20.0	0.4	85.2	86.5	84.9	85.5	0.9

3.1.4 The rheology of gels containing ZnO

The flow curves of the Lutrol® F127 systems with different amount of zinc oxide at different temperature, 4°C, 27°C and 37°C, are shown in Figures 24, 25 and 26, respectively. Without an incorporation of ZnO, the Lutrol® F127 system was a liquid at 4°C and the flow curves was linear, indicating a Newtonian behavior. Incorporation of ZnO caused an apparent change in the flow curve of the Lutrol® F127 systems. The curves moved to a higher shear stress with the increased ZnO concentration, indicating the compact gel structure. The flow curve also shifted from less shear stress to higher shear stress when the temperature was increased. All systems showed the non-Newtonian flow characteristic at 27°C and 37°C. However, the area of the hysteresis loop did not follow up with an increase in ZnO amount.

The flow parameters of the Lutrol® F127 systems containing different amount of ZnO are shown in Table 16. All gels could not provide a N value greater than unity at 4°C, indicating that the flow type was Newtonian. On the other hand, the N values of all systems were higher than one as the temperature was increased, suggesting that the gel containing ZnO shifted the flow from Newtonian to non-Newtonian as the temperature was enhanced. The viscosity coefficient of systems increased when the temperature was increased. Similar result has been reported for an increased Aerosil® amount that could move the shear stress value of system containing Pluronic® F127 to higher value (Maheshwari *et al*., 2006). The increased shear stress value with the enhanced amount of ZnO indicated the higher compact structure of the gels in this experiment. The apparent viscosity of the gels were increased with the concentration of lecithin has been reported previously (Bentley *et al*., 1999). Such behaviour could be as a result of a decrease in the amount of the water in the formulation, resulting from the addition of lecithin. The increase of the concentration of lecithin increased the hysteresis area, indicating that it enhanced the thixotropic properties of the poloxamers gels.

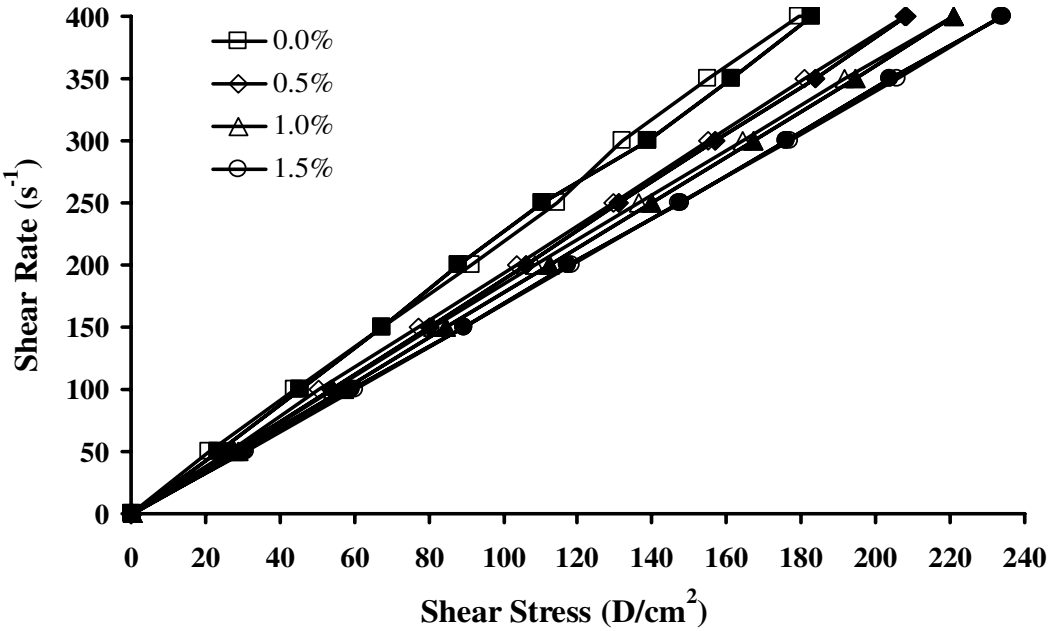

Figure 24 Flow curve of Lutrol® F127 system containing different amount of ZnO BP at 4°C. Open symbols represent the up-curve, and closed symbols represent the down-curve.

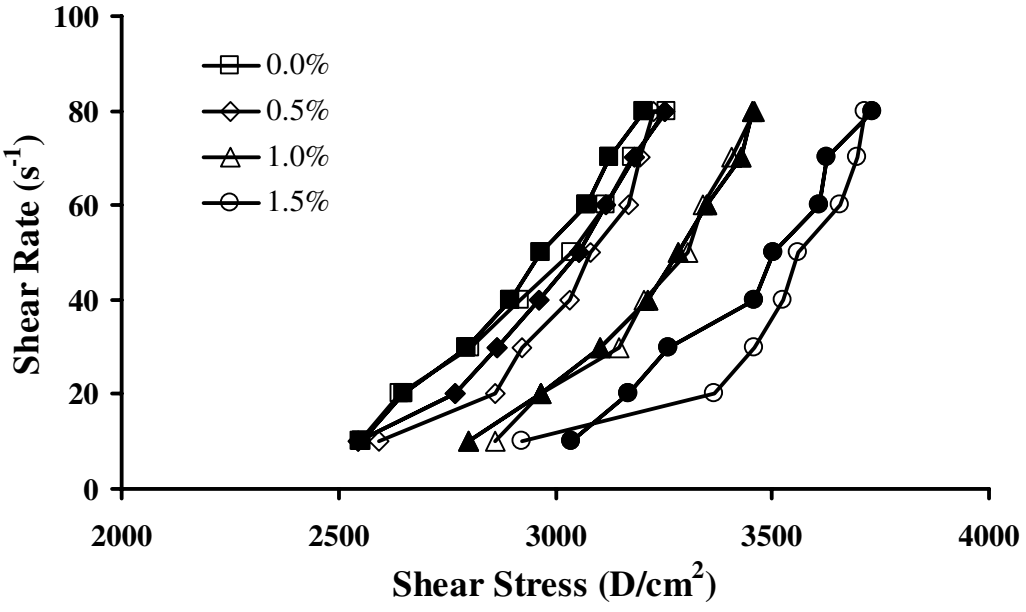

Figure 25 Flow curve of Lutrol® F127 system containing different amount of ZnO BP at 27°C. Open symbols represent the up-curve, and closed symbols represent the down-curve.

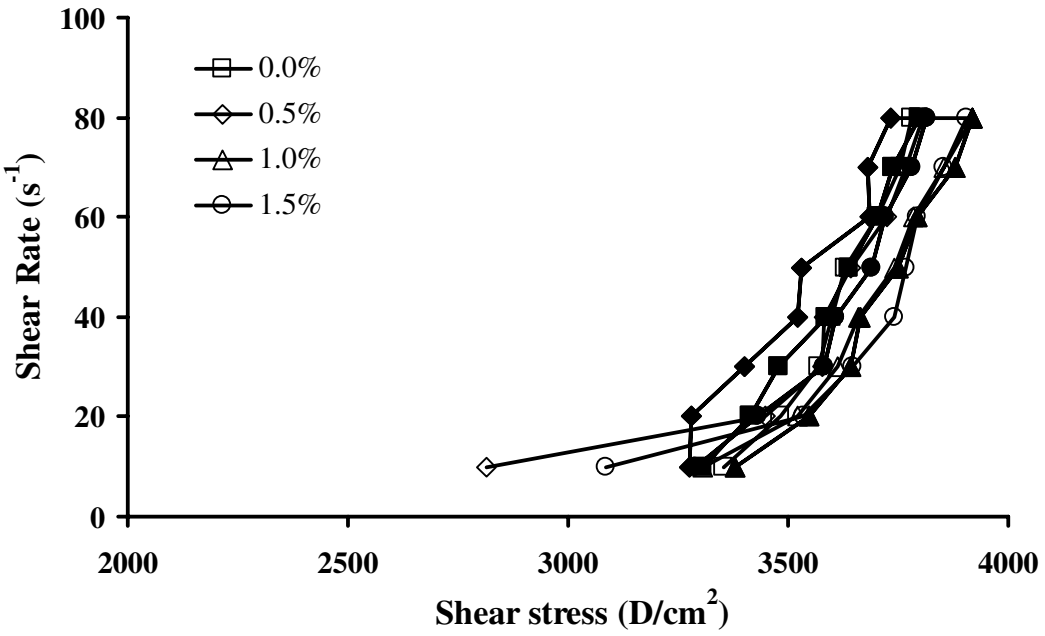

Figure 26 Flow curve of Lutrol® F127 system containing different amount of ZnO BP at 37°C. Open symbols represent the up-curve, and closed symbols represent the down-curve.

Table 16 Flow parameters of Lutrol® F127 aqueous gel containing different amount of zinc oxide at 4°C 27°C and 37°C (n=3)

Lutrol® F127 system						
Amount of	4°C		27°C		37°C	
ZnO BP (% w/w)	N (mean±S.D.)	Viscosity Coefficient (mean±S.D., $[D/cm^2]^N$ s)	N (mean±S.D.)	Viscosity Coefficient (mean±S.D., $[D/cm^2]^N$ s)	N (mean±S.D.)	Viscosity Coefficient (mean±S.D., $[D/cm^2]^N$ s)
0	0.98 ± 0.01	-0.39 ± 0.02	9.61 ± 1.72	31.65 ± 5.96	11.99 ± 1.42	41.13 ± 5.15
0.5	0.99 ± 0.01	-0.30 ± 0.02	9.36 ± 0.64	31.27 ± 2.29	7.95 ± 1.14	26.71 ± 4.10
1	1.00 ± 0.01	-0.26 ± 0.01	9.18 ± 1.08	30.59 ± 3.80	15.03 ± 2.23	51.96 ± 7.90
1.5	1.05 ± 0.02	-0.13 ± 0.04	6.93 ± 3.47	22.68 ± 12.28	8.99 ± 0.76	30.43 ± 2.69

3.2 The influence of doxycycline hyclate concentration on gel properties

3.2.1 The appearance of gels containing doxycycline hyclate

The 20%w/w Lutrol® F127 systems containing different concentrations of doxycycline hyclate were prepared. The prepared gels containing doxycycline hyclate were yellowish and transparent. The color was increased as the doxycycline hyclate concentration increased. The system contained the doxycycline hyclate ≥ 7.5%w/w exhibited the undissolved drug crystals in this systems after storage in the refrigerator (4°C). The previous study found that the undissolved drug crystals were formed in the Lutrol system containing ≥ 9%w/w tetracycline HCl (Maheshwari *et al*., 2006).

3.2.2 The pH of gels containing doxycycline hyclate

The effect of doxycycline hyclate on the pH values of Lutrol® F127 gels are shown in Table 17. The pH value of the gel base containing 20%w/w Lutrol® F127 was 6.0 ± 0.1. While the pH value of 1%w/v doxycycline hyclate in water was 2.23 ± 0.06. The pH values of all systems were between 2.9 ± 0.0 to 3.2 ± 0.1. It was obvious that the pH values of the systems were reduced after addition of doxycycline hyclate due to the acid property of this drug.

Table 17 pH of Lutrol® F127 gel containing different concentrations of doxycycline hyclate (n=3)

Amount of Doxycycline hyclate (%w/w)	pH				
	1	2	3	Mean	S.D.
0.0	5.89	5.92	6.06	5.96	0.09
2.5	3.20	3.23	3.26	3.23	0.03
5.0	3.13	3.22	3.22	3.19	0.05
7.5	2.93	2.98	3.01	2.97	0.04
10.0	2.85	2.88	2.94	2.89	0.05

3.2.3 The gelation and gel melting temperature of gels containing doxycycline hyclate

The gelation temperature and gel melting temperature were gradually increased as the amount of doxycycline hyclate was increased (Figure 27 and Table 18). Recently, many studies reported that there were many factors affecting on the gelation temperature of Lutrol such as drug, menthol, vitamin B12 and sorbitol (Yong *et al*., 2004; Pisal *et al*., 2004; Scherlund *et al*., 2000). Ibuprofen increased the gelation temperature (Yong *et al*., 2004), whereas lidocaine and prilocaine, menthol, inorganic salts, vitamin B12 and sorbitol decreased the gelation temperature of poloxamer gel (Pisal *et al*., 2004; Scherlund *et al*., 2000). Sodium dodecylsulfate was known to increase the gelling point due to micellar solubilization (Vednere *et al.,* 1984). Alcohol also increased the gelling point due to a disruption of the hydration sphered presumably around the hydrophobic portion of the poloxamer (Bahadur, 1993). Most of flavors increased the viscosity of the poloxamer aqueous solution and decreased the gelling point of poloxamer 407 aqueous solution in proportion to the addition of flavor amount. The flavors might bind to the hydrophilic end chains of poloxamer, promoting dehydration and causing gelation of the polymer solution at lower temperatures (Rhee *et al.,* 2006).

Therefore, it was obvious that the hydroxyl groups on doxycycline hyclate might form hydrogen bonding with Lutrol® F127, which it might disrupt the hydration sphere around the hydrophobic portion of the poloxamer and then increased the gelling point similar to that of alcohol and sodium dodecylsulfate did (Bahadur, 1993; Vednere *et al.,* 1984).

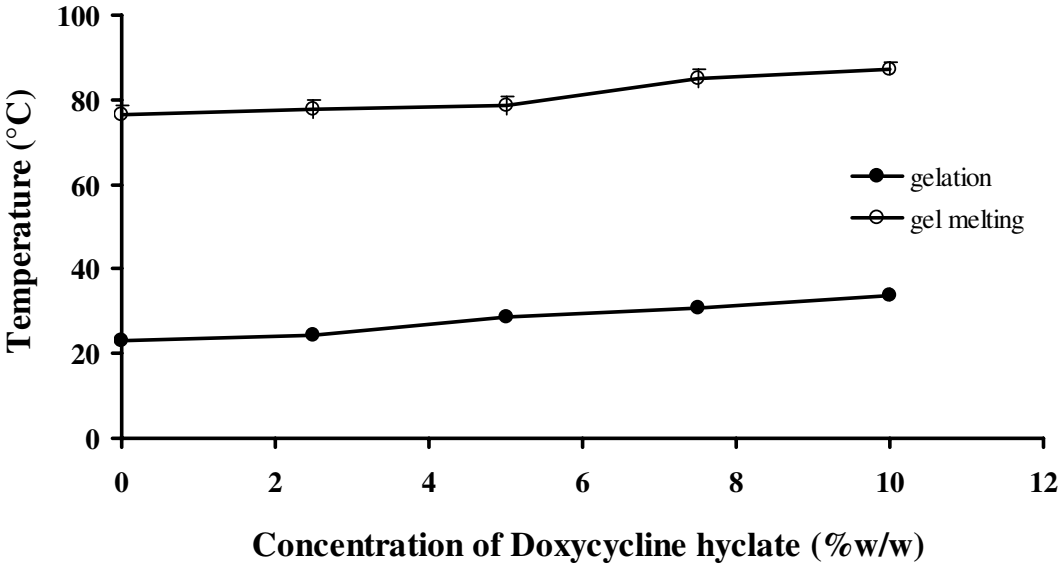

Figure 27 Effect of doxycycline hyclate on gelation and gel melting temperature of systems comprising 20%w/w Lutrol® F127

Table 18 Gelation and gel melting temperature of Lutrol® F127 systems containing different concentrations of doxycycline hyclate (n=3)

Concentration of	Gelation temperature (°C)					Gel melting temperature (°C)				
Doxycycline (%w/w)	1	2	3	Mean	S.D.	1	2	3	Mean	S.D.
0	23.0	23.0	23.0	23.0	0.0	79.0	76.0	74.6	76.5	2.2
2.5	23.5	24.0	25.4	24.3	1.0	80.0	76.0	77.0	77.7	2.1
5	27.5	29.1	28.8	28.5	0.9	81.0	77.0	78.2	78.7	2.1
7.5	30.0	31.7	30.8	30.8	0.9	87.6	83.9	84.0	85.2	2.1
10	33.0	35.6	33.1	33.9	1.5	89.0	86.0	87.0	87.3	1.5

3.2.4 The rheology of gels containing doxycycline hyclate

The flow curves of the Lutrol® F127 gels containing doxycycline hyclate at different temperatures, 4°C, 27°C and 37°C, are shown in Figures 28, 29 and 30, respectively. The incorporation of doxycycline hyclate caused an apparent change in the flow curve of the Lutrol® F127 gels. The flow curve shifted from low shear stress to higher shear stress when the temperature was increased from 4 to 37°C. Increase in amount of doxycycline hyclate shifted of flow curve from low to high at 4 and 37°C. In contrast, the flow curve shifted from high shear stress to lower shear stress when the concentration of doxycycline hyclate was increased at 27°C. The results suggested that the gel structures at this condition were less compact. Particularly, at 27°C, the flow of the prepared gels with doxycycline hyclate < 5%w/w were Newtonian characteristic whereas that systems containing doxycycline hyclate ≥ 5%w/w were non-Newtonian characteristic. The flow parameters of Lutrol® F127 gels containing different concentrations of doxycycline hyclate at 4°C, 27°C and 37°C are listed in Table 19. The N values of all gels were near to 1 at 4°C indicating a Newtonian flow characteristic. Meanwhile, the obtained N values of all gels were > 1 at 37°C, indicating the non-Newtonian flow of all gels. Moreover, the N values of the prepared gel containing doxycycline hyclate less than 5%w/w were > 1 at 27°C but the N values of the others gels were near to 1. These results were correlated with the apparent state of the prepared gels containing 5%w/w doxycycline hyclate that was a liquid at 4 and 27°C, and a solid at 37°C. Therefore the viscosity coefficient (η) of the systems containing doxycycline hyclate was apparently increased when the temperature was increased to 37°C.

The flow curves of the Lutrol® F127 gels containing different concentrations of doxycycline hyclate with 20%w/w NMP at 4°C, 27°C and 37°C**,** are shown in Figures 31, 32 and 33, respectivly. The 20%w/w of NMP changed the shear stress. The flow curves of the Lutrol® F127 systems containing different doxycycline hyclate with 20%w/w NMP shifted to more shear rate when the 20%w/w NMP was added. At 27°C, the flow curve shifted from high shear stress to lower shear stress when the concentration of doxycycline hyclate was increased as well as the prepared systems without NMP. The flow curves of the prepared gels containing 10%w/w doxycycline hyclate was Newtonian flow, whereas the systems containing doxycycline hyclate < 10%w/w indicated the non-Newtonian characteristic. The flow curve of all gel systems were

shifted to high shear stress as the temperature was increased. The flow parameters of Lutrol® F127 gels containing different concentrations of doxycycline hyclate with 20%w/w NMP at 4°C, 27°C and 37°C, are listed in Table 20. The N values of all gels were close to 1 at 4°C, indicating a Newtonian flow characteristic. Meanwhile, the N values of all gels were > 1 at 37°C, signified the non-Newtonian flow. Moreover, at 27°C, the N values of the prepared gel containing doxycycline hyclate higher than 7.5%w/w were closed to 1 but the N values of gels containing doxycycline hyclate ≤ 5%w/w were greater than 1. The viscosity coefficient (η) of the systems containing doxycycline hyclate notably increased when the temperature was increased to 37°C.

Thus the doxycycline hyclate amounts were added into the system affecting the strength of gel structure. The decreasing strength of gel structure was evident as the doxycycline hyclate amount was increased. This could be correlated with the previous study (3.2.3) which the gelation temperature were increased for the system containing doxycycline hyclate. The enhancement of the gelation temperature of the poloxamer systems with the doxycycline/HP-β-cyclodextrin complexes has been reported (He *et al.*, 2008).

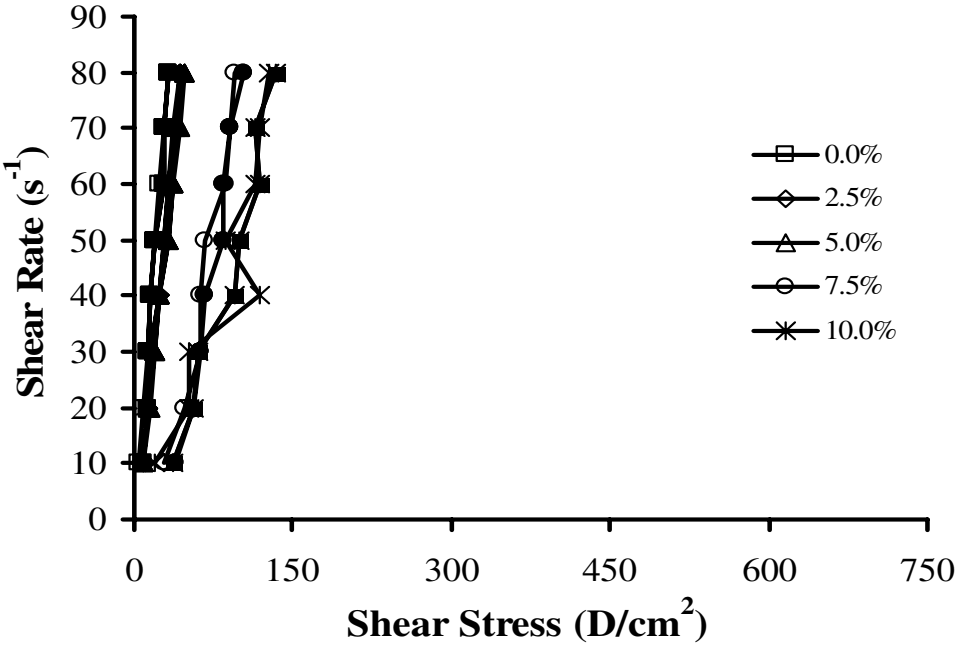

Figure 28 Flow curve of Lutrol® F127 systems containing different concentrations of doxycycline hyclate without NMP at 4°C. Open symbols represent the up-curve, and closed symbols represent the down-curve.

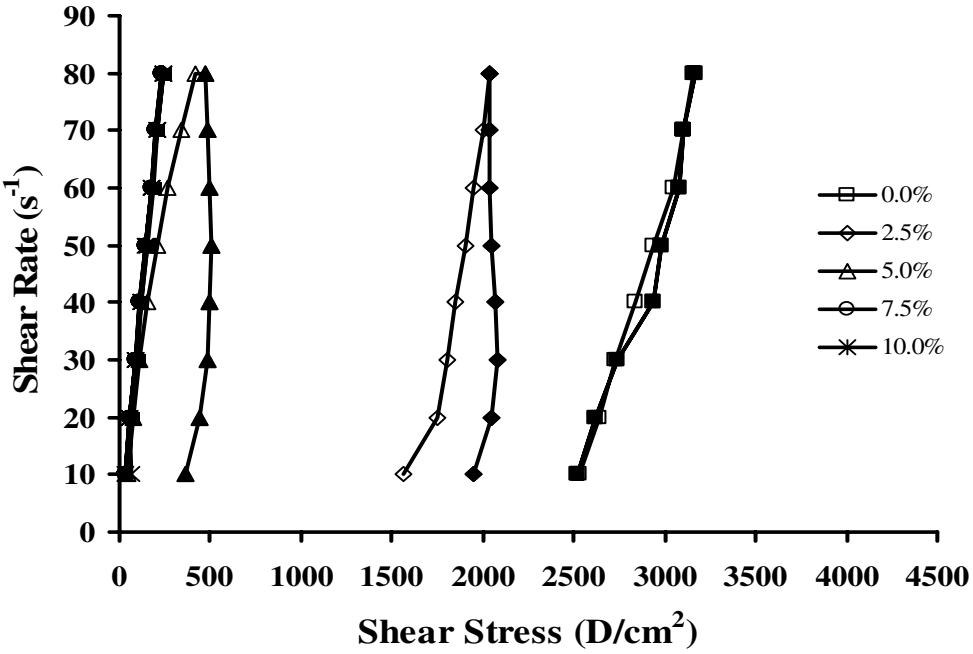

Figure 29 Flow curve of Lutrol® F127 systems containing different concentrations of doxycycline hyclate without NMP at 27°C. Open symbols represent the up-curve, and closed symbols represent the down-curve.

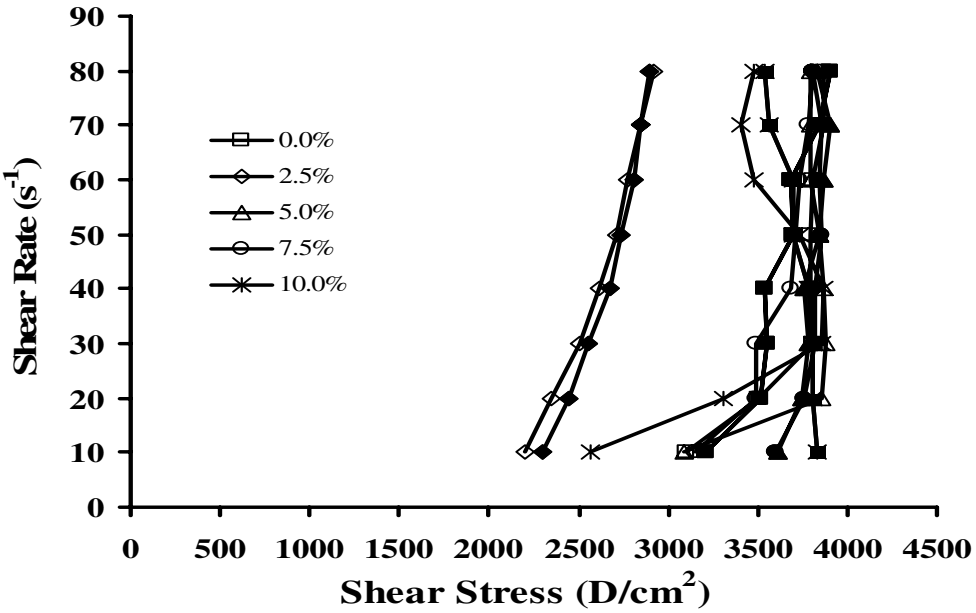

Figure 30 Flow curve of Lutrol® F127 systems containing different concentrations of doxycycline hyclate without NMP at 37°C. Open symbols represent the up-curve, and closed symbols represent the down-curve.

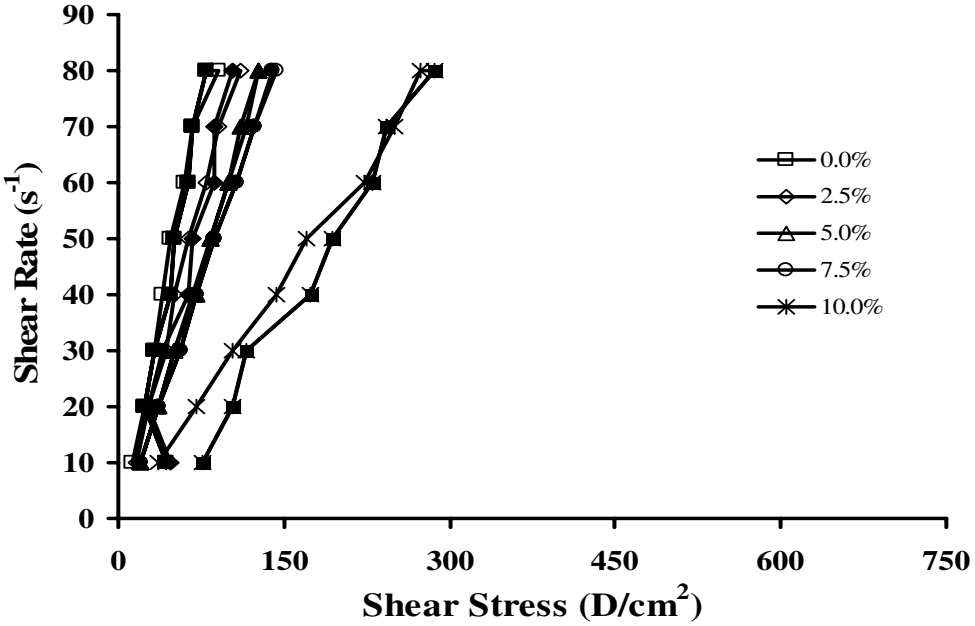

Figure 31 Flow curve of Lutrol® F127 systems containing different concentrations of doxycycline hyclate with 20%w/w NMP at 4°C. Open symbols represent the up-curve, and closed symbols represent the down-curve.

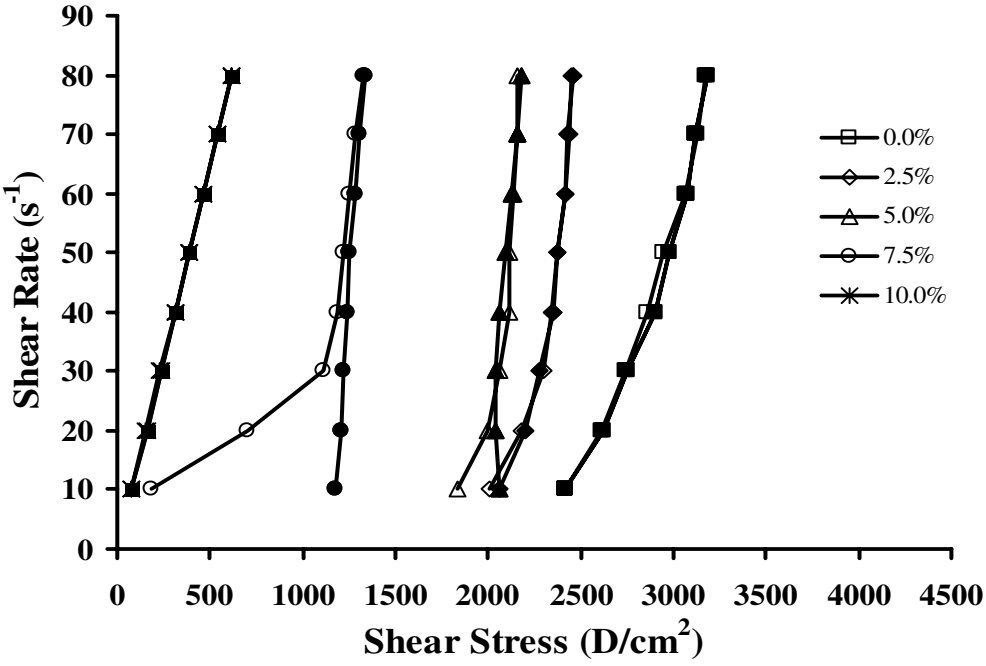

Figure 32 Flow curve of Lutrol® F127 systems containing different concentrations of doxycycline hyclate with 20%w/w NMP at 27°C. Open symbols represent the up-curve, and closed symbols represent the down-curve.

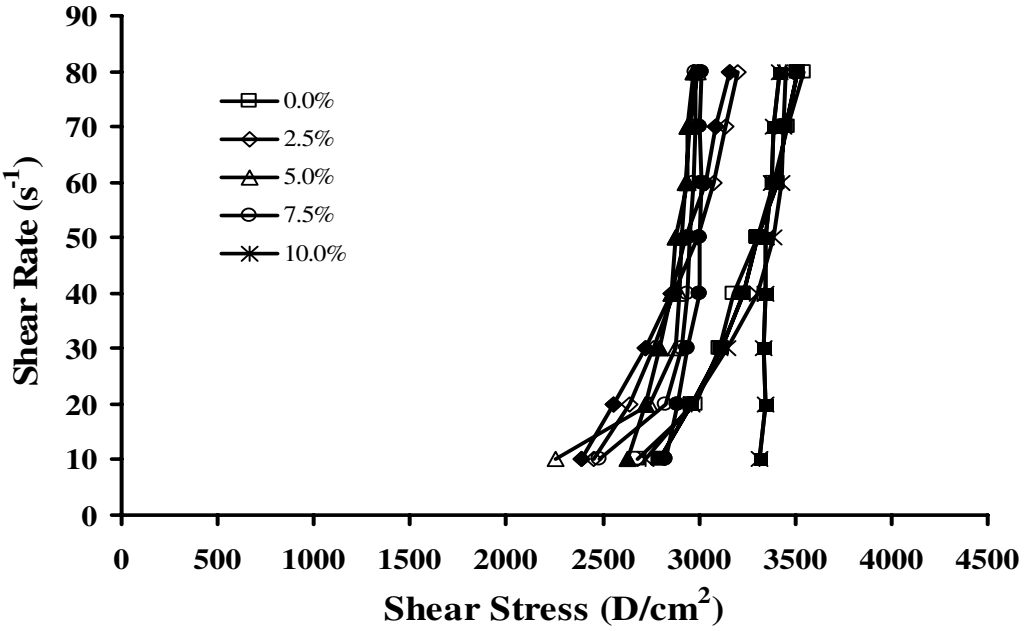

Figure 33 Flow curve of Lutrol® F127 systems containing different concentrations of doxycycline hyclate with 20%w/w NMP at 37°C. Open symbols represent the up-curve, and closed symbols represent the down-curve.

Table 19 Flow parameters of Lutrol® F127 gel containing different doxycycline hyclate without NMP at 4°C 27°C and 37°C (n=3)

Lutrol® F127 gel, without NMP						
Concentration of Doxycycline hyclate (% w/w)	4°C N (mean±S.D.)	4°C Viscosity Coefficient (mean±S.D., $[D/cm^2]^N$ s)	27°C N (mean±S.D.)	27°C Viscosity Coefficient (mean±S.D., $[D/cm^2]^N$ s)	37°C N (mean±S.D.)	37°C Viscosity Coefficient (mean±S.D., $[D/cm^2]^N$ s)
0	1.15 ± 0.27	0.05 ± 0.42	7.76 ± 0.63	25.32 ± 2.16	10.22 ± 0.95	34.85 ± 3.38
2.5	1.12 ± 0.17	-0.11 ± 0.25	9.57± 1.61	29.21 ± 5.17	8.13 ± 0.85	26.08 ± 2.79
5	1.19 ± 0.13	-0.13 ± 0.19	0.72 ± 0.15	0.17 ± 0.26	6.69 ± 0.36	22.16 ± 1.20
7.5	1.56 ± 0.18	1.02 ± 0.64	1.00 ± 0.04	0.49 ± 0.10	9.39 ± 1.88	31.84 ± 6.73
10	1.00 ± 0.07	0.32 ± 0.16	1.10 ± 0.14	0.72 ± 0.29	6.51 ± 4.21	21.16 ± 14.45

Table 20 Flow parameters of Lutrol® F127 gel containing different doxycycline hyclate with 20% w/w NMP at 4°C 27°C and 37°C (n=3)

Lutrol® F127 gel contain 20% NMP						
Concentration of	4°C		27°C		37°C	
Doxycycline hyclate (% w/w)	N (mean±S.D.)	Viscosity Coefficient (mean±S.D., $[D/cm^2]^N$ s)	N (mean±S.D.)	Viscosity Coefficient (mean±S.D., $[D/cm^2]^N$ s)	N (mean±S.D.)	Viscosity Coefficient (mean±S.D., $[D/cm^2]^N$ s)
0	1.11 ± 0.03	0.22 ± 0.03	7.47 ± 0.15	24.30 ± 0.50	7.90 ± 0.35	26.26±1.20
2.5	1.07 ± 0.05	0.23 ± 0.12	9.26 ± 0.77	29.57 ± 2.42	7.65 ± 0.09	24.66±0.25
5	1.12 ± 0.01	0.44 ± 0.01	11.48 ± 1.19	36.32 ± 4.17	7.15 ± 1.32	23.06±4.29
7.5	1.17 ± 0.19	0.69 ± 0.47	1.00 ± 0.11	1.39 ± 0.35	9.32 ± 1.26	30.86±4.22
10	1.06 ± 0.05	0.65 ± 0.08	1.01 ± 0.02	0.92 ± 0.10	7.84 ± 0.24	25.76±1.09

3.3 The influence of ZnO and doxycycline hyclate amounts on gel properties

3.3.1 The appearance of doxycycline hyclate gels containing ZnO

The 20%w/w Lutrol® F127 system containing 5%w/w doxycycline hyclate, with or without 20%w/w NMP were a yellowish clear system. The doxycycline hyclate-Lutrol® F127 systems containing ZnO were opaque yellowish incompatible gel, whereas the doxycycline hyclate-Lutrol® F127 systems with 20%w/w NMP were homogeneous opaque yellowish gel.

3.3.2 The pH of doxycycline hyclate gels containing ZnO

The pH value of Lutrol® F127 gel containing 5%w/w doxycycline hyclate containing different amount of ZnO with or without NMP were measured and results were shown in Figure 34 and Table 21. The pH value of 5%w/w doxycycline hyclate gel with or without 20%w/w NMP were 3.21 $\pm$ 0.04 and 3.18 $\pm$ 0.04, respectively. The addition of ZnO into the doxycycline hyclate-Lutrol F127® gel enhanced the pH value of the prepared gel, whereas the effect of NMP on the pH value of doxycycline hyclate gels was quite slightly thus an addition of ZnO influenced the pH value of the systems.

Table 21 pH of Lutrol® F127 gel containing 5% w/w doxycycline hyclate and different amount of zinc oxide BP with or without NMP (n=3)

	pH									
Amount of	without NMP					20% NMP				
ZnO BP (%w/w)	1	2	3	Mean	S.D.	1	2	3	Mean	S.D.
0	3.16	3.15	3.22	3.18	0.04	3.22	3.16	3.24	3.21	0.04
0.5	3.29	3.23	3.25	3.26	0.03	3.34	3.36	3.40	3.37	0.03
1	4.53	4.35	4.41	4.43	0.09	4.66	4.65	4.70	4.67	0.03
1.5	4.61	4.63	4.49	4.58	0.08	4.63	4.62	4.65	4.63	0.02
2	4.90	4.93	4.70	4.84	0.13	4.68	4.59	4.69	4.65	0.06

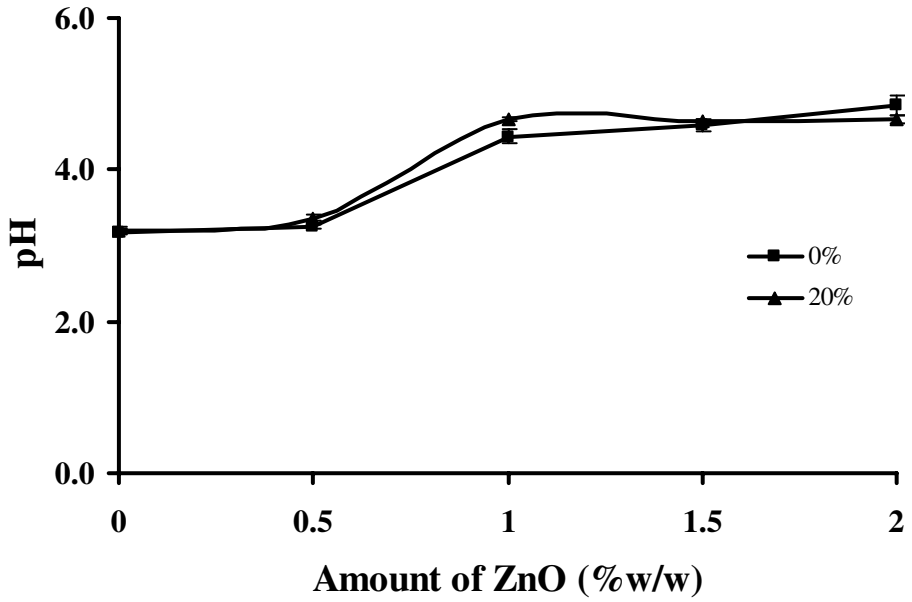

Figure 34 Effect of amount of ZnO BP on the pH of Lutrol® F127 gel containing 5%w/w doxycycline hyclate with or without 20%w/w NMP (n=3).

3.3.3 The gelation and gel melting temperature of 5% w/w doxycycline hyclate gels containing ZnO

The Lutrol® F127 (20%w/w) containing doxycycline hyclate (5%w/w), NMP (20% w/w) and various ZnO amounts were prepared. The effect of ZnO on sol-gel transition is shown in Figure 35. Incorporation of ZnO into the doxycycline hyclate-Lutrol® F127 systems with 20%w/w NMP shifted sol-gel transition to a lower temperature. The doxycycline hyclate-Lutrol® F127 systems comprising ZnO without NMP were gel state even at low temperature, thus the sol-gel transition temperature were not found.

Maheshwari *et al*. (2006) reported that the concentration of the Aerosil® increased, the gel structure became more closely packed, with the arrangement in a lattice pattern. It was obvious that the sol-gel transition temperature of this system decreased as the amount of was ZnO increased therefore, the gel structure became more closely packed and increased dehydration of PPO block as same as the previous studies (3.1.3).

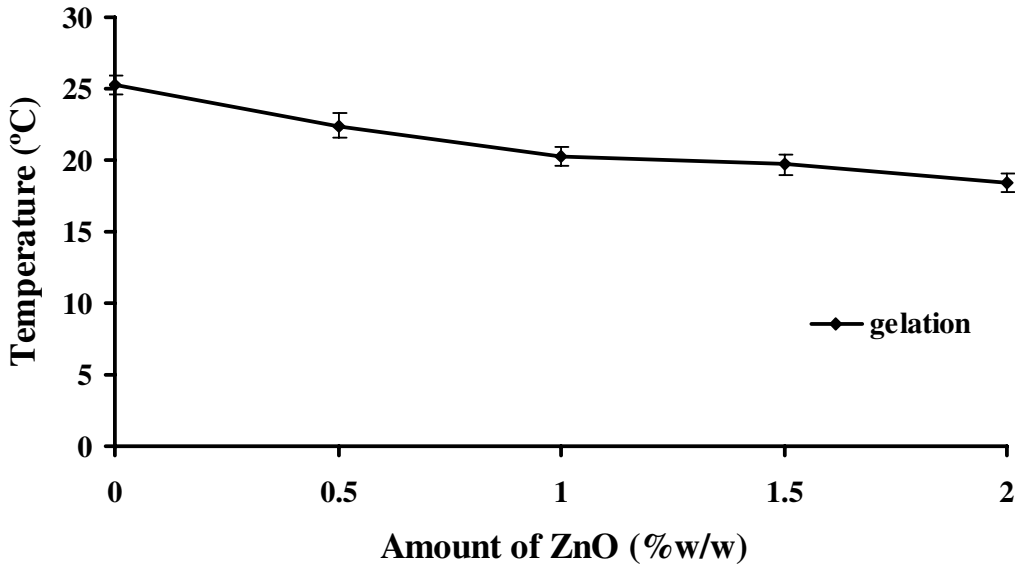

Figure 35 Gelation temperature of Lutrol® F127 gel containing 5%w/w doxycycline hyclate and 20%w/w NMP different amount of zinc oxide (n=3)

Table 22 Gelation and gel melting temperature of Lutrol® F127 gel containing 5%w/w doxycycline hyclate and 20%w/w NMP different amount of zinc oxide (n=3)

Amount of	Gelation temperature (°C)				
ZnO BP(%w/w)	1	2	3	Mean	S.D.
0.0	24.6	25.4	25.9	25.3	0.7
0.5	22.3	21.6	23.3	22.4	0.9
1.0	19.6	20.3	20.9	20.3	0.7
1.5	19.1	19.5	20.5	19.7	0.7
2.0	18.9	17.7	18.6	18.4	0.6

3.3.4 The rheology of doxycycline hyclate gels containing ZnO

The 20%w/w Lutrol® F127, 5%w/w doxycycline hyclate without NMP and different amount of ZnO were prepared. The flow curves of the prepared gels at different temperature, 4°C, 27°C and 37°C are shown in Figures 36, 37 and 38, respectively. The flow curve of the systems was changed which depended on the amount of the incorporated ZnO. The flow curve of the prepared gel containing ZnO ≥ 1%w/w could not be investigated because the viscosity was to high to measure. The flow curve of the prepared gels without ZnO was Newtonian flow at 4°C. The flow curve shifted from low shear stress to higher shear stress along the temperature increased and higher amount of added ZnO, indicating non-Newtonian flow. The flow parameters of the doxycycline hyclate-Lutrol® F127 gels containing ZnO without NMP at 4°C, 27°C and 37°C are listed in Table 23. The N values of the doxycycline hyclate-Lutrol® F127 gels without ZnO was 1 at 4°C indicating a Newtonian flow characteristic. Meanwhile, the obtained N values of the doxycycline hyclate-Lutrol® F127 gels containing ZnO were > 1 at all temperatures, indicating a non-Newtonian flow. The viscosity coefficient (η) of the doxycycline hyclate-Lutrol® F127 systems were increased with an increase in temperature and amount of ZnO incorporation.

The flow curves of the Lutrol® F127 gels containing 5%w/w doxycycline hyclate, 20%w/w NMP with various amount of ZnO at 4°C, 27°C and 37°C are shown in Figures

39, 40 and 41, respectively. The addition of NMP into the systems containing ZnO resulted to decrease the viscosity of the system. The flow curve shifted from low shear stress to higher shear stress as the temperature was increased and ZnO was added, indicating a non-Newtonian flow. However, the area of hysteresis loop were not increased as the amount of ZnO were increased, indicating that it did not enhance the thixotropic properties of the systems. However, the thixotropic properties of poloxamer gel has been previously reported. The increased lecithin concentration enhanced the hysteresis area of the poloxamer gels that the thixotropic properties of the poloxamer gels were enhanced (Bentley *et al*., 1999). Maheshwari *et al*. (2006) found that the area of the hysteresis loop increased with the concentration of Aerosil® and tetracycline and the recovery of the consistency was slow when there were higher amounts of Aerosil® and tetracycline.

The flow parameters of Lutrol® F127 gels containing 5%w/w doxycycline hyclate, 20%w/w NMP and different amount of ZnO at 4°C, 27°C and 37°C are listed in Table 24. The obtained N values of all gels were closed to 1 at 4°C indicating a Newtonian flow characteristic. Meanwhile, the N values of all gels were > 1 at 27°C and 37°C, indicating a non-Newtonian flow. The viscosity coefficient (η) of all systems was notably increased when the temperature was increased.

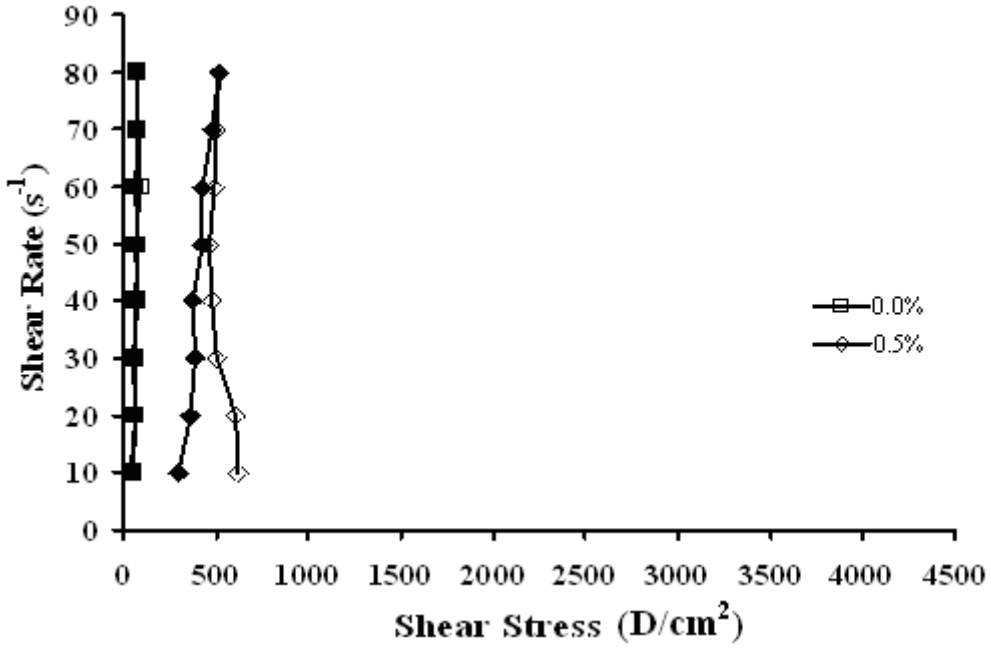

Figure 36 Flow curve of 5%w/w doxycycline hyclate systems containing 0.5%w/w ZnO without NMP at 4°C. Open symbols represent the up-curve, and closed symbols represent the down-curve.

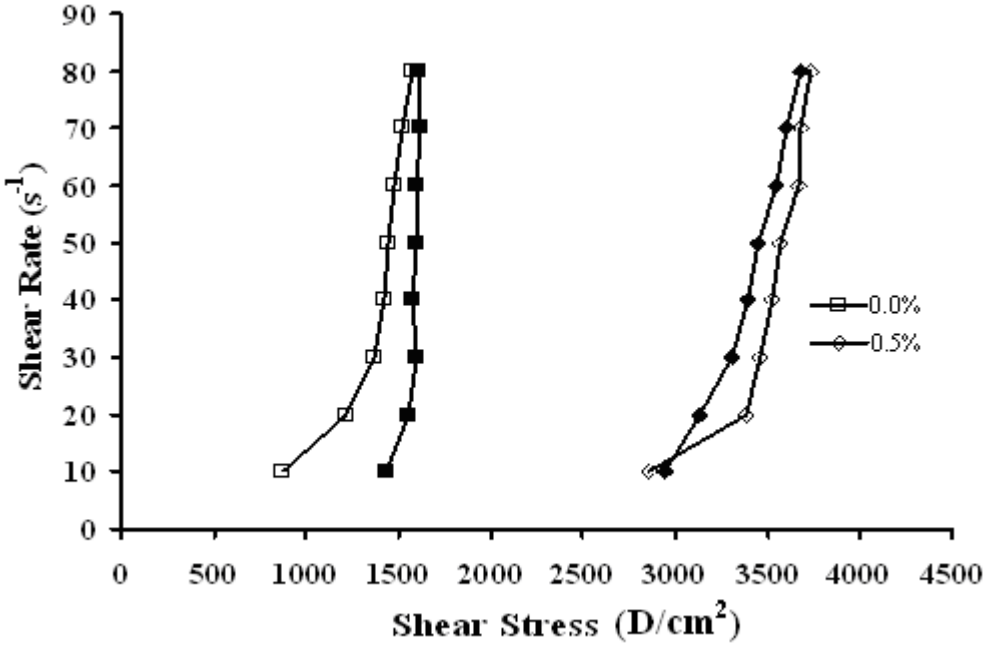

Figure 37 Flow curve of 5%w/w doxycycline hyclate system containing 0.5%w/w ZnO and without NMP at 27°C. Open symbols represent the up-curve, and closed symbols represent the down-curve.

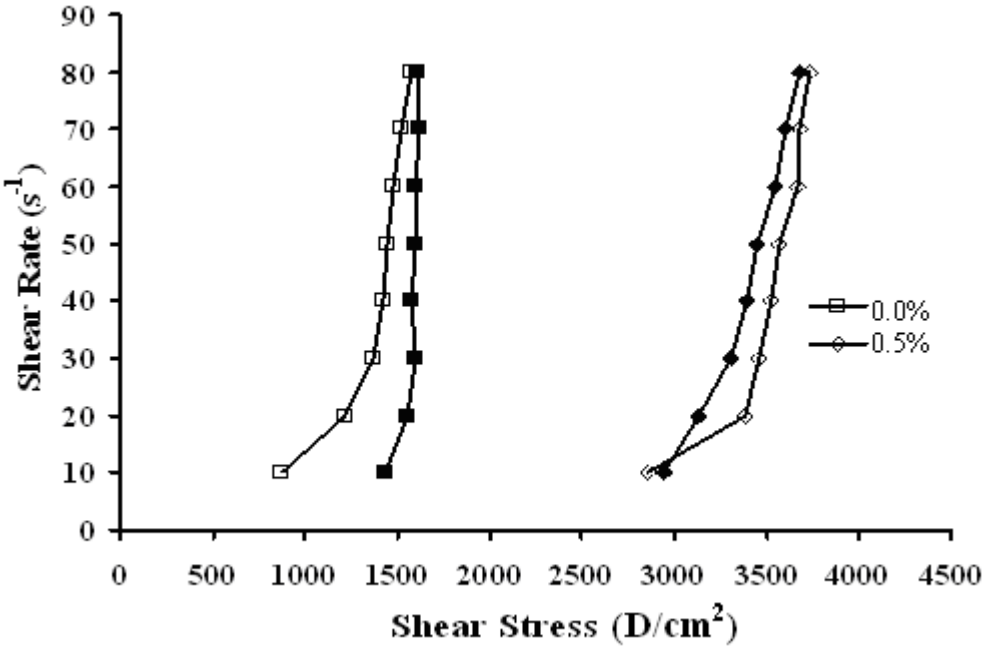

Figure 38 Flow curve of 5%w/w doxycycline hyclate system containing 0.5%w/w ZnO and without NMP at 37°C. Open symbols represent the up-curve, and closed symbols represent the down-curve.

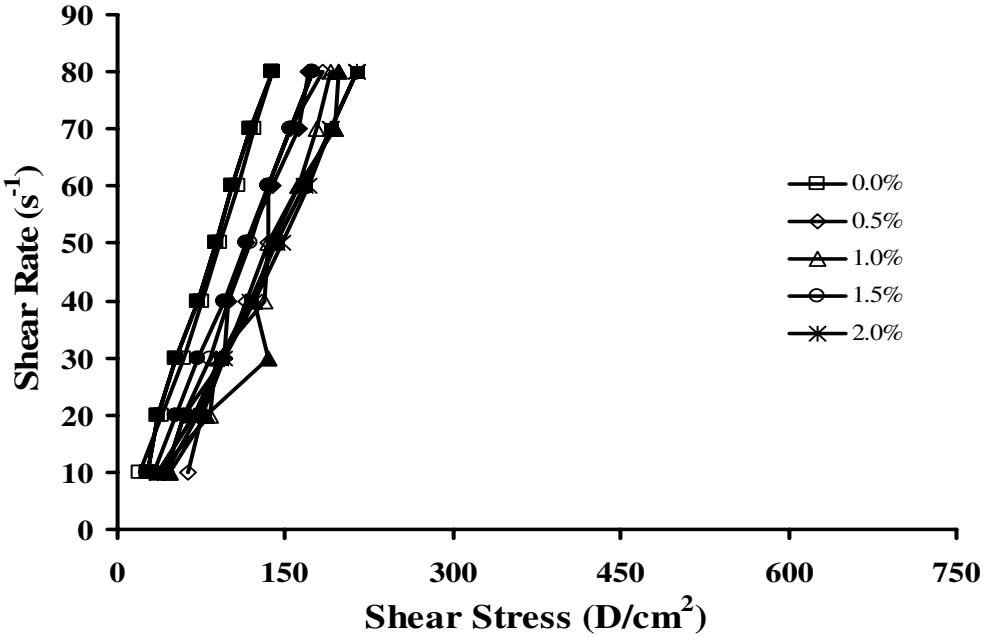

Figure 39 Flow curve of doxycycline hyclate system containing different amount of ZnO with 20%w/w NMP at 4°C. Open symbols represent the up-curve, and closed symbols represent the down-curve.

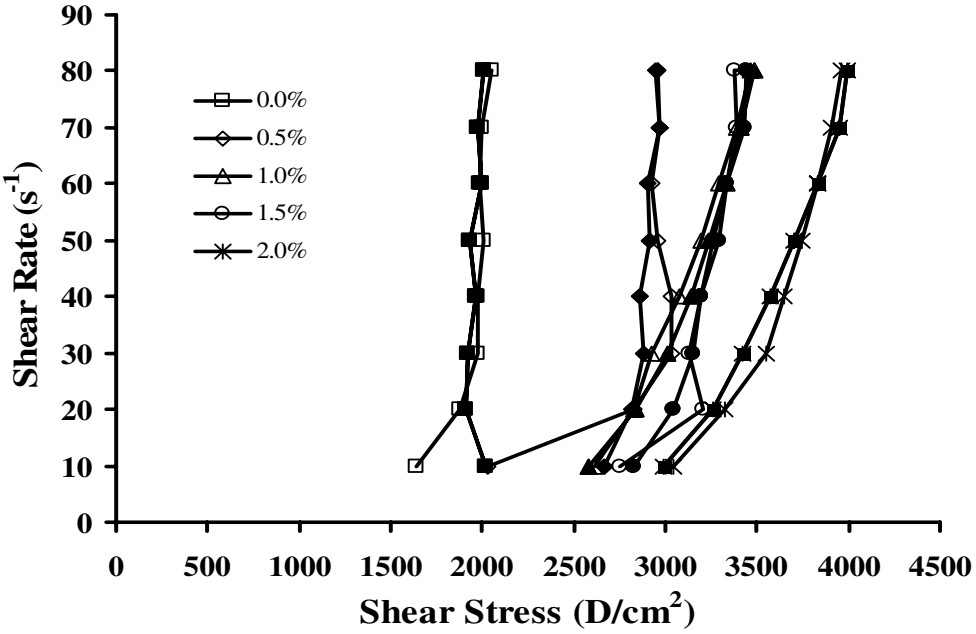

Figure 40 Flow curve of doxycycline hyclate system containing different amount of ZnO with 20%w/w NMP at 27°C. Open symbols represent the up-curve, and closed symbols represent the down-curve.

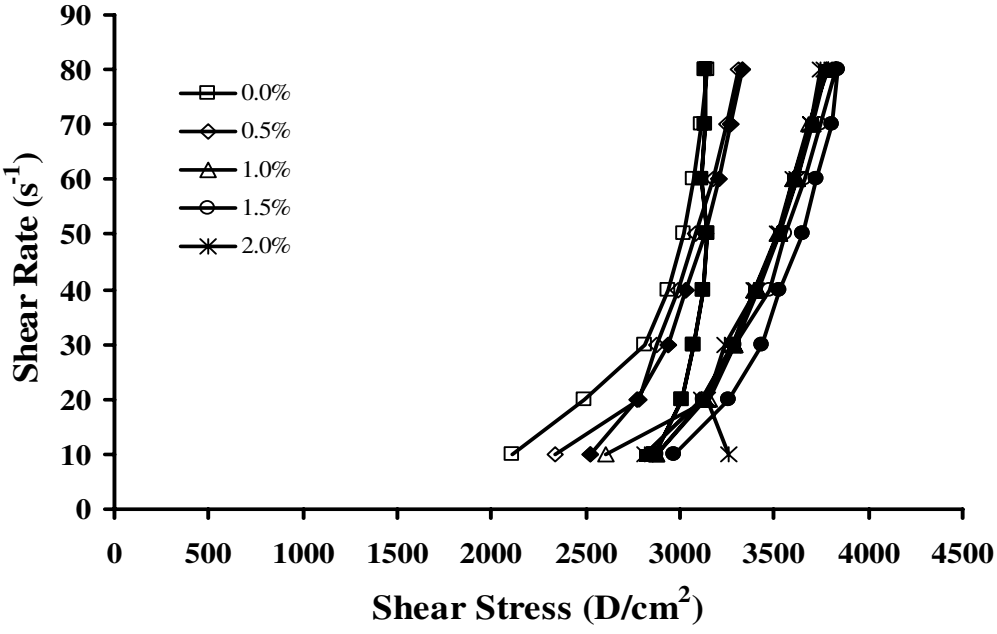

Figure 41 Flow curve of doxycycline hyclate system containing different amount of ZnO with 20%w/w NMP at 37°C. Open symbols represent the up-curve, and closed symbols represent the down-curve.

Table 23 Flow parameters of 5%w/w doxycycline hyclate system containing different amount of ZnO and without NMP at 4°C 27°C and 37°C (n=3)

Lutrol® F127 gel, without NMP						
Concentration of ZnO (% w/w)	4°C		27°C		37°C	
	N (Mean±S.D.)	Viscosity Coefficient (Mean±S.D., $[D/cm^2]^N$ s)	N (Mean±S.D.)	Viscosity Coefficient (Mean±S.D., $[D/cm^2]^N$ s)	N (Mean±S.D.)	Viscosity Coefficient (Mean±S.D., $[D/cm^2]^N$ s)
0	1.00 ± 0.27	2.23 ± 0.39	3.17 ± 0.99	8.37 ± 3.14	7.50 ± 0.95	25.07 ± 7.87
0.5	5.81 ± 0.27	13.27 ± 0.78	6.10 ± 1.51	20.06 ± 5.24	6.55 ± 0.85	21.75 ± 11.45

Table 24 Flow parameters of 5%w/w doxycycline hyclate system containing different amount of ZnO and with 20%w/w NMP at 4°C 27°C and 37°C (n=3)

Lutrol® F127 gel containing 20% NMP						
Amount of ZnO BP (% w/w)	4°C		27°C		37°C	
	N (Mean±S.D.)	Viscosity Coefficient (mean±S.D., $[D/cm^2]^N$ s)	N (Mean±S.D.)	Viscosity Coefficient (mean±S.D., $[D/cm^2]^N$ s)	N (Mean±S.D.)	Viscosity Coefficient (Mean±S.D., $[D/cm^2]^N$ s)
0	1.13 ± 0.03	9.23 ± 1.53	8.36 ± 0.24	28.56±4.89	6.31 ± 1.63	20.38±5.76
0.5	1.64 ± 0.28	4.77 ± 32.56	4.77 ± 1.57	15.08±5.67	6.29 ± 0.18	20.30±0.62
1	1.24 ± 0.06	7.42 ± 0.24	7.42 ± 0.24	24.44±0.91	6.62 ± 0.68	21.86±2.45
1.5	1.35 ± 0.11	8.37 ± 1.08	8.37 ± 1.08	27.77±3.80	7.22 ± 1.01	23.98±3.41
2	1.29 ± 0.06	9.27 ± 1.26	9.27 ± 1.26	23.36±18.25	7.87 ± 1.40	26.32±4.92

4. The antimicrobial activity studies

4.1 Effect of ZnO amount on antimicrobial activity

The growth inhibition of microbes (*S. aureus*, *E. coli* and *C. albicans*) was studied by the direct-exposure method with colony count. The amount of ZnO BP in the range of 5-200 mg/10mL was tested for antimicrobial activity. The inhibition profiles against *S. aureus*, *E. coli* and *C. albicans* of ZnO are shown in Figure 42. At lower concentration of 50 mg/10mL, ZnO BP inhibited the *S. aureus* growth stronger than *C. albicans* and *E. coli*. The concentration of ZnO BP at 5 mg/10mL inhibited *S. aureus* growth about 90%. Approximately 50% growth inhibition were found by both *C. albicans* and *E. coli* in all concentrations. At lower 50 mg/10ml, ZnO BP inhibit *C. albicans* better than *E. coli*. These results indicated that the ZnO could be inhibited all microbes (*S. aureus*, *E. coli* and *C. albicans*). ZnO inhibited about 90% of *S. aureus* growth and

about 50% of *C. albicans* at concentration 5 mg/10ml, whereas ZnO againsted *E. coli* as dose dependent from 0 - 100 mg/10mL ZnO and the highest inhibition was 50% of *E. coli* growth.

Many reports (Yamamoto 2001; Yamamoto *et al.,* 1998; Brayner *et al.,* 2006; Cassanho *et al.,* 2005; Yamamoto and Iida 2003) showed that ZnO could be used as antimicrobial agent. It had been demonstrated that ZnO exhibited antimicrobial activity against *S. aureus* (Yamamoto 2001) and *E. coli* (Yamamoto *et al.,* 1998; Brayner *et al.,* 2006). The antibacterial activity of ZnO increased with the concentration was increased (Yamamoto 2001) which this could correlate to this investigation in anti-*E. coli*. Tam *et al*. (2008) reported that ZnO is more effective for gram-positive than gram-negative bacteria because the formers have simpler cell membrane structure. The antifungal activity was evident in the carbon samples containing ZnO (Yamamoto and Iida 2003). The zinc oxide-eugenol cement was more effective in reducing *Candida* spp. colony count than the glass ionomer cement. The counts of *C. albicans* after treatment with the former were zero after 48 hours (Junior *et al*., 2000; Cassanho *et al.,* 2005), whereas the present study result of the implies that ZnO could inhibited *C. albicans* about 50% after 4 hours. All these results supported that ZnO had antifungal activity.

Many studies suggested that the release of H_2O_2 had been proposed as a mechanism responsible for antibacterial activity (Sawai *et al.,* 1998; Yamamoto 2001; Yamamoto *et al.,* 2004), however it was still not clear yet the antibacterial activity of ZnO could be attributed to the damage of cell membranes, which lead to leakage of cell contents and cell death (Tam *et al.,* 2008). The difference in activity against these two types of bacteria can be attributed to different organization of the cell wall. Gram-positive bacteria typically have one cytoplasmic membrane and thick wall composed of multilayers of peptidogycan (Fu *et al.,* 2005). Gram-negative bacteria have more complex cell wall structure, with a layer of peptidoglycan between outer membrane and cytoplasmic membrane (Fu *et al.,* 2005; Brayner *et al.,* 2006). Therefore, the cell wall membrane of gram-positive bacteria can be damaged more easily. Membrane damage attributed to photocatalytic processes was claimed as the mechanism of antibacterial activity for TiO_2 (Fu *et al*., 2005).

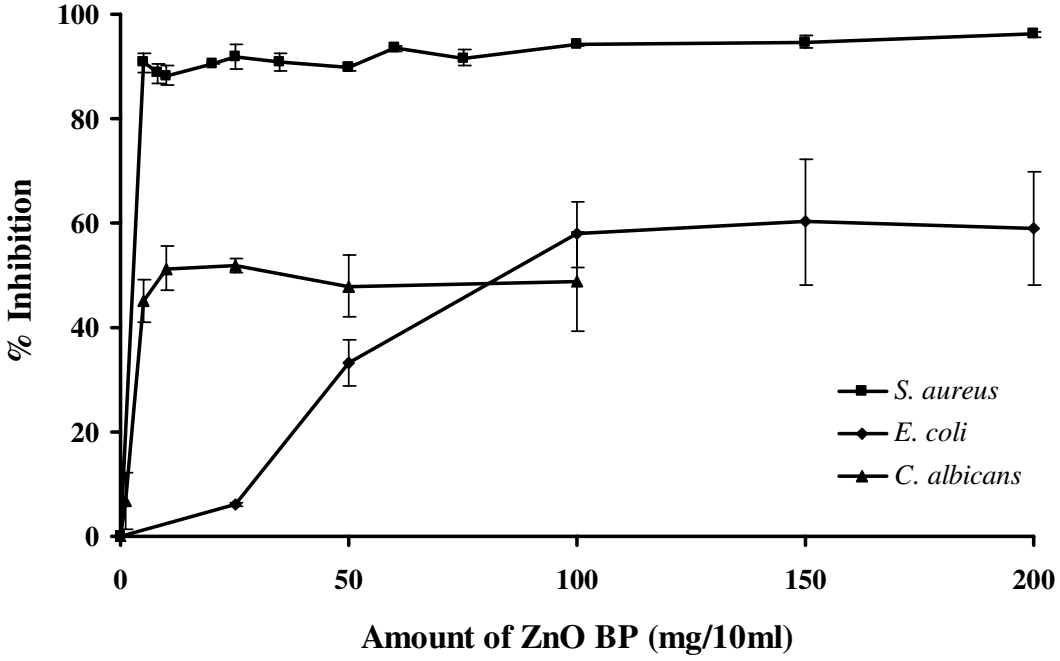

Figure 42 Inhibition profile towards *Staphylococcus aureus*, *Escherichia coli* and *Candida albicans* of zinc oxide BP (n=3)

4.2 Effect of type of ZnO on antimicrobial activity

The inhibition profiles against *S. aureus*, *E. coli* and *C. albicans* of various ZnO are shown in Figures 43, 44 and 45, respectively. The control was initial amount of cell that there was no addition of the samples. From previous study, the different concentrations of ZnO were selected to further study the antimicrobial activity in different type of ZnO, which depended on its efficacy. ZnO at concentration of 5 mg/10ml was used for *S. aureus* and *C. albicans* while at concentration of 150 mg/10ml was used for *E. coli*. Antibacterial activity of type of ZnO against *S. aureus* and *E. coli* showed no significant difference ($p > 0.05$). Micronized ZnO exhibited the antibacterial activity against *S. aureus* higher than that of powder, BP, tetrapod II and I ZnO. While antbacterial activity of powder ZnO against the *E. coli* growth was higher than that of micronized, BP, tetrapod I and II forms. Antifungal activity of type of ZnO against *C. albicans* showed no significant difference ($p > 0.05$). All types of ZnO could inhibit *C. albicans* growth as the same level. Both colloidal silicon dioxides, Aerosil® 200 and Aerosil® R972, had no the

antimicrobial activity. Thus, it was obvious that the particle size of ZnO affected the antibacterial activity but not antifungal activity.

Antibacterial activity of ZnO depended on the particle sizes (Yamamoto 2001) and shapes (Tam *et al*., 2008; Zhang *et al.,* 2008). From our studies, the particle size of ZnO influenced the antibacterial activity. The antibacterial activity of ZnO powder increased with the smaller particle size and the activity against *S. aureus* was less than that against *E. coli* (Yamamoto 2001). The antibacterial behaviors of ZnO nanofluids against *E. coli* bacteria are exhibited that the number of the bacterial colonies dropped with the increasing concentration of ZnO particles (Zhang *et al.,* 2008). Mungkornasawakul *et al.* (2005) investigated that ZnO nanopowders could inhibit the growth of microbes as *Rhizopus oligosporus*, *Penicillium oxalicum*, *Aspergillus fumigatus*, *Aspergillus awamori, Escherichia coli*, *Bacillus subtilis* and *Staphylococcus aureus* that the antibacterial activity against *S. aureus* was more than that against *E. coli*. From the present study also found that ZnO could inhibit *S. aureus* was more than *E . coli*.

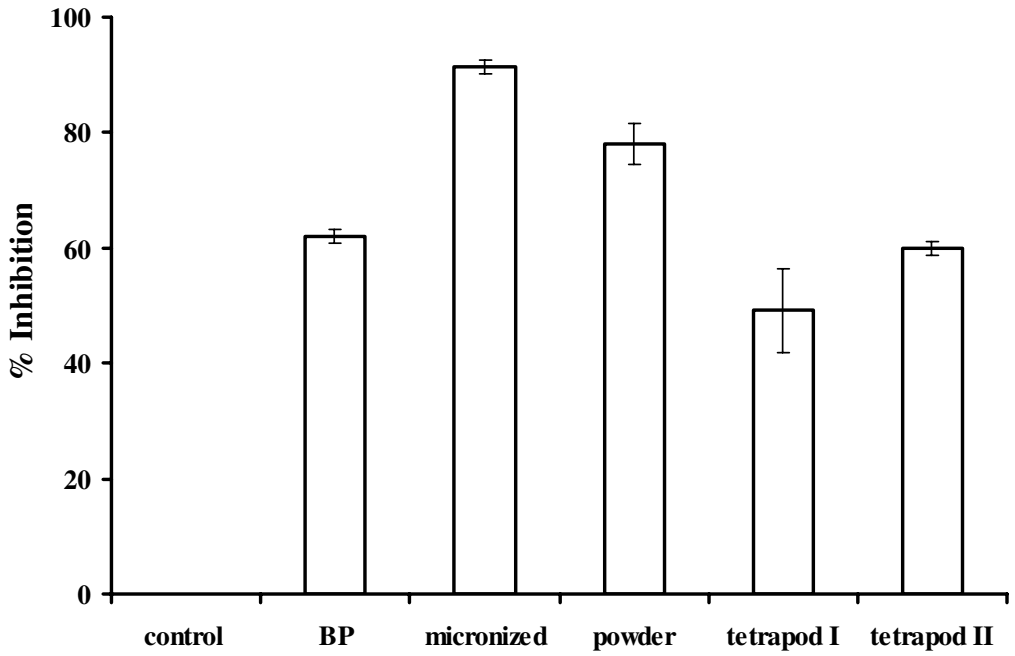

Figure 43 Inhibition profiles against *Staphylococcus aureus* of various zinc oxide at concentration of 5mg/10ml (n=3)

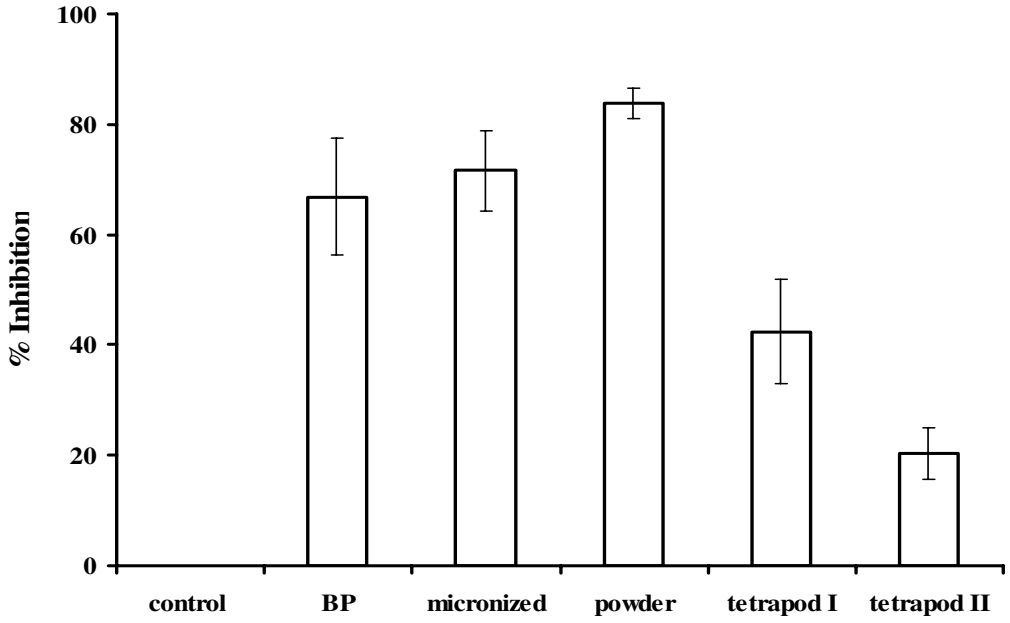

Figure 44 Inhibition profiles against *Escherichia coli* of various zinc oxide at concentration of 150mg/10ml (n=3)

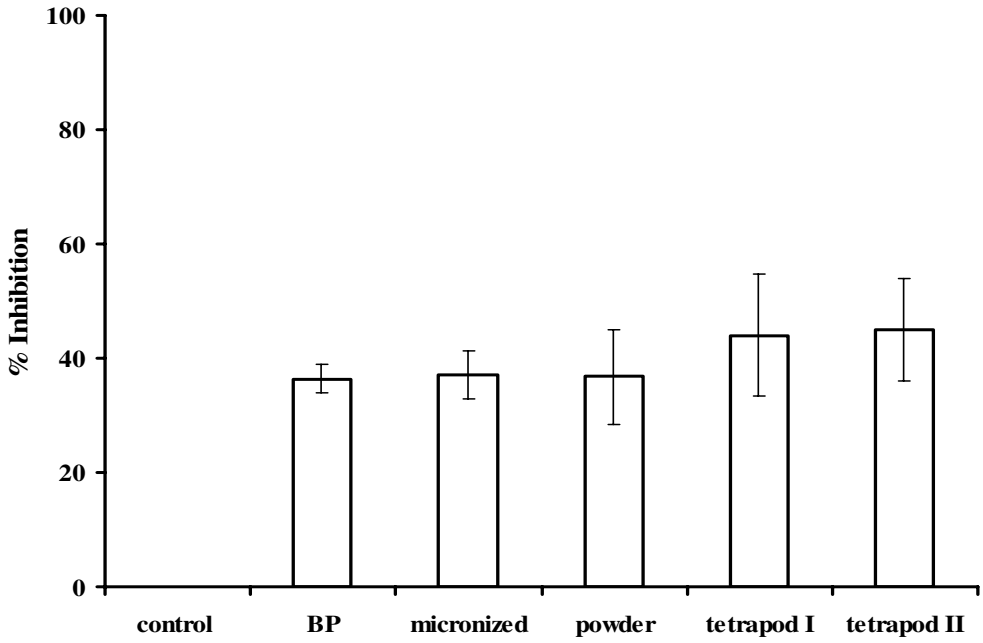

Figure 45 Inhibition profiles against *Candida albicans* of various zinc oxide at concentration of 5mg/10ml (n=3)

4.3 The antimicrobial activity of gels comprising different amount of NMP concentrations

The antimicrobial activity of gels containing different amount of NMP against *S. aureus, E. coli* and *C. albicans* (Figures 46 and 47) were tested by agar diffusion method. Antibacterial activity against *S. aureus* and *E. coli* was increased as the amount of NMP was increased from 20 – 40 %w/w,. Whereas the antifungal activity against *C. albicans* was enhanced by increasing the amount of NMP from 10 - 80% w/w. However, there was no antimicrobial effect for the gel base. The inhibition zone of pure NMP against *S. aureus*, *E. coli* and *C. albicans* were 1.9 ± 0.1, 2.0 ± 0.2 and 3.5 ± 0.1 cm., respectively (Figure 48). Thus, NMP could be inhibited all tested microbes.

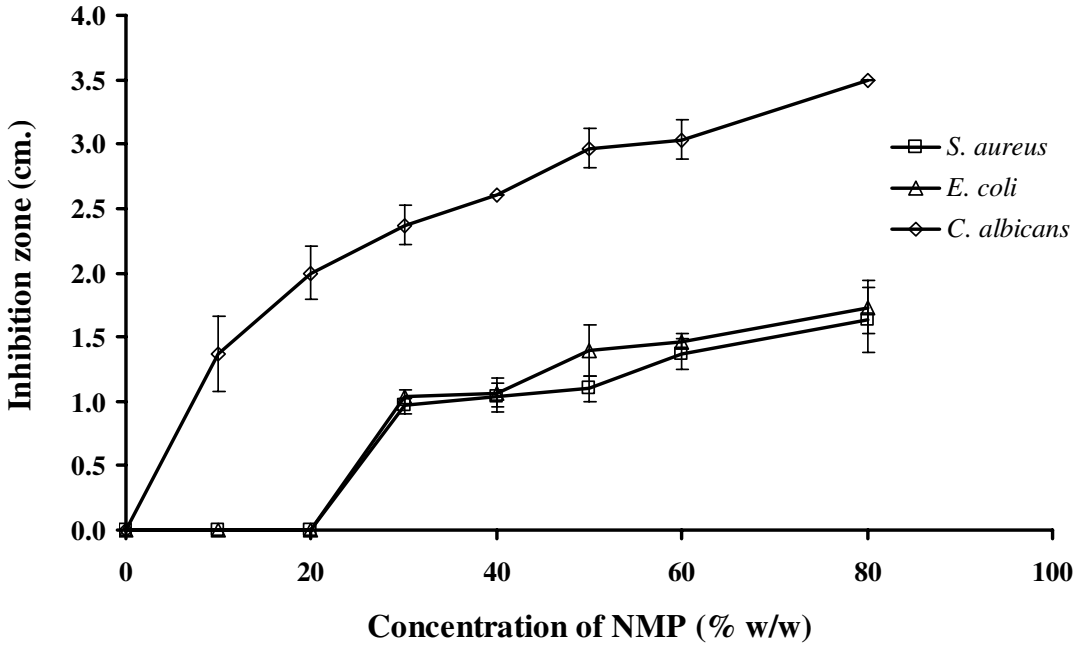

Figure 46 Inhibition zone diameter of 20% Lutrol® F 127 gel containing different concentrations of NMP obtained from the agar diffusion method

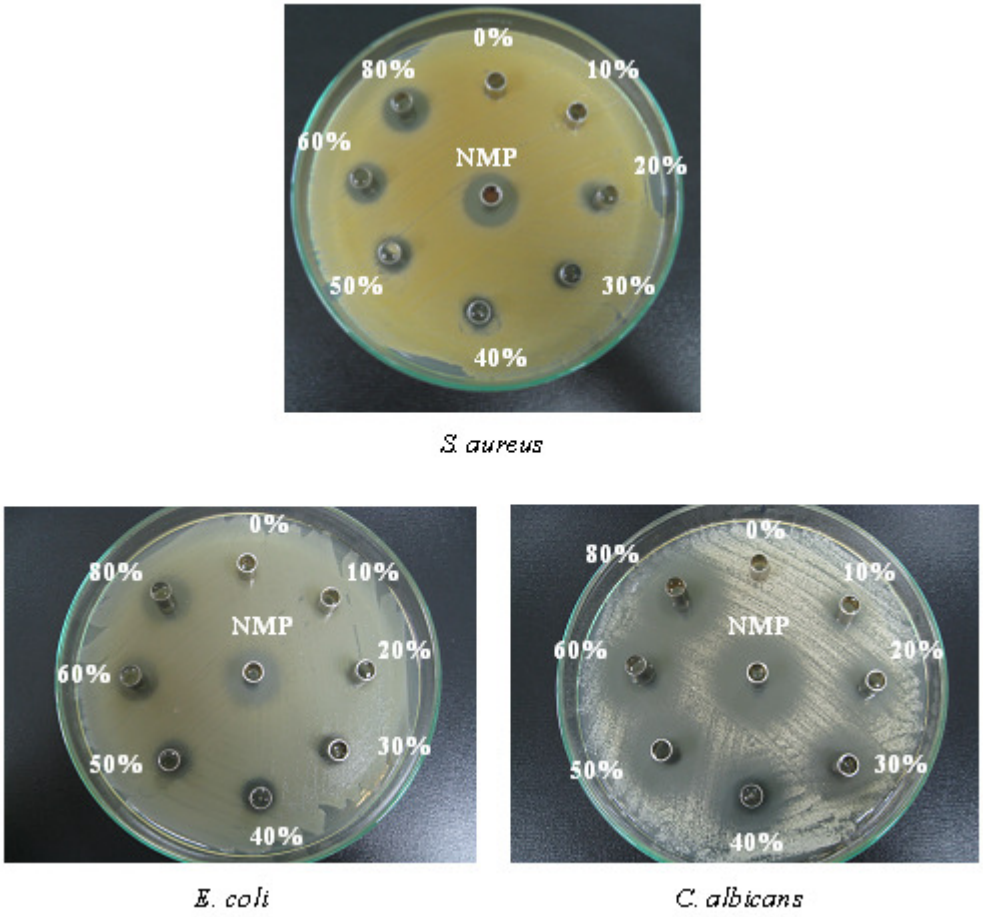

Figure 47 Photographs of inhibition zone of Lutrol® F 127 gels containing different NMP concentrations against *Staphylococcus aureus*, *Escherichia coli* and *Candida albicans*

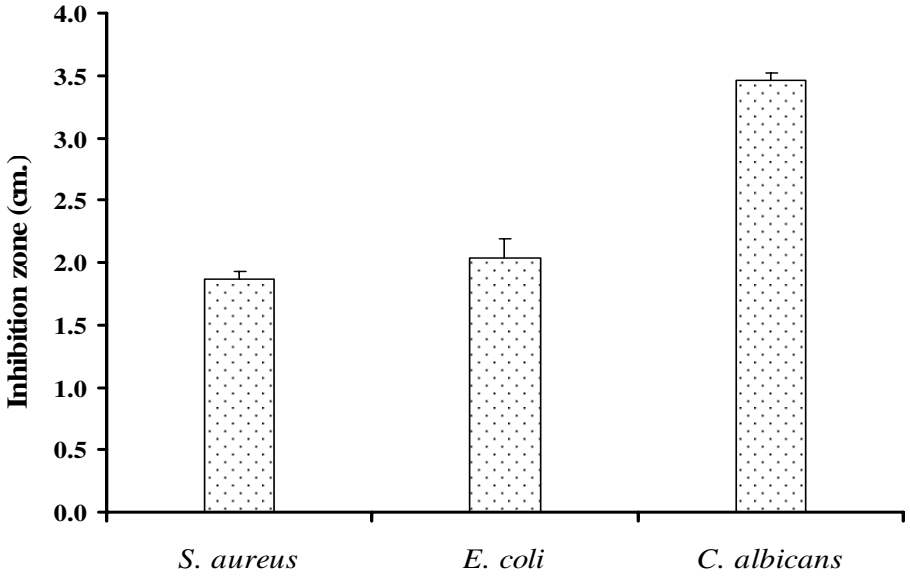

Figure 48 Inhibition zone of NMP against three microbes obtained from the agar diffusion method (n=3)

4.4 The antimicrobial activity of gels containing various ZnO concentrations

The prepared gels containing different amount of ZnO BP were tested the antimicrobial activity against *S. aureus*, *E. coli* and *C. albicans* using the agar diffusion method. There was no inhibition zone for the Lutrol® F127 gel without ZnO BP indicating that Lutrol® F127 had no the antimicrobial activity. All gels containing different concentrations of ZnO BP showed no inhibition zone (Figure 49), due to ZnO BP could not diffuse pass the gels to the agar. Thus, the antimicrobial activity of prepared gel containing ZnO BP were not detected in this agar diffusion method. Therefore the contact direction methods were used to assay the antimicrobial activity of gel preparation. The percentage of growth inhibition against *S. aureus*, *E. coli* and *C. albicans* are shown in Figures 50, 51 and 52, respectively. The percentage of growth inhibition against *S. aureus* of the gel base containing 20%w/w NMP was 31.8 $\pm$ 4.9 % which was less than that without NMP which was 54.5 $\pm$ 3.5 %. This result suggested that the 20%w/w NMP did not enhance the antibacterial activity of the system. The growth inhibition againsted *S. aureus* of the prepared gel containing ZnO alone was increased as the ZnO amount were increased. Whereas the percentage of growth inhibition againsted *S. aureus* by the prepared gel containing 20%w/w NMP and ZnO (1%, 5% or 10%w/w) were 37.5 $\pm$ 6.2, 79.3 $\pm$ 4.3 or 78.5 $\pm$ 3.0, respectively

(Table 25). The percentage of the growth inhibition against *E. coli* by the prepared gels without NMP containing 1, 5 and 10% w/w ZnO were 61.7 ± 8.6 %, 63.1 ± 11.3 % and 62.9 ± 10.0 %, respectively, which were not different. The addition of 20% w/w NMP into the systems containing ZnO (1, 5 and 10%w/w) could inhibit *E. coli* growth as 27.5 ± 7.0, 51.4 ± 3.9 and 63.3 ± 4.8 %, respectively (Table 26). The percentage of growth inhibition against *C. albicans* by the prepared gel containing 5 and 10%w/w ZnO were not different (55.2 ± 4.5 and 56.2 ± 5.9, respectively), but higher than by that of 1%w/w ZnO (15.1 ± 0.4 %). When the added NMP (20%w/w) into the systems, the percentage of the growth inhibition against *C. albicans* by the prepared gels were less than that without NMP (Table 27). However, the pure NMP (20%w/w) were tested antimicrobial activity using contact direction method. The percent inhibition against *S. aureus, E. coli* and *C. albicans* were 26.3 ± 8.0 %, 49.6 ± 10.9 % and 1.6 ± 0.8 %, respectively. These results supported that the addition of 20%w/w NMP into the Lutrol® F127 systems containing ZnO could not enhance the antimicrobial activity of these systems. However, the increased ZnO amount enhanced the antimicrobial activity of these systems.

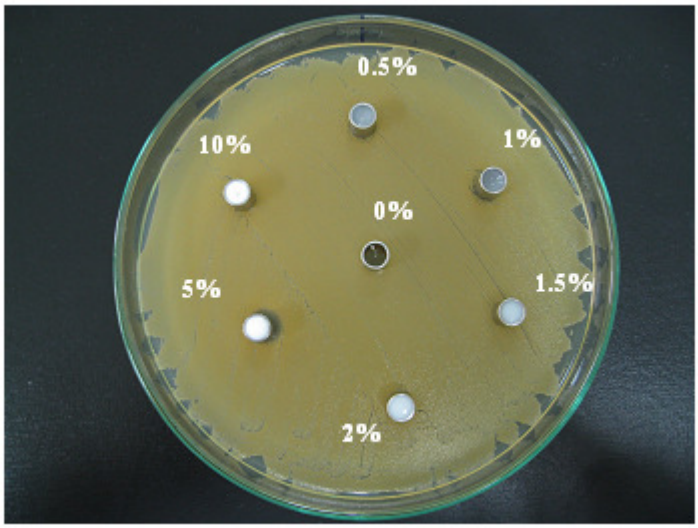

Figure 49 Inhibition zone photographs of the systems against *Staphylococcus aureus* by Lutrol® F127 gel containing different concentrations of zinc oxide by the agar diffusion method

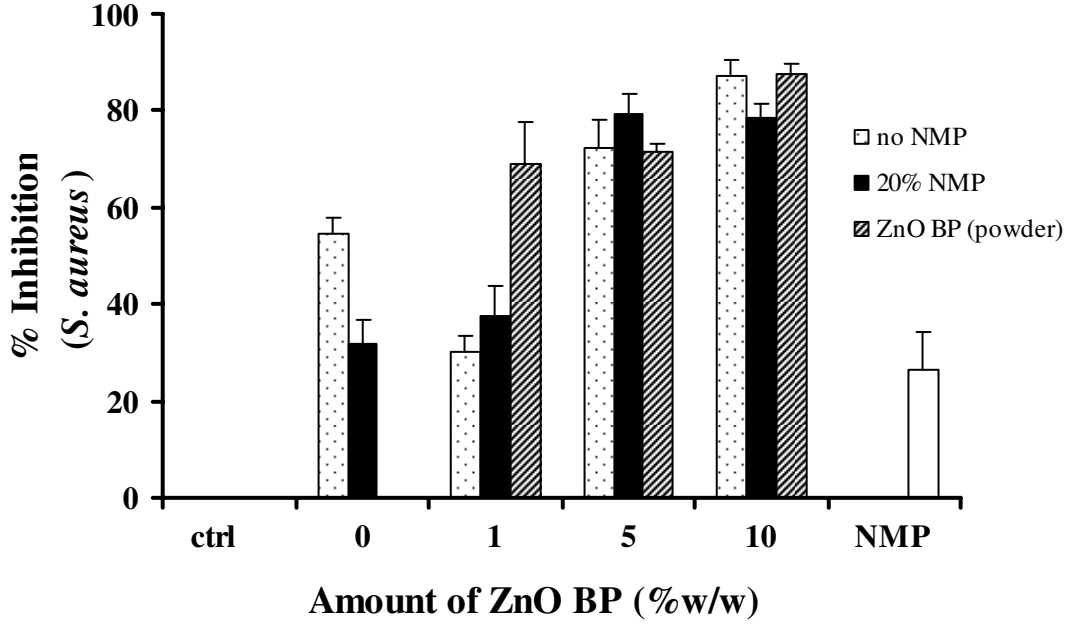

Figure 50 Percentage of *S. aureus* growth inhibition of Lutrol® F127 gel containing different amount of zinc oxide and *N*-methyl-2-pyrrolidone (n=3)

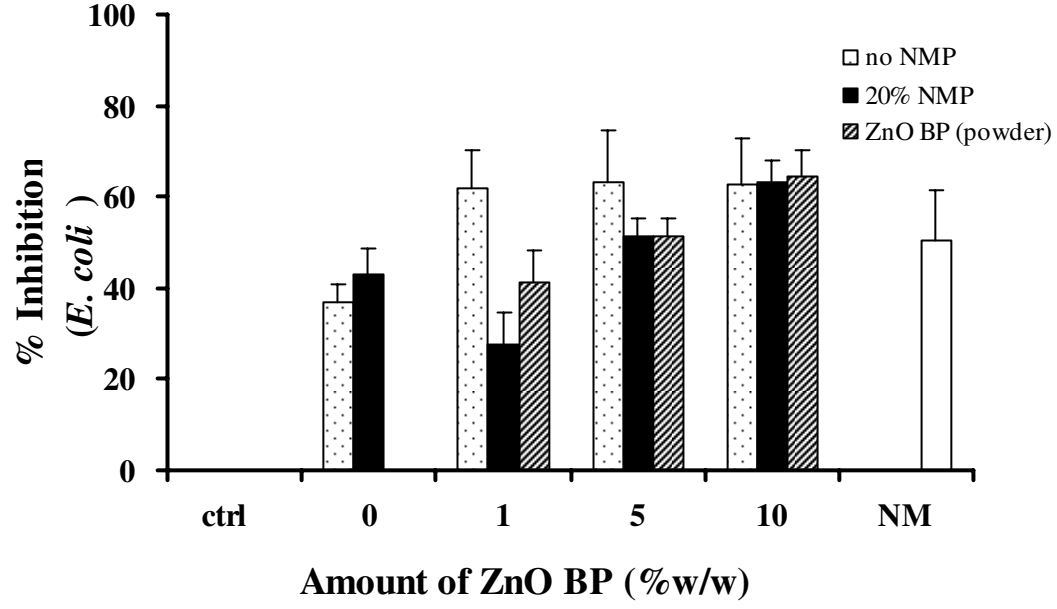

Figure 51 Percentage of *E. coli* growth inhibition of Lutrol® F127 gel containing different amount of zinc oxide and *N*-methyl-2-pyrrolidone (n=3)

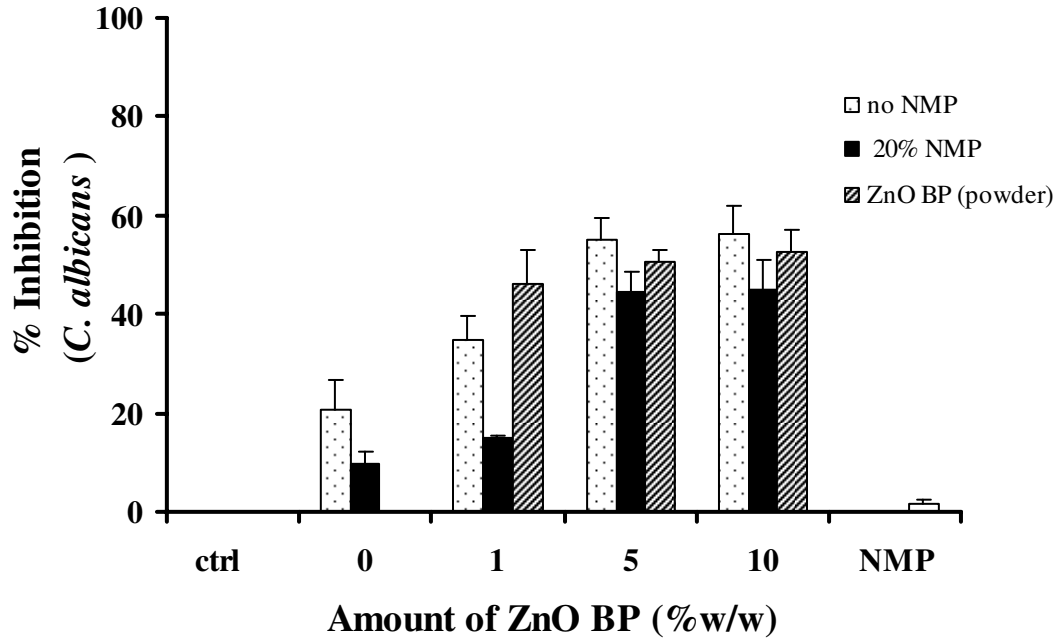

Figure 52 Percentage of *C. albicans* growth inhibition of Lutrol® F127 gel containing different amount of zinc oxide and *N*-methyl-2-pyrrolidone (n=3)

Table 25 Percentage of *S. aureus* growth inhibition of ZnO BP (powder) and Lutrol® F127 gel containing different amount of ZnO and NMP (n=3)

Percentage of *S. aureus* growth inhibition (%)				
	ZnO BP (%w/w)			
	0	1	5	10
ZnO BP (powder)	-	69.0 ± 8.9	71.5 ± 1.5	87.5 ± 2.2
Lutrol® F 127 (20%w/w)				
without NMP	54.5 ± 3.5	30.3 ± 3.2	72.5 ± 5.6	87.3 ± 3.3
20% NMP	31.8 ± 4.9	37.5 ± 6.2	79.3 ± 4.3	78.5 ± 3.0

Table 26 Percentage of *E. coli* growth inhibition of ZnO BP (powder) and Lutrol® F127 gel containing different amount of ZnO and NMP (n=3)

Percentage of *E. coli* growth inhibition (%)				
	ZnO (%w/w)			
	0	1	5	10
ZnO (powder)	-	41.1 ± 7.2	51.3 ± 4.1	64.6 ± 5.4
Lutrol® F 127 (20%w/w)				
without NMP	36.7 ± 4.3	61.7 ± 8.6	63.1 ± 11.3	62.9 ± 10.0
20% NMP	42.9 ± 5.8	27.5 ± 7.0	51.4 ± 3.9	63.3 ± 4.8

Table 27 Percentage of *C. albicans* growth inhibition of ZnO BP (powder) and Lutrol® F127 gel containing different amount of ZnO and NMP (n=3)

Percentage of *C. albicans* growth inhibition (%)				
	ZnO (%w/w)			
	0	1	5	10
ZnO (powder)	-	46.0 ± 6.9	50.6 ± 2.5	52.8 ± 4.3
Lutrol® F 127 (20%w/w)				
without NMP	20.6 ± 5.9	15.1 ± 0.4	55.2 ± 4.5	56.2 ± 5.9
20% NMP	9.8 ± 2.5	11.2 ± 6.8	44.6 ± 3.9	44.8 ± 6.3

4.5 The antimicrobial activity of gels comprising different amount of doxycycline hyclate

The 20%w/w Lutrol® F127 gels containing various amount doxycycline hyclate with or without 20%w/w NMP were tested the antimicrobial activity against *S. aureus*, *E. coli* and *C. albicans* using the agar diffusion method (Figure 53 and Table 28). Because the doxyxycline hyclate has a potent antibacterial activity, thus the antibacterial activity of doxycycline hyclate was rather difficult to observe when the contact direction method was employed. The inhibition zone diameter against *C. albicans* of the gel base containing 20%w/w NMP was 1.8 $\pm$ 0.1 cm., whereas the gel base containing with and without 20%w/w NMP did not exhibit the inhibition zone against *S. aureus* and *E. coli*, indicating that the addition of 20%w/w NMP could be inhibit *C. albicans*. The inhibition zone diameter were increased as the doxycycline hyclate concentration was increased, indicating the antimicrobial activity of doxycycline hyclate was dose response. The inhibition zone diameter against *S. aureus* was greater than that against *E. coli* and *C. albicans*, indicated that the doxycycline hyclate influenced on the gram-positive bacteria, gram-negative bacteria and fungal, respectively. Generally, doxycycline is bacteriostatic against a wide variety of organisms, both gram-positive and gram-negative. The addition of NMP into the gel system affected the activity against *C. albicans* since the inhibition zone of the prepared gel with 20%w/w NMP were notably higher than that without NMP. Therefore, NMP enhanced the antifungal activity of doxycycline hyclate.

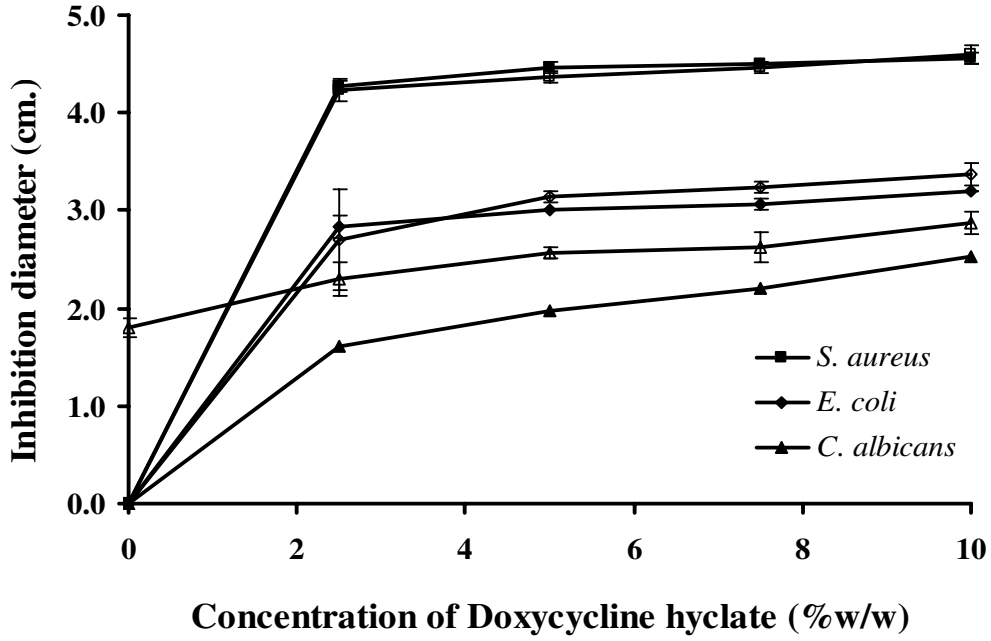

Figure 53 Inhibition zone diameter of 20%w/w Lutrol® F 127 gel containing different concentrations of doxycycline hyclate obtained from the agar diffusion method. Closed symbols represent the prepared gel without NMP, and opened symbols represent the prepared gels with 20%w/w NMP.

Table 28 Inhibition zone diameter of the Lutrol® F127 gels containing different doxycycline hyclate concentration with and without NMP

Concentration of Doxycycline hyclate (%w/w)	Inhibition zone diameter (cm.)					
	no NMP			20% NMP		
	S. aureus (Mean ± S.D.)	*E. coli* (Mean ± S.D.)	*C. albicans* (Mean ± S.D.)	*S. aureus* (Mean ± S.D.)	*E. coli* (Mean ± S.D.)	*C. albicans* (Mean ± S.D.)
0.0	0.0 ± 0.0	0.0 + 0.0	0.0 ± 0.0	0.0 ± 0.0	0.0 ± 0.0	1.8 ± 0.1
2.5	4.3 ± 0.1	2.8 ± 0.1	1.6 ± 0.1	4.2 ± 0.1	2.7 ± 0.1	2.3 ± 0.2
5.0	4.5 ± 0.1	3.0 ± 0.0	2.0 ± 0.1	4.4 ± 0.1	3.1 ± 0.0	2.6 ± 0.1
7.5	4.5 ± 0.0	3.1 ± 0.1	2.2 ± 0.1	4.5 ± 0.1	3.2 ± 0.0	2.6 ± 0.2
10.0	4.6 ± 0.1	3.2 ± 0.0	2.5 ± 0.2	4.6 ± 0.1	3.4 ± 0.0	2.9 ± 0.1

4.6 The antimicrobial activity of doxycycline hyclate gels on various amount zinc oxide

The effect of ZnO and NMP on the antimicrobial activity of doxycycline hyclate gels are shown in Figure 54 and Table 29. The agar diffusion method was tested for the antimicrobial activity against *S. aureus*, *E. coli* and *C. albicans*. Inhibition zone diameters against *S. aureus*, *E. coli* of the doxycycline hyclate gels with or without NMP were not different. Whereas the inhibition zone diameters against *C. albicans* of the doxycycline hyclate gels with 20%w/w NMP were higher than that without NMP. It suggested that the 20%w/w NMP could enhance the antifungal activity against *C. albicans* of doxycycline hyclate-Lutrol® F127 gel. The inhibition zone of the prepared gel containing 0.5%w/w ZnO were lower than that without ZnO, indicated that the diffusion of doxycyline hyclate from gel decreased when the systems containing ZnO. For *S. aureus*, the inhibition zone of the doxycycline hyclate-Lutrol® F127 gel were decreased with the amountof ZnO, whereas the inhibition zone of the prepared gel with 20% NMP did not depend on the ZnO amount. For *E. coli* and *C. albicans*, the inhibition zone of the doxycycline hyclate-Lutrol® F127 gel with or without 20% w/w NMP were decreased when the amount ZnO were increased. These results showed that the amount of ZnO affected to the diffusion of drug from gels. The incorporation of 20% w/w NMP increased the antimicrobial activity of the systems. These mentioned results correlated well with the drug release at the first 16 hours which indicated for the structure of the gel functioned as barrier to drug release.

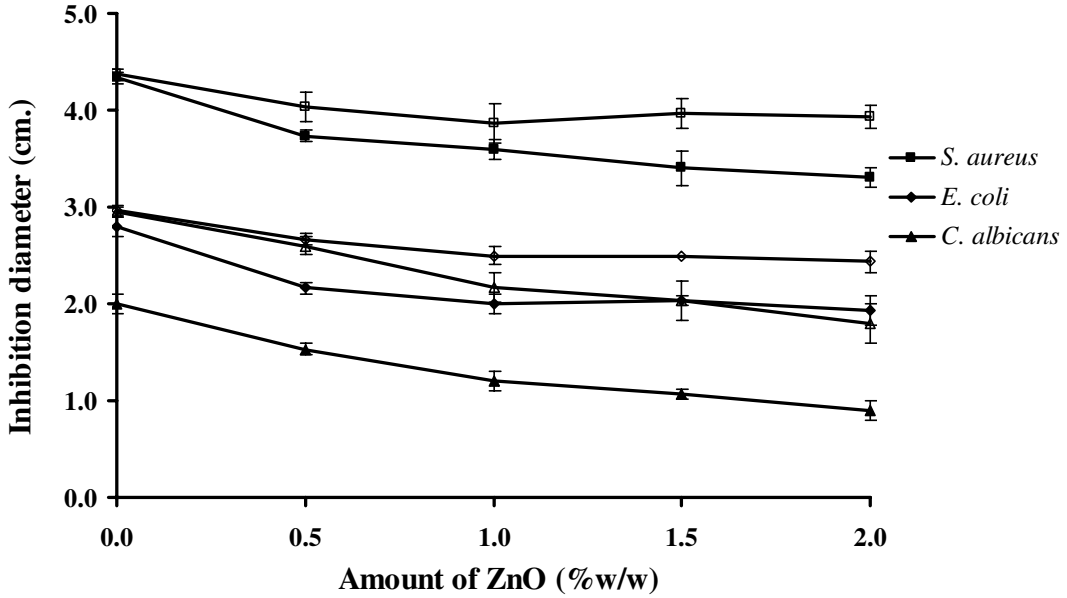

Figure 54 Inhibition zone of 5%w/w doxycycline hyclate gels containing different zinc oxide concentrations with and without NMP against *S. aureus*, *E. coli* and *C. albicans*. (Opened symbols show the prepared gel with NMP. Closed symbols show the prepared gel without NMP).

Table 29 Inhibition zone diameter of the 5%w/w doxycycline hyclate gels containing different zinc oxide concentration with and without NMP

Amount of ZnO BP (%w/w)	Inhibition zone diameter (cm.)					
	without NMP			20% NMP		
	S. aureus (Mean ± S.D.)	*E. coli* (Mean ± S.D.)	*C. albicans* (Mean ± S.D.)	*S. aureus* (Mean ± S.D.)	*E. coli* (Mean ± S.D.)	*C. albicans* (Mean ± S.D.)
0.0	4.3 ± 0.1	2.8 ± 0.1	2.0 ± 0.1	4.4 ± 0.1	3.0 ± 0.1	3.0 ± 0.1
0.5	3.7 ± 0.1	2.2 ± 0.1	1.5 ± 0.1	4.0 ± 0.2	2.7 ± 0.1	2.6 ± 0.1
1.0	3.6 ± 0.1	2.0 ± 0.1	1.2 ± 0.1	3.9 ± 0.2	2.5 ± 0.1	2.2 ± 0.2
1.5	3.4 ± 0.2	2.0 ± 0.1	1.1 ± 0.1	4.0 ± 0.2	2.5 ± 0.2	2.0 ± 0.2
2.0	3.3 ± 0.1	1.9 ± 0.2	0.9 ± 0.2	3.9 ± 0.2	2.4 ± 0.1	1.8 ± 0.2

5. Effect of ingredients on the drug release from gels

In vitro release profile provides insight into the efficiency of the drug delivery system proposed for the controlled release of the drug. The drug release was tested in phosphate buffer pH 7.2 to imitate the environment of periodontitis (Maheshwari *et al*., 2006). The drug release profile of system containing doxycycline hyclate (5% w/w) without polymer showed a fast release with about 90% drug release at 5 hours (Figure 55), whereas that of systems containing 5 %w/w doxycycline hyclate in 20%w/w Lutrol® F127 was about 80% drug release in 5 hours. It suggested that Lutrol® F127 could retard the release of drug since the structure of the gel functioned as barrier to the drug release. Tan *et al*. (2000) suggested that the polyvinylpyrrolidone K90 (PVP) concentration was negatively correlated with gel hardness and compressibility, however the drug release was reduced as the PVP increased.

The influence of NMP on drug release from gels containing 20%w/w Lutrol® F127 and 5%w/w doxycycline hyclate was investigated (Figure 55). The added 20%w/w NMP into the gel systems enhanced the release of doxycycline hyclate. This result signified that NMP might decrease the gel strength. NMP was a more effective solvent than ethanol in improvement of estradiol solubility (Koizumi *et al*., 2004). Yoneto *et al*. (1995, 1997) reported that N-alkyl-pyrrolidone derivatives increased drug solubility in skin and also fluidized lipids in stratum corneum.

The influence of amount of ZnO (0.5, 1, 2, 5%w/w) on drug release from gels containing 20%w/w Lutrol® F127 with 20% w/w NMP and 5%w/w doxycycline hyclate was investigated (Figure 56). Doxycycline hyclate released from gel without ZnO as a biphasic characteristic, with a relatively fast release at the initial hours, then the drug release was almost completed and the amount of drug released was about 90% after 10 hours. The release of doxycycline hyclate in 20%w/w Lutrol® F127 containing 0.5 % w/w ZnO showed the drug release about 15% at 16 hours. During the first 16 hours, the release of doxycycline hyclate were decreased as the amount of ZnO were increased. Subsequently, the drug release from gel containing 5%w/w ZnO were faster than that containing ZnO of 2% and 1%w/w, respectively. However, a slow release at the late stage was evident which the drug release was about 60% at 216 hours. Whereas, the drug release from gel containing ZnO 1.0% was slow at the beginning and a fast release was found at the late stage which later the amount of drug released was about

60% at the end of the test. These results indicated that ZnO influenced on the structure of the gel functioned as barrier to drug release. This result was similar to Maheshwari's report (Maheshwari *et al.*, 2006), however, the drug release was different for the first stage because the structure of gels were changed after the ZnO was separated from the systems. Maheshwari *et al.* (2006) reported that the release of tetracycline from 20%w/w pluronic gel were decreased when the concentration of Aerosil® were increased (at 8 hours), indicated that structure of gel functioned as barrier to drug release and it suggested that Aerosil® supplemented hydrogen bonding, which enhanced the dehydration of PPO block of the micelle and micelle entanglement thus micelles could not separate easily from each other, which accounts for the rigidity and slow dissolution of these gels. The enhanced resistance may be due to the increase in size of micelles within the gel structure, which led to higher viscosity and lower drug release (Maheshwari *et al.*, 2006). Pandit and Wang (1998) investigated the release of propranolol from 21% F127 gels containing various amounts of added NaCl, Na_2SO_4 or Na_2HPO_4 that most salts decreased the diffusion of propranolol across a membrane. It was explained as water structure-making salts reduced the cmc and cmt of F127, make the PEO-PEO chain interactions stronger due to a decrease in hydrogen bonding with water, and thus make the PEO chain network tighter. Thus, diffusion of a drug molecule through the aqueous channel network was expected to decrease in the presence of salts. However, this study implied that the incorporated zinc oxide into the Lutrol® F127 systems could be sustained the drug release from the systems.

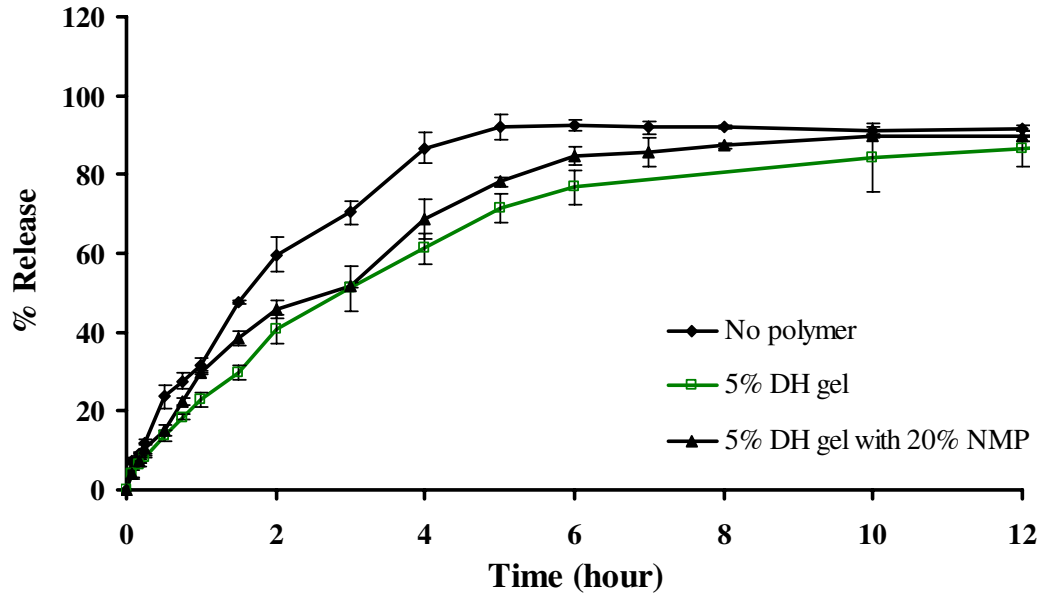

Figure 55 Drug release profiles of 5%w/w doxycycline hyclate (DH) systems containing Lutrol® F127 (20% w/w) with and without NMP in phosphate buffer pH 7.2 (n=3)

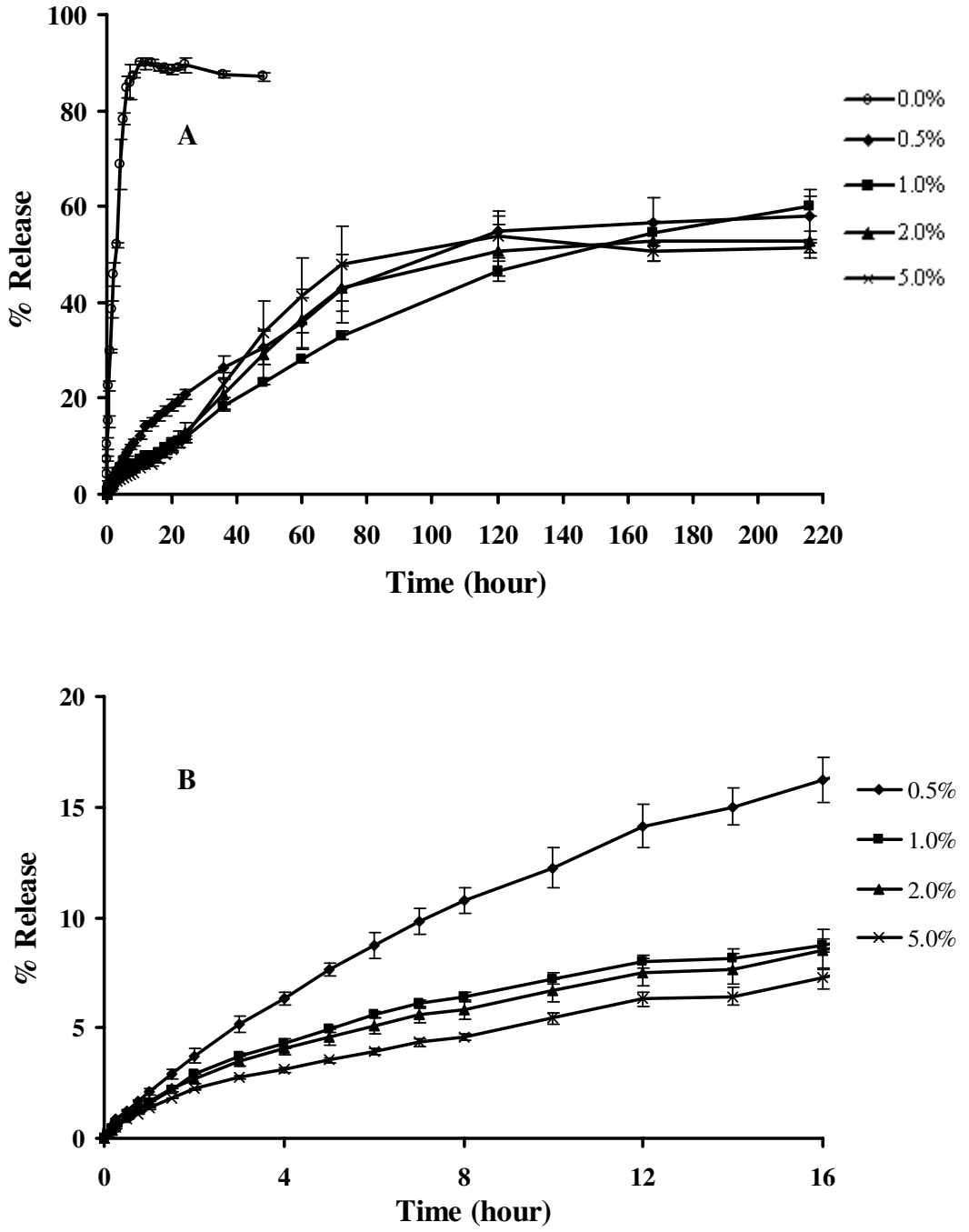

Figure 56 Drug release profiles of 5%w/w doxycycline hyclate gels containing 20%w/w NMP and different amount of zinc oxide in phosphate buffer pH 7.2 (n=3); (A: 0 - 216 hour, B: 0 - 16 hour)

6. Texture analysis

Texture analysis could provide the informative data on the dynamic properties such as, the elasticity modulus (G') and the viscous modulus (G"). The elasticity modulus (G') is low for a solution and increases drastically with temperature as a result of gel formation processes (Edsman *et al*., 1998). When the sol-gel transition has taken place G' becomes independent of further increase in temperature. The sol-gel transition temperature for the Lutrol® F127 systems are shown in Figure 57. The sol-gel transition temperature of the Lutrol® F127 system containing 5%w/w doxycycline hyclate and 20%w/w NMP was about 28°C. The sol-gel transition temperature of the systems decreased with the ZnO amount. The results indicated the change of sol-gel transition which they were similar to those where a sol-gel transition was determined by the visual method. Maheshwari *et al*. (2006) suggested that the increased of elasticity with the increased in the concentration of Aerosil®.

Syringeability of various Lutrol® F127 system was examined to determine the effect of the incorporated excipient and temperature on the force required to expel the product. This is an importance to indicate the ability of the product to be delivered from a syringe through a needle, in order to fulfill the requirement for the ease or feasibility of application. The systems examined for syringeability are listed in Table 30. The effect of temperature on syringeability of the system could be notably evident. The syringeability was tested at temperature of 4°C and 20°C because these were temperature during storage and during applying from the syringe through the needle, respectively (Kelly *et al.,* 2004). System 1 had a syringeability of 7.11 $\pm$ 0.14 N at 4°C and 13.68 $\pm$ 1.49 N at 20°C, which was an 2- fold increase in resistance to syringing over this temperature range. When the 5%w/w doxycycline hyclate was added into Lutrol® F127 system (system 2), the syringeability was increased to be 8.65 $\pm$ 0.48 N at 4°C and 17.31 $\pm$ 1.77 N at 20°C, that were slight higher than that from system 1. The syringeability of the 20%w/w Lutrol® F127 system containing 5%w/w doxycycline hyclate and 20%w/w NMP (system 3) were 17.15 $\pm$ 0.54 N and 21.21 $\pm$ 1.37 N at 4°C and 20°C, respectively. The syringeability of the systems containing 1%w/w ZnO were increased be 22.07 $\pm$ 4.24 N at 4°C and 25.79 $\pm$ 2.30 N at 20°C. The syringeability correlated well with the rheology results. The addition of doxycycline hyclate, ZnO and NMP affected the syringeability of systems. This was correlated with our

previous studies (3.3.4) that the added ZnO increased shear stress of the doxycycline hyclate-Lutrol® F127 systems.

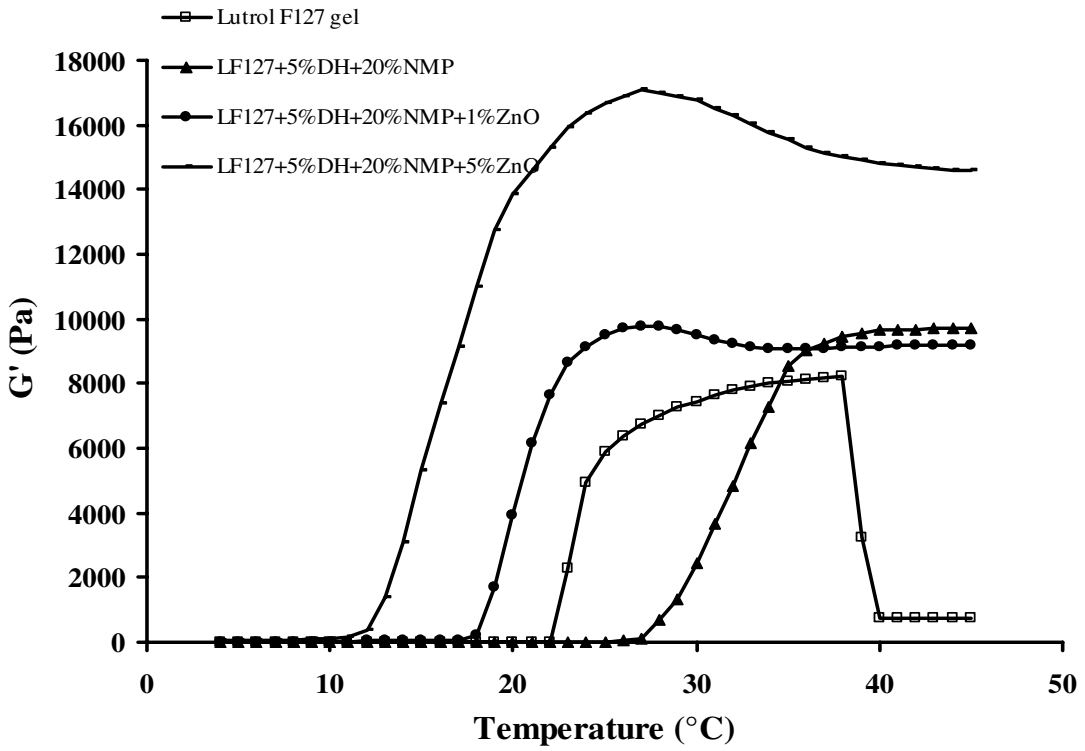

Figure 57 Storage modulus (G') of 20%w/w Lutrol® F127 systems; Lutrol® F127 system containing 5%w/w doxycycline hyclate (DH) and 20%w/w NMP; Lutrol® F127 system containing 5%w/w doxycycline hyclate, 20%w/w NMP and 1%w/w ZnO; and Lutrol® F127 system containing 5%w/w doxycycline hyclate, 20%w/w NMP and 5%w/w ZnO.

Table 30 Syringeability of various systems at 4ºC and 20ºC

System no.	System	Syringeability at 4°C (N)	Syringeability at 20°C (N)
1	20% Lutrol® F127	7.11 ± 0.14	13.68 ± 1.49
2	20% Lutrol® F127, 5%DH	8.65 ± 0.48	17.31 ± 1.77
3	20% Lutrol® F127, 5%DH, 20%NMP	17.15 ± 0.54	21.21 ± 1.37
4	20% Lutrol® F127, 5%DH, 20%NMP, 1%ZnO	22.07 ± 4.24	25.79 ± 2.30

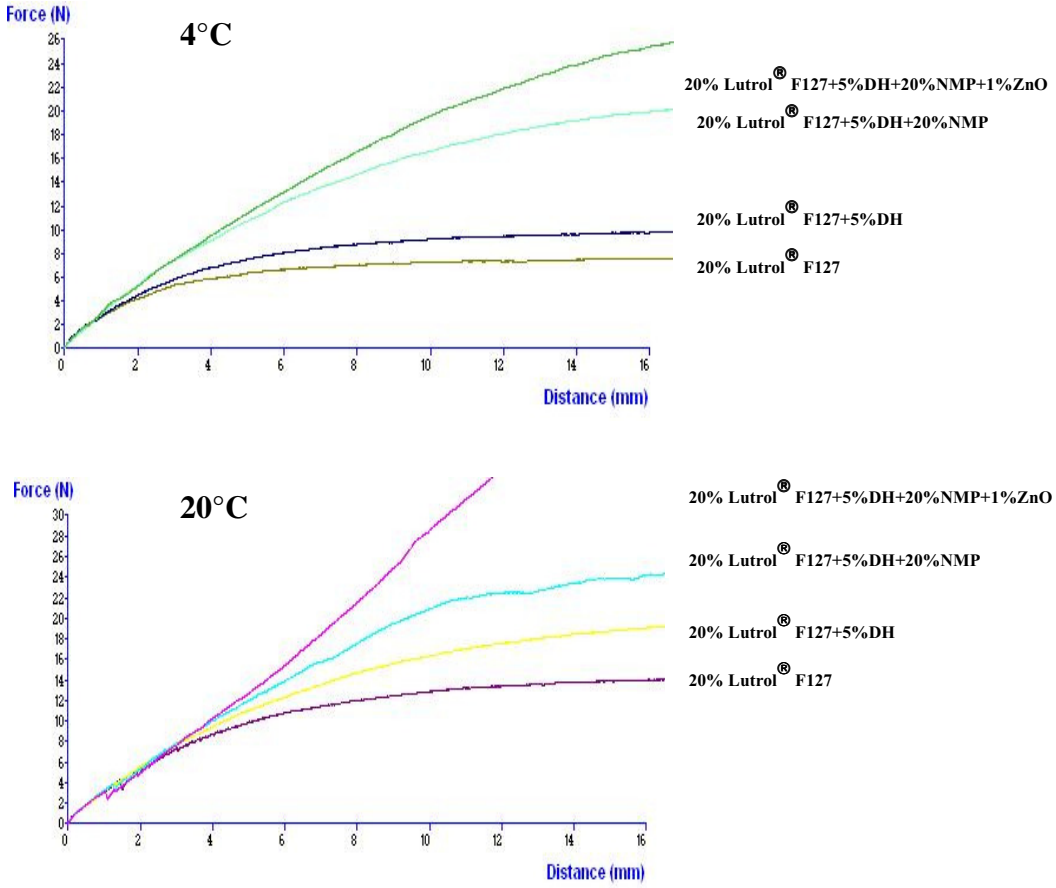

Figure 58 Force-displacement profiles for the gel systems containing Lutrol® F127 gel (20%w/w); Lutrol® F127 (20%w/w) system containing 5%w/w doxycycline hyclate (DH); Lutrol® F127 (20%w/w) system containing 5%w/w doxycycline hyclate and 20%w/w NMP; Lutrol® F127 (20%w/w) system containing 5%w/w doxycycline hyclate, 20%w/w NMP and 1%w/w ZnO at temperature of 4 and 20ºC

7. Surface morphology of gels

Surface morphology and cross section area of the prepared gel was characterized using scanning electron microscopy. Freeze-dried was utilized for sample preparation to maintain the porous structure without any collapse during water sublimation. The SEM images of Lutrol® F127 dried gel containing 5%w/w doxycycline hyclate and different amounts of ZnO at different magnifications are shown in Figures 59 - 60. The porous surface was evident for 20%w/w Lutrol® F127 system (Figure 59A). The enlarged images of the surface of the wall were seen at magnification 100X and 350X which the porous structure was more evident. The structures of 20%w/w Lutrol® F127 systems were notably different from that of gel comprising doxycycline hyclate. The structure of the doxycycline hyclate-Lutrol® F127 system contained the continuous cell, whereas the wall surface were smooth (Fig. 59B). The cell of structures were decreased with an increase of ZnO contents and the porous structure was more compact and smaller. This was explained by the entangling between ZnO and Lutrol® F127 being enhanced with the increase of ZnO content. For samples of 0.5%, 1.0%, 2.0%, 5.0% and 10.0% w/w ZnO content, the SEM micrographs were further magnified to clearify their structure as presented in Figs. 59(C-D) and 60(A-C). The addition of Aerosil® transformed the poloxamer system from the cubic into the hexagonal phase (Maheshwari *et al*., 2006). Therefore, this study suggested that the increased of zinc oxide amount decreased the size of the continuous cell and increased the compact of the wall surface because the Lutrol® F127 systems changed be the hexagonal phase as the addition of Aerosil®.

The SEM photographs of cross-sectional morphology of Lutrol® F127 dried gel containing 5%w/w doxycycline hyclate, 20%w/w NMP and different amount of ZnO after release test for 216 hours in phosphate buffer pH 7.2 at different magnifications are shown in Figures 61. As shown in the micrographs, the continuous cell diameters were decreased after the released test. It was obvious that the structure of Lutrol® F127 dried gel were fragile and the pores surface were decreased. It was obvious that the Lutrol®F127 has a molecular weight of 12,600, which could not diffuse pass dialysis tube (MW cutoff: 6000-8000) therefore the structure of these systems were more compacted.

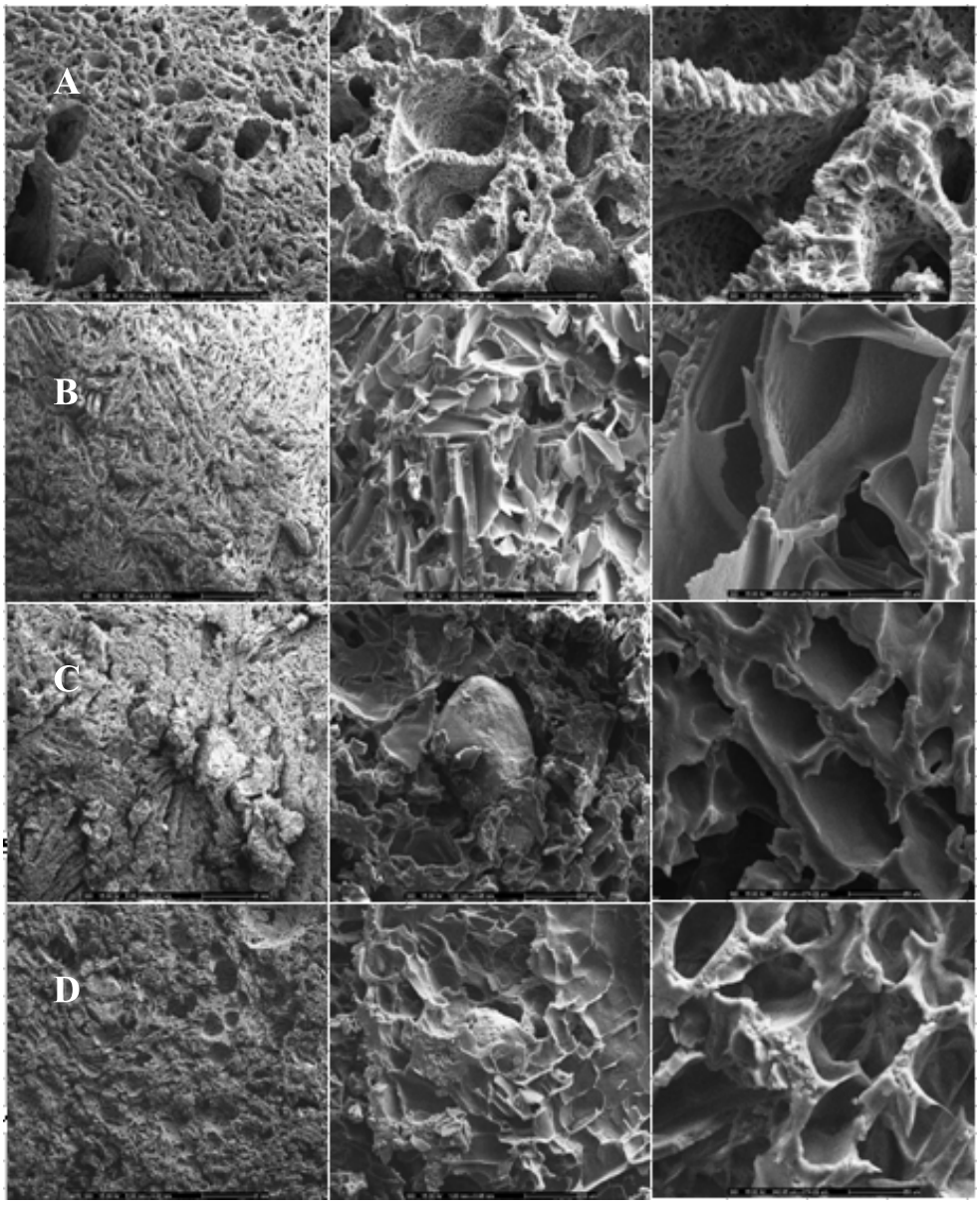

Figure 59 SEM micrographs of the dried gel systems; 20%w/w Lutrol® F127 systems (A); and 5%w/w doxycycline hyclate-Lutrol® F127 systems (B) containing with 0.5%w/w ZnO (c) and 1.0%w/w ZnO (D) with different magnifications (20X, 100X and 350X).

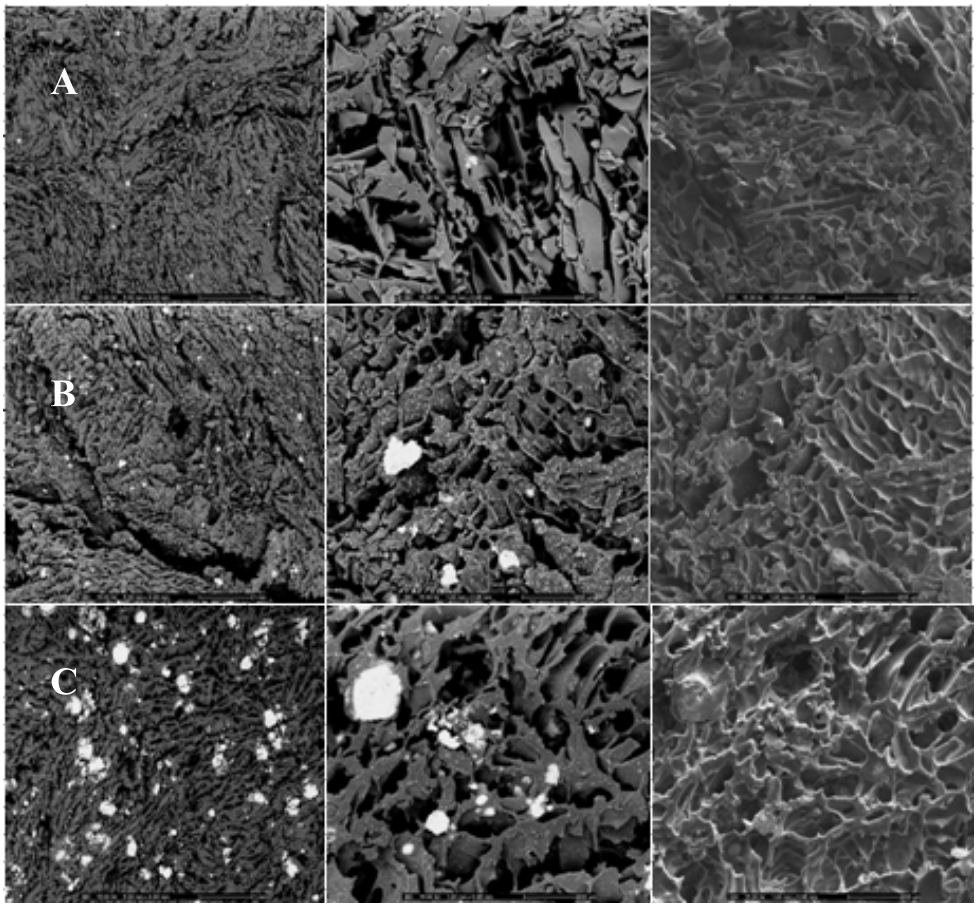

Figure 60 SEM micrographs of 20%w/w Lutrol® F127 systems containing 5%w/w doxycycline hyclate and different amount of ZnO with different magnifications; (A) 2%w/w ZnO; (B) 5%w/w ZnO and (C) 10%w/w ZnO.

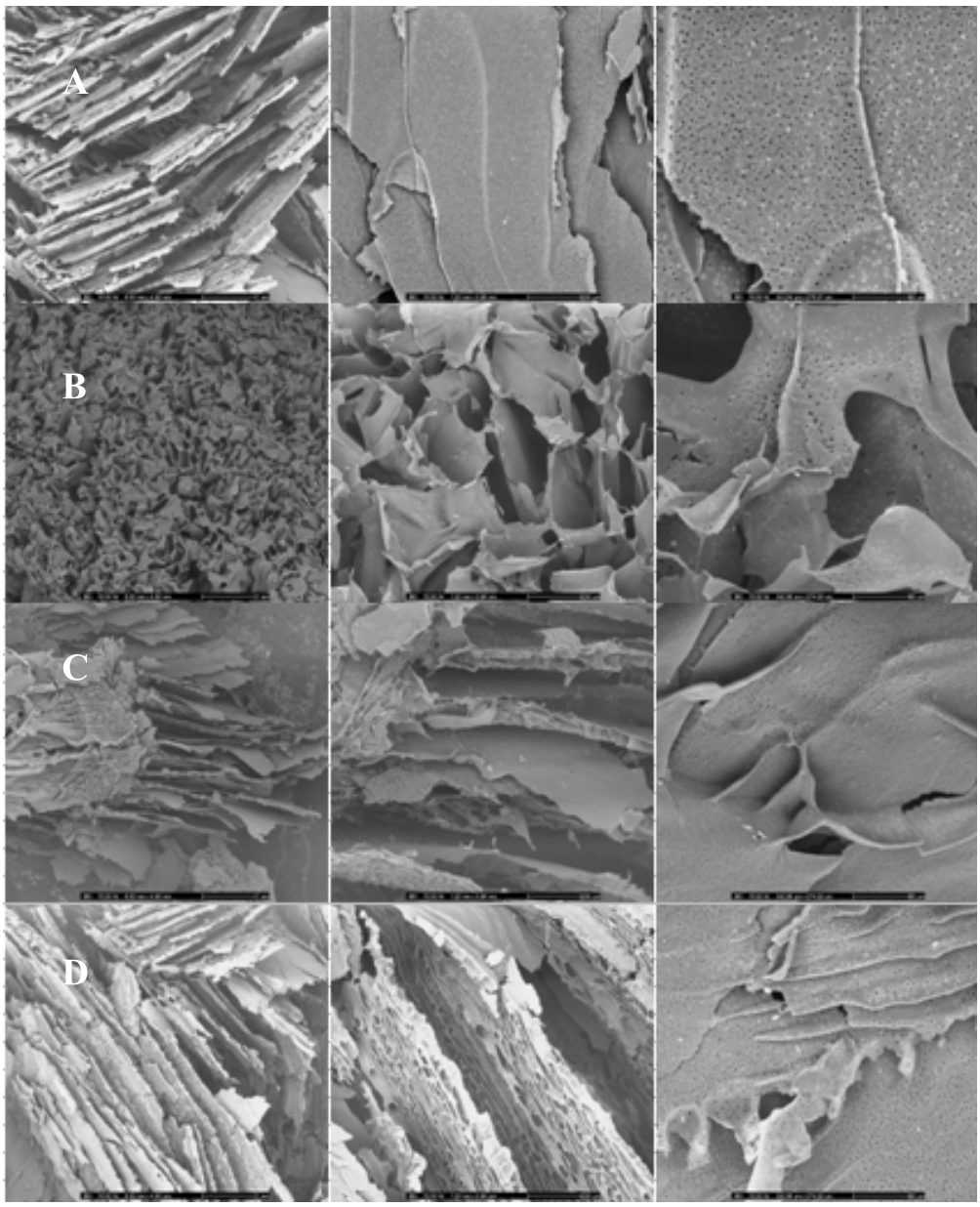

Figure 61 SEM micrographs of 20%w/w Lutrol® F127 systems containing 20%w/w NMP, 5%w/w doxycycline hyclate and different amount of ZnO after release test for 216 hours in phosphate buffer pH 7.2 with different magnifications; (A) 0.5%w/w ZnO; (B) 1%w/w ZnO; (C) 2%w/w ZnO and (D) 5%w/w ZnO.

8. Analysis of the drug release data

Large value of coefficient of determination (r^2) or model selection criteria (msc) indicated a superiority of the release profile fitting to mathematical equations. The r^2 and msc from curve fitting to power law, first order, Higuchi's and zero order equations are shown in Table 31. From curve fitting, the drug release data of the Lutrol F127® system containing 5% w/w doxyxycline hyclate with or without 20% w/w NMP were fitted well with first order model since r^2 and msc from curve fitting were higher than Higuchi's model and zero order curve fitting. The release data of gels containing different amount of ZnO were fitted well on power law equation since, r^2 and msc of curve fitting to Power law model were higher than those fitting to first order and zero order (Table 31). The estimate parameters from curve fitting to power law equation are shown in Table 32. By comparison, the drug release rate (k) following power law kinetic of gel containing ZnO of 5% was slower than that containing ZnO of 2%, 1% and 0.5%, respectively. From the n values of the prepared gel containing ZnO of 0% and 0.5% which were also near to 0.45 indicated that the drug release should also follow Fickian diffusion. On the other hand, the n values of the prepared gel containing ZnO of 1% were 0.63, indicated that the drug release should also follow anomalous (non-Fickian) transport. However, the n values of the prepared gel containing ZnO of 2% and 5% were 1.04 and 1.18, respectively, indicated that the drug release should also follow Case-II transport and Super case-II transport, respectively.

The release profiles of drugs from Pluronic® F127 gels have been reported (Lu and Jun, 1998; Suh and Jun, 1996). Most of these studies have examined the diffusion of drug out of the gel in either aqueous or non-aqueous media, and with or without an intervening membrane. In general, these systems showed that drug released follows the Higuchi square root low (Higuchi, 1962), and that the diffusion coefficients of the drug in the gel decrease with increasing Pluronic® F127 content, which was consistent with a consequent increase in bulk viscosity and gel rigidity. In many applications of controlled drug delivery, a constant drug release rate or zero order delivery is desired. Fickian release, which is the usual diffusion-controlled release from drug delivery systems, has a rate of drug release that decreased as a function of time, due to a decrease in the concentration gradient. Where the rate of dissolution of the polymer matrix controls the drug release rate (Lee and Peppas, 1987), zero-order release is observed

(Mallapragada *et al*., 1997). The decrease in the diffusion rate of drug with time due to decrease in concentration gradient can be offset by an increase in the release rate due to gel dissolution.

Moore *et al.* (2000) suggested that the drug release of the Pluronic® F127 systems were zero order, and the drug release was controlled by gel dissolution rather than by drug diffusion. The addition of inorganic salts had no significant effect on dissolution rate or drug release. Increasing F127 concentration in the gel decreased gel dissolution and drug release rate. The zero-order drug release rate was not influenced by the properties of the drug and was dependent solely on the gel dissolution rate. Esposito *et al*. (1997) investigated the mechanism of drug release from the poloxamer gel indicated that was anomalous (non-Fickian) release process.

In our studies, it was indicated that the increased zinc oxide amounts decreased the drug release rate (k) therefore zinc oxide could be sustained the doxycycline hyclate release from the Lutrol® F127 systems.

Table 31 Comparison of degree of goodness-of-fit from curve fitting of the release profiles of doxycycline hyclate in phosphate buffer pH 7.2 to different release models.

Formula	**Power law**		**First order**		**Higuchi's**		**Zero order**	
	r^2	**msc**	**r^2**	**msc**	**r^2**	**msc**	**r^2**	**msc**
Doxycycline hyclate solution	0.9788	3.19	0.9163	2.04	0.5838	0.43	0.9734	3.18
Doxycycline hyclate containing 20% Lutrol® F127 without NMP	0.9488	2.42	0.9870	3.98	0.9488	2.61	0.8314	1.42
Doxycycline hyclate containing 20% Lutrol® F127 and 20% NMP								
ZnO 0.0%	0.9850	3.70	0.9921	4.51	0.9605	2.90	0.9285	2.31
ZnO 0.5%	0.9759	3.37	0.8535	1.69	0.9700	3.27	0.7753	1.26
ZnO 1.0%	0.9880	3.88	0.9699	3.14	0.9410	2.47	0.9456	2.55
ZnO 2.0%	0.9933	4.27	0.9150	1.96	0.6582	0.57	0.9921	4.35
ZnO 5.0%	0.8770	0.90	0.7337	0.52	0.6021	0.12	0.8625	1.18

Table 32 Estimate parameter from curve fitting of drug release in phosphate buffer pH 7.2 to power law expression.

Formula	k ± sd*10^{-1}	tl ± sd (min)	n ± sd
Doxycycline hyclate solution	0.0051 ± 0.0112	-12.57 ± 45.78	1.29 ± 0.35
Doxycycline hyclate containing 20% Lutrol® F127 without NMP	0.3683 ± 0.1964	13.67 ± 19.74	0.50 ± 0.08
Doxycycline hyclate containing 20% Lutrol® F127 and 20% NMP			
ZnO 0.0%	0.4251 ± 0.0967	10.98 ± 4.27	0.50 ± 0.04
ZnO 0.5%	0.1029 ± 0.0300	300.00 ± 93.66	0.44 ± 0.03
ZnO 1.0%	0.0162 ± 0.0113	300.00 ± 367.37	0.63 ± 0.07
ZnO 2.0%	0.0013 ± 0.0023	300.00 ± 371.85	1.04 ± 0.21
ZnO 5.0%	0.0005 ± 0.0084	300.00 ± 3890.66	1.18 ± 1.92

k = release rate; tl = lag time and n = diffusional exponent

CHAPTER V

CONCLUSION

The characterization of zinc oxide with DSC and FT-IR indicated that the physicochemical properties were not different for different types of zinc oxide. SEM-EDS study indicated the tetrapod I and II ZnO were four needle-like arms with pyramidal tips that were different from the others type. However, EDS analysis implied the different shapes of ZnO could release the different energy after activation, indicating the arrangement of molecules. The particle size affected the antibacterial activity of zinc oxide, whereas the antifungal activity was less affected by the particle size. The physical properties of the gel systems depended on the ingredients which were added into the systems. The Lutrol® F127 system was Newtonian flow at low temperature (4°C), and altered be non-Newtonian flow when the temperature was increased. The NMP, biocompatible solvent, was used in this system. The amount of NMP affected the thermosensitive property of the Lutrol® F127. The amount of NMP ≥ 60% reversed the phase of the Lutrol® F127 system that were non-Newtonian flow at 4°C and were Newtonian at high temperature. The gelation temperature of the Lutrol® F127 was decreased as the amount of zinc oxide was increased. Whereas the gelation temperature of the Lutrol® F127 was increased as the amount of doxycycline hyclate was increased. All flow behavior of the Lutrol® F127 systems containing zinc oxide were Newtonian flow at 4°C, and were non-Newtonian flow at high temperature (27 and 37°C). The amount of doxycycline hyclate affected the flow behaviors of the Lutrol® F127 systems. The Lutrol® F127 systems comprising doxycycline hyclate ≥ 7.5% were still Newtonian flow at high temperature (27°C), whereas the added 20% NMP into the Lutrol® F127 system containing ≤ 7.5% doxyxcycline hyclate were non-Newtonian flow. However, the flow behavior of the 5% doxycycline hyclate-Lutrol® F127 systems comprising 20% NMP and zinc oxide were Newtonian flow at 4°C, and were non-Newtonian flow at high temperature (27°C and 37°C). The increased zinc oxide amount into the doxycycline hyclate-Lutrol® F127 systems decreased the inhibition zone diameters against all microbes due to zinc oxide affected to diffusion of drug from gels. Whereas the direct contaction method, the antimicrobial activity of

doxycycline hyclate-Lutrol® F127 systems comprising with 20% NMP were increased with the amount of zinc oxide were increased. For the rheology study, the increased of zinc oxide in the doxycycline hyclate-Lutrol® F127 systems increased its viscosity and reduced the drug release rate. The morphology of freeze-dried Lutrol® F127 system was continuous cell and pore surface, whereas the addition of doxycycline hyclate changed the structure of Lutrol® F127 that was the continuous cell and the surface was smooth. The sizes of continuous cells were decreased with an increase of zinc oxide contents and the structure was more compact and smaller. However, the structures of the Lutrol® F127 systems comprising zinc oxide after the release study were the fragile continuous cells and the surfaces were small pores. The surface structures of these systems were compacted. The syringeability of the doxycycline hyclate-Lutrol® F127 system were increased as the amount of zinc oxide was increased, however the syringeability of them were decreased as the temperature was decreased. The release of doxycycline hyclate from Lutrol® F127 system were fitted well with first order model, whereas the systems incorporated with 0.5% w/w zinc oxide followed the anomalous (non-Fickian) transport. Whereas, the increasing amount of zinc oxide to 2% and 5% altered the drug release to Case-II transport and Super case-II transport, respectively. However, the power law kinetic implied that the drug release rate was decreased as the amount of zinc oxide was increased. Therefore zinc oxide could be sustained the doxycycline hyclate release from the Lutrol® F127 systems.

In conclusion, the development of thermosensitive gel of doxycycline hyclate with containing zinc oxide was successful. The added NMP could modify the thermosensitive property of the doxycycline hyclate-Lutrol F127® systems comprising zinc oxide. System comprising zinc oxide could prolong the release of doxycycline hyclate from Lutrol® F127 systems and could be delivered from a syringe through a needle for utilizing in periodontitis therapy at the periodontal pocket.

BIBLIOGRAPHY

Addy, M, Langeroudi, M. "Comparison of the immediate effects on the sub-gingival microflora of acrylic strips containing 40% chlorhexidine, metronidazole or tetracycline." J. Clin. Periodontol. 11 (1984) : 379 – 386.

Ahuja, A., Ali, J., Rahman, S. "Biodegradable periodontal intrapocket device containing metronidazole and amoxycillin: formulation and characterization." Pharmazie. 61(1) (2006) : 25 – 29.

Akhter, S., Barry, B.W. "Absorption through human skin of ibuprofen and flurbiprofen; effect of dose variation, deposited drug film, occlusion and the penetration enhancer N-methyl-2-pyrrolidone." J. Pharm. Pharmacol. 37 (1985) : 27 - 37.

Alexander, M.B., Damoulis, P.D. "The role of cytokines in the pathogenesis of periodontal disease." Curr. Opin. Periodontol. (1994) : 39 - 53.

Alexandridis, P., Hatton, T.A. "Poly(ethylene oxide)-poly(propylene oxide)-poly(ethylene oxide) block copolymer surfactants in aqueous solutions and at interfaces:thermodynamics, structure, dynamics, and modeling." Colloids Surf. A. 96 (1995) : 1 - 46.

Alxandridis, P., Holtzwarth, J.F., Hatton, T.A. "Micellization of poly (ethylene oxide)-poly (propyleneoxide) poly (ethylene oxide) triblock copolymers in aqueous solutions: thermodynamics of copolymer association." Macromol. 27 (1994) : 2414 - 2425.

Attwood, D., Collett, J.H., Tait, C.J. "The micellar properties of the poly(oxyethylene)-poly(oxypropylene) copolymer Pluronic F 127 in water and electrolyte solution." Int. J. Pharm. 26 (1985) : 25 - 33.

Bahadur, P., Pandya, K., Almgren, M. *et al*. "Effect of inorganic salts on the micellar behaviour of ethylene oxide-propylene oxide block copolymers in aqueous solution." Colloid. Polym. Sci. 271 (1993) : 657 - 667.

Baker, E.N., Rumballa, S.V., Anderson, B.F. "Transferrins: insights into structure and function from studies on lactoferrin." Trends Biochem. Sci. 12 (1987) : 350 - 353.

Barichello, J.M., Morishita, M., Takayama, K. *et al*. "Enhanced rectal absorption of insulin loaded Pluronic F-127 gels containing unsaturated fatty acids." Int. J. Pharm. 183(2) (1999) : 125 - 132.

Barnard, A.S., Xiao, Y., Cai, Z. "Modeling the shape and orientation of ZnO nanobelts. Chemical." Physics Letters 419 (2006) : 313 – 316.

Bentley, M.V.L.B., Marchetti, J.M., Ricardo, N. *et al.* "Influence of lecithin on some physical chemical properties of poloxamer gels: rheological, microscopic and in vitro permeation studies." Int. J. Pharm. 193 (1999) : 49 – 55.

Bohorquez, M., Koch, C., Trygstad, T. *et al*. "A study of the temperature-dependent micellization of Pluronic F127." J. Colloid Interf. Sci. 216(1) (1999) : 34 - 40.

Bollen, C.M., Quirynen, M. "Microbiological response to mechanical treatment in combination with adjunctive therapy." J. Periodontol. 67 (1996) : 1143 - 1158.

Brayner, R., Ferrari-Iliou, N., Bravois, N. "Toxicological impact studies based on *Escherichia coli* bacteria in ultrafine ZnO nanoparticles colloid medium." Nano. Lett. 6 (2006) : 866 - 870.

Bruschi, M.L. Jones, D.S., Panzeri, H. *et al*. "Semisolid systems containing propolis for the treatment of periodontal disease: in vitro release kinetics, syringeability, rheological, textural, and mucoadhesive properties." J. Pharm. Sci. 96 (2007) : 2074 – 2089.

Cassanho, A.C.A., Rernandes, A.M., Oliveira, L.D. *et al*. "In vitro activity of zinc oxide-eugenol and glass ionomer cements on *Candida albicans*." Braz. Oral Res. 19(2) (2005) : 134 - 138.

Castro L.J., Sahagún, A.M., Diez, M.J. *et al*. "Pharmacokinetics of doxycycline in sheep after intravenous and oral administration." Vet. J. 180(3) (2009) : 389 - 395.

Chang, J.Y., Oh, Y.K., Choi, H.G. *et al.* "Rheological evaluation of thermosensitive and mucoadhesive vaginal gels in physiological conditions." Int. J. Pharm. 241(1) (2002) : 155 - 163.

Charrueau, C., Tuleu, C., Astre, V. *et. al*. "Poloxamer 407 as a thermogelling and adhesive polymer for rectal administration of short-chain fatty acids." Drug Dev. Ind. Pharm. 27(4) (2001) : 351 - 357.

Choi, H., Lee, M., Kim, M. *et al*. "Effect of additives on the physicochemical properties of liquid suppository bases." Int. J. Pharm. 190(1) (1999): 13 - 19.

Choi, D.H., Moon, I.S., Choi, B.K. *et al*. "Effects of sub-antimicrobial dose doxycycline therapy on cervicular fluid MMP-2, and gingival tissue MMP-9, TIMP-1 and IL-6 levels in chronic periodontitis." J. Periodont. Res. 39 (2004) : 20 - 26.

Choopun, S., Hongsith, N., Mangkorntong, P. *et al*. "Zinc oxide nanobelts by RF sputtering for ethanol sensor." Physica. E. 39 (2007) : 53 - 56.

Coleman, N.J., Bishop, A.H., Booth, S.E. *et al*. "Ag^{+}- and Zn^{2+}-exchange kinetics and antimicrobial properties of 11Å tobermorites." J. Eur. Ceram. Soc. 29 (2009) : 1109 – 1117.

Degussa. Aerosil – Fumed silica [online]. Accessed February 2009. Available from http:/www.degussa.huls.com

Desai, P.R., Jain, N.J., Sharma, R.K. *et al*. "Effects of additives on micellization of PEO/PPO/PEO block copolymer F127 in aqueous solution." Colloids Surf. A: Physicochem. Eng. Aspects. 178 (2001) : 57 - 69.

Dimitrova, E., Bogdanova, S,. Mitcheva, M. *et al*. "Development of model aqueous ophthalmic solution of indomethacin." Drug Dev. Ind. Pharm 26(12) (2000) : 1297 - 1301.

Dumortier, G., Grossiord, J.L., Agnely, F. *et al*. "A Review of Poloxamer 407 Pharmaceutical and Pharmacological Characteristics." Pharm. Res. 23(12) 2006 : 2709 - 2728.

Dumortier, G., Grossiord, J.L., Zuber, M. *et al*. "Thermoreversible morphine gel." Drug Dev. Ind. Pharm. 17(9) (1991) : 1255 - 1265.

Edsman, K., Carlfors, J., Petersson, R. "Rheological evaluation of poloxamer as an in situ gel for ophthalmic use." Eur. J. Pharm. Sci. 6 (1998) : 105 - 112.

Esposito, P., Ortesi, R., Cervellati, F. *et al*. "Biodegradable microparticles for sustained delivery of tetracycline to the periodontal pocket: formulatory and drug release studies." J. Microencapsul. 14 (1997): 175 – 187.

Fu, G., Vary, P.S., Lin, C.T. *et al.* "Anatase TiO_2 nanocomposites for antimicrobial coatings." J. Phys. Chem. B 109 (2005) : 8889 - 8898.

Gad, H.A., El-Nabarawi, M.A., El-Hady, S.S. "Formulation and Evaluation of PLA and PLGA In Situ Implants Containing Secnidazole and/or Doxycycline for Treatment of Periodontitis." AAPS PharmSciTech. 9 (2008) : 878 - 884.

Gapski, R., Barr, J.L., Sarment, D.P. *et al*. "Effect of systemic matrix metalloproteinase inhibition on periodontal wound repair: A proof of concept trial." J. Periodont. 75 (2004) : 441 – 452.

Gates, K.A., Grad, H., Birek, P. *et al*. "A new bioerodible polymer insert for a controlled release of metronidazole." Pharm. Res. 11(1994) : 1605 – 1609.

Gilbert, J.C., Richardson, J.L., Davies, M.C. *et al*. "The effect of solutes and polymers on the gelation properties of pluronic F-127 solutions for controlled drug delivery." J. Control. Rel. 5 (1987) : 113 - 118.

Gillissen, M., Streendam, R., Vanderlaan, A. *et al*. "Develpoment of doxycycline- eluting delivery systems based on SynBiosys™ biodegradable multi-block copolymers." J. Periodontol. 89 (2000) : 453 - 457.

Golomb, G., Friedman, M., Soskolne, A. *et al*. "Sustained release device containing metronidazole for periodontal use." J. Dent. Res. 63 (1984) : 1149 – 1153.

Goodson, J.M., Holborow, D., Dunn, R.L. *et al*. "Monolithic tetracycline-containing fibers for controlled delivery to periodontal pockets." J. Periodontol. 54 (1983) : 575 - 579.

Goodson, J.M., Haffajee., A., Socransky, S.S. "Periodontal therapy by local delivery of tetracycline." J. Clin. Periodontol. 6 (1979) : 83 – 92.

Greenstein, G. "Local drug delivery in the treatment of periodontal diseases: assessing the clinical significance of the results." J. Periodontol. 77 (2006) : 565 – 578.

Gui, Y., Xie, C., Zhang, Q., Hu, M. *et al*. "Synthesis and characterization of ZnO nanostructures by two-step oxidation of Zn nano- and microparticles." J. Cryst. Growth 289 (2006) : 663 – 669.

Guzman, M., Aberturas, M.R., Garcia, F. *et al*. "Gelatin gels and polyoxyethylene polyoxypropylene gels: comparative study of their properties." Drug Dev. Ind. Pharm. 20 (1994) : 2041 - 2048.

Haffajee, A.D., Socransky, S.S. "Attachment level changes in destructive periodontal diseases." J. Clin. Periodontol. 13 (1986) : 461 – 472.

Hansen, C.M., Just, L. "Prediction of environmental stress cracking in plastics with Hansen solubility parameters." Ind. Eng. Chem. Res. 40 (2001) : 21 – 25.

He, Z.,. Chen, M., Wang, R. *et al.* "The Complex with Doxycycline and Hydroxypropyl-cyclodextrin in Thermal Sensitive Hydrogel for Ophthalmic Delivery." AAPS PharmSciTech. 9 (2008) : 1287 - 1292.

Higashi, K., Morisaki, K., Hayashi, S. *et al*. "Local ofloxacin delivery using a controlled release insert (PT-01) in the human periodontal pocket." J. Periodontol. Res. 25 (1990) : 1 – 5.

Higuchi, W.I. "Analysis of data on medicament release from ointments." J. Pharm. Sci. 51 (1962) : 802 – 804.

Higuchi, T. "Mechanism of sustained-action medication. Theoretical analysis of rate of release of solid drugs dispersed in solid matrices." J. Pharm. Sci. 52 (1963) : 1145 – 1149.

Huang, K., Lee, B.P., Ingram, D.R. *et al*. "Synthesis and characterization of self-assembling block copolymers containing bioadhesive end groups." Biomacromol. 3(2) (2002) : 397 - 406.

Iqbal, Z., Jain, N., Jain, G.K. *et al*. "Dental therapeutic systems." Recent Pat Drug Deliv. Formul. 2 (1) (2008) : 58 – 67.

Ivanova, R., Alexandridis, P., Lindman, B. "Interaction of poloxamers block copolymers with cosolvents and surfactants." Colloids Surf. A. Physic. Eng. Aspects. 183-185 (2001) : 41 - 53.

Ivanova, R., Lindman, B., Alexandridis, P. "Effect of Pharmaceutically Acceptable Glycols on the Stability of the Liquid Crystalline Gels Formed by Poloxamer 407 in Water." J. Colloid Interf. Sci. 252(1) (2002) : 226 - 235.

Jain, N., Jain, G.K., Javed, S. *et al.* "Recent approaches for the treatment of periodontitis." Drug Discov. Today 13(21-22) (2008) : 932 - 943.

Jeong, B., Kim, S.W., Bae, Y.H. "Thermosensitive sol–gel reversible hydrogels." Adv. Drug Deliv. Rev. 54 (2002) : 37 – 51.

Jeong, B., Lee, D.S., Shon, J.I. *et al*. "Thermoreversible gelation of poly(ethylene oxide) biodegradable polyester block copolymers." J. Polym. Sci. Polym. Chem. 37 (1999) : 751 – 760.

Jones, D.S., Woolfson, A.D., Djokic, J. *et al*. "Development and mechanical characterization of bioadhesive semi-solid, polymeric systems containing tetracycline for the treatment of periodontal diseases." Pharm. Res. 13 (1996) : 1734 - 1738.

Jones, D.S., Woolfson, A.D., Brown, A.F. *et al*. "Mucoadhesive, syringeable drug delivery systems for controlled application of metronidazole to the periodontal pocket: in vitro

release kinetics, syringeability, mechanical and mucoadhesive properties." J. Control. Rel. 4 (1997) : 71 – 79.

Jorgenson, E.B., Hvidt, S., Schillen, K. *et al*. "Effects of salts on micellization and gelation of triblock copolymer studied by rheology and light scattering." Macromol. 30 (1997) : 2355 - 2364.

Juhasz, J., Lenaerts, V., Raymond, P. *et al*. "Diffusion of rat atrial natriuretic factor in thermoreversible poloxamer gels." Biomater. 10(4) (1989) : 265 - 268.

Junior, S.J.F., Favieri, A., Gahyva, S.M. *et al*. "Antimicrobial activity and flow rate of newer and established root canal sealers." J. Endod. 26 (2000) : 274 - 277.

Kelly, H.M., Deasy, P.B., Ziaka, E. *et al*. "Formulation and preliminary in vivo dog studies of a novel drug delivery system for the treatment of periodontitis." Int. J. Pharm. 274 (2004) : 167 - 183.

Khattar, J.A., Musharrafieh, M., Tamim, H. "Topical zinc oxide vs. salicylic acid–lactic acid combination in the treatment of warts." Int. J. Dermatol. 46(4) (2007) : 427 - 430.

Koizumi, A., Fujii, M., Kondoh, M. *et al*. "Effect of N-methyl-2-pyrrolidone on skin permeation of estradiol." Eur. J. Pharma. Biopharm. 57(3) (2004) : 473 - 478.

Kranz, H., Bodmeier, R. "Structure formation and characterization of injectable drug loaded biodegradable devices: In situ implants versus in situ microparticles." Eur. J. Pharm. Sci. 34(2-3) (2008) : 164 - 172.

Kumari, P.G., Venkatesu, P., Rao, M.V.P. *et al*. "Excess molar volumes and ultrasonic studies of N-methyl-2-pyrrolidone with ketones at T = 303.15 K." J. Chem. Thermodyn. 41 (2009) : 586 – 590.

Kumar, P.S., Raj, A.D., Mangalaraj, D. *et al*. "Growth and characterization of ZnO nanostructured thin films by a two step chemical method." Appl. Surf. Sci. 255 (2008) : 2382 – 2387.

Lee, P.I., Peppas, N.A. "Prediction of polymer dissolution in swellable controlled-release systems." J. Control. Rel. 6 (1987) : 201 – 215.

Leung, Y.H., Djurišic, A.B., Gao, J. *et al*. "Zinc oxide ribbon and comb structures: synthesis and optical properties." Chem. Phys. Lett. 394 (2004) : 452 - 457.

Listgarten, M.A. “Nature of periodontal diseases: pathogenic mechanisms.” J. Periodontol Res. 22 (1987) : 172 – 178.

Lim, Y.S., Park, J.W., Hong, S.T. *et al*. “Carbothermal synthesis of ZnO nanocomb structure.” Mat. Sci. Eng. B. 129 (2006) : 100 - 103.

Liu, T., Chu., B. “Formation of homogeneous gel-like phases by mixed triblock copolymer micelles in aqueous solution: FCC to BCC phase transition.” J. Appl. Cryst 33 (2000) : 727 - 730.

Lu, G., Jun, H.W. “Diffusion studies of methotrexate in Carbopol and poloxamer gels.” Int. J. Pharm. 160 (1998) : 1 – 9.

Maheshwari, M., Paradkar, A., Yamamura, S., *et al*. “Preparation and Characterization of Pluronic–Colloidal Silicon Dioxide Composite Particles as Liquid Crystal Precursor.” AAPS PharmSciTech. 7(4) (2006) : E1 - E7.

Maheshwari, M., Miglani,G., Mali, A. *et al*. “Development of tetracycline-serratiopeptidase-containing periodontal gel: formulation and preliminary clinical study.” AAPS PharmSciTech. 7(3) (2006) : E1 - E10.

Mallapragada, S.K., Peppas, N.A., Colombo, P. “Crystal dissolution-controlled release systems: II. Metronidazole release from semicrystalline poly(vinyl alcohol).” J. Biomed. Mater. Res. 36 (1997) : 125 – 130.

Malmsten M., Lindman B. “Self-assembly in aqueous block copolymer solutions.” Macromol. 25 (1992) : 5440 - 5445.

Marriott, C. Rheology and flow of fluids. In: Aulton ME, ed. Pharmaceutics: The Science of Dosage Form Design. New York, NY: Churchill Livingstone; 1988, pp. 264 - 287.

Marsh, P.D. “Host defences and microbial homeostasis: role of microbial interactions.” J. Dent. Res. 68 (1989) : 1567 - 1575.

Martin, A. Physical Pharmacy. Philadelphia, PA: Lea and Febiger; 1993 : 393 – 422.

Martindale: The complete drug reference, 34th edition; The Pharmceutical Press, Grayslake, USA; 2005, pp. 206 - 207.

Maze, G.I. Reinhardt, R.A., Agarwal, R.K. *et al*. “Response to intracrevicular controlled delivery of 25% tetracycline from poly(lactide:glycolide) film strips in SPT patients.” J. Clin.Periodontol. 22 (1995) : 860 - 867.

McDonald, C., Wong, C.K. “The effect of temperature on the micellar properties of a polyoxyethylene-polyoxypropylene polymer in water.” J. Pharm. Pharmacol. 26 (1974) : 556 - 557.

MicroMath Scientist Handbook Rev. 7EEF, MicroMath: Salt Lake City, 1995, pp: 467.

Miller, S.C., Donovan, M.D. “Effect of poloxamer 407 gel on the miotic activity of pilocarpine nitrate in rabbits.” Int. J. Pharm. 12 (1982) : 147 - 152.

Miller, S.C., Drabik, B.R. “Rheological properties of poloxamer vehicles.” Int. J. Pharm. 18 (1984) : 269 - 276.

Miyazaki, S., Tobiyama, T., Takada, M. *et al.* “Percutaneous absorption of indomethacin from Pluronic F127 gels in rats.” J. Pharm. Pharmacol. 47 (1995) : 455 – 457.

Moore, T., Croy, S., Mallapragad, S. *et al*. “Experimental investigation and mathematical modeling of Pluronic F127 gel dissolution: drug release in stirred systems.” J. Control. Rel. 67 (2000) : 191 – 202.

Morishita, M., Barichello, J.M., Takayama, K., *et al*. “Pluronic F-127 gels incorporating highly purified unsaturated fatty acids for buccal delivery of insulin.” Int. J. Pharm. 212(2) (2001) : 289 - 293.

Mortensen, K., Brown, W., Norde´n, B. “Inverse melting transition and evidence of three-dimensional cubatic structure in a block-copolymer micellar system.” Phys. Rev. Lett. 68 (1992) : 2340 - 2343.

Mungkornasawakul, P, Rattanakit, N., Sirita, J. *et al.* “Antimicrobial zinc oxide nanoparticle.” 31st Congress on Science and Technology of Thailand at Suranaree University of Technology (2005), pp. 1 - 3.

Noyan, U., Yilmaz, S., Kuru, B. *et al*. “A clinical and microbiological evaluation of systemic and local metronidazole delivery in adult periodontitis patients.” J. Clin. Periodontol. 24 (1997) : 158 – 165.

Olivieri, L., Seiller, M., Bromberg, L. *et al*. “Optimization of a thermally reversible W/O/W multiple emulsion for shear-induced drug release.” J. Control. Rel. 88(3) (2003) : 401 - 412.

Paolantonio, M. Dangelo, M., Grassi, R. *et al*. "Clinical and microbiologic effects of subgingival controlled-release delivery of chlorhexidine chip in the treatment of periodontitis: a multicenter study." J. Periodontol. 79 (2008) : 271 – 282.

Paquette, D.W., Waters, G.S., Stefanidou, V.L., *et al*. "Inhibition of experimental gingivitis in beagle dogs with topical salivary histatins." J. Clin. Periodontol. 24 (1997) : 216 - 222.

Pandit, N., Trygstad, T., Croy, S. *et al*. "Effect of salts on the micellization, clouding, and solubilization behavior of Pluronic F127 solutions." J. Colloid Interf. Sci. 222 (2) (2000) : 213 - 220.

Pandit, N.K., Wang, D. "Salt effects on the diffusion and release rate of propranolol from poloxamer 407 gels." Int. J. Pharm. 167 (1998) : 183 - 189.

Peppas, N.A. "Analysis of Fickian and non-Fickian drug release from polymers." Pharm. Acta. Helv. 60 (1985) : 110 – 111.

Pisal, S.S., Paradkar, A.R., Mahadik, K.R. *et al*. "Pluronic gels for nasal delivery of Vitamin B12. Part I: preformulation study." Int. J. Pharm. 270 (2004) : 37 - 45.

Pitcher, G.R., Newman, H.N., Strahan, J.D. "Access to subgingival plaque by disclosing agents using mouthrinsing and direct irrigation." J. Clin. Periodontol. 7 (1980) : 300 – 308.

Polson, A.M., Garrett, S., Stoller, N.H. *et al*. "Multi-center comparative evaluation of subgingivally delivered sanguinarine and doxycycline in the treatment of periodontitis. II. Clinical results." J. Periodontol. 68 (1997) : 119 – 126.

Polson, A.M., Garrett, S., Stoller, N.H. *et al*. "Multi-center comparative evaluation of subgingivally delivered sanguinarine and doxycycline in the treatment of periodontitis II. Clinical results." J. Periodontol. 68 (1997) : 119 – 126.

Rassing, J., Atwood, D. "Ultrasonic velocity and light scattering studies on polyoxyethylene-polyoxypropylene copolymer pluronic F-127 in aqueous solution." Int. J. Pharm. 13 (1983) : 47 - 55.

Remington, Alfonso R. The science and practice of pharmacy, Easton, USA, Mack Pub. Co., 2000, pp. 1207.

Reynolds, J.J., Meikle, M.C. "Mechanisms of connective tissue matrix destruction in periodontitis." Periodontol. (1997) : 144 - 157.

Rhee, Y.S., Shin, Y.H., Park, C.W. *et al*. "Effect of flavors on the viscosity and gelling point of aqueous poloxamer solution." Arch. Pharm.Res. 29(12) (2006) : 1171 - 1178.

Ritger, P.I., Peppas, N.A. "A simple equation for description of solute release. I. Fickian and non-Fickian release from non-swellable devices in the form of slabs, spheres, cylinders or discs." J. Control. Rel. 5 (1987) : 23 – 26.

Sa, T., Colombo, P., Catellani, P.L. *et al*. "Swelling characteristics of hydrophilic matrices for controlled release: new dimensionless number to describe the swelling and release behaviour." Int. J. Pharm. 88 (1990) : 99 – 109.

Sasaki, H., Kojima, M., Mori, Y. *et al*. "Acute toxicity and skin irritation of pyrrolidone derivatives as transdermal penetration enhancer." Chem. Pharm. Bull 38 (1990) : 2308 - 2310.

Sasaki, H., Kojima, M., Nakamura, J. *et al*. "Enhancing effect of pyrrolidone derivatives on transdermal drug delivery I." Int. J. Pharm. 44 (1988) : 15 - 24.

Sauvetre, E., Glupczynsky, Y., Yourassowsky, E. *et al*. "The effect of clindamycin gel insert in periodontal pockets, as observed on smears and cultures." Infect. 21(1993) : 245 - 247.

Sawai, J. "Quantitative evaluation of antibacterial activities of metallic oxide powders (ZnO, MgO and CaO) by conductimetric assay." J. Microbiol. Meth. 54 (2003) : 177 - 182.

Sawai, J., Shoji, S., Igarashi, H., *et al*. "Hydrogen Peroxide as an Antibacterial Factor in Zinc Oxide Powder Slurry." J. Ferment. Bioengineer. 86(5) (1998) : 521 - 522.

Sawai, J., Kawada, E., Kanou, F. *et al*. "Detection of active oxygen generated from ceramic powders having antibacterial activity." J. Chem. Eng. Jpn. 29(4) (1996) : 627 – 633.

Sawai, J., Kojima, H., Igarashi, H. *et al*. "Escherichia coli damage by ceramic powder slurries." J. Chem. Eng. Jpn. 30(6) (1997) :1034 – 1039.

Scherlund, M., Malmsten, M., Holmqvist, P. *et al*. "Thermosetting microemulsions and mixed micellar solutions as drug delivery systems for periodontal anesthesia." Int. J. Pharm. 194 (2000) : 103 - 116.

Schmolka, I.R. "Artificial skin I. preparation and properties of pluronic F-127 gels for treatment of burns." J. Biomed. Mater. Res. 6(6) (1972) : 571 - 582.

Schwach, A.K., Vivien, C.N., Gurny, R. "Local delivery of antimicrobial agents for the treatment of periodontal diseases." Eur. J. Pharm. Biopharm. 50 (2000) : 83 - 99.

Schwartz, J.B., Simonelli, A.P., Higuchi, W. “Drug release from wax matrices.” J. Control. Rel. 29 (1968) : 32 – 45.

Seymour, R.A., Heasman, P.A. “Tetracyclines in the management of periodontal diseases: a review.” J. Clin. Periodontol. 22 (1995) : 22 - 35.

Shane, S.M. “Infectious diseases and parasites of ratites.” Vet. Clin. North. Am. Food Anim. Pract. 14 (1998) : 455 - 483.

Shawesh, A., Kallioinen, S., Antikainen, O. *et al*. “Influence of storage time and temperature on the stability of indomethacin Pluronic F-127 gels.” Pharmazie. 57(10) (2002) : 690 - 694.

Shin, S.C., Cho, C.W. “Physicochemical characterizations of piroxicam-poloxamer solid dispersion.” Pharm. Dev. Technol. 2(4) (1997) : 403 - 407.

Slots, J., Rams, T.E. “Antibiotics in periodontal therapy: advantages and disadvantages.” J. Clin. Periodontol. 17 (1990) : 479 – 493.

Stratton, C.W., Lorian, V. Mechanisms of action for antimicrobial agents: general principals and mechanisms for selected classes of antibiotics, antibiotics in laboratory medicine, 4th ed.,Williams &Wilkins, Baltimore, 1996, pp. 579 - 603.

Stratton, L.P., Dong, A., Manning, M. *et al*. “Drug delivery matrix containing native protein precipitates suspended in a poloxamer gel.” J. Pharm. Sci. 86 (1997) :1006 - 1010.

Stoimenov, P.K., Klinger, R.L., Marchin, G.L. *et al*. “Metal oxide nanoparticles as bactericidal agents.” Lang. 18(17) (2002) : 6679 – 6686.

Suh, H., Jun, H.W. “Physicochemical and release studies of naproxen in poloxamer gels.” Int. J. Pharm. 129 (1996) : 13 – 20.

Takeuchi, H., Nagira, S., Yamamoto, H. *et al*. “Solid dispersion particles of tolbutamide prepared with fine silica particles by the spray-drying method.” Powder Technol. 141(3) (2004) : 187 - 195.

Tam, K.H., Djurišic, A.B., Chan, C.M.N. *et al* “Antibacterial activity of ZnO nanorods prepared by a hydrothermal method.” Thin Sol. Films 516 (2008) : 6167 – 6174.

Tan, Y.T.F., Peh, K.K., Al-Hanbali, O. “Effect of carbopol and polyvinylpyrrolidone on the mechanical, rheological, and release properties of bioadhesive polyethylene glycol gels.” AAPS PharmSciTech. 1(3)(24) (2000) :1 - 10.

The pharmaceutical Codex 12th edition, Principles and practice of pharmaceutics, The Pharmaceutical Press, London,1994, pp. 850 - 852.

Tonetti, M.S., Pini-Prato, G., Cortellini, P. "Principles and clinical applications of periodontal controlled drug delivery with tetracycline fibers." Int. J. Periodontol. Res. Dent. 14 (1994) : 421 - 435.

Tonetti, M., Cugini, M.A., Goodson, J.M. "Zero-order delivery with periodontal placement of tetracycline-loaded ethylene vinyl acetate fibres." J. Periodontol. Res. 25 (1990) : 243 – 249.

Vadnere, M., Amidon, G., Lindenbaum, S. *et al*. "Thermodynamic studies on the sol-gel transition of som pluronic polyols." Int. J. Pharm. 22 (1984) : 207 - 218.

Vernardou, D., Kenanakis, G., Couris, S. *et al*. "pH effect on the morphology of ZnO nanostructures grown with aqueous chemical growth." Thin Sol. Films 515 (2007) : 8764 - 8767.

Veyries, M.L., Couarraze, G., Geiger, S. *et al*. "Controlled release of vancomycin from poloxamer 407 gels." Int. J. Pharm. 192(2) (1999) : 183 - 193.

Vyas, S.P., Sihorkar, V., Mishra, V. "Controlled and targeted drug delivery strategies towards intra periodontal pocket diseases." J. Clin. Pharm. Ther. 25 (2005) : 21 – 42.

Wang, J.X., Wen, L.X., Wang, Z.H. *et al*. "Immobilization of silver on hollow silica nanospheres and nanotubes and their antibacterial effects." Mater. Chem. Phys. 96(1) (2006) : 90 – 97.

Wang, P., Johnston, T.P. "Enhanced stability of two model proteins in an agitated solution environment using poloxamer 407." J. Parenter. Sci. Technol. 47 (1993) : 183 - 189.

Wang, Z.L. "Nanostructures of zinc oxide." Mater. Today. (2004) : 26 - 33.

Wanka, G., Hoffmann, H., Ulbricht, W. "The aggregation behavior of poly(oxyethylene)-poly(propylene oxide)-poly(ethylene oxide) block copolymers in aqueous solution." Colloid Polym. Sci. 268 (1990) : 101 - 117.

Wanka, G., Hoffmann, H., Ulbricht, W. "Phase diagrams and aggregation behavior of poly(oxyethylene)-poly (oxypropylene)-poly (oxyethylene) triblock coplymers in aqueous solutions." Macromol. 27 (1990) : 4115 - 4159.

Wenzel, J.G., Balaji, K.S., Koushik, K., *et al*. "Pluronic F127 gel formulations of deslorelin and GnRH reduce drug degradation and sustain drug release and effect in cattle." J. Control. Rel. 85 (2002) : 51 - 59.

Yamamoto, O. "Influence of particle size on the antibacterial activity of zinc oxide." Int. J. Inorg. Mat. 3 (2001) : 643 - 646.

Yamamoto, O., Hotta, M., Sawai, J., *et al*. "Influence of powder characteristic of ZnO on antibacterial activity – effect of specific surface area." J. Ceramic. Soc. Jpn. 106 (10) (1998) :1007 - 1011.

Yamamoto, O., Iida, Y. "Antifungal characteristics of spherical carbon materials with zinc oxide." J. Ceram. Soc. Jpn. 111(8) (2003) : 614 - 616.

Yoneto, K., Ghanem, A.H., Higuchi, W.I. *et al.* "Mechanistic studies of the 1-alkyl-2-pyrrolidones as skin permeation enhancers." J. Pharm. Sci. 84 (1995) : 312 - 317.

Yoneto, K., Li, S.K., Higuchi, W.I. *et al.* "Influence of the permeation enhancers 1-alkyl-2-pyrrolidones on permeant partitioning into the stratum corneum." J. Pharm. Sci. 87 (1997) : 209 - 214.

Yong, C.S., Choi, J., Quan, Q.Z. *et al*. "Effect of sodium chloride on the gelation temperature, gel strength and bioadhesive force of poloxamer gels containing diclofenac sodium." Int. J. Pharm. 226 (1-2) (2001) : 195 - 205.

Yong, C.S., Oh. Y.K., Jung, S.H. *et al*. "Preparation of ibuprofen-loaded liquid suppository using eutectic mixture system with mentol." Eur. J. Pharm. Sci. 23 (2004) : 347 - 353.

Yu, Z., Ramamurthy, N.S., Leung, M. *et al*. "Chemically-modifed tetracycline normalizes collagen metabolism in diabetic rats; A dose-response study." J. Periodontol. Res. 28 (1993) : 420 - 428.

Zhang, L., Ding, Y., Povey, M. *et al*. "ZnO nanofluids - A potential antibacterial agent." Prog. Nat. Sci. 18 (2008) : 939 – 944.

APPENDICES

APPENDIX I

The particle size of various zinc oxide and colloidal silicon dioxide

Table 33 The particle size of various zinc oxide and colloidal silicon dioxide

	particle size (μm)							
	1		2		3		Mean	S.D.
	mean size	std.dev	mean size	std.dev	mean size	std.dev		
ZnO BP	**19.325**	**9.672**	**18.032**	**6.032**	**17.924**	**6.775**	**18.427**	**7.493**
micronized ZnO*	**4.752**	**2.987**	**4.373**	**2.926**	**4.182**	**2.760**	**4.436**	**2.891**
powder ZnO	**14.663**	**8.010**	**12.438**	**6.467**	**13.655**	**5.669**	**13.585**	**6.715**
tetrapod I	**32.524**	**22.725**	**31.017**	**19.222**	**35.674**	**21.467**	**33.072**	**21.138**
tetrapod II	**30.631**	**35.643**	**41.079**	**27.704**	**40.524**	**29.274**	**37.411**	**30.874**
Aerosil® 200	**52.472**	**34.983**	**54.963**	**26.230**	**50.810**	**32.616**	**52.748**	**31.276**
Aerosil® R972*	**95.990**	**71.298**	**85.862**	**56.943**	**87.051**	**64.834**	**89.634**	**64.358**

* dispersed in absolute ethanol

APPENDICES II

Table 34 The rheology data of the Lutrol® F127 systems containing different N-methyl-2-pyrrolidone at 4°C

(A)

Shear Rate	Shear Stress (D/cm²) NMP 0%					Shear Rate	Shear Stress (D/cm²) NMP 10%				
(s^{-1})	1	2	3	Mean	S.D.	(s^{-1})	1	2	3	Mean	S.D.
50	25.02	25.51	27.47	26.00	1.30	50	32.37	34.83	33.84	33.68	1.23
100	48.56	51.99	53.46	51.34	2.52	100	66.22	66.22	69.16	67.20	1.70
150	74.56	73.58	78.48	75.54	2.60	150	103.01	99.57	103.01	101.86	1.98
200	101.04	103.50	99.57	101.37	1.98	200	137.34	135.38	133.42	135.38	1.96
250	129.49	123.12	126.06	126.22	3.19	250	175.11	173.64	171.68	173.47	1.72
300	156.96	145.19	151.07	151.07	5.89	300	204.54	208.95	206.99	206.83	2.21
350	178.05	171.68	179.52	176.42	4.17	350	231.03	245.74	245.25	240.67	8.36
400	199.14	202.58	208.95	203.56	4.98	400	267.81	269.78	286.94	274.84	10.52
400	203.07	202.09	201.60	202.25	0.75	400	274.68	264.87	281.06	273.54	8.15
350	180.01	180.50	174.62	178.38	3.27	350	242.80	236.42	236.91	238.71	3.55
300	156.96	151.07	150.09	152.71	3.71	300	210.42	204.54	204.05	206.34	3.55
250	132.44	122.13	127.04	127.20	5.15	250	176.58	173.64	173.15	174.45	1.86
200	103.01	100.55	105.95	103.17	2.70	200	134.40	143.23	143.23	140.28	5.10
150	76.52	75.54	79.95	77.34	2.32	150	110.36	105.95	107.42	107.91	2.25
100	51.99	55.43	52.48	53.30	1.86	100	70.63	68.18	72.59	70.47	2.21
50	28.94	26.00	26.00	26.98	1.70	50	54.45	33.35	34.83	40.88	11.78

(B)

Shear Rate	Shear Stress (D/cm²) NMP 20%					Shear Rate	Shear Stress (D/cm²) NMP 30%				
(s^{-1})	1	2	3	Mean	S.D.	(s^{-1})	1	2	3	Mean	S.D.
50	51.99	52.48	54.45	52.97	1.30	10	2854.31	2857.54	2774.19	2828.68	47.22
100	102.02	104.97	105.95	104.31	2.04	20	3000.41	3210.76	3163.13	3124.77	110.30
150	153.04	155.49	155.98	154.83	1.58	30	3309.98	3436.98	3508.42	3418.46	100.51
200	202.09	206.01	207.97	205.36	3.00	40	3683.05	3536.20	3583.83	3601.02	74.92
250	251.63	257.51	258.49	255.88	3.71	50	3762.42	3655.26	3694.95	3704.21	54.18
300	302.64	310.00	311.96	308.20	4.91	60	3877.52	3782.27	3790.20	3816.66	52.85
350	353.16	360.52	361.99	358.56	4.73	70	3978.48	3885.46	3897.36	3920.43	50.62
400	402.70	410.06	412.02	408.26	4.91	80	4005.36	3960.86	3964.83	3977.02	24.63
400	406.62	411.04	412.02	409.89	2.87	80	4059.36	3964.83	3974.25	3999.48	52.07
350	357.08	360.52	361.99	359.86	2.52	70	3942.12	3877.52	3917.21	3912.28	32.58
300	306.56	311.96	310.98	309.83	2.87	60	3801.33	3798.14	3790.20	3796.56	5.73
250	255.06	260.46	261.93	259.15	3.62	50	3758.45	3675.11	3698.92	3710.83	42.93
200	203.56	206.01	209.44	206.34	2.96	40	3619.55	3571.92	3540.17	3577.21	39.95
150	154.02	155.49	155.98	155.16	1.02	30	3425.07	3401.26	3417.14	3414.49	12.12
100	102.51	103.50	104.97	103.66	1.23	20	3079.79	3202.82	3230.60	3171.07	80.26
50	52.97	52.97	52.97	52.97	0.00	10	2854.11	2932.94	2865.47	2884.18	42.61

(continued)

(C)

Shear Rate	Shear Stress (D/cm^2) NMP 40%					Shear Rate	Shear Stress (D/cm^2) NMP 50%				
(s^{-1})	1	2	3	Mean	S.D.	(s^{-1})	1	2	3	Mean	S.D.
10	2925.01	2877.38	2984.54	2928.97	53.69	10	381.00	254.00	460.38	365.13	104.10
20	3313.95	3246.48	3385.39	3315.27	69.46	20	448.47	392.91	583.41	474.93	97.97
30	3385.39	3524.29	3802.11	3570.60	212.19	30	480.22	452.44	646.91	526.53	105.18
40	3480.64	3615.58	3821.95	3639.39	171.90	40	504.04	496.10	694.54	564.89	112.35
50	3619.55	3722.73	3937.05	3759.78	161.96	50	571.51	527.85	742.17	613.84	113.26
60	3706.86	3837.83	3948.96	3831.21	121.18	60	635.01	555.63	789.79	660.14	119.09
70	3786.24	3913.24	3985.55	3895.01	100.90	70	702.48	583.41	829.48	705.12	123.05
80	3901.33	3925.22	4005.97	3944.17	54.83	80	722.32	611.20	877.10	736.87	133.55
80	3853.70	3899.69	3997.15	3916.85	73.25	80	670.73	607.23	873.14	717.03	138.87
70	3750.52	3893.39	3870.25	3838.05	76.69	70	603.26	575.48	845.35	674.70	148.45
60	3694.95	3829.89	3966.14	3830.33	135.59	60	547.69	543.73	825.51	638.98	161.56
50	3532.23	3726.70	3814.02	3690.98	144.25	50	515.94	511.98	789.79	605.90	159.26
40	3464.76	3599.70	3706.86	3590.44	121.31	40	420.69	476.26	758.04	551.66	180.87
30	3230.60	3436.98	3560.01	3409.20	166.45	30	365.13	440.54	722.32	509.33	188.27
20	3036.13	3270.29	3333.79	3213.41	156.77	20	297.66	384.97	670.73	451.12	195.13
10	2909.13	3000.41	3063.91	2991.15	77.81	10	218.28	281.78	599.29	366.45	204.13

(D)

Shear Rate	Shear Stress (D/cm^2) NMP 60%					Shear Rate	Shear Stress (D/cm^2) NMP 80%				
(s^{-1})	1	2	3	Mean	S.D.	(s^{-1})	1	2	3	Mean	S.D.
10	912.82	1817.71	706.45	1145.66	591.09	10	2901.19	1297.80	2230.47	2143.15	805.26
20	1770.08	3933.08	1476.39	2393.19	1341.65	20	3087.73	1420.83	3004.38	2504.31	939.25
30	1925.11	3433.08	1837.55	2398.58	896.97	30	3458.69	1341.45	3313.95	2704.70	1182.82
40	2154.66	2500.34	2182.84	2279.28	191.96	40	3532.23	1012.04	3500.48	2681.59	1445.95
50	2236.87	1162.86	2353.50	1917.74	656.34	50	2563.84	1004.11	3468.73	2345.56	1246.73
60	2400.36	1464.49	2569.22	2144.69	595.09	60	2222.53	1027.92	3591.76	2280.74	1282.91
70	3625.36	1377.17	1845.49	2282.68	1186.14	70	2012.18	1087.45	3300.25	2133.29	1111.36
80	1785.96	1210.48	1758.36	1584.93	324.58	80	2012.18	1182.70	2960.72	2051.87	889.68
80	1139.05	1174.76	1514.14	1275.98	207.02	80	1793.90	1131.11	2151.09	1692.03	517.56
70	1067.61	912.82	1325.17	1101.87	208.30	70	1420.83	1035.86	1682.77	1379.82	325.40
60	885.04	865.20	1135.08	961.77	150.41	60	1337.49	940.61	1460.52	1246.20	271.71
50	762.01	765.98	960.45	829.48	113.44	50	992.20	817.57	1234.30	1014.69	209.27
40	813.60	829.48	900.92	848.00	46.51	40	809.64	722.32	1047.76	859.91	168.44
30	762.01	579.44	873.14	738.20	148.29	30	619.13	599.29	849.32	689.25	138.98
20	595.32	567.54	845.35	669.40	153.01	20	511.98	448.47	694.54	551.66	127.74
10	496.10	464.35	769.95	576.80	168.02	10	440.54	313.54	642.95	465.67	166.14

Table 35 The rheology data of the Lutrol® F127 systems containing different *N*-methyl-2-pyrrolidone at 27°C

(A)

Shear Rate	Shear Stress (D/cm^2) NMP 0%					Shear Rate	Shear Stress (D/cm^2) NMP 10%				
(s^{-1})	1	2	3	Mean	S.D.	(s^{-1})	1	2	3	Mean	S.D.
10	2786.10	2730.53	2694.82	2737.15	46.00	10	2480.50	2500.34	2345.56	2442.13	84.22
20	3032.16	2992.48	2925.01	2983.21	54.18	20	2774.19	2798.00	2547.97	2706.72	138.00
30	3425.07	3401.26	3040.10	3288.81	215.72	30	3000.41	2877.38	2671.00	2849.60	166.45
40	3484.61	3500.48	3135.35	3373.48	206.38	40	3083.76	3012.32	2782.13	2959.40	157.62
50	3560.01	3563.98	3214.73	3446.24	200.51	50	3194.88	3111.54	2885.32	3063.91	160.18
60	3603.67	3643.36	3306.01	3517.68	184.38	60	3274.26	3202.82	2968.66	3148.58	159.86
70	3651.30	3687.02	3385.39	3574.57	164.80	70	3357.60	3282.20	3044.07	3227.96	163.65
80	3698.92	3774.33	3440.95	3638.07	174.82	80	3429.04	3341.73	3119.48	3296.75	159.61
80	3690.98	3734.64	3460.79	3628.81	147.13	80	3433.01	3357.60	3115.51	3302.04	165.88
70	3639.39	3675.11	3405.23	3573.24	146.60	70	3377.45	3313.95	3059.94	3250.45	168.01
60	3575.89	3607.64	3349.67	3511.07	140.67	60	3309.98	3242.51	3020.26	3190.92	151.60
50	3500.48	3500.48	3274.26	3425.07	130.61	50	3242.51	3179.01	2932.94	3118.15	163.51
40	3401.26	3401.26	3179.01	3327.18	128.32	40	3155.20	3087.73	2865.47	3036.13	151.60
30	3306.01	3298.07	3087.73	3230.60	123.80	30	3052.01	2992.48	2742.44	2928.97	164.26
20	3163.13	3139.32	2956.76	3086.40	112.91	20	2901.19	2849.60	2591.63	2780.81	165.85
10	2988.51	2976.60	2766.25	2910.45	125.02	10	2667.03	2599.56	2420.97	2562.52	127.15

(B)

Shear Rate	Shear Stress (D/cm^2) NMP 20%					Shear Rate	Shear Stress (D/cm^2) NMP 30%				
(s^{-1})	1	2	3	Mean	S.D.	(s^{-1})	1	2	3	Mean	S.D.
10	3016.29	2587.66	2504.31	2702.75	274.71	10	2865.47	2857.54	2774.19	2832.40	50.57
20	3270.29	3048.04	2861.50	3059.94	204.65	20	3079.79	3210.76	3163.13	3151.23	66.29
30	3607.64	3198.85	2889.29	3231.93	360.32	30	3206.79	3436.98	3508.42	3384.06	157.62
40	3635.42	3306.01	3000.41	3313.95	317.58	40	3333.79	3536.20	3583.83	3484.61	132.76
50	3738.61	3425.07	3115.51	3426.40	311.55	50	3448.89	3655.26	3694.95	3599.70	132.11
60	3817.99	3520.33	3214.73	3517.68	301.64	60	3571.92	3782.27	3790.20	3714.80	123.80
70	3905.30	3607.64	3298.07	3603.67	303.63	70	3651.30	3885.46	3897.36	3811.37	138.76
80	3968.80	3698.92	3381.42	3683.05	294.01	80	3730.67	3960.86	3964.83	3885.46	134.06
80	3968.80	3698.92	3381.42	3683.05	294.01	80	3718.77	3964.83	3917.21	3866.93	130.51
70	3897.36	3623.51	3313.95	3611.61	291.89	70	3643.36	3877.52	3817.21	3779.36	121.58
60	3829.89	3544.14	3246.48	3540.17	291.73	60	3571.92	3798.14	3790.20	3720.09	128.38
50	3746.55	3448.89	3155.20	3450.21	295.68	50	3480.64	3675.11	3698.92	3618.22	119.75
40	3631.45	3349.67	3063.91	3348.34	283.77	40	3369.51	3571.92	3540.17	3493.87	108.86
30	3524.29	3222.67	2936.91	3227.96	293.73	30	3234.57	3401.26	3417.14	3350.99	101.13
20	3353.64	3055.98	2782.13	3063.91	285.84	20	3063.91	3202.82	3230.60	3165.78	89.31
10	3079.79	2790.07	2559.88	2809.91	260.52	10	2809.91	2932.94	2865.47	2869.44	61.61

(continued)

(C)

Shear Rate	Shear Stress (D/cm^2) NMP 40%					Shear Rate	Shear Stress (D/cm^2) NMP 50%				
(s^{-1})	1	2	3	Mean	S.D.	(s^{-1})	1	2	3	Mean	S.D.
10	2925.01	2833.72	2913.10	2890.61	49.62	10	381.00	254.00	460.38	365.13	104.10
20	3313.95	3210.76	3282.20	3268.97	52.85	20	448.47	392.91	583.41	474.93	97.97
30	3385.39	3266.32	3409.20	3353.64	76.55	30	480.22	452.44	646.91	526.53	105.18
40	3480.64	3413.17	3532.23	3475.35	59.71	40	504.04	496.10	694.54	564.89	112.35
50	3619.55	3548.11	3647.33	3604.99	51.19	50	571.51	527.85	742.17	613.84	113.26
60	3706.86	3671.14	3734.64	3704.21	31.83	60	635.01	555.63	789.79	660.14	119.09
70	3786.24	3778.30	3817.99	3794.17	21.00	70	702.48	583.41	829.48	705.12	123.05
80	3901.33	3857.67	3921.17	3893.39	32.49	80	722.32	611.20	877.10	736.87	133.55
80	3853.70	3869.58	3905.30	3876.19	26.43	80	670.73	607.23	873.14	717.03	138.87
70	3750.52	3774.33	3814.02	3779.62	32.08	70	603.26	575.48	845.35	674.70	148.45
60	3694.95	3706.86	3722.73	3708.18	13.94	60	547.69	543.73	825.51	638.98	161.56
50	3532.23	3556.04	3611.61	3566.63	40.73	50	515.94	511.98	789.79	605.90	159.26
40	3464.76	3448.89	3484.61	3466.09	17.90	40	420.69	476.26	758.04	551.66	180.87
30	3230.60	3270.29	3349.67	3283.52	60.62	30	365.13	440.54	722.32	509.33	188.27
20	3036.13	3075.82	3159.16	3090.37	62.79	20	297.66	384.97	670.73	451.12	195.13
10	2909.13	2849.60	2861.50	2873.41	31.50	10	218.28	281.78	599.29	366.45	204.13

(D)

Shear Rate	Shear Stress (D/cm^2) NMP 60%					Shear Rate	Shear Stress (D/cm^2) NMP 80%				
(s^{-1})	1	2	3	Mean	S.D.	(s^{-1})	1	2	3	Mean	S.D.
10	31.75	31.75	27.78	30.43	2.29	50	3.97	0.00	0.00	1.32	2.29
20	63.50	63.50	55.56	60.85	4.58	100	7.94	3.97	3.97	5.29	2.29
30	95.25	91.28	87.31	91.28	3.97	150	7.94	7.94	7.94	7.94	0.00
40	123.03	123.03	115.10	120.39	4.58	200	11.91	7.94	7.94	9.26	2.29
50	154.78	150.81	146.85	150.81	3.97	250	15.88	11.91	7.94	11.91	3.97
60	182.56	182.56	174.63	179.92	4.58	300	15.88	11.91	7.94	11.91	3.97
70	214.32	214.32	206.38	211.67	4.58	350	19.84	15.88	11.91	15.88	3.97
80	242.10	242.10	234.16	239.45	4.58	400	19.84	19.84	15.88	18.52	2.29
80	242.10	242.10	234.16	239.45	4.58	400	19.84	19.84	15.88	18.52	2.29
70	210.35	210.35	206.38	209.02	2.29	350	19.84	15.88	11.91	15.88	3.97
60	182.56	182.56	178.60	181.24	2.29	300	15.88	11.91	11.91	13.23	2.29
50	150.81	154.78	146.85	150.81	3.97	250	15.88	11.91	11.91	13.23	2.29
40	123.03	123.03	119.06	121.71	2.29	200	11.91	7.94	7.94	9.26	2.29
30	95.25	95.25	87.31	92.61	4.58	150	7.94	7.94	3.97	6.61	2.29
20	63.50	63.50	59.53	62.18	2.29	100	7.94	3.97	3.97	5.29	2.29
10	31.75	31.75	31.75	31.75	0.00	50	3.97	0.00	0.00	1.32	2.29

Table 36 The rheology data of the Lutrol® F127 systems containing different *N*-methyl-2-pyrrolidone at 37°C

(A)

Shear Rate	Shear Stress (D/cm^2) NMP 0%					Shear Rate	Shear Stress (D/cm^2) NMP 10%				
(s^{-1})	1	2	3	Mean	S.D.	(s^{-1})	1	2	3	Mean	S.D.
10	2750.38	3270.29	3274.26	3098.31	301.32	10	3151.23	2960.72	2940.88	3017.61	116.14
20	3476.67	3548.11	3345.70	3456.82	102.65	20	3321.89	3306.01	3262.35	3296.75	30.83
30	3544.14	3560.01	3357.60	3487.25	112.56	30	3587.80	3337.76	3607.64	3511.07	150.41
40	3607.64	3643.36	3429.04	3560.01	114.82	40	3603.67	3448.89	3635.42	3562.66	99.80
50	3671.14	3683.05	3464.76	3606.32	122.73	50	3655.26	3524.29	3706.86	3628.81	94.11
60	3726.70	3698.92	3540.17	3655.26	100.64	60	3742.58	3635.42	3758.45	3712.15	66.92
70	3742.58	3766.39	3591.76	3700.24	94.70	70	3810.05	3718.77	3833.86	3787.56	60.75
80	3810.05	3829.89	3647.33	3762.42	100.17	80	3877.52	3774.33	3897.36	3849.74	66.05
80	3774.33	3841.80	3675.11	3763.75	83.85	80	3885.46	3810.05	3889.42	3861.64	44.73
70	3698.92	3798.14	3623.51	3706.86	87.58	70	3814.02	3762.42	3845.77	3807.40	42.06
60	3663.20	3710.83	3579.86	3651.30	66.29	60	3774.33	3706.86	3730.67	3737.29	34.22
50	3567.95	3675.11	3532.23	3591.76	74.36	50	3683.05	3639.39	3675.11	3665.85	23.26
40	3528.26	3591.76	3480.64	3533.55	55.75	40	3611.61	3548.11	3548.11	3569.27	36.66
30	3413.17	3571.92	3401.26	3462.12	95.28	30	3452.86	3436.98	3516.36	3468.73	42.00
20	3333.79	3500.48	3341.73	3392.00	94.03	20	3325.85	3313.95	3369.51	3336.44	29.25
10	3290.14	3306.01	3238.54	3278.23	35.28	10	3182.98	3111.54	3095.66	3130.06	46.51

(B)

Shear Rate	Shear Stress (D/cm^2) NMP 20%					Shear Rate	Shear Stress (D/cm^2) NMP 30%				
(s^{-1})	1	2	3	Mean	S.D.	(s^{-1})	1	2	3	Mean	S.D.
10	3016.29	2841.66	2968.66	2942.20	90.27	10	2829.75	2885.32	2897.22	2870.77	36.01
20	3270.29	3171.07	3222.67	3221.34	49.62	20	3333.79	2944.85	3234.57	3171.07	202.10
30	3607.64	3286.17	3186.95	3360.25	219.91	30	3464.76	3052.01	3389.36	3302.04	219.79
40	3635.42	3401.26	3317.92	3451.53	164.61	40	3587.80	3194.88	3512.39	3431.69	208.52
50	3738.61	3508.42	3405.23	3550.75	170.67	50	3710.83	3298.07	3611.61	3540.17	215.45
60	3817.99	3607.64	3516.36	3647.33	154.68	60	3814.02	3413.17	3698.92	3642.04	206.39
70	3905.30	3690.98	3599.70	3731.99	156.87	70	3909.27	3496.51	3786.24	3730.67	211.91
80	3960.10	3770.36	3659.23	3796.56	152.14	80	3954.21	3560.01	3857.67	3790.63	205.47
80	3968.80	3774.33	3679.08	3807.40	147.67	80	3992.12	3579.86	3857.67	3809.88	210.25
70	3897.36	3714.80	3615.58	3742.58	142.93	70	3909.27	3516.36	3782.27	3735.96	200.51
60	3829.89	3635.42	3544.14	3669.82	145.95	60	3829.89	3440.95	3694.95	3655.26	197.49
50	3746.55	3560.01	3468.73	3591.76	141.60	50	3718.77	3353.64	3599.70	3557.37	186.21
40	3631.45	3448.89	3373.48	3484.61	132.64	40	3607.64	3258.38	3476.67	3447.56	176.44
30	3524.29	3353.64	3250.45	3376.13	138.30	30	3440.95	3131.38	3373.48	3315.27	162.79
20	3353.64	3202.82	3107.57	3221.34	124.07	20	3266.32	2976.60	3202.82	3148.58	152.29
10	3079.79	2932.94	2861.50	2958.08	111.29	10	3012.32	2718.63	2921.04	2883.99	150.31

(continued)

(C)

Shear Rate	Shear Stress (D/cm^2) NMP 40%					Shear Rate	Shear Stress (D/cm^2) NMP 50%				
(s^{-1})	1	2	3	Mean	S.D.	(s^{-1})	1	2	3	Mean	S.D.
10	2671.00	2750.38	2710.69	2710.69	39.69	10	31.75	39.69	39.69	37.04	4.58
20	3163.13	3016.29	2980.57	3053.33	96.76	20	59.53	71.44	87.31	72.76	13.94
30	3234.57	3123.45	3079.79	3145.94	79.80	30	91.28	103.19	111.13	101.87	9.99
40	3341.73	3242.51	3194.88	3259.71	74.92	40	119.06	130.97	162.72	137.59	22.57
50	3472.70	3349.67	3317.92	3380.09	81.75	50	146.85	162.72	190.50	166.69	22.10
60	3544.14	3452.86	3385.39	3460.79	79.67	60	178.60	190.50	226.22	198.44	24.79
70	3595.73	3532.23	3472.70	3533.55	61.53	70	206.38	218.28	254.00	226.22	24.79
80	3647.33	3603.67	3560.01	3603.67	43.66	80	234.16	250.03	265.91	250.03	15.88
80	3667.17	3623.51	3556.04	3615.58	55.99	80	234.16	246.07	273.85	251.36	20.37
70	3560.01	3536.20	3500.48	3532.23	29.96	70	206.38	210.35	238.13	218.28	17.30
60	3536.20	3460.79	3401.26	3466.09	67.63	60	178.60	174.63	210.35	187.86	19.58
50	3417.14	3361.57	3317.92	3365.54	49.73	50	146.85	146.85	186.53	160.07	22.91
40	3345.70	3250.45	3210.76	3268.97	69.35	40	119.06	119.06	158.75	132.29	22.91
30	3123.45	3127.41	3087.73	3112.86	21.86	30	91.28	91.28	115.10	99.22	13.75
20	2968.66	2956.76	2932.94	2952.79	18.19	20	59.53	63.50	87.31	70.12	15.03
10	2746.41	2686.88	2651.16	2694.82	48.12	10	31.75	31.75	51.59	38.37	11.46

(D)

Shear Rate	Shear Stress (D/cm^2) NMP 60%					Shear Rate	Shear Stress (D/cm^2) NMP 80%				
(s^{-1})	1	2	3	Mean	S.D.	(s^{-1})	1	2	3	Mean	S.D.
10	16.68	15.70	14.22	15.53	1.23	50	12.75	9.81	12.75	11.77	1.70
20	32.86	31.39	29.43	31.23	1.72	100	24.03	20.11	25.02	23.05	2.60
30	48.07	48.07	43.65	46.60	2.55	150	34.34	30.41	35.81	33.52	2.79
40	63.27	62.29	58.37	61.31	2.60	200	44.15	40.71	47.58	44.15	3.43
50	77.99	78.48	72.59	76.35	3.27	250	54.45	50.52	58.37	54.45	3.92
60	93.20	93.69	87.31	91.40	3.55	300	66.22	60.82	69.65	65.56	4.45
70	108.40	108.40	102.02	106.28	3.68	350	77.50	71.12	80.44	76.35	4.76
80	123.12	123.61	116.74	121.15	3.83	400	87.80	81.42	91.23	86.82	4.98
80	122.63	123.61	116.74	120.99	3.71	400	87.80	80.93	90.74	86.49	5.03
70	106.93	108.89	102.02	105.95	3.54	350	77.50	71.12	80.44	76.35	4.76
60	92.21	93.69	87.80	91.23	3.06	300	66.71	60.82	69.16	65.56	4.29
50	76.52	77.50	73.08	75.70	2.32	250	55.92	51.01	57.88	54.94	3.54
40	56.90	62.78	58.37	59.35	3.06	200	45.13	40.71	46.60	44.15	3.06
30	42.67	46.60	44.15	44.47	1.98	150	34.34	30.41	35.32	33.35	2.60
20	28.94	31.39	29.43	29.92	1.30	100	23.05	20.60	24.03	22.56	1.77
10	15.21	15.70	14.72	15.21	0.49	50	11.77	10.30	12.26	11.45	1.02

Table 37 The rheology data of the Lutrol® F127 systems containing different amount ZnO at 4°C

(A)

Shear Rate	Shear Stress (D/cm^2)					Shear Rate	Shear Stress (D/cm^2)				
	ZnO 0%						ZnO 0.5%				
(s^{-1})	1	2	3	Mean	S.D.	(s^{-1})	1	2	3	Mean	S.D.
50	21.09	21.09	19.62	20.60	0.85	50	25.02	26.49	26.00	25.83	0.75
100	44.64	44.15	40.71	43.16	2.14	100	48.07	50.52	51.99	50.19	1.98
150	70.14	67.69	61.31	66.38	4.56	150	72.10	77.01	78.97	76.03	3.54
200	93.69	91.23	80.93	88.62	6.77	200	97.12	103.50	105.46	102.02	4.36
250	115.76	114.29	98.10	109.38	9.80	250	122.13	129.49	132.93	128.18	5.51
300	141.75	131.94	119.68	131.13	11.06	300	147.64	155.00	161.87	154.83	7.11
350	169.71	155.00	141.75	155.49	13.99	350	172.66	180.99	189.33	180.99	8.34
400	198.16	179.52	163.34	180.34	17.43	400	198.65	207.97	215.82	207.48	8.59
400	197.18	182.96	165.30	181.81	15.97	400	199.14	208.46	216.80	208.14	8.83
350	167.26	161.37	144.70	157.78	11.70	350	175.11	183.94	189.82	182.96	7.41
300	144.21	138.81	119.19	134.07	13.16	300	150.58	156.96	164.32	157.29	6.87
250	122.63	110.36	99.57	110.85	11.53	250	125.57	130.96	137.34	131.29	5.89
200	100.06	87.80	80.44	89.43	9.91	200	101.04	105.95	109.38	105.46	4.19
150	75.05	67.69	61.31	68.02	6.87	150	76.03	79.95	82.40	79.46	3.22
100	48.56	45.62	41.69	45.29	3.45	100	51.01	53.96	54.94	53.30	2.04
50	24.53	23.54	21.09	23.05	1.77	50	26.00	27.47	27.96	27.14	1.02

(B)

Shear Rate	Shear Stress (D/cm^2)					Shear Rate	Shear Stress (D/cm^2)				
	ZnO 1.0%						ZnO 1.5%				
(s^{-1})	1	2	3	Mean	S.D.	(s^{-1})	1	2	3	Mean	S.D.
50	27.96	27.96	27.96	27.96	0.00	50	32.37	30.90	32.37	31.88	0.85
100	54.45	54.45	55.43	54.77	0.57	100	59.84	60.33	60.82	60.33	0.49
150	81.91	80.93	83.88	82.24	1.50	150	88.29	89.27	90.25	89.27	0.98
200	108.89	108.40	112.32	109.87	2.14	200	115.27	118.21	118.70	117.39	1.86
250	136.85	136.36	141.75	138.32	2.98	250	142.74	147.15	148.62	146.17	3.06
300	165.79	164.32	170.20	166.77	3.06	300	169.22	177.07	177.56	174.62	4.68
350	193.26	191.79	199.63	194.89	4.17	350	196.69	206.01	206.01	202.90	5.38
400	221.22	220.73	229.55	223.83	4.96	400	223.18	233.48	233.97	230.21	6.09
400	222.20	220.73	230.54	224.49	5.29	400	222.69	233.97	234.46	230.37	6.66
350	194.73	194.73	197.67	195.71	1.70	350	196.20	204.05	205.03	201.76	4.84
300	168.24	167.26	162.85	166.12	2.87	300	168.24	176.09	177.07	173.80	4.84
250	140.28	139.79	136.85	138.98	1.86	250	141.75	147.64	148.62	146.01	3.71
200	112.32	112.32	111.83	112.16	0.28	200	114.78	117.23	119.19	117.07	2.21
150	84.86	84.37	84.86	84.69	0.28	150	86.82	89.27	90.25	88.78	1.77
100	56.90	57.39	57.88	57.39	0.49	100	59.35	59.35	60.82	59.84	0.85
50	28.94	28.94	28.94	28.94	0.00	50	30.41	30.41	31.39	30.74	0.57

Table 38 The rheology data of the Lutrol® F127 systems containing different amount ZnO at 27°C

(A)

Shear Rate	Shear Stress (D/cm²) ZnO 0%					Shear Rate	Shear Stress (D/cm²) ZnO 0.5%				
(s^{-1})	1	2	3	Mean	S.D.	(s^{-1})	1	2	3	Mean	S.D.
10	2547.97	2484.47	2742.44	2591.63	134.41	10	2591.63	2746.41	2980.57	2772.87	195.82
20	2643.22	2547.97	2726.57	2639.25	89.36	20	2861.50	3147.26	3294.10	3100.96	219.99
30	2805.94	2627.35	2817.85	2750.38	106.72	30	2925.01	3226.63	3433.01	3194.88	255.49
40	2917.07	2734.50	2921.04	2857.54	106.57	40	3032.16	3298.07	3516.36	3282.20	242.49
50	3036.13	2809.91	3020.26	2955.43	126.28	50	3079.79	3377.45	3556.04	3337.76	240.60
60	3115.51	2897.22	3055.98	3022.90	112.84	60	3167.10	3436.98	3611.61	3405.23	223.95
70	3179.01	2968.66	3119.48	3089.05	108.42	70	3194.88	3476.67	3663.20	3444.92	235.77
80	3258.38	2984.54	3175.04	3139.32	140.37	80	3226.63	3500.48	3679.08	3468.73	227.89
80	3202.82	3016.29	3163.13	3127.41	98.26	80	3254.42	3524.29	3687.02	3488.58	218.50
70	3127.41	2964.69	3127.41	3073.17	93.95	70	3182.98	3444.92	3639.39	3422.43	229.04
60	3071.85	2893.26	3032.16	2999.09	93.78	60	3115.51	3409.20	3571.92	3365.54	231.32
50	2968.66	2849.60	2976.60	2931.62	71.14	50	3055.98	3302.04	3575.89	3311.30	260.08
40	2897.22	2766.25	2881.35	2848.28	71.48	40	2960.72	3258.38	3436.98	3218.70	240.60
30	2794.04	2678.94	2813.88	2762.28	72.86	30	2865.47	3111.54	3361.57	3112.86	248.05
20	2651.16	2579.72	2698.78	2643.22	59.93	20	2770.22	3016.29	3234.57	3007.03	232.31
10	2555.91	2389.22	2512.25	2485.79	86.44	10	2544.00	2869.44	2992.48	2801.97	231.72

(B)

Shear Rate	Shear Stress (D/cm²) ZnO 1.0%					Shear Rate	Shear Stress (D/cm²) ZnO 1.5%				
(s^{-1})	1	2	3	Mean	S.D.	(s^{-1})	1	2	3	Mean	S.D.
10	2583.69	2742.44	2861.50	2729.21	139.38	10	2127.28	2710.69	2984.54	2607.50	437.85
20	2925.01	3143.29	2968.66	3012.32	115.51	20	2603.53	2932.94	3142.51	2893.00	271.70
30	3012.32	3234.57	3147.26	3131.38	111.97	30	2754.35	3452.86	3209.98	3139.06	354.61
40	3107.57	3321.89	3202.82	3210.76	107.38	40	2889.29	3389.36	3398.07	3225.57	291.26
50	3179.01	3397.29	3306.01	3294.10	109.63	50	3226.63	3333.79	3490.14	3350.19	132.51
60	3186.95	3436.98	3341.73	3321.89	126.19	60	3452.86	3409.20	3418.70	3426.92	22.96
70	3274.26	3484.61	3405.23	3388.03	106.22	70	3397.29	3222.67	3321.89	3313.95	87.58
80	3309.98	3500.48	3460.79	3423.75	100.51	80	3270.29	3139.32	3250.45	3220.02	70.59
80	3329.82	3488.58	3452.86	3423.75	83.28	80	3309.98	3079.79	3167.10	3185.62	116.21
70	3246.48	3425.07	3429.04	3366.87	104.28	70	3282.20	3079.79	3155.20	3172.39	102.29
60	3127.41	3321.89	3349.67	3266.32	121.10	60	2897.22	3103.60	3016.29	3005.70	103.60
50	3091.70	3266.32	3282.20	3213.41	105.70	50	2944.85	3119.48	2928.97	2997.77	105.70
40	3040.10	3167.10	3214.73	3140.64	90.27	40	2853.57	3059.94	2686.88	2866.80	186.89
30	3024.23	3123.45	3103.60	3083.76	52.50	30	2980.57	2889.29	2607.50	2825.79	194.47
20	2893.26	2992.48	2968.66	2951.46	51.80	20	2686.88	2873.41	2448.75	2669.68	212.85
10	2659.10	2770.22	2798.00	2742.44	73.50	10	2532.09	2782.13	2119.34	2477.85	334.71

Table 39 The rheology data of the Lutrol® F127 systems containing different amount ZnO at 37°C

(A)

Shear Rate	Shear Stress (D/cm^2) ZnO 0%					Shear Rate	Shear Stress (D/cm^2) ZnO 0.5%				
(s^{-1})	1	2	3	Mean	S.D.	(s^{-1})	1	2	3	Mean	S.D.
10	3306.01	3103.60	3353.64	3254.42	132.76	10	2813.88	3087.73	3028.19	2976.60	144.03
20	3520.33	3306.01	3484.61	3436.98	114.82	20	3448.89	3536.20	3599.70	3528.26	75.72
30	3611.61	3591.76	3567.95	3590.44	21.86	30	3575.89	3647.33	3702.89	3642.04	63.67
40	3659.23	3587.80	3599.70	3615.58	38.27	40	3579.86	3742.58	3730.67	3684.37	90.71
50	3742.58	3647.33	3631.45	3673.79	60.10	50	3643.36	3766.39	3754.48	3721.41	67.86
60	3786.24	3671.14	3702.89	3720.09	59.44	60	3722.73	3794.17	3730.67	3749.19	39.16
70	3853.70	3706.86	3754.48	3771.68	74.92	70	3766.39	3853.70	3726.70	3782.27	64.97
80	3917.21	3762.42	3782.27	3820.63	84.22	80	3806.08	3905.30	3802.11	3837.83	58.46
80	3917.21	3726.70	3798.14	3814.02	96.24	80	3730.67	3814.02	3766.39	3770.36	41.81
70	3877.52	3671.14	3738.61	3762.42	105.23	70	3683.05	3778.30	3663.20	3708.18	61.53
60	3794.17	3627.48	3702.89	3708.18	83.47	60	3687.02	3718.77	3508.42	3638.07	113.39
50	3750.52	3548.11	3639.39	3646.00	101.37	50	3532.23	3690.98	3540.17	3587.80	89.45
40	3663.20	3504.45	3587.80	3585.15	79.41	40	3520.33	3607.64	3536.20	3554.72	46.51
30	3643.36	3440.95	3476.67	3520.33	108.04	30	3401.26	3583.83	3492.54	3492.54	91.28
20	3548.11	3361.57	3413.17	3440.95	96.32	20	3278.23	3433.01	3417.14	3376.13	85.15
10	3377.45	3262.35	3306.01	3315.27	58.10	10	3274.26	3290.14	3258.38	3274.26	15.88

(B)

Shear Rate	Shear Stress (D/cm^2) ZnO 1.0%					Shear Rate	Shear Stress (D/cm^2) ZnO 1.5%				
(s^{-1})	1	2	3	Mean	S.D.	(s^{-1})	1	2	3	Mean	S.D.
10	3412.39	3306.01	3322.60	3347.00	57.23	10	3087.73	3032.03	3235.28	3118.35	105.03
20	3507.64	3520.33	3595.73	3541.23	47.62	20	3536.20	3401.06	3389.22	3442.16	81.66
30	3571.92	3611.61	3643.36	3608.96	35.79	30	3647.33	3505.02	3408.09	3520.15	120.33
40	3595.73	3659.23	3647.33	3634.10	33.75	40	3742.58	3640.74	3549.53	3644.28	96.57
50	3660.01	3742.58	3718.77	3707.12	42.50	50	3766.39	3732.81	3645.56	3714.92	62.37
60	3655.26	3786.24	3790.20	3743.90	76.79	60	3794.17	3782.81	3770.15	3782.38	12.02
70	3775.11	3853.70	3825.92	3818.25	39.86	70	3853.70	3881.21	3821.75	3852.22	29.76
80	3851.30	3917.21	3782.27	3850.26	67.48	80	3905.30	3920.90	3966.18	3930.79	31.63
80	3832.23	3917.21	3786.24	3845.22	66.44	80	3814.02	3809.77	3953.50	3859.10	81.78
70	3716.36	3877.52	3683.05	3758.97	104.00	70	3778.30	3702.62	3838.40	3773.11	68.04
60	3684.92	3794.17	3683.05	3720.71	63.63	60	3718.77	3654.99	3778.87	3717.54	61.95
50	3650.64	3750.52	3603.67	3668.27	74.99	50	3690.98	3690.71	3796.31	3726.00	60.89
40	3591.57	3663.20	3540.17	3598.32	61.79	40	3607.64	3658.96	3640.74	3635.78	26.02
30	3540.92	3643.36	3413.17	3532.48	115.33	30	3583.83	3658.96	3560.59	3601.12	51.42
20	3494.88	3548.11	3357.60	3466.87	98.29	20	3433.01	3647.05	3477.24	3519.10	112.99
10	3342.37	3377.45	3175.04	3298.29	108.17	10	3290.14	3527.99	3362.93	3393.68	121.87

Table 40 The rheology data of the Lutrol® F127 systems containing different amount doxycycline hyclate at 4°C

(A)

Shear Stress (D/cm^2)						Shear Stress (D/cm^2)					
Shear Rate	Doxycycline hyclate 0%					Shear Rate	Doxycycline hyclate 2.5%				
(s^{-1})	1	2	3	Mean	S.D.	(s^{-1})	1	2	3	Mean	S.D.
10	3.97	15.88	15.88	11.91	6.87	10	7.94	7.94	3.97	6.61	2.29
20	7.94	11.91	27.78	15.88	10.50	20	11.91	11.91	11.91	11.91	0.00
30	11.91	35.72	15.88	21.17	12.76	30	15.88	15.88	15.88	15.88	0.00
40	15.88	23.81	35.72	25.14	9.99	40	23.81	19.84	19.84	21.17	2.29
50	19.84	31.75	31.75	27.78	6.87	50	27.78	23.81	23.81	25.14	2.29
60	23.81	55.56	35.72	38.37	16.04	60	31.75	31.75	31.75	31.75	0.00
70	27.78	59.53	43.66	43.66	15.88	70	35.72	35.72	35.72	35.72	0.00
80	31.75	59.53	43.66	44.98	13.94	80	43.66	39.69	39.69	41.01	2.29
80	31.75	63.50	47.63	47.63	15.88	80	43.66	39.69	39.69	41.01	2.29
70	27.78	51.59	51.59	43.66	13.75	70	39.69	35.72	35.72	37.04	2.29
60	27.78	59.53	31.75	39.69	17.30	60	31.75	31.75	31.75	31.75	0.00
50	19.84	51.59	35.72	35.72	15.88	50	27.78	27.78	23.81	26.46	2.29
40	15.88	51.59	23.81	30.43	18.76	40	23.81	23.81	19.84	22.49	2.29
30	11.91	27.78	43.66	27.78	15.88	30	15.88	15.88	15.88	15.88	0.00
20	11.91	35.72	23.81	23.81	11.91	20	11.91	11.91	11.91	11.91	0.00
10	7.94	43.66	7.94	19.84	20.62	10	7.94	7.94	7.94	7.94	0.00

(B)

Shear Stress (D/cm^2)						Shear Stress (D/cm^2)					
Shear Rate	Doxycycline hyclate 5%					Shear Rate	Doxycycline hyclate 7.5%				
(s^{-1})	1	2	3	Mean	S.D.	(s^{-1})	1	2	3	Mean	S.D.
10	7.94	7.94	11.91	9.26	2.29	10	27.78	55.56	11.91	31.75	22.10
20	11.91	15.88	15.88	14.55	2.29	20	47.63	55.56	27.78	43.66	14.31
30	19.84	19.84	19.84	19.84	0.00	30	63.50	63.50	39.69	55.56	13.75
40	23.81	27.78	27.78	26.46	2.29	40	63.50	75.41	27.78	55.56	24.79
50	31.75	35.72	31.75	33.07	2.29	50	67.47	79.38	39.69	62.18	20.37
60	35.72	39.69	39.69	38.37	2.29	60	87.31	63.50	35.72	62.18	25.82
70	39.69	47.63	43.66	43.66	3.97	70	91.28	91.28	43.66	75.41	27.50
80	47.63	51.59	51.59	50.27	2.29	80	95.25	103.19	39.69	79.38	34.60
80	47.63	51.59	51.59	50.27	2.29	80	103.19	99.22	47.63	83.34	31.00
70	43.66	47.63	43.66	44.98	2.29	70	91.28	99.22	39.69	76.73	32.32
60	35.72	39.69	39.69	38.37	2.29	60	83.34	83.34	39.69	68.79	25.21
50	31.75	35.72	31.75	33.07	2.29	50	83.34	71.44	43.66	66.15	20.37
40	23.81	27.78	27.78	26.46	2.29	40	67.47	63.50	39.69	56.89	15.03
30	19.84	19.84	19.84	19.84	0.00	30	63.50	67.47	39.69	56.89	15.03
20	15.88	15.88	11.91	14.55	2.29	20	55.56	51.59	47.63	51.59	3.97
10	7.94	15.88	7.94	10.58	4.58	10	39.69	35.72	43.66	39.69	3.97

(continued)

(C)

	Shear Stress (D/cm^2)				
Shear Rate	**Doxycycline hyclate 10%**				
(s^{-1})	**1**	**2**	**3**	**Mean**	**S.D.**
10	**43.66**	**19.84**	**15.88**	**26.46**	**15.03**
20	**31.75**	**51.59**	**23.81**	**35.72**	**14.31**
30	**91.28**	**51.59**	**35.72**	**59.53**	**28.62**
40	**166.69**	**119.06**	**55.56**	**113.77**	**55.75**
50	**75.41**	**87.31**	**55.56**	**72.76**	**16.04**
60	**83.34**	**115.10**	**55.56**	**84.67**	**29.79**
70	**91.28**	**119.06**	**67.47**	**92.61**	**25.82**
80	**119.06**	**127.00**	**79.38**	**108.48**	**25.52**
80	**103.19**	**134.94**	**75.41**	**104.51**	**29.79**
70	**87.31**	**115.10**	**83.34**	**95.25**	**17.30**
60	**83.34**	**119.06**	**55.56**	**85.99**	**31.83**
50	**67.47**	**99.22**	**55.56**	**74.08**	**22.57**
40	**63.50**	**95.25**	**39.69**	**66.15**	**27.88**
30	**43.66**	**59.53**	**67.47**	**56.89**	**12.12**
20	**27.78**	**55.56**	**55.56**	**46.30**	**16.04**
10	**39.69**	**35.72**	**11.91**	**29.10**	**15.03**

Table 41 The rheology data of the Lutrol® F127 systems containing different amount doxycycline hyclate at 27°C

(A)

Shear Stress (D/cm^2)						Shear Stress (D/cm^2)					
Shear Rate	Doxycycline hyclate 0%					Shear Rate	Doxycycline hyclate 2.5%				
(s^{-1})	1	2	3	Mean	S.D.	(s^{-1})	1	2	3	Mean	S.D.
10	2536.06	2297.94	2492.41	2442.13	126.77	10	1567.68	1516.08	1281.92	1455.23	152.29
20	2639.25	2698.78	2754.35	2697.46	57.56	20	1750.24	1579.58	1349.39	1559.74	201.16
30	2730.53	2718.63	2845.63	2764.93	70.14	30	1805.80	1623.24	1369.24	1599.43	219.26
40	2833.72	2853.57	2956.76	2881.35	66.05	40	1853.43	1674.83	1416.86	1648.37	219.48
50	2932.94	2936.91	3044.07	2971.31	63.04	50	1901.06	1702.62	1472.42	1692.03	214.51
60	3044.07	3028.19	3127.41	3066.56	53.30	60	1952.65	1738.33	1520.05	1737.01	216.30
70	3107.57	3119.48	3206.79	3144.61	54.18	70	2004.24	1774.05	1559.74	1779.35	222.30
80	3163.13	3182.98	3274.26	3206.79	59.27	80	2035.99	1817.71	1583.55	1812.42	226.27
80	3167.10	3202.82	3294.10	3221.34	65.50	80	2039.96	1829.62	1615.30	1828.29	212.33
70	3099.63	3171.07	3242.51	3171.07	71.44	70	2032.03	1845.49	1623.24	1833.59	204.65
60	3079.79	3103.60	3179.01	3120.80	51.80	60	2039.96	1861.37	1639.11	1846.81	200.82
50	2980.57	3052.01	3115.51	3049.36	67.51	50	2051.87	1897.09	1662.93	1870.63	195.82
40	2932.94	2964.69	3020.26	2972.63	44.19	40	2063.78	1912.96	1682.77	1886.50	191.88
30	2742.44	2877.38	2936.91	2852.24	99.64	30	2083.62	1932.81	1698.65	1905.02	193.98
20	2619.41	2750.38	2809.91	2726.57	97.46	20	2047.90	1972.49	1734.37	1918.25	163.65
10	2520.19	2540.03	2611.47	2557.23	48.01	10	1948.68	1920.90	1766.12	1878.57	98.37

(B)

Shear Stress (D/cm^2)						Shear Stress (D/cm^2)					
Shear Rate	Doxycycline hyclate 5%					Shear Rate	Doxycycline hyclate 7.5%				
(s^{-1})	1	2	3	Mean	S.D.	(s^{-1})	1	2	3	Mean	S.D.
10	39.69	39.69	75.41	51.59	20.62	10	27.78	31.75	35.72	31.75	3.97
20	75.41	83.34	194.47	117.74	66.57	20	55.56	63.50	67.47	62.18	6.06
30	111.13	142.88	702.48	318.83	332.63	30	87.31	95.25	99.22	93.93	6.06
40	154.78	273.85	861.23	429.95	378.21	40	115.10	130.97	130.97	125.68	9.17
50	206.38	603.26	920.76	576.80	357.93	50	142.88	162.72	162.72	156.11	11.46
60	265.91	742.17	952.51	653.53	351.78	60	170.66	198.44	194.47	187.86	15.03
70	337.35	809.64	972.36	706.45	329.84	70	202.41	234.16	230.19	222.25	17.30
80	420.69	849.32	992.20	754.07	297.42	80	230.19	265.91	261.94	252.68	19.58
80	468.32	873.14	1008.08	783.18	280.90	80	230.19	269.88	261.94	254.00	21.00
70	484.19	873.14	1008.08	788.47	272.01	70	202.41	238.13	230.19	223.58	18.76
60	500.07	865.20	1000.14	788.47	258.71	60	174.63	206.38	198.44	193.15	16.52
50	508.01	865.20	1000.14	791.11	254.29	50	142.88	170.66	162.72	158.75	14.31
40	500.07	853.29	992.20	781.85	253.72	40	115.10	138.91	130.97	128.32	12.12
30	480.22	845.35	996.17	773.92	265.29	30	87.31	103.19	99.22	96.57	8.26
20	444.51	829.48	980.29	751.43	276.29	20	59.53	67.47	67.47	64.82	4.58
10	361.16	789.79	940.61	697.19	300.62	10	27.78	35.72	31.75	31.75	3.97

(continued)

(C)

	Shear Stress (D/cm^2)				
Shear Rate	**Doxycycline hyclate 10%**				
(s^{-1})	**1**	**2**	**3**	**Mean**	**S.D.**
10	**63.50**	**31.75**	**35.72**	**43.66**	**17.30**
20	**59.53**	**59.53**	**63.50**	**60.85**	**2.29**
30	**91.28**	**91.28**	**95.25**	**92.61**	**2.29**
40	**119.06**	**123.03**	**127.00**	**123.03**	**3.97**
50	**146.85**	**150.81**	**166.69**	**154.78**	**10.50**
60	**178.60**	**182.56**	**194.47**	**185.21**	**8.26**
70	**206.38**	**214.32**	**218.28**	**212.99**	**6.06**
80	**242.10**	**242.10**	**254.00**	**246.07**	**6.87**
80	**238.13**	**246.07**	**254.00**	**246.07**	**7.94**
70	**206.38**	**214.32**	**222.25**	**214.32**	**7.94**
60	**178.60**	**182.56**	**190.50**	**183.89**	**6.06**
50	**150.81**	**154.78**	**158.75**	**154.78**	**3.97**
40	**119.06**	**123.03**	**127.00**	**123.03**	**3.97**
30	**87.31**	**95.25**	**95.25**	**92.61**	**4.58**
20	**59.53**	**63.50**	**63.50**	**62.18**	**2.29**
10	**31.75**	**31.75**	**31.75**	**31.75**	**0.00**

Table 42 The rheology data of the Lutrol® F127 systems containing different amount doxycycline hyclate at 37°C

(A)

Shear Stress (D/cm^2)						Shear Stress (D/cm^2)					
Shear Rate	Doxycycline hyclate 0%					Shear Rate	Doxycycline hyclate 2.5%				
(s^{-1})	1	2	3	Mean	S.D.	(s^{-1})	1	2	3	Mean	S.D.
10	3103.60	3171.07	3182.98	3152.55	42.81	10	2198.72	2198.72	2194.75	2197.39	2.29
20	3504.45	3413.17	3563.98	3493.87	75.96	20	2349.53	2321.75	2226.50	2299.26	64.53
30	3802.11	3702.89	3690.98	3731.99	61.01	30	2504.31	2409.06	2377.31	2430.23	66.09
40	3798.14	3734.64	3742.58	3758.45	34.60	40	2611.47	2492.41	2440.81	2514.90	87.52
50	3790.20	3762.42	3825.92	3792.85	31.83	50	2710.69	2571.78	2524.16	2602.21	96.92
60	3810.05	3786.24	3814.02	3803.43	15.03	60	2778.16	2667.03	2587.66	2677.62	95.69
70	3861.64	3825.92	3841.80	3843.12	17.90	70	2845.63	2726.57	2647.19	2739.79	99.88
80	3861.64	3869.58	3929.11	3886.78	36.88	80	2913.10	2770.22	2722.60	2801.97	99.14
80	3901.33	3869.58	3861.64	3877.52	21.00	80	2893.26	2790.07	2718.63	2800.65	87.79
70	3837.83	3817.99	3825.92	3827.25	9.99	70	2845.63	2734.50	2667.03	2749.06	90.18
60	3683.05	3746.55	3687.02	3705.54	35.57	60	2805.94	2686.88	2607.50	2700.11	99.88
50	3694.95	3687.02	3651.30	3677.75	23.26	50	2734.50	2627.35	2551.94	2637.93	91.74
40	3536.20	3607.64	3516.36	3553.40	48.01	40	2674.97	2555.91	2472.56	2567.81	101.73
30	3556.04	3575.89	3567.95	3566.63	9.99	30	2559.88	2452.72	2405.09	2472.56	79.28
20	3512.39	3488.58	3468.73	3489.90	21.86	20	2444.78	2345.56	2293.97	2361.44	76.65
10	3210.76	3306.01	3290.14	3268.97	51.03	10	2293.97	2166.96	2103.46	2188.13	97.00

(B)

Shear Stress (D/cm^2)						Shear Stress (D/cm^2)					
Shear Rate	Doxycycline hyclate 5%					Shear Rate	Doxycycline hyclate 7.5%				
(s^{-1})	1	2	3	Mean	S.D.	(s^{-1})	1	2	3	Mean	S.D.
10	3087.73	2821.82	2730.53	2880.03	185.57	10	3147.26	2909.13	3250.45	3102.28	175.05
20	3853.70	3429.04	3369.51	3550.75	264.05	20	3484.61	3381.42	3484.61	3450.21	59.58
30	3881.49	3560.01	3468.73	3636.74	216.81	30	3492.54	3448.89	3583.83	3508.42	68.86
40	3873.55	3599.70	3524.29	3665.85	183.78	40	3687.02	3619.55	3790.20	3698.92	85.95
50	3837.83	3639.39	3532.23	3669.82	155.05	50	3714.80	3722.73	3853.70	3763.75	78.01
60	3790.20	3619.55	3611.61	3673.79	100.90	60	3730.67	3790.20	3877.52	3799.46	73.86
70	3790.20	3611.61	3587.80	3663.20	110.63	70	3778.30	3849.74	3901.33	3843.12	61.78
80	3798.14	3655.26	3544.14	3665.85	127.33	80	3802.11	3869.58	3952.92	3874.87	75.55
80	3833.86	3667.17	3556.04	3685.69	139.83	80	3806.08	3944.99	3921.17	3890.75	74.28
70	3909.27	3651.30	3540.17	3700.24	189.36	70	3857.67	3964.83	3925.14	3915.88	54.18
60	3865.61	3623.51	3532.23	3673.79	172.28	60	3841.80	3937.05	3901.33	3893.39	48.12
50	3845.77	3579.86	3512.39	3646.00	176.26	50	3853.70	3968.80	3881.49	3901.33	60.06
40	3758.45	3544.14	3472.70	3591.76	148.71	40	3814.02	3917.21	3833.86	3855.03	54.75
30	3786.24	3492.54	3417.14	3565.31	195.01	30	3817.99	3897.36	3821.95	3845.77	44.73
20	3742.58	3413.17	3357.60	3504.45	208.09	20	3762.42	3885.46	3746.55	3798.14	76.03
10	3611.61	3337.76	3234.57	3394.65	194.85	10	3603.67	3655.26	3631.45	3630.13	25.82

(continued)

(C)

Shear Rate (s^{-1})	Shear Stress (D/cm^2) Doxycycline hyclate 10%				
	1	2	3	Mean	S.D.
10	2571.78	2516.22	2766.25	2618.09	131.29
20	3302.04	3306.01	2976.60	3194.88	189.05
30	3849.74	3274.26	2996.44	3373.48	435.21
40	3871.12	3230.60	3103.60	3401.77	411.40
50	3730.67	2869.44	3063.91	3221.34	451.68
60	3480.64	2825.79	2944.85	3083.76	348.83
70	3409.20	2742.44	2873.41	3008.35	353.27
80	3476.67	2813.88	3016.29	3102.28	339.66
80	3544.14	2869.44	2980.57	3131.38	361.75
70	3563.98	2948.82	3020.26	3177.69	336.44
60	3694.95	2932.94	3048.04	3225.31	410.77
50	3694.95	2964.69	3040.10	3233.25	401.62
40	3778.30	3218.70	3067.88	3354.96	374.30
30	3810.05	3167.10	3079.79	3352.31	398.81
20	3806.08	3139.32	3048.04	3331.15	413.83
10	3829.89	3250.45	2996.44	3358.93	427.18

Table 43 The rheology data of the Lutrol® F127 systems containing different amount doxycycline hyclate with 20%NMP at 4°C

(A)

Shear Rate	Shear Stress (D/cm^2)					Shear Rate	Shear Stress (D/cm^2)				
	Doxycycline hyclate 0%						Doxycycline hyclate 2.5%				
(s^{-1})	1	2	3	Mean	S.D.	(s^{-1})	1	2	3	Mean	S.D.
10	11.91	11.91	11.91	11.91	0.00	10	15.88	15.88	11.91	14.55	2.29
20	23.81	23.81	35.72	27.78	6.87	20	27.78	31.75	23.81	27.78	3.97
30	31.75	31.75	27.78	30.43	2.29	30	43.66	39.69	35.72	39.69	3.97
40	39.69	43.66	39.69	41.01	2.29	40	51.59	55.56	47.63	51.59	3.97
50	47.63	51.59	47.63	48.95	2.29	50	63.50	63.50	59.53	62.18	2.29
60	59.53	63.50	55.56	59.53	3.97	60	79.38	87.31	67.47	78.05	9.99
70	67.47	75.41	67.47	70.12	4.58	70	91.28	95.25	79.38	88.64	8.26
80	91.28	79.38	75.41	82.02	8.26	80	111.13	99.22	95.25	101.87	8.26
80	79.38	83.34	75.41	79.38	3.97	80	103.19	107.16	95.25	101.87	6.06
70	67.47	71.44	67.47	68.79	2.29	70	87.31	95.25	83.34	88.64	6.06
60	63.50	63.50	55.56	60.85	4.58	60	87.31	83.34	71.44	80.70	8.26
50	51.59	59.53	47.63	52.92	6.06	50	67.47	79.38	59.53	68.79	9.99
40	47.63	47.63	39.69	44.98	4.58	40	63.50	63.50	47.63	58.21	9.17
30	31.75	35.72	31.75	33.07	2.29	30	39.69	51.59	35.72	42.33	8.26
20	23.81	27.78	19.84	23.81	3.97	20	27.78	59.53	23.81	37.04	19.58
10	43.66	11.91	11.91	22.49	18.33	10	47.63	15.88	15.88	26.46	18.33

(B)

Shear Rate	Shear Stress (D/cm^2)					Shear Rate	Shear Stress (D/cm^2)				
	Doxycycline hyclate 5%						Doxycycline hyclate 7.5%				
(s^{-1})	1	2	3	Mean	S.D.	(s^{-1})	1	2	3	Mean	S.D.
10	19.84	19.84	19.84	19.84	0.00	10	19.84	23.81	55.56	33.07	19.58
20	35.72	35.72	35.72	35.72	0.00	20	35.72	51.59	51.59	46.30	9.17
30	51.59	51.59	51.59	51.59	0.00	30	55.56	67.47	87.31	70.12	16.04
40	67.47	67.47	67.47	67.47	0.00	40	71.44	91.28	95.25	85.99	12.76
50	83.34	79.38	83.34	82.02	2.29	50	87.31	111.13	130.97	109.80	21.86
60	99.22	95.25	95.25	96.57	2.29	60	107.16	130.97	138.91	125.68	16.52
70	115.10	111.13	111.13	112.45	2.29	70	123.03	150.81	158.75	144.20	18.76
80	127.00	127.00	127.00	127.00	0.00	80	142.88	166.69	190.50	166.69	23.81
80	127.00	127.00	127.00	127.00	0.00	80	138.91	166.69	182.56	162.72	22.10
70	111.13	111.13	107.16	109.80	2.29	70	123.03	150.81	158.75	144.20	18.76
60	99.22	95.25	91.28	95.25	3.97	60	107.16	127.00	142.88	125.68	17.90
50	83.34	79.38	75.41	79.38	3.97	50	87.31	111.13	115.10	104.51	15.03
40	71.44	63.50	63.50	66.15	4.58	40	71.44	83.34	95.25	83.34	11.91
30	51.59	47.63	47.63	48.95	2.29	30	55.56	75.41	71.44	67.47	10.50
20	35.72	31.75	31.75	33.07	2.29	20	35.72	51.59	47.63	44.98	8.26
10	19.84	15.88	19.84	18.52	2.29	10	19.84	23.81	31.75	25.14	6.06

(continued)

(C)

	Shear Stress (D/cm^2)				
Shear Rate	**Doxycycline hyclate 10%**				
(s^{-1})	**1**	**2**	**3**	**Mean**	**S.D.**
10	**35.72**	**35.72**	**31.75**	**34.40**	**2.29**
20	**71.44**	**79.38**	**79.38**	**76.73**	**4.58**
30	**103.19**	**99.22**	**95.25**	**99.22**	**3.97**
40	**142.88**	**138.91**	**119.06**	**133.62**	**12.76**
50	**170.66**	**166.69**	**142.88**	**160.07**	**15.03**
60	**222.25**	**190.50**	**170.66**	**194.47**	**26.03**
70	**250.03**	**226.22**	**202.41**	**226.22**	**23.81**
80	**273.85**	**254.00**	**226.22**	**251.36**	**23.92**
80	**285.75**	**261.94**	**226.22**	**257.97**	**29.96**
70	**242.10**	**230.19**	**198.44**	**223.58**	**22.57**
60	**230.19**	**190.50**	**170.66**	**197.12**	**30.31**
50	**194.47**	**174.63**	**142.88**	**170.66**	**26.03**
40	**174.63**	**127.00**	**115.10**	**138.91**	**31.50**
30	**115.10**	**119.06**	**87.31**	**107.16**	**17.30**
20	**103.19**	**95.25**	**59.53**	**85.99**	**23.26**
10	**75.41**	**35.72**	**31.75**	**47.63**	**24.14**

Table 44 The rheology data of the Lutrol® F127 systems containing different amount doxycycline hyclate with 20%NMP at 27°C

(A)

Shear Stress (D/cm^2)						Shear Stress (D/cm^2)					
Shear Rate	Doxycycline hyclate 0%					Shear Rate	Doxycycline hyclate 2.5%				
(s^{-1})	1	2	3	Mean	S.D.	(s^{-1})	1	2	3	Mean	S.D.
10	2417.00	2349.53	2520.19	2428.91	85.95	10	2004.24	1928.84	2079.65	2004.24	75.41
20	2611.47	2512.25	2663.06	2595.60	76.65	20	2174.90	2178.87	2333.65	2229.14	90.53
30	2738.47	2591.63	2841.66	2723.92	125.65	30	2293.97	2278.09	2492.41	2354.82	119.42
40	2861.50	2734.50	2948.82	2848.28	107.77	40	2341.59	2333.65	2540.03	2405.09	116.93
50	2940.88	2809.91	3071.85	2940.88	130.97	50	2373.34	2357.47	2571.78	2434.20	119.42
60	3059.94	2881.35	3139.32	3026.87	132.13	60	2413.03	2393.19	2524.16	2443.46	70.59
70	3127.41	2968.66	3210.76	3102.28	122.99	70	2436.84	2428.91	2524.16	2463.30	52.85
80	3171.07	3016.29	3306.01	3164.46	144.97	80	2448.75	2436.84	2547.97	2477.85	61.01
80	3186.95	3032.16	3278.23	3165.78	124.39	80	2456.69	2452.72	2512.25	2473.89	33.28
70	3115.51	2992.48	3214.73	3107.57	111.34	70	2428.91	2444.78	2492.41	2455.36	33.05
60	3071.85	2885.32	3151.23	3036.13	136.51	60	2420.97	2405.09	2460.66	2428.91	28.62
50	2980.57	2841.66	3052.01	2958.08	106.96	50	2377.31	2401.12	2444.78	2407.74	34.22
40	2905.16	2734.50	2968.66	2869.44	121.10	40	2353.50	2353.50	2420.97	2375.99	38.95
30	2750.38	2674.97	2861.50	2762.28	93.84	30	2278.09	2345.56	2393.19	2338.95	57.83
20	2619.41	2536.06	2714.66	2623.38	89.36	20	2202.68	2286.03	2317.78	2268.83	59.44
10	2417.00	2270.15	2520.19	2402.45	125.65	10	2055.84	2135.21	2166.96	2119.34	57.24

(B)

Shear Stress (D/cm^2)						Shear Stress (D/cm^2)					
Shear Rate	Doxycycline hyclate 5%					Shear Rate	Doxycycline hyclate 7.5%				
(s^{-1})	1	2	3	Mean	S.D.	(s^{-1})	1	2	3	Mean	S.D.
10	1833.59	1690.71	1817.71	1780.67	78.31	10	178.60	1277.95	246.07	567.54	616.16
20	1996.31	1813.74	1873.27	1894.44	93.10	20	706.45	1400.99	936.64	1014.69	353.79
30	2063.78	1901.06	1944.71	1969.85	84.22	30	1115.23	1452.58	1139.05	1235.62	188.27
40	2111.40	1960.59	1984.40	2018.80	81.08	40	1186.67	1543.86	1178.73	1303.09	208.55
50	2115.37	1992.34	1996.31	2034.67	69.92	50	1218.42	1619.27	1202.55	1346.75	236.15
60	2139.18	2000.28	2020.12	2053.19	75.13	60	1250.17	1678.80	1250.17	1393.05	247.47
70	2155.06	2024.09	2043.93	2074.36	70.59	70	1285.89	1750.24	1281.92	1439.35	269.25
80	2163.00	2051.87	2067.74	2094.20	60.10	80	1329.55	1813.74	1317.64	1486.98	283.05
80	2182.84	2059.81	2067.74	2103.46	68.86	80	1341.45	1821.68	1337.49	1500.21	278.41
70	2159.03	2043.93	2047.90	2083.62	65.33	70	1301.77	1762.15	1305.74	1456.55	264.66
60	2131.25	1984.40	2016.15	2043.93	77.26	60	1281.92	1686.74	1289.86	1419.51	231.46
50	2091.56	1964.56	1976.46	2010.86	70.14	50	1254.14	1643.08	1270.02	1389.08	220.12
40	2059.81	1912.96	1956.62	1976.46	75.41	40	1242.23	1595.46	1258.11	1365.27	199.51
30	2039.96	1932.81	1936.77	1969.85	60.75	30	1222.39	1583.55	1222.39	1342.78	208.52
20	2039.96	1936.77	1940.74	1972.49	58.46	20	1206.52	1559.74	1210.48	1325.58	202.80
10	2063.78	1940.74	1996.31	2000.28	61.61	10	1178.73	1587.52	1190.64	1318.96	232.65

(continued)

(C)

	Shear Stress (D/cm^2)				
Shear Rate	**Doxycycline hyclate 10%**				
(s^{-1})	**1**	**2**	**3**	**Mean**	**S.D.**
10	**75.41**	**99.22**	**71.44**	**82.02**	**15.03**
20	**150.81**	**194.47**	**138.91**	**161.40**	**29.25**
30	**230.19**	**293.69**	**206.38**	**243.42**	**45.14**
40	**309.57**	**396.88**	**273.85**	**326.76**	**63.29**
50	**388.94**	**492.13**	**341.32**	**407.46**	**77.09**
60	**468.32**	**583.41**	**412.76**	**488.16**	**87.04**
70	**539.76**	**666.76**	**476.26**	**560.92**	**97.00**
80	**611.20**	**750.10**	**547.69**	**636.33**	**103.52**
80	**611.20**	**746.13**	**547.69**	**635.01**	**101.34**
70	**535.79**	**666.76**	**476.26**	**559.60**	**97.46**
60	**460.38**	**591.35**	**412.76**	**488.16**	**92.48**
50	**388.94**	**511.98**	**345.29**	**415.40**	**86.44**
40	**313.54**	**428.63**	**273.85**	**338.67**	**80.39**
30	**238.13**	**341.32**	**206.38**	**261.94**	**70.55**
20	**158.75**	**242.10**	**138.91**	**179.92**	**54.75**
10	**79.38**	**138.91**	**67.47**	**95.25**	**38.27**

Table 45 The rheology data of the Lutrol® F127 systems containing different amount doxycycline hyclate with 20%NMP at 37°C

(A)

Shear Stress (D/cm^2)						Shear Stress (D/cm^2)					
Shear Rate	Doxycycline hyclate 0%					Shear Rate	Doxycycline hyclate 2.5%				
(s^{-1})	1	2	3	Mean	S.D.	(s^{-1})	1	2	3	Mean	S.D.
10	2678.94	2734.50	2940.88	2784.77	138.02	10	2452.72	2274.12	2226.50	2317.78	119.26
20	2984.54	3163.13	3369.51	3172.39	192.65	20	2643.22	2345.56	2373.34	2454.04	164.42
30	3107.57	3198.85	3353.64	3220.02	124.39	30	2766.25	2468.59	2508.28	2581.04	161.62
40	3182.98	3341.73	3492.54	3339.08	154.80	40	2869.44	2591.63	2623.38	2694.82	152.06
50	3306.01	3436.98	3591.76	3444.92	143.04	50	2992.48	2663.06	2710.69	2788.74	178.04
60	3385.39	3560.01	3694.95	3546.78	155.21	60	3079.79	2778.16	2766.25	2874.73	177.68
70	3456.82	3635.42	3782.27	3624.84	162.98	70	3139.32	2845.63	2841.66	2942.20	170.72
80	3544.14	3675.11	3841.80	3687.02	149.19	80	3202.82	2881.35	2905.16	2996.44	179.12
80	3516.36	3718.77	3853.70	3696.28	169.79	80	3159.16	2901.19	2909.13	2989.83	146.70
70	3452.86	3623.51	3786.24	3620.87	166.71	70	3083.76	2845.63	2869.44	2932.94	131.15
60	3409.20	3595.73	3675.11	3560.01	136.51	60	3036.13	2798.00	2786.10	2873.41	141.05
50	3302.04	3476.67	3607.64	3462.12	153.32	50	2928.97	2722.60	2730.53	2794.04	116.93
40	3234.57	3417.14	3468.73	3373.48	123.03	40	2857.54	2643.22	2627.35	2709.37	128.56
30	3119.48	3218.70	3401.26	3246.48	142.93	30	2722.60	2512.25	2559.88	2598.24	110.30
20	2964.69	3055.98	3246.48	3089.05	143.77	20	2559.88	2377.31	2409.06	2448.75	97.54
10	2798.00	2921.04	2917.07	2878.70	69.92	10	2393.19	2170.93	2159.03	2241.05	131.89

(B)

Shear Stress (D/cm^2)						Shear Stress (D/cm^2)					
Shear Rate	Doxycycline hyclate 5%					Shear Rate	Doxycycline hyclate 7.5%				
(s^{-1})	1	2	3	Mean	S.D.	(s^{-1})	1	2	3	Mean	S.D.
10	2258.25	2174.90	2373.34	2268.83	99.64	10	2488.44	2631.31	2631.31	2583.69	82.49
20	2746.41	2460.66	2968.66	2725.24	254.66	20	2829.75	2964.69	2956.76	2917.07	75.72
30	2877.38	2536.06	3107.57	2840.34	287.55	30	2905.16	3190.92	3079.79	3058.62	144.05
40	2897.22	2627.35	3171.07	2898.55	271.87	40	2940.88	3258.38	3135.35	3111.54	160.09
50	2913.10	2663.06	3214.73	2930.30	276.23	50	2952.79	3302.04	3194.88	3149.90	178.92
60	2932.94	2726.57	3234.57	2964.69	255.49	60	2968.66	3321.89	3214.73	3168.43	181.11
70	2952.79	2762.28	3254.42	2989.83	248.15	70	2980.57	3345.70	3230.60	3185.62	186.67
80	2996.44	2762.28	3254.42	3004.38	246.16	80	2984.54	3381.42	3262.35	3209.44	203.66
80	2972.63	2790.07	3242.51	3001.74	227.62	80	3012.32	3389.36	3290.14	3230.60	195.44
70	2936.91	2770.22	3226.63	2977.92	230.95	70	3004.38	3385.39	3313.95	3234.57	202.53
60	2936.91	2754.35	3190.92	2960.72	219.26	60	3012.32	3381.42	3325.85	3239.86	199.01
50	2881.35	2730.53	3167.10	2926.33	221.73	50	3000.41	3361.57	3349.67	3237.22	205.17
40	2857.54	2694.82	3123.45	2891.93	216.38	40	3000.41	3349.67	3325.85	3225.31	195.13
30	2798.00	2651.16	3087.73	2845.63	222.15	30	2944.85	3309.98	3325.85	3193.56	215.54
20	2718.63	2595.60	3000.41	2771.55	207.53	20	2889.29	3258.38	3302.04	3149.90	226.75
10	2627.35	2452.72	2837.69	2639.25	192.76	10	2821.82	3143.29	3190.92	3052.01	200.77

(continued)

(C)

	Shear Stress (D/cm^2)				
Shear Rate	**Doxycycline hyclate 10%**				
(s^{-1})	**1**	**2**	**3**	**Mean**	**S.D.**
10	**2718.63**	**3357.60**	**2428.91**	**2835.05**	**475.17**
20	**2964.69**	**3448.89**	**2663.06**	**3025.55**	**396.43**
30	**3147.26**	**3579.86**	**2782.13**	**3169.75**	**399.34**
40	**3306.01**	**3651.30**	**2940.88**	**3299.40**	**355.25**
50	**3385.39**	**3683.05**	**3032.16**	**3366.87**	**325.84**
60	**3433.01**	**3746.55**	**3095.66**	**3425.07**	**325.51**
70	**3440.95**	**3734.64**	**3107.57**	**3427.72**	**313.74**
80	**3452.86**	**3683.05**	**3147.26**	**3427.72**	**268.78**
80	**3421.11**	**3675.11**	**3179.01**	**3425.07**	**248.07**
70	**3389.36**	**3639.39**	**3171.07**	**3399.94**	**234.34**
60	**3373.48**	**3655.26**	**3182.98**	**3403.91**	**237.61**
50	**3349.67**	**3659.23**	**3179.01**	**3395.97**	**243.44**
40	**3345.70**	**3690.98**	**3214.73**	**3417.14**	**246.03**
30	**3337.76**	**3587.80**	**3147.26**	**3357.60**	**220.94**
20	**3349.67**	**3552.08**	**3206.79**	**3369.51**	**173.50**
10	**3313.95**	**3444.92**	**3206.79**	**3321.89**	**119.26**

Table 46 The rheology data of the Lutrol® F127 systems containing 5% w/w doxycycline hyclate and different amount ZnO with 20%w/w NMP at 4°C

(A)

Shear Stress (D/cm^2)						Shear Stress (D/cm^2)					
Shear Rate	**ZnO 0%**					**Shear Rate**	**ZnO 0.5%**				
(s^{-1})	**1**	**2**	**3**	**Mean**	**S.D.**	**(s^{-1})**	**1**	**2**	**3**	**Mean**	**S.D.**
10	19.84	19.84	23.81	21.17	2.29	10	59.53	63.50	47.63	56.89	8.26
20	39.69	39.69	39.69	39.69	0.00	20	95.25	75.41	59.53	76.73	17.90
30	59.53	55.56	59.53	58.21	2.29	30	130.97	95.25	87.31	104.51	23.26
40	75.41	71.44	75.41	74.08	2.29	40	158.75	115.10	91.28	121.71	34.22
50	91.28	87.31	91.28	89.96	2.29	50	186.53	134.94	111.13	144.20	38.55
60	107.16	103.19	107.16	105.83	2.29	60	222.25	134.94	123.03	160.07	54.18
70	123.03	119.06	123.03	121.71	2.29	70	250.03	154.78	138.91	181.24	60.10
80	138.91	134.94	138.91	137.59	2.29	80	277.82	182.56	158.75	206.38	63.00
80	138.91	134.94	138.91	137.59	2.29	80	277.82	170.66	154.78	201.09	66.92
70	119.06	119.06	123.03	120.39	2.29	70	246.07	162.72	142.88	183.89	54.75
60	103.19	99.22	107.16	103.19	3.97	60	234.16	138.91	127.00	166.69	58.73
50	87.31	83.34	91.28	87.31	3.97	50	190.50	115.10	107.16	137.59	46.00
40	71.44	71.44	75.41	72.76	2.29	40	174.63	99.22	91.28	121.71	46.00
30	51.59	55.56	67.47	58.21	8.26	30	123.03	95.25	79.38	99.22	22.10
20	35.72	39.69	39.69	38.37	2.29	20	91.28	59.53	55.56	68.79	19.58
10	27.78	19.84	23.81	23.81	3.97	10	87.31	43.66	51.59	60.85	23.26

(B)

Shear Stress (D/cm^2)						Shear Stress (D/cm^2)					
Shear Rate	**ZnO 1%**					**Shear Rate**	**ZnO 2%**				
(s^{-1})	**1**	**2**	**3**	**Mean**	**S.D.**	**(s^{-1})**	**1**	**2**	**3**	**Mean**	**S.D.**
10	35.72	47.63	35.72	39.69	6.87	10	43.66	43.66	39.69	43.66	0.00
20	83.34	47.63	63.50	64.82	17.90	20	59.53	79.38	63.50	69.45	14.03
30	87.31	91.28	87.31	88.64	2.29	30	83.34	95.25	91.28	89.30	8.42
40	130.97	87.31	115.10	111.13	22.10	40	99.22	115.10	119.06	107.16	11.23
50	134.94	119.06	138.91	130.97	10.50	50	119.06	142.88	138.91	130.97	16.84
60	162.72	134.94	158.75	152.14	15.03	60	134.94	166.69	162.72	150.81	22.45
70	178.60	162.72	182.56	174.63	10.50	70	154.78	186.53	186.53	170.66	22.45
80	190.50	186.53	206.38	194.47	10.50	80	174.63	210.35	206.38	192.49	25.26
80	198.44	174.63	206.38	193.15	16.52	80	174.63	210.35	206.38	192.49	25.26
70	194.47	162.72	182.56	179.92	16.04	70	154.78	186.53	182.56	170.66	22.45
60	162.72	150.81	158.75	157.43	6.06	60	134.94	162.72	158.75	148.83	19.64
50	138.91	119.06	130.97	129.65	9.99	50	115.10	134.94	134.94	125.02	14.03
40	123.03	111.13	111.13	115.10	6.87	40	95.25	111.13	111.13	103.19	11.23
30	134.94	83.34	87.31	101.87	28.71	30	71.44	87.31	87.31	79.38	11.23
20	79.38	59.53	59.53	66.15	11.46	20	51.59	59.53	63.50	55.56	5.61
10	47.63	55.56	31.75	44.98	12.12	10	31.75	31.75	35.72	31.75	0.00

(continued)

(C)

	Shear Stress (D/cm^2)				
Shear Rate	**ZnO 2%**				
(s^{-1})	**1**	**2**	**3**	**Mean**	**S.D.**
10	43.66	39.69	43.66	42.33	2.29
20	71.44	67.47	75.41	71.44	3.97
30	95.25	95.25	95.25	95.25	0.00
40	123.03	119.06	127.00	123.03	3.97
50	146.85	138.91	146.85	144.20	4.58
60	170.66	166.69	158.75	165.37	6.06
70	190.50	190.50	186.53	189.18	2.29
80	214.32	218.28	210.35	214.32	3.97
80	214.32	214.32	214.32	214.32	0.00
70	190.50	186.53	190.50	189.18	2.29
60	166.69	170.66	158.75	165.37	6.06
50	142.88	142.88	142.88	142.88	0.00
40	119.06	119.06	111.13	116.42	4.58
30	91.28	91.28	99.22	93.93	4.58
20	67.47	63.50	79.38	70.12	8.26
10	35.72	63.50	35.72	44.98	16.04

Table 47 The rheology data of the Lutrol® F127 systems containing 5% w/w doxycycline hyclate and different amount ZnO with 20%w/w NMP at 27°C

(A)

Shear Stress (D/cm^2)						Shear Stress (D/cm^2)					
Shear Rate	ZnO 0%					Shear Rate	ZnO 0.5%				
(s^{-1})	1	2	3	Mean	S.D.	(s^{-1})	1	2	3	Mean	S.D.
10	1635.15	1654.99	1591.49	1627.21	32.49	10	2028.06	1992.34	2698.78	2239.73	397.96
20	1877.24	1647.05	1694.68	1739.66	121.51	20	2829.75	2909.13	3123.45	2954.11	151.92
30	1972.49	1694.68	1785.96	1817.71	141.60	30	3028.19	3135.35	3413.17	3192.24	198.69
40	1976.46	1698.65	1837.55	1837.55	138.91	40	3032.16	3159.16	3508.42	3233.25	246.62
50	2008.21	1742.30	1857.40	1869.30	133.35	50	2960.72	3147.26	3571.92	3226.63	313.23
60	1984.40	1801.84	1857.40	1881.21	93.58	60	2928.97	3119.48	3583.83	3210.76	336.83
70	1992.34	1837.55	1889.15	1906.35	78.81	70	2964.69	3151.23	3595.73	3237.22	324.19
80	2051.87	1817.71	1924.87	1931.48	117.22	80	2944.85	3182.98	3611.61	3246.48	337.88
80	2008.21	1869.30	1924.87	1934.13	69.92	80	2956.76	3123.45	3560.01	3213.41	311.53
70	1972.49	1849.46	1901.06	1907.67	61.78	70	2964.69	3071.85	3476.67	3171.07	270.02
60	2000.28	1829.62	1869.30	1899.73	89.31	60	2901.19	3000.41	3421.11	3107.57	276.02
50	1936.77	1825.65	1833.59	1865.34	61.99	50	2909.13	2976.60	3357.60	3081.11	241.81
40	1964.56	1809.77	1813.74	1862.69	88.24	40	2857.54	2928.97	3286.17	3024.23	229.64
30	1916.93	1809.77	1805.80	1844.17	63.04	30	2881.35	2928.97	3234.57	3014.97	191.67
20	1912.96	1825.65	1797.87	1845.49	60.06	20	2813.88	2857.54	3163.13	2944.85	190.30
10	2020.12	1829.62	1833.59	1894.44	108.86	10	2663.06	2702.75	3048.04	2804.62	211.74

(B)

Shear Stress (D/cm^2)						Shear Stress (D/cm^2)					
Shear Rate	ZnO 1%					Shear Rate	ZnO 1.5%				
(s^{-1})	1	2	3	Mean	S.D.	(s^{-1})	1	2	3	Mean	S.D.
10	2611.47	2726.57	2663.06	2667.03	57.65	10	2750.38	2551.94	2821.82	2651.16	140.32
20	2829.75	3052.01	3119.48	3000.41	151.60	20	3206.79	3004.38	3115.51	3105.59	143.12
30	2928.97	3107.57	3171.07	3069.21	125.53	30	3127.41	2976.60	3206.79	3052.01	106.64
40	3075.82	3230.60	3270.29	3192.24	102.76	40	3194.88	3000.41	3357.60	3097.65	137.51
50	3190.92	3345.70	3349.67	3295.43	90.53	50	3254.42	3167.10	3357.60	3210.76	61.74
60	3294.10	3436.98	3429.04	3386.71	80.30	60	3337.76	3282.20	3540.17	3309.98	39.29
70	3385.39	3524.29	3496.51	3468.73	73.50	70	3385.39	3270.29	3607.64	3327.84	81.38
80	3468.73	3603.67	3579.86	3550.75	72.02	80	3381.42	3337.76	3726.70	3359.59	30.87
80	3480.64	3595.73	3563.98	3546.78	59.44	80	3444.92	3373.48	3714.80	3409.20	50.51
70	3413.17	3524.29	3532.23	3489.90	66.57	70	3429.04	3361.57	3563.98	3395.31	47.71
60	3333.79	3440.95	3429.04	3401.26	58.73	60	3333.79	3266.32	3536.20	3300.06	47.71
50	3242.51	3345.70	3357.60	3315.27	63.29	50	3290.14	3226.63	3381.42	3258.38	44.90
40	3135.35	3242.51	3238.54	3205.47	60.75	40	3194.88	3163.13	3313.95	3179.01	22.45
30	3012.32	3115.51	3151.23	3093.02	72.13	30	3147.26	3044.07	3179.01	3095.66	72.97
20	2837.69	2944.85	2988.51	2923.68	77.60	20	3040.10	2948.82	2996.44	2994.46	64.55
10	2575.75	2694.82	2754.35	2674.97	90.94	10	2825.79	2738.47	2718.63	2782.13	61.74

(continued)

(C)

	Shear Stress (D/cm^2)				
Shear Rate	**ZnO 2%**				
(s^{-1})	**1**	**2**	**3**	**Mean**	**S.D.**
10	3040.10	3155.20	2996.44	3063.91	82.01
20	3325.85	3651.30	3409.20	3462.12	169.05
30	3548.11	3698.92	3413.17	3553.40	142.95
40	3647.33	3782.27	3464.76	3631.45	159.35
50	3746.55	3782.27	3512.39	3680.40	146.60
60	3829.89	3782.27	3623.51	3745.22	108.06
70	3909.27	3810.05	3651.30	3790.20	130.13
80	3956.14	3817.99	3690.98	3821.70	132.62
80	3987.95	3726.70	3710.83	3808.49	155.62
70	3952.92	3647.33	3631.45	3743.90	181.19
60	3829.89	3548.11	3571.92	3649.97	156.27
50	3698.92	3421.11	3488.58	3536.20	144.90
40	3575.89	3353.64	3389.36	3439.63	119.35
30	3425.07	3238.54	3206.79	3290.14	117.93
20	3258.38	3071.85	3075.82	3135.35	106.57
10	2992.48	2877.38	2809.91	2893.26	92.31

Table 48 The rheology data of the Lutrol® F127 systems containing 5% w/w doxycycline hyclate and different amount ZnO with 20%w/w NMP at 37°C

(A)

Shear Stress (D/cm^2)						Shear Stress (D/cm^2)					
Shear Rate	**ZnO 0%**					**Shear Rate**	**ZnO 0.5%**				
(s^{-1})	**1**	**2**	**3**	**Mean**	**S.D.**	**(s^{-1})**	**1**	**2**	**3**	**Mean**	**S.D.**
10	2115.37	2464.62	2333.65	2304.55	176.44	10	2333.65	2393.19	2488.44	2405.09	78.08
20	2492.41	2956.76	2817.85	2755.67	238.34	20	2782.13	2710.69	2885.32	2792.71	87.79
30	2813.88	3115.51	3000.41	2976.60	152.22	30	2877.38	2885.32	3048.04	2936.91	96.32
40	2940.88	3182.98	3079.79	3067.88	121.49	40	2992.48	2976.60	3155.20	3041.42	98.85
50	3020.26	3230.60	3131.38	3127.41	105.23	50	3083.76	3107.57	3250.45	3147.26	90.15
60	3071.85	3246.48	3171.07	3163.13	87.58	60	3175.04	3171.07	3353.64	3233.25	104.28
70	3111.54	3242.51	3222.67	3192.24	70.59	70	3246.48	3242.51	3440.95	3309.98	113.44
80	3143.29	3262.35	3250.45	3218.70	65.58	80	3313.95	3313.95	3516.36	3381.42	116.86
80	3139.32	3250.45	3250.45	3213.41	64.16	80	3329.82	3317.92	3524.29	3390.68	115.87
70	3131.38	3250.45	3218.70	3200.18	61.65	70	3270.29	3254.42	3452.86	3325.85	110.27
60	3115.51	3246.48	3179.01	3180.33	65.50	60	3206.79	3190.92	3373.48	3257.06	101.13
50	3143.29	3226.63	3139.32	3169.75	49.30	50	3135.35	3095.66	3286.17	3172.39	100.51
40	3127.41	3210.76	3107.57	3148.58	54.75	40	3036.13	3008.35	3182.98	3075.82	93.84
30	3075.82	3159.16	3036.13	3090.37	62.79	30	2932.94	2897.22	3055.98	2962.05	83.28
20	3008.35	3067.88	2984.54	3020.26	42.93	20	2770.22	2750.38	2893.26	2804.62	77.40
10	2861.50	2925.01	2853.57	2880.03	39.16	10	2524.16	2528.13	2643.22	2565.17	67.63

(B)

Shear Stress (D/cm^2)						Shear Stress (D/cm^2)					
Shear Rate	**ZnO 1%**					**Shear Rate**	**ZnO 1.5%**				
(s^{-1})	**1**	**2**	**3**	**Mean**	**S.D.**	**(s^{-1})**	**1**	**2**	**3**	**Mean**	**S.D.**
10	2611.47	2897.22	2786.10	2764.93	144.05	10	2873.41	2889.29	2817.85	2881.35	11.23
20	3155.20	3341.73	3294.10	3263.68	96.92	20	3127.41	3683.05	3139.32	3405.23	392.89
30	3286.17	3433.01	3433.01	3384.06	84.78	30	3294.10	3698.92	3194.88	3496.51	286.25
40	3397.29	3579.86	3540.17	3505.77	96.02	40	3476.67	3734.64	3313.95	3605.65	182.41
50	3520.33	3687.02	3575.89	3594.41	84.87	50	3556.04	3726.70	3421.11	3641.37	120.67
60	3603.67	3794.17	3587.80	3661.88	114.84	60	3659.23	3873.55	3500.48	3766.39	151.54
70	3683.05	3885.46	3710.83	3759.78	109.72	70	3746.55	3909.27	3575.89	3827.91	115.06
80	3790.20	3925.14	3774.33	3829.89	82.87	80	3825.92	3965.32	3659.23	3895.62	98.57
80	3778.30	3941.02	3837.83	3852.38	82.33	80	3837.83	3989.87	3655.26	3913.85	107.51
70	3706.86	3853.70	3770.36	3776.97	73.65	70	3802.11	3941.02	3587.80	3871.56	98.22
60	3615.58	3730.67	3627.48	3657.91	63.29	60	3722.73	3877.52	3508.42	3800.13	109.45
50	3524.29	3651.30	3552.08	3575.89	66.77	50	3651.30	3821.95	3421.11	3736.63	120.67
40	3417.14	3536.20	3421.11	3458.15	67.63	40	3528.26	3714.80	3321.89	3621.53	131.90
30	3294.10	3417.14	3313.95	3341.73	66.05	30	3436.98	3567.95	3210.76	3502.47	92.61
20	3135.35	3270.29	3171.07	3192.24	69.92	20	3258.38	3452.86	3052.01	3355.62	137.51
10	2877.38	2972.63	2901.19	2917.07	49.57	10	2964.69	3202.82	2805.94	3083.76	168.38

(continued)

(C)

	Shear Stress (D/cm^2)				
Shear Rate	**ZnO 2%**				
(s^{-1})	**1**	**2**	**3**	**Mean**	**S.D.**
10	3254.42	2936.91	2849.60	3013.64	213.04
20	3147.26	3405.23	3405.23	3319.24	148.94
30	3238.54	3472.70	3520.33	3410.52	150.83
40	3405.23	3619.55	3575.89	3533.55	113.26
50	3520.33	3683.05	3607.64	3603.67	81.43
60	3619.55	3746.55	3817.99	3728.03	100.51
70	3694.95	3829.89	3897.36	3807.40	103.06
80	3742.58	3881.49	3948.23	3857.43	104.91
80	3766.39	3905.30	3968.41	3880.03	103.35
70	3694.95	3845.77	3897.36	3812.69	105.18
60	3595.73	3706.86	3778.30	3693.63	92.00
50	3528.26	3675.11	3702.89	3635.42	93.84
40	3397.29	3524.29	3563.98	3495.19	87.07
30	3278.23	3500.48	3460.79	3413.17	118.53
20	3111.54	3353.64	3302.04	3255.74	127.52
10	2809.91	3032.16	3016.29	2952.79	123.99

APPENDICES III

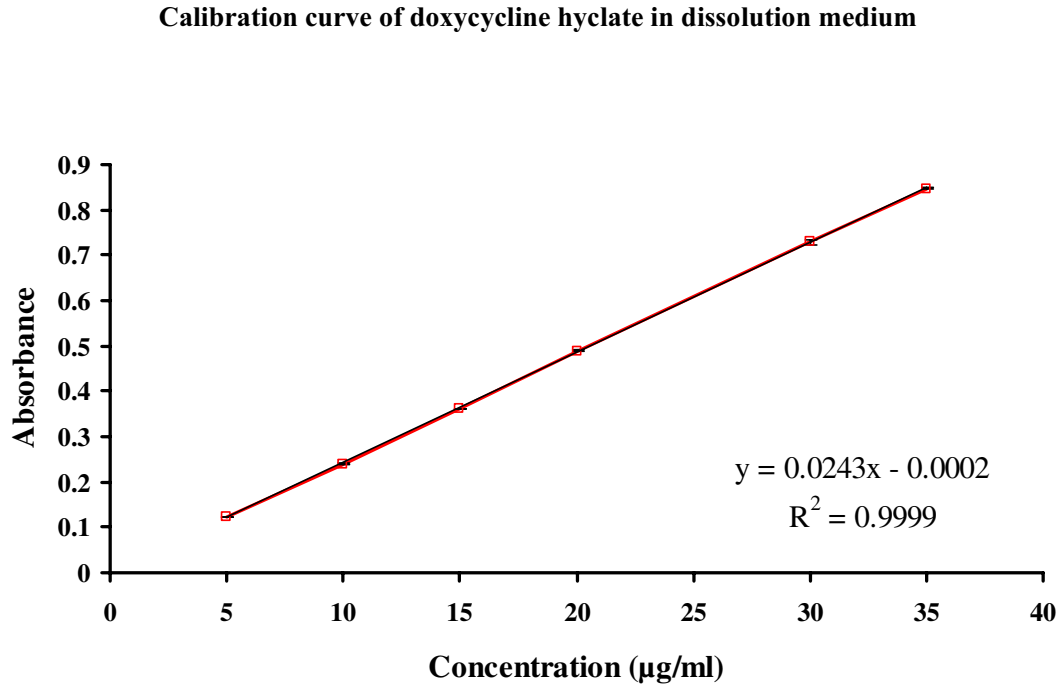

Figure 62 Calibration curve of doxycycline hyclate in in phosphate buffer pH 7.2

APPENDICES IV

The percentage of cumulative release of doxycycline hyclate

Table 49 The percentage of cumulative release of doxycycline hyclate in phosphate buffer pH 7.2 using dialysis tube method at 100 rpm

5% doxycycline hyclate					
TIME (min)	**1**	**2**	**3**	**mean**	**S.D.**
0	**0.00**	**0.00**	**0.00**	**0.00**	**0.00**
5	**7.18**	**8.42**	**6.82**	**7.47**	**0.84**
10	**9.84**	**9.24**	**8.85**	**9.31**	**0.50**
15	**13.04**	**11.70**	**11.65**	**12.13**	**0.79**
30	**26.95**	**21.47**	**22.60**	**23.67**	**2.90**
45	**29.52**	**25.66**	**27.76**	**27.65**	**1.93**
60	**33.21**	**29.38**	**31.59**	**31.39**	**1.92**
90	**48.27**	**47.38**	**47.64**	**47.76**	**0.45**
120	**61.94**	**54.96**	**62.38**	**59.76**	**4.17**
180	**72.95**	**66.85**	**71.19**	**70.33**	**3.14**
240	**89.72**	**82.26**	**87.99**	**86.66**	**3.91**
300	**93.37**	**94.53**	**88.40**	**92.10**	**3.25**
360	**94.26**	**92.06**	**91.31**	**92.54**	**1.54**
420	**92.57**	**93.08**	**90.08**	**91.91**	**1.61**
480	**91.63**	**92.30**	**92.31**	**92.08**	**0.39**
600	**90.13**	**91.63**	**91.90**	**91.22**	**0.95**
720	90.89	91.94	92.14	**91.66**	**0.67**

Table 50 The percentage of cumulative release of doxycycline hyclate from Lutrol® F127 gel into phosphate buffer pH 7.2 using dialysis tube method at 100 rpm

5% doxycycline hyclate+20% Lutrol® F127					
TIME (min)	1	2	3	mean	S.D.
0	0.00	0.00	0.00	0.00	0.00
5	4.36	3.28	4.89	4.18	0.82
10	6.77	5.87	6.45	6.36	0.46
15	8.62	8.49	8.18	8.43	0.23
30	14.75	14.14	12.04	13.64	1.42
45	18.91	18.75	17.76	18.47	0.62
60	23.21	24.34	20.65	22.74	1.89
90	28.50	32.11	29.01	29.87	1.95
120	36.70	43.21	42.38	40.76	3.54
180	52.05	56.21	45.09	51.12	5.62
240	64.02	62.97	56.89	61.29	3.85
300	71.57	75.07	67.80	71.48	3.64
360	78.09	80.46	71.99	76.84	4.37
600	88.40	90.21	74.18	84.26	8.78
720	86.74	90.91	82.09	86.58	4.41
840	88.24	90.67	89.29	89.40	1.22
960	83.64	91.15	90.22	88.34	4.09
1080	83.80	91.24	90.73	88.59	4.16
1200	83.02	89.52	90.87	87.80	4.20
1320	85.08	88.95	90.77	88.27	2.91
1440	81.27	88.32	90.34	86.64	4.76
2160	81.92	86.03	88.07	85.34	3.13
2880	81.04	85.91	87.34	84.76	3.30
3600	81.50	85.27	86.81	84.53	2.74

Table 51 The percentage of cumulative release of doxycycline hyclate from Lutrol® F127 gel containing 20% *N*-methyl-2-pyrrolidone and different amount of zinc oxide in phosphate buffer pH 7.2 using dialysis tube method at 100 rpm

(A)

5% doxycycline hyclate+20% Lutrol® F127+20% NMP					
TIME (min)	**1**	**2**	**3**	**mean**	**S.D.**
0	**0.00**	**0.00**	**0.00**	**0.00**	**0.00**
5	**2.73**	**4.40**	**5.58**	**4.23**	**1.43**
10	**7.94**	**7.20**	**6.97**	**7.37**	**0.50**
15	**12.07**	**9.85**	**9.74**	**10.55**	**1.31**
30	**15.15**	**16.29**	**13.95**	**15.13**	**1.17**
45	**22.60**	**23.39**	**21.47**	**22.48**	**0.96**
60	**30.18**	**29.61**	**29.78**	**29.86**	**0.29**
90	**39.63**	**36.46**	**39.63**	**38.58**	**1.83**
120	**45.86**	**43.47**	**48.20**	**45.84**	**2.37**
180	**51.34**	**52.49**	**52.05**	**51.96**	**0.58**
240	**62.92**	**72.58**	**70.61**	**68.70**	**5.11**
300	**77.28**	**79.57**	**77.91**	**78.25**	**1.18**
360	**86.72**	**82.29**	**85.54**	**84.85**	**2.30**
420	**86.19**	**81.95**	**89.20**	**85.78**	**3.64**
480	**87.44**	**86.71**	**87.64**	**87.26**	**0.49**
600	**89.59**	**90.30**	**89.76**	**89.88**	**0.37**
720	**88.38**	**90.43**	**90.66**	**89.82**	**1.26**
840	**89.68**	**90.68**	**89.79**	**90.05**	**0.55**
960	**88.38**	**89.42**	**88.73**	**88.84**	**0.53**
1080	**87.81**	**89.07**	**89.53**	**88.81**	**0.89**
1200	**87.36**	**89.35**	**88.83**	**88.51**	**1.04**
1320	**88.34**	**89.46**	**89.28**	**89.03**	**0.60**
1440	**88.03**	**91.21**	**89.11**	**89.45**	**1.61**
2160	**86.59**	**88.08**	**87.61**	**87.43**	**0.76**
2880	**86.11**	87.63	87.45	**87.06**	**0.83**

(continued)

(B)

5% doxycycline hyclate+20% Lutrol® F127+ 20% NMP+0.5% ZnO						5% doxycycline hyclate+20% Lutrol® F127+ 20% NMP+1.0% ZnO					
TIME (min)	1	2	3	mean	S.D.	TIME (min)	1	2	3	mean	S.D.
0	0.00	0.00	0.00	0.00	0.00	0	0.00	0.00	0.00	0.00	0.00
5	0.24	0.19	0.20	0.21	0.03	5	0.19	0.11	0.09	0.13	0.05
10	0.53	0.52	0.62	0.56	0.05	10	0.34	0.42	0.48	0.41	0.07
15	0.86	0.77	0.88	0.84	0.06	15	0.62	0.57	0.64	0.61	0.04
30	1.20	1.24	1.28	1.24	0.04	30	0.85	0.89	0.90	0.88	0.03
45	1.53	1.69	1.74	1.65	0.11	45	1.29	1.32	1.26	1.29	0.03
60	1.98	2.29	2.14	2.14	0.15	60	1.47	1.68	1.60	1.58	0.10
90	2.64	3.07	2.94	2.88	0.22	90	2.14	2.30	2.15	2.20	0.09
120	3.41	3.67	4.09	3.72	0.34	120	3.02	2.99	2.78	2.93	0.13
180	4.96	4.94	5.56	5.16	0.35	180	3.85	3.61	3.60	3.69	0.14
240	6.09	6.22	6.67	6.32	0.30	240	4.08	4.48	4.36	4.31	0.21
300	7.32	7.60	7.90	7.61	0.29	300	4.86	5.14	4.86	4.95	0.16
360	8.07	8.90	9.22	8.73	0.59	360	5.45	5.77	5.55	5.59	0.16
420	9.20	9.98	10.35	9.84	0.59	420	5.88	6.29	6.05	6.08	0.21
480	10.14	10.78	11.35	10.76	0.61	480	6.15	6.58	6.37	6.37	0.22
600	11.34	12.21	13.21	12.25	0.94	600	6.95	7.40	7.31	7.22	0.24
720	13.03	14.39	14.95	14.13	0.99	720	7.66	8.18	8.21	8.02	0.31
840	14.35	14.67	15.94	14.99	0.84	840	7.62	8.45	8.30	8.12	0.44
960	15.24	16.23	17.28	16.25	1.02	960	8.39	8.94	8.90	8.74	0.31
1080	16.39	17.42	18.44	17.42	1.02	1080	9.27	9.70	9.77	9.58	0.27
1200	17.37	18.64	19.59	18.54	1.11	1200	10.00	10.34	10.48	10.28	0.25
1320	18.30	19.72	20.77	19.59	1.24	1320	10.80	11.25	11.23	11.09	0.25
1440	19.63	20.77	21.96	20.79	1.16	1440	11.58	12.21	11.99	11.93	0.32
2160	24.13	29.02	26.06	26.40	2.46	2160	17.76	18.75	18.40	18.30	0.50
2880	27.25	34.31	30.52	30.69	3.53	2880	22.83	23.73	23.75	23.44	0.52
3600	30.99	41.16	35.00	35.72	5.12	3600	27.45	28.60	28.25	28.10	0.59
4320	39.55	48.12	40.81	42.83	4.63	4320	32.01	33.75	33.47	33.08	0.93
7200	51.09	59.40	54.54	55.01	4.17	7200	44.93	48.83	45.71	46.49	2.06
10080	51.33	61.62	57.31	56.75	5.16	10080	54.80	56.59	52.16	54.52	2.23
12960	51.82	62.72	59.08	57.88	5.55	12960	61.23	61.15	57.73	60.03	2.00

(continued)

(C)

5% doxycycline hyclate+20% Lutrol® F127+ 20% NMP+2.0% ZnO						5% doxycycline hyclate+20% Lutrol® F127+ 20% NMP+5.0% ZnO					
TIME (min)	1	2	3	mean	S.D.	TIME (min)	1	2	3	mean	S.D.
0	0.00	0.00	0.00	0.00	0.00	0	0.00	0.00	0.00	0.00	0.00
5	0.30	0.13	0.19	0.21	0.09	5	0.21	0.16	0.20	0.19	0.03
10	0.41	0.36	0.42	0.40	0.03	10	0.35	0.36	0.32	0.34	0.02
15	0.63	0.58	0.58	0.59	0.03	15	0.53	0.51	0.46	0.50	0.04
30	1.09	0.96	1.01	1.02	0.06	30	0.94	0.84	0.88	0.89	0.05
45	1.49	1.29	1.31	1.37	0.11	45	1.13	1.10	1.13	1.12	0.02
60	1.77	1.55	1.66	1.66	0.11	60	1.32	1.40	1.37	1.36	0.04
90	2.37	2.12	2.21	2.23	0.13	90	1.82	1.84	1.82	1.83	0.01
120	2.86	2.45	2.76	2.69	0.21	120	2.18	2.24	2.25	2.23	0.04
180	3.68	3.28	3.56	3.51	0.20	180	2.71	2.83	2.71	2.75	0.07
240	4.33	3.73	4.16	4.08	0.31	240	2.99	3.21	3.11	3.10	0.11
300	4.89	4.23	4.66	4.59	0.34	300	3.45	3.65	3.52	3.54	0.10
360	5.39	4.70	5.23	5.11	0.36	360	3.80	4.10	3.94	3.95	0.15
420	5.86	5.16	5.72	5.58	0.37	420	4.20	4.51	4.31	4.34	0.16
480	6.16	5.31	5.95	5.80	0.44	480	4.44	4.76	4.53	4.58	0.17
600	7.00	6.07	6.91	6.66	0.51	600	5.23	5.72	5.35	5.43	0.26
720	7.86	6.83	7.86	7.52	0.60	720	6.04	6.66	6.18	6.30	0.33
840	7.99	6.85	8.12	7.65	0.70	840	6.06	6.83	6.37	6.42	0.39
960	8.86	7.53	9.23	8.54	0.89	960	6.82	7.78	7.16	7.25	0.49
1080	9.80	8.28	10.58	9.55	1.17	1080	7.66	8.91	8.19	8.25	0.62
1200	10.75	9.01	11.77	10.51	1.40	1200	8.62	10.14	9.32	9.36	0.76
1320	11.77	9.78	13.07	11.54	1.66	1320	9.72	11.61	10.68	10.67	0.95
1440	12.93	10.63	14.76	12.77	2.07	1440	10.93	13.22	11.96	12.03	1.15
2160	21.70	17.15	23.74	20.86	3.37	2160	20.09	22.65	25.55	22.76	2.73
2880	32.09	23.40	31.91	29.13	4.97	2880	27.27	33.61	40.20	33.69	6.46
3600	41.33	29.35	38.36	36.34	6.24	3600	33.07	42.93	48.27	41.42	7.71
4320	49.49	35.23	43.93	42.88	7.19	4320	39.09	51.61	53.28	47.99	7.76
7200	55.02	44.63	52.74	50.80	5.46	7200	49.28	54.15	57.72	53.72	4.24
10080	54.83	48.02	55.79	52.88	4.24	10080	49.50	52.92	49.22	50.55	2.06
12960	53.30	50.24	54.69	52.75	2.28	12960	49.61	53.39	50.72	51.24	1.95

APPENDICES V

Table 52 The Storage modulus and Loss modulus of the Lutrol® F 127 system

Temperature (°C)	Storage modulus(G') (Pa)					Loss modulus (G") (Pa)				
	1	2	3	mean	S.D.	1	2	3	mean	S.D.
4	1.39	1.36	1.03	1.26	0.20	19.15	14.97	17.43	17.18	2.10
5	1.59	1.11	1.13	1.28	0.27	18.90	15.18	17.15	17.08	1.86
6	1.57	1.35	1.21	1.38	0.18	19.12	14.67	16.64	16.81	2.23
7	1.35	1.02	1.23	1.20	0.17	17.99	14.51	16.41	16.30	1.74
8	1.53	1.03	0.99	1.18	0.30	17.61	14.06	16.08	15.92	1.78
9	1.20	0.98	0.84	1.01	0.18	17.29	13.76	15.58	15.54	1.77
10	1.26	0.94	0.63	0.95	0.31	16.64	13.39	15.06	15.03	1.62
11	1.13	0.95	0.55	0.88	0.29	16.20	13.09	14.51	14.60	1.56
12	1.07	1.04	0.64	0.92	0.24	15.63	12.74	14.09	14.15	1.44
13	1.03	0.98	0.73	0.92	0.16	15.24	12.53	13.86	13.87	1.36
14	1.12	0.94	0.85	0.97	0.14	15.13	12.50	14.01	13.88	1.32
15	1.06	0.97	0.80	0.94	0.13	15.44	13.09	14.22	14.25	1.18
16	1.37	1.42	1.10	1.30	0.17	16.18	14.16	15.43	15.26	1.02
17	1.73	1.92	1.58	1.74	0.17	18.01	16.04	17.29	17.11	1.00
18	2.40	2.43	2.20	2.34	0.12	21.52	19.58	20.62	20.57	0.97
19	3.45	3.69	3.63	3.59	0.13	27.56	25.59	27.00	26.72	1.01
20	5.32	5.70	5.51	5.51	0.19	37.04	35.00	37.43	36.49	1.30
21	8.34	8.71	9.59	8.88	0.64	51.39	49.74	57.49	52.87	4.08
22	15.78	33.11	27.91	25.60	8.90	91.31	174.34	155.95	140.54	43.61
23	2262.94	2687.15	2890.08	2613.39	320.01	4824.29	5164.18	5581.66	5190.04	379.34
24	4934.57	5029.53	6160.66	5374.92	682.13	7829.58	7203.18	8727.79	7920.18	766.33
25	5880.66	5641.93	7456.97	6326.52	986.24	8402.02	7580.81	9419.09	8467.31	920.88
26	6396.93	6115.65	7875.38	6795.99	945.30	8714.03	7844.33	9607.95	8722.10	881.84
27	6759.04	6444.90	8126.85	7110.26	894.29	8926.07	8012.50	9706.40	8881.66	847.83
28	7028.49	6671.51	8249.93	7316.64	827.72	9099.44	8129.79	9762.55	8997.26	821.16
29	7265.40	6866.19	8457.87	7529.82	828.13	9244.82	8224.03	9867.52	9112.12	829.74
30	7458.25	7014.22	8608.39	7693.62	822.73	9360.75	8303.52	9931.34	9198.54	825.95
31	7646.57	7125.89	8741.78	7838.08	824.79	9458.23	8360.90	9986.75	9268.62	829.34
32	7789.93	7227.62	8831.20	7949.58	813.62	9515.78	8406.17	10025.86	9315.94	828.13
33	7919.92	7309.91	8905.81	8045.21	805.29	9495.33	8423.23	10045.23	9321.26	824.89
34	8010.55	7371.45	8974.36	8118.79	806.92	9487.01	8430.86	10039.34	9319.07	817.29
35	8087.71	7416.64	9020.34	8174.89	805.40	9483.75	8417.41	10029.17	9310.11	819.79
36	8145.31	7456.48	9056.31	8219.37	802.48	9474.42	8395.07	10006.15	9291.88	820.91
37	8186.16	7473.35	9090.30	8249.94	810.36	9460.15	8362.33	9976.82	9266.43	824.49
38	8215.86	7497.37	9110.81	8274.68	808.32	9440.38	8334.95	9948.37	9241.23	824.94
39	7930.01	7508.75	9114.74	8184.50	832.69	8677.91	8299.37	9906.40	8961.23	840.14
40	728.96	751.74	911.56	797.42	99.50	800.62	826.49	867.53	831.55	33.74
41	727.00	750.37	910.79	796.05	100.05	795.72	821.33	823.71	813.58	15.52
42	726.03	749.67	910.48	795.39	100.36	790.62	816.29	757.22	788.04	29.62
43	725.66	749.31	912.75	795.91	101.88	785.21	810.15	683.18	759.51	67.27
44	724.50	747.86	909.37	793.91	100.67	779.29	805.48	622.53	735.77	98.94
45	721.92	744.50	906.02	790.81	100.41	773.27	799.61	561.03	711.30	130.80

Table 53 The Storage modulus and Loss modulus of the Lutrol® F 127 system containing 5%w/w doxycycline hyclate

Temperature (°C)	Storage modulus(G') (Pa)					Loss modulus (G") (Pa)				
	1	2	3	mean	S.D.	1	2	3	mean	S.D.
4	0.83	0.83	0.83	0.83	0.83	19.81	17.73	16.21	17.92	1.81
5	0.32	0.32	0.32	0.32	0.32	18.55	17.49	16.92	17.65	0.83
6	0.35	0.35	0.35	0.35	0.35	18.30	16.93	16.80	17.34	0.83
7	0.30	0.30	0.30	0.30	0.30	17.64	16.42	16.38	16.81	0.72
8	0.27	0.27	0.27	0.27	0.27	16.86	15.93	16.04	16.28	0.51
9	0.25	0.25	0.25	0.25	0.25	16.28	15.29	15.60	15.73	0.50
10	0.32	0.32	0.32	0.32	0.32	15.68	14.89	15.03	15.20	0.42
11	0.36	0.36	0.36	0.36	0.36	14.84	14.31	14.63	14.59	0.27
12	0.36	0.36	0.36	0.36	0.36	14.91	13.97	14.35	14.41	0.47
13	0.61	0.61	0.61	0.61	0.61	14.62	14.34	14.20	14.39	0.21
14	0.55	0.55	0.55	0.55	0.55	15.11	14.78	14.80	14.90	0.18
15	0.70	0.70	0.70	0.70	0.70	16.07	15.56	16.24	15.96	0.36
16	0.67	0.67	0.67	0.67	0.67	18.12	17.19	18.14	17.82	0.55
17	0.66	0.66	0.66	0.66	0.66	20.99	20.08	19.61	20.23	0.70
18	1.26	1.26	1.26	1.26	1.26	23.82	23.22	23.83	23.62	0.35
19	2.31	2.31	2.31	2.31	2.31	28.91	27.02	28.46	28.13	0.99
20	3.38	3.38	3.38	3.38	3.38	34.32	32.12	32.79	33.08	1.13
21	4.50	4.50	4.50	4.50	4.50	39.45	38.47	38.69	38.87	0.52
22	5.62	5.62	5.62	5.62	5.62	46.29	47.13	44.63	46.01	1.27
23	6.80	6.80	6.80	6.80	6.80	52.42	53.28	50.50	52.06	1.42
24	8.15	8.15	8.15	8.15	8.15	58.86	59.89	58.17	58.97	0.87
25	9.55	9.55	9.55	9.55	9.55	66.31	67.28	66.29	66.63	0.56
26	13.04	13.04	13.04	13.04	13.04	84.18	76.25	79.13	79.85	4.01
27	18.11	18.11	18.11	18.11	18.11	110.43	128.04	110.02	116.16	10.29
28	92.14	92.14	92.14	92.14	92.14	535.25	304.79	224.44	354.83	161.33
29	3452.92	3452.92	3452.92	3452.92	3452.92	7405.47	7705.79	7928.78	7680.01	262.60
30	6384.93	6384.93	6384.93	6384.93	6384.93	10732.72	10154.66	10320.34	10402.57	297.68
31	7525.10	7525.10	7525.10	7525.10	7525.10	11456.19	11451.29	10408.56	11105.35	603.44
32	9282.36	9282.36	9282.36	9282.36	9282.36	11683.45	11719.96	11219.71	11541.04	278.88
33	9994.06	9994.06	9994.06	9994.06	9994.06	11864.11	11889.63	11532.92	11762.22	198.99
34	10322.64	10322.64	10322.64	10322.64	10322.64	11999.78	11982.68	11903.00	11961.82	51.65
35	10477.32	10477.32	10477.32	10477.32	10477.32	12067.15	12039.51	12180.48	12095.71	74.70
36	10652.30	10652.30	10652.30	10652.30	10652.30	12122.92	12084.63	12359.33	12188.96	148.78
37	10804.88	10804.88	10804.88	10804.88	10804.88	12179.39	12113.85	12454.51	12249.25	180.75
38	10939.95	10939.95	10939.95	10939.95	10939.95	12224.69	12157.93	12533.41	12305.34	200.32
39	11084.64	11084.64	11084.64	11084.64	11084.64	12285.63	12170.47	12574.71	12343.60	208.26
40	11219.03	11219.03	11219.03	11219.03	11219.03	12308.52	12234.67	12588.37	12377.18	186.58
41	11351.90	11351.90	11351.90	11351.90	11351.90	12336.09	12268.42	12627.78	12410.76	190.96
42	11500.36	11500.36	11500.36	11500.36	11500.36	12381.74	12301.55	12694.18	12459.16	207.45

(continued)

Temperature	Storage modulus(G') (Pa)					Loss modulus (G") (Pa)				
(°C)	1	2	3	mean	S.D.	1	2	3	mean	S.D.
43	11624.45	11624.45	11624.45	11624.45	11624.45	12402.74	12328.27	12741.26	12490.76	220.11
44	11739.74	11739.74	11739.74	11739.74	11739.74	12445.07	12376.07	12822.16	12547.77	240.12
45	11877.05	11877.05	11877.05	11877.05	11877.05	12458.31	12401.72	12865.07	12575.04	252.77

Table 54 The Storage modulus and Loss modulus of the Lutrol® F 127 system containing 5%w/w doxycycline hyclate with 20%w/w NMP

Temperature	Storage modulus(G') (Pa)					Loss modulus (G") (Pa)				
(°C)	1	2	3	mean	S.D.	35.59	39.86	39.47	38.31	2.36
4	0.87	3.65	11.86	5.46	5.71	35.70	39.23	39.30	38.08	2.06
5	0.80	3.23	11.32	5.11	5.51	36.30	39.62	40.55	38.82	2.23
6	0.50	3.09	10.81	4.80	5.36	37.28	41.01	41.41	39.90	2.28
7	0.45	3.07	10.46	4.66	5.19	39.47	43.36	43.44	42.09	2.27
8	0.56	3.40	10.46	4.81	5.09	42.30	46.51	46.75	45.19	2.50
9	0.52	3.88	10.55	4.98	5.11	45.14	49.94	50.06	48.38	2.80
10	1.08	4.86	11.06	5.67	5.04	49.52	53.76	54.59	52.63	2.72
11	1.72	5.40	11.76	6.29	5.08	52.69	58.32	59.65	56.89	3.69
12	2.55	6.36	12.22	7.04	4.87	58.78	63.19	65.09	62.35	3.24
13	3.73	7.26	13.36	8.11	4.87	65.64	70.09	70.21	68.65	2.61
14	4.81	8.48	14.34	9.21	4.80	71.70	77.83	77.20	75.58	3.37
15	6.17	10.06	15.50	10.57	4.69	77.99	83.73	85.69	82.47	4.00
16	7.44	11.41	17.23	12.03	4.92	84.99	92.16	91.00	89.38	3.85
17	8.87	13.00	18.29	13.38	4.72	93.10	98.25	95.43	95.59	2.58
18	10.28	14.43	19.32	14.68	4.53	100.64	104.57	103.91	103.04	2.10
19	11.69	15.75	21.01	16.15	4.67	108.05	111.34	112.08	110.49	2.15
20	13.33	16.96	22.87	17.72	4.81	115.63	118.89	118.63	117.72	1.81
21	14.70	18.73	24.32	19.25	4.83	123.67	125.34	125.61	124.87	1.05
22	16.31	20.09	25.99	20.80	4.88	130.58	131.04	131.63	131.08	0.53
23	17.67	21.49	27.56	22.24	4.99	137.64	137.55	138.04	137.74	0.26
24	18.95	23.01	29.16	23.71	5.14	144.38	147.63	149.78	147.26	2.72
25	20.38	25.36	32.27	26.00	5.97	196.58	172.25	172.68	180.50	13.92
26	32.27	30.73	37.91	33.64	3.78	513.57	383.54	262.93	386.68	125.35
27	118.75	75.15	57.17	83.69	31.67	2608.24	1420.36	803.82	1610.80	917.16
28	678.21	320.89	175.29	391.47	258.78	4366.19	5064.94	3309.98	4247.04	883.53
29	1336.34	1617.28	964.01	1305.88	327.70	6910.75	7303.26	5595.08	6603.03	894.70
30	2431.37	2593.55	1862.15	2295.69	384.11	9001.63	8957.76	8117.13	8692.18	498.48
31	3664.81	3677.72	3149.44	3497.32	301.34	10487.21	10277.31	9617.51	10127.34	453.83
32	4837.46	4893.46	4267.09	4666.01	346.60	11439.35	11077.75	10501.30	11006.13	473.11
33	6167.16	6040.01	5194.22	5800.47	528.86	11787.27	11461.48	11134.96	11461.24	326.15
34	7266.67	7046.34	6226.94	6846.65	547.87	11637.14	11501.43	11517.08	11551.88	74.25
35	8568.00	8006.62	7234.76	7936.46	669.38	11568.60	11394.28	11471.10	11477.99	87.36
36	9048.91	8796.63	8255.59	8700.38	405.32	11701.84	11467.07	11357.90	11508.94	175.75
37	9258.41	9028.51	8722.96	9003.29	268.62	11820.56	11501.21	11427.75	11583.17	208.84
38	9445.86	9168.93	8906.43	9173.74	269.75	11855.68	11467.24	11521.19	11614.70	210.43
39	9582.33	9242.98	9070.35	9298.56	260.48	11849.06	11402.25	11583.38	11611.56	224.74
40	9639.07	9250.07	9213.42	9367.52	235.88	11817.97	11321.22	11559.36	11566.18	248.45
41	9648.84	9236.58	9290.90	9392.11	223.99	11765.87	11235.60	11508.86	11503.44	265.18
42	9653.23	9209.31	9335.69	9399.41	228.71	11657.30	11121.60	11439.88	11406.26	269.43

(continued)

Temperature (°C)	Storage modulus(G') (Pa)					Loss modulus (G") (Pa)				
	1	2	3	mean	S.D.	1	2	3	mean	S.D.
43	9696.15	9163.13	9339.32	9399.54	271.56	11594.66	11015.86	11382.86	11331.13	292.85
44	9702.55	9121.38	9376.48	9400.14	291.31	11548.58	10872.53	11249.56	11223.56	338.78
45	9703.80	9000.16	9317.84	9340.60	352.37	35.59	39.86	39.47	38.31	2.36

Table 55 The Storage modulus and Loss modulus of the Lutrol® F 127 system containing 5%w/w doxycycline hyclate and 1.0%w/w ZnO with 20%w/w NMP

Temperature	Storage modulus(G') (Pa)					Loss modulus (G") (Pa)				
(°C)	1	2	3	mean	S.D.	83.24	79.56	101.08	87.96	11.51
4	9.83	11.54	12.50	11.29	1.35	84.71	82.05	98.53	88.43	8.85
5	10.08	12.00	12.59	11.56	1.31	91.21	87.81	103.47	94.16	8.24
6	11.29	13.06	13.92	12.76	1.34	102.26	95.63	114.53	104.14	9.59
7	13.44	14.61	16.84	14.96	1.73	112.20	106.05	127.43	115.22	11.01
8	15.48	16.67	20.16	17.44	2.43	125.96	119.02	139.22	128.07	10.27
9	18.22	19.43	22.81	20.15	2.38	139.97	133.94	155.32	143.07	11.02
10	20.91	22.68	26.39	23.33	2.80	157.58	151.61	184.83	164.67	17.71
11	24.61	26.38	33.38	28.12	4.63	177.75	171.81	208.31	185.96	19.58
12	28.84	30.88	39.20	32.97	5.49	202.07	193.54	230.28	208.63	19.23
13	33.99	35.78	44.75	38.17	5.76	226.65	217.49	265.51	236.55	25.49
14	39.22	41.02	54.32	44.85	8.24	256.15	243.40	293.84	264.46	26.22
15	45.70	46.70	63.59	52.00	10.05	290.08	272.98	343.96	302.34	37.04
16	53.47	53.39	83.48	63.45	17.35	393.76	338.72	1034.78	589.09	386.96
17	76.37	68.34	297.70	147.47	130.16	991.37	765.75	3417.39	1724.84	1470.13
18	214.25	164.39	1148.52	509.06	554.36	4687.28	3398.38	6375.58	4820.41	1493.06
19	1706.19	1034.22	3184.31	1974.91	1099.94	7279.88	6161.27	8459.54	7300.23	1149.27
20	3950.16	3145.52	4851.63	3982.44	853.52	9541.75	8852.28	9564.37	9319.47	404.75
21	6173.55	5193.50	6125.36	5830.80	552.44	10235.10	9794.29	10222.52	10083.97	250.95
22	7669.46	6728.45	7579.92	7325.94	519.38	10650.37	10206.90	10616.90	10491.39	246.94
23	8663.94	7528.20	8430.12	8207.42	599.73	10826.96	10462.92	10754.77	10681.55	192.75
24	9112.70	8010.09	8809.39	8644.06	569.59	10945.69	10622.53	10802.75	10790.32	161.94
25	9508.95	8375.57	9095.55	8993.36	573.56	10961.53	10652.05	10741.86	10785.15	159.22
26	9741.80	8635.56	9160.13	9179.16	553.36	10898.56	10598.84	10688.01	10728.47	153.90
27	9776.67	8753.99	9232.15	9254.27	511.70	10817.78	10486.41	10579.77	10627.99	170.87
28	9756.17	8725.48	9171.95	9217.87	516.88	10703.79	10382.67	10463.63	10516.70	167.01
29	9657.08	8682.67	9085.14	9141.63	489.66	10583.52	10300.10	10365.83	10416.48	148.34
30	9518.98	8643.83	9005.02	9055.94	439.79	10419.93	10243.28	10295.11	10319.44	90.80
31	9331.95	8625.98	8964.24	8974.06	353.08	10320.32	10192.23	10237.33	10249.96	64.97
32	9218.93	8598.41	8924.10	8913.81	310.39	10248.44	10192.14	10181.03	10207.20	36.14
33	9137.25	8670.64	8884.49	8897.46	233.57	10201.76	10178.59	10156.16	10178.83	22.80
34	9099.24	8712.24	8879.84	8897.11	194.08	10165.60	10166.56	10137.05	10156.40	16.76
35	9086.45	8741.66	8873.32	8900.48	173.99	10142.15	10151.50	10128.33	10140.66	11.66
36	9087.68	8753.14	8898.57	8913.13	167.74	10134.12	10139.26	10120.56	10131.31	9.66
37	9105.21	8770.24	8919.60	8931.69	167.81	10118.81	10129.01	10109.65	10119.16	9.69
38	9122.78	8778.46	8937.52	8946.25	172.33	10098.67	10119.67	10094.07	10104.14	13.64
39	9130.82	8794.19	8938.41	8954.47	168.89	10085.37	10111.65	10088.41	10095.14	14.38
40	9145.67	8810.07	8959.69	8971.81	168.13	10073.44	10101.87	10077.46	10084.26	15.39
41	9165.78	8822.87	8967.97	8985.54	172.13	10056.44	10085.53	10060.65	10067.54	15.72
42	9175.27	8827.09	8960.96	8987.77	175.64	10041.37	10066.63	10041.95	10049.98	14.42

(continued)

Temperature	Storage modulus(G') (Pa)					Loss modulus (G") (Pa)				
(°C)	1	2	3	mean	S.D.	1	2	3	mean	S.D.
43	9178.88	8833.94	8965.85	8992.89	174.05	10014.06	10050.81	10021.91	10028.93	19.35
44	9186.55	8843.88	8967.28	8999.24	173.56	9986.64	10034.27	10001.60	10007.51	24.35
45	9202.24	8849.56	8962.41	9004.74	180.11	83.24	79.56	101.08	87.96	11.51

Table 56 The Storage modulus and Loss modulus of the Lutrol® F 127 system containing 5%w/w doxycycline hyclate and 5.0%w/w ZnO with 20%w/w NMP

Temperature	Storage modulus(G') (Pa)					Loss modulus (G") (Pa)				
(°C)	1	2	3	mean	S.D.	1	2	3	mean	S.D.
4	50.80	65.19	50.38	55.46	8.44	242.77	348.18	241.87	277.61	61.12
5	53.64	61.28	53.56	56.16	4.43	249.27	324.38	248.43	274.03	43.61
6	58.71	66.22	53.88	59.60	6.22	269.11	337.34	250.49	285.65	45.73
7	66.36	73.02	58.68	66.02	7.18	300.08	360.48	269.22	309.93	46.42
8	75.51	84.52	66.06	75.36	9.23	334.75	399.01	299.65	344.47	50.39
9	89.74	99.25	75.29	88.09	12.07	381.69	443.75	334.42	386.62	54.83
10	111.66	134.25	89.62	111.84	22.32	445.69	526.40	381.31	451.13	72.70
11	166.59	234.50	111.50	170.86	61.61	556.92	710.04	445.44	570.80	132.84
12	394.08	2111.57	165.91	890.52	1063.60	938.61	4998.26	557.24	2164.70	2461.33
13	1387.28	3645.68	387.13	1806.70	1669.27	3430.55	7662.57	922.91	4005.35	3406.40
14	3085.84	6092.81	461.56	3213.40	2817.79	6314.98	9448.12	1076.31	5613.14	4229.80
15	5328.38	8185.30	1386.02	4966.57	3414.05	8235.56	10380.94	3483.24	7366.58	3530.00
16	7405.96	9761.30	3045.84	6737.70	3407.24	9713.72	10938.84	6269.51	8974.02	2420.95
17	9115.05	11483.66	5338.14	8645.62	3099.54	10637.46	11427.96	8220.12	10095.18	1671.26
18	11006.04	12237.79	7407.02	10216.95	2510.20	11294.06	11581.44	9704.55	10860.02	1010.92
19	12732.09	12837.34	9115.07	11561.50	2119.33	11646.54	11652.74	10635.98	11311.75	585.25
20	13838.87	13337.13	11003.04	12726.35	1513.37	11826.39	11709.11	11290.77	11608.76	281.56
21	14616.98	13736.93	12733.54	13695.82	942.39	11911.34	11750.07	11640.46	11767.29	136.26
22	15298.31	14048.31	13840.56	14395.73	788.53	11945.12	11770.48	11826.08	11847.23	89.22
23	15903.14	14285.98	14622.18	14937.10	853.33	11952.05	11767.80	11915.51	11878.46	97.55
24	16355.56	14520.84	15283.77	15386.72	921.68	11931.39	11758.26	11943.24	11877.63	103.55
25	16665.03	14749.28	15903.32	15772.54	964.55	11897.74	11760.13	11948.68	11868.85	97.54
26	16878.63	14893.75	16350.73	16041.04	1028.04	11858.29	11737.56	11929.75	11841.86	97.14
27	17085.62	15011.41	16664.21	16253.75	1096.33	11748.39	11701.91	11893.88	11781.39	100.15
28	16991.42	15112.15	16876.28	16326.62	1053.33	11672.51	11678.61	11857.27	11736.13	104.96
29	16910.04	15200.44	17073.16	16394.55	1037.34	11577.16	11632.43	11745.95	11651.85	86.06
30	16755.48	15282.07	16985.63	16341.06	924.30	11451.09	11596.34	11672.52	11573.32	112.50
31	16529.78	15345.77	16898.64	16258.06	811.31	11362.35	11552.68	11578.46	11497.83	118.04
32	16303.37	15411.75	16745.81	16153.64	679.51	11245.26	11508.44	11450.54	11401.41	138.30
33	16014.03	15480.96	16522.80	16005.93	520.97	11111.63	11457.64	11361.70	11310.32	178.63
34	15758.61	15503.15	16292.57	15851.44	402.82	11002.93	11417.44	11247.57	11222.65	208.37
35	15555.42	15510.44	16001.24	15689.03	271.31	10881.06	11369.94	11107.07	11119.36	244.67
36	15308.27	15533.47	15746.07	15529.27	218.93	10738.27	11331.33	11004.36	11024.65	297.05
37	15143.65	15561.63	15548.34	15417.87	237.57	10627.08	11296.26	10901.60	10941.65	336.39
38	15016.99	15583.22	15294.00	15298.07	283.13	10512.60	11269.04	10740.93	10840.86	387.99
39	14923.87	15613.61	15130.80	15222.76	353.95	10393.05	11226.80	10627.06	10748.97	430.03
40	14834.97	15635.92	15011.98	15160.96	420.75	10281.44	11189.79	10509.23	10660.16	472.61
41	14757.57	15655.06	14932.55	15115.06	475.77	10205.02	11151.73	10385.43	10580.72	502.66
42	14697.89	15683.39	14836.26	15072.51	533.54	10115.70	11106.15	10279.86	10500.57	530.83

(continued)

Temperature (°C)	Storage modulus(G') (Pa)					Loss modulus (G") (Pa)				
	1	2	3	mean	S.D.	1	2	3	mean	S.D.
43	14652.64	15709.34	14749.56	15037.18	584.12	10029.89	11058.12	10209.04	10432.35	549.29
44	14613.63	15731.93	14689.91	15011.82	624.79	9952.17	11007.03	10116.96	10358.72	567.46
45	14581.36	15775.63	14643.66	15000.22	672.25	9854.16	10917.97	10032.31	10268.15	569.77

APPENDICES VI

The preparation of different solutions and others

Tryptic soy agar (TSA)

Suspend 40.0 g of the powder in 1 L of purified water. Mix completely. Heat with frequent agitation and boil for 1 minute to completely dissolve the powder. Autoclave at 121°C for 15 minutes.

Tryptic soy broth (TSB)

Suspend 30.0 g of the powder in 1 L of purified water. Mix throughly. Warm slightly to completely dissolve the powder. Autoclave at 121°C for 15 minutes.

Sabouraud dextrose agar (SDA)

Suspend 65.0 g of the powder in 1 L of purified water. Mix completely. Heat with frequent agitation and boil for 1 minute to completely dissolve the powder. Autoclave at 121°C for 15 minutes.

Sabouraud dextrose broth (SDB)

Dissolve 30 g of the powder in 1 L of purified water. Autoclave at 121°C for 15 minutes.

Preparation of phosphate buffer pH 7.2 using as solvent for determination of content uniformity

Phosphate buffer pH 7.2 was prepared by dissolving 6.81 g of potassium dihydrogen orthophosphate and 1.41 g of sodium hydroxide in distilled water to obtain 1000 mL.

APPENDICES VII

LIST OF ABBREVIATIONS

BEI	backscatter electron image
$^{\circ}C$	degree Celsius
cd	coefficient of determination
CFU/mL	colony forming unit/milliliter
D/cm^2	Dyne/centimeter^2
et al.	and others
g	gram
mg	milligram
mm	millimeter
mL	mililiter
msc	model selection criterion
N	newton
nm	nanometer
NMP	*N*-methyl-2-pyrrolidone
PVP	polyvinyl pyrrolidone
rpm	round per minute
SEI	secondary electron image
SEM	scanning electron microscope
S.D.	standard deviation
ZnO	zinc oxide
%w/w	percent of weight by weight
μm	micrometer
μg	microgram

BIOGRAPHY

Name	Jongjan Mahadlek, Miss.
Date of Birth	October 1, 1982
Place of Birth	Ratchaburi
Institution Attended	
2004	Silpakorn University, Bachelor of Pharmacy
2008	Silpakorn University, Master of Pharmacy (Pharmaceutical Technology)
PRESENTATION	Jongjan Mahadlek, Thawatchai Phaechamud, Supab Choopun and Juree Charoenteeraboon. “Characterization of Typical and Nano Zinc Oxide” The Silpakorn University Research Fair, Silpakorn University, Thailand. December 18 - 19, 2008.